UNIVERSITAT DE BARCELONA

Nuevos materiales en el uso de la técnica de gradiente de difusión en capa fina (DGT) en estudios de la contaminación por mercurio en ambientes impactados por la mineria de oro

Siday Marrugo-Madrid

Siday Marrugo-Madrid

UNIVERSITAT DE BARCELONA

CSIC
CONSEJO SUPERIOR DE INVESTIGACIONES CIENTÍFICAS

TESIS DOCTORAL

NUEVOS MATERIALES EN EL USO DE LA
TÉCNICA DE GRADIENTE DE DIFUSIÓN EN CAPA FINA (DGT)
EN ESTUDIOS DE LA CONTAMINACIÓN POR MERCURIO EN
AMBIENTES IMPACTADOS POR LA MINERÍA DE ORO

Siday Marrugo-Madrid

2023

Facultad de Química

Departamento de Ingeniería Química y Química Analítica

Doctorado en Química Analítica y Medio Ambiente

NUEVOS MATERIALES EN EL USO DE LA TÉCNICA DE GRADIENTE DE DIFUSIÓN EN CAPA FINA (DGT) EN ESTUDIOS DE LA CONTAMINACIÓN POR MERCURIO EN AMBIENTES IMPACTADOS POR LA MINERÍA DE ORO

SIDAY MARRUGO-MADRID

Tesis presentada para obtener el título de Doctor (PhD)
por la Universidad de Barcelona

Director	Tutor
Dr. Sergi Díez Salvador	**Dra. Cristina Ariño Blasco**
Instituto de Diagnóstico Ambiental y Estudios del Agua – IDÆA	Departamento de Ingeniería Química y Química Analítica
Consejo Superior de Investigaciones Científicas– CSIC	Facultad de Química
	Universidad de Barcelona

Barcelona, 2023

Cuanto mayor es la dificultad,
más gloria hay en superarla.
Los buenos navegantes logran su reputación
en las tormentas y tempestades.
—Epicteto

A Jose bonito, mi madre y mi padre,
gracias por tanto amor

Agradecimientos

Si mencionara a todas las personas de las que estoy profundamente agradecida por ayudarme a cumplir este sueño, seguramente tendría que sumarle otro capítulo a mi tesis doctoral. Pero no puedo dejar pasar la oportunidad de expresar mi gratitud hacia aquellos que han dejado una huella imborrable en este increíble viaje hacia la culminación de mi doctorado:

En primer lugar, mi más sincero agradecimiento a mi director de tesis y amigo, Sergi Díez. ¡Sin duda alguna es un crack en investigación! Además, su calidez humana, sus consejos certeros y sus palabras de apoyo me han acompañado en todo momento durante este proceso doctoral, especialmente en las horas más difíciles durante la pandemia. Gracias Sergi, the best boss ever!

A mi tutora, Cristina Ariño, de la Universidad de Barcelona, quiero agradecerle su valiosa guía, los consejos oportunos, todos los certificados que me ha firmado rápidamente para mis interminables gestiones burocráticas. Gracias Cristina por la confianza que depositaste en mí desde el principio.

A mi papá, José Marrugo Negrete, a quien amo y admiro infinitamente, quiero darle las gracias por sus valiosos consejos y su apoyo cariñoso e incondicional en todos los proyectos académicos, laborales que emprendo. Tú me has enseñado con tu ejemplo las bases de una investigación científica de calidad. Y a mi mamá, Siday Madrid, ¡tu buen sentido del humor es insuperable!

Admiro tu habilidad para mantener la calma en medio de la tempestad. A mis padres, gracias por tanto amor.

A mis hermanos, José Luis (¡bonito! jejeje) y José David, gracias por su constante atención y palabras de aliento. Y a ti, *Jose "bonito"*, nuestras conversaciones son tan enriquecedoras y espectaculares que me emociona mucho cuando hacemos largas llamadas. Gracias por compartir tu tiempo y conocimientos conmigo. El aprendizaje es constante.

Un agradecimiento especial a mis primos Germán, Alex y Adrián, pues nuestras discusiones sobre temas económicos y mineros relacionados con esta tesis me han ayudado a crecer y aprender más en este campo.

Mis más sinceros agradecimientos a Anuar "el Nino", Manuel Hamilton, Harry, Carlos, Leo e Iván, sin ustedes no habría sido posible realizar los muestreos necesarios para llevar a cabo esta investigación.

Quiero extender mi gratitud a la Universidad de Barcelona y al Ministerio de Ciencia, Tecnología e Innovación de Colombia por brindarme esta oportunidad única y otorgarme la beca que me ha permitido vivir y estudiar en Barcelona. Vivir en esta ciudad había sido mi sueño desde hace 15 años o más, así que ha sido maravilloso también sentirme parte de esta cultura.

Al grupo de investigación EPA del IDAEA-CSIC, y en especial a Carmen, Sandra, Yolanda, Marta, Mónica, Jess, Alicia, Edu, Víctor y Mercè, quiero agradecerles de corazón por su valiosa ayuda a lo largo de estos años. También a los que ya no están, pero dejaron su inigualable huella: Gerlaine, Ana, Vítor, Dorde, Abbas, Rui y Josep María. Y a los nuevos que han ido

llegando. Son las personas más guays que he conocido en entornos laborales. Los admiro muchísimo porque siempre mantienen un excelente ambiente, en el que da mucho gusto trabajar.

Dicen que los amigos son la familia que uno elige, y a ellos les tengo un profundo cariño. Quiero agradecer a mis amigos de Barcelona, mi fuente de risas y serotonina para seguir adelante: Alba, Raúl, Kenny, Pablo, Akash, Miguel Ángel, Pamela, Yenifer, Simón (Bro) y Eunice (quien además ilustró con mucho entusiasmo la portada de esta tesis). A mis amigos de vóley: Romà, Gema, Diego, Pooya, Sina, Anne, Michelangelo y Suzane. Y en la distancia a Johana, Teonila y Daniel. Gracias por acompañarme estos años, sin duda somos una familia numerosa.

Agradezco a Dios por la vida, porque siento su presencia en todas las personas maravillosas que he conocido en este difícil camino y que me llenan de ánimo y alegría.

Por último, pero no menos importante, quiero dedicar esta tesis a la memoria de mis familiares y amigos que ya no están conmigo. A mis tías Sury, Necho y Maritza, a mi abuelita Emi, a mi padrino y a mi amigo Jeison Malo, los llevo siempre en mi corazón. Sé que estarían orgullosos y felices de verme culminar este doctorado. Agradezco el cariño y los buenos momentos que me brindaron. Los extraño mucho.

¡Gracias a todos por ser parte de este logro!

TABLA DE CONTENIDO

LISTA DE ACRÓNIMOS Y SÍMBOLOS

3MFS	Sílica funcionalizada con 3-mercaptopropilo
Acetil-CoA	Acetil coenzima A
ADN	Ácido desoxirribonucleico
AMPs	Pozas mineras abandonadas
As	Arsénico
BAF	Factores de bioacumulación
BC	Biocarbón base u original
BTP1	Polímero poli(4-((2-aminonaftaleno-6-carbonotioil) carbamoil) isotiocianato de benzoilo)
BTP2	Polímero poli(4-((4-aminobencil) fenilcarbonotioil) carbamoil) benzoil isotiocianato)
Cd	Cadmio
CHD	Población infantil
Co	Cobalto
Co-HgcA	Cobalamina-HgcA
CR	Riesgo carcinogénico
Cr	Cromo
Cu	Cobre
Cys	Cisteína
D	Coeficiente de difusión
DGT	Gradiente de difusión en capa fina
DMA80	Analizador directo de mercurio
DOM	Materia orgánica disuelta
EDI	Ingesta diaria estimada
EDXRF	Espectrometría de fluorescencia de rayos X de dispersión de energía
EtHg	Etilmercurio
FAO	Organización de las Naciones Unidas para la alimentación y la agricultura
FBC	Biocarbón de plumas

FDA	Administración de alimentos y medicamentos de los Estados Unidos
Fe	Hierro
FeRB o IRB	Bacterias ferro-reductoras
FT-IR	Espectroscopía infrarroja por transformada de Fourier
GMA	Global mercury assessment
Hg	Mercurio
Hg$^+$, Hg$_2^{2+}$	Ion mercurioso
Hg^0	Mercurio elemental o metálico
Hg^{2+}	Ion mercúrico
HgcA	Proteínas corrinoides putativas, codificadas por el gen *hgcA*
hgcAB	Gen esencial para la metilación del mercurio
HgcB	Ferredoxinas 2[4Fe–4S] asociadas a la proteína corrinoide putativa, codificadas por el gen *hgcB*
Hg$_p$	Mercurio particulado
HI	Índice de peligrosidad
INSST	Instituto nacional de seguridad y salud en el trabajo
JECFA	Comité Mixto FAO/OMS de expertos en aditivos alimentarios
MAPE / ASGM	Minería de oro artesanal y en pequeña escala
Me$_2$Hg / DMHg	Dimetilmercurio
MeHg	Metilmercurio
MerA	Enzimas organomercurio reductasa
MerB	Enzimas organomercurio liasa
Mn	Manganeso
Ni	Níquel
ODS	Objetivos de desarrollo sostenible
OMS / WHO	Organización mundial de la salud
OSHA	Agencia europea para la seguridad y la salud en el trabajo
PASAHg	Plan de acción sectorial ambiental de mercurio
Pb	Plomo
PBTU	Polímero de polibenzoiltiourea
PEL	Límite de exposición permisible

PIB	Producto interno bruto
PNUMA / UNEP	Programa de las Naciones Unidas para el medio ambiente
PTWI	Ingesta semanal tolerable provisional
PUNHg	Plan único nacional de mercurio
PVC	Cloruro de polivinilo
S	Azufre
SAM	S-adenosilmetionina
SBC	Biocarbón sulfurado
Se	Selenio
SeH	Grupo selenol
SH	Grupo tiol o mercapto
Sn	Estaño
SRB	Bacterias sulfato-reductoras
TEMED	N,N,N´,N´-tetrametiletilendiamina
THF	Tetrahidrofolato
THQ	Cociente de peligrosidad total
USEPA	Agencia de protección ambiental de los Estados Unidos
USGS	Servicio geológico de Estados Unidos
VCM	Monómero de cloruro de vinilo
WCBA	Mujeres en edad fértil
Zn	Zinc

LISTA DE FIGURAS

LISTA DE PUBLICACIONES

Abstract

Mercury (Hg) is widely recognized as one of the most toxic, complex and persistent pollutants in the environment. Despite extensive public awareness of the known environmental risks and numerous adverse effects on human health, it continues to be extensively used in various mining and industrial sectors. Artisanal and small-scale gold mining (ASGM), chloride monomer, chlor-alkali and acetaldehyde production are the most important Hg uses globally. Therefore, a significant increase in global anthropogenic Hg emissions has been observed in the last decades. Based on this situation and the special toxicodynamics of Hg, there is a persistent need to further investigate the dynamics and bioavailability of Hg in highly polluted ecosystems.

In this doctoral thesis, priority has been given to the *in situ* implementation of the diffusive gradients in thin-films technique (DGT) in order to quantify the bioavailable fraction of Hg in aqueous medium. Furthermore, an exhaustive exploration and evaluation of new polymeric materials and derivatives of residual biomass has been carried out, with the aim of incorporating them in the DGT technique as alternatives for the uptake of labile Hg. The efforts have been oriented to developing an efficient and reliable strategy for the assessment and monitoring of Hg in aquatic systems in remote and hard-to-reach areas.

In the first part of the thesis, the results of the evaluation of the level of contamination, the risk to human health and the carcinogenic risk from the consumption of Hg and As contaminated food in hard-to-reach areas highly impacted by ASGM in the Colombian rainforest are presented. The results of the hazard index (HI) of Hg and As through the consumption of fruits, tubers and fish exceeded the acceptable level (HI>1) and the carcinogenic risk related to As is shown. Concerning the quantification of the bioavailable

fraction of Hg, DGT devices were deployed along the Atrato river (Colombia) and in abandoned mining ponds (AMPs) close to local populations. These DGT devices were manufactured and calibrated in the laboratory using 3-mercaptopropyl functionalized silica (3MFS) as the binding layer for Hg. In addition, it was considered relevant to quantify the bioavailable fraction of other trace metals (Pb, Cu, Zn, Cd, Ni, Mn and Cr) that could potentially have a common source with Hg contamination. Therefore, commercial DGT devices with Chelex-100 as a specific binding layer for the analysed metals were used. The results presented were consistent with other studies of Hg in the Atrato river and AMPs, and were compared with other studies with similar methods, which allowed us to conclude that the application of the DGT technique is efficient for the quantification and monitoring of bioavailable Hg in aquatic systems of this type of highly vulnerable and hard-to-reach ecosystems.

The second part of the thesis focused on the exploration and evaluation of new materials for incorporation in the DGT technique through the valorization of agro-industrial biomass residues and the application of new polymeric materials for the determination of the labile fraction of Hg in aqueous medium. Biomass-derived materials (biochar, chicken feathers, cork, rice husk and canola) were evaluated with respect to its Hg removal potential, the facility of preparation of the binding layers (agarose and polyacrylamide hydrogels), and its efficiency in the determination of the labile fraction of Hg by time series experiments in aqueous medium, in the absence and presence of other trace elements (Mn, Cu, Zn, Ni, Pb, Cd and As), under controlled laboratory conditions. Similarly, three polymers synthesized from benzoylthiourea (BTP1, BTP2 and PBTU) with demonstrated affinity for Hg were evaluated for inclusion within the DGT technique. In this investigation of new materials, the BTP1 polymer demonstrated to be more effective in the uptake and quantification of labile Hg, and the efficacy of the DGT-BTP1 devices was compared to DGT devices prepared with 3MFS during *in situ* Hg deployments in the Quito river (Colombia). The results showed a good performance in the quantification of the labile Hg fraction and, furthermore,

it was also demonstrated that DGT-BTP1 devices are a useful tool for *in situ* monitoring of bioavailable Hg in freshwaters. In conclusion, the results obtained for the inclusion of new materials in the DGT technique could be considered satisfactory and promising. At the same time, this thesis provides a solid basis for future research and applications in Hg contamination studies, as well as, supporting the principles of green chemistry and residue valorization.

Resum

El mercuri (Hg) és un dels contaminants més tòxics, complexos i persistents en el medi ambient. Malgrat els riscos ambientals coneguts i els nombrosos efectes adversos per a la salut humana, encara s'utilitza àmpliament en diversos sectors miners i industrials. Així doncs, el Hg s'usa principalment en la mineria d'or artesanal i en petita escala (MAPE) i en la producció de clorur de vinil, clor-alcali i acetaldehid, amb un increment significatiu d'emissions mundials de Hg antropogènic en les últimes dècades. Degut a aquesta situació, i a l'especial toxicodinàmica del Hg, existeix la necessitat de profunditzar en la dinàmica i biodisponibilitat del Hg en ecosistemes altament contaminats.

En aquesta tesi doctoral s'ha investigat sobre la implementació in situ de la tècnica de gradient de difusió en capa prima (DGT) amb la finalitat de quantificar la fracció biodisponible de Hg en medi aquàtic. Així mateix, s'ha dut a terme una exhaustiva exploració i avaluació de nous materials polimèrics i derivats de biomassa residual, amb l'objectiu d'incorporar-los en aquesta tècnica com a alternatives per a la captació del Hg làbil. Aquests esforços han estat orientats al desenvolupament d'una estratègia eficient i fiable per a l'avaluació i el monitoratge del Hg en sistemes aquàtics d'àrees remotes.

En la primera part de la tesi, es presenten els resultats de l'avaluació del nivell de contaminació, el risc per a la salut humana i el risc carcinogènic derivat del consum d'aliments contaminats amb Hg i As en àrees de difícil accés altament impactades per MAPE a la selva tropical colombiana. En termes generals, els resultats dels índexs de perillositat (HI) per a Hg i As pel consum d'aliments locals, van superar el nivell acceptable (HI>1), existint també un risc carcinogènic relacionat amb l'As. Pel que fa a la quantificació de la fracció biodisponible de Hg, es van desplegar dispositius DGT al llarg

del riu Atrato (Colòmbia) i en basses abandonades (AMPs) per la MAPE, properes a poblacions locals. Aquests dispositius DGT es van fabricar i calibrar al laboratori utilitzant sílice funcionalitzada amb 3-mercaptopropil (3MFS) com a capa de resina per al Hg. A més, es va considerar rellevant quantificar la fracció biodisponible d'altres metalls traça (Pb, Cu, Zn, Cd, Ni, Mn i Cr) que podrien compartir un origen comú amb la contaminació per Hg. Amb aquesta finalitat es van utilitzar dispositius DGT de tipus comercial amb Chelex-100 com a capa d'unió específica per als metalls analitzats. Els resultats presentats van ser coherents amb altres estudis de Hg al riu Atrato i AMPs, i es van comparar amb altres estudis amb mètodes similars. Això ens va permetre concloure que l'aplicació de la tècnica DGT és eficient per a la quantificació i el monitoratge del Hg biodisponible en sistemes aquàtics en aquests tipus d'ecosistemes altament vulnerables i de difícil accés.

La segona part de la tesi es va centrar en l'exploració i avaluació de nous materials per a la seva incorporació en la tècnica DGT mitjançant la revalorització de residus agroindustrials i l'aplicació de nous materials polimèrics per a la determinació de la fracció làbil de Hg en medi aquàtic. Els materials derivats de biomassa (biocarbó, plomes de pollastre, suro, closca de arròs i colza) van ser avaluats en relació amb la seva capacitat de captació del Hg, la facilitat de preparació de les capes d'unió (hidrogels d'agarosa i poliacrilamida) i la seva eficàcia en la determinació de la fracció làbil de Hg. Es van dissenyar experiments de sèrie temporal en medi aquàtic, en absència i presència d'altres elements traça (Mn, Cu, Zn, Ni, Pb, Cd i As) i en condicions controlades de laboratori. De manera similar, es van avaluar tres polímers sintetitzats a partir de la benzotioamida (BTP1, BTP2 i PBTU) amb demostrada afinitat amb el Hg per al seu ús en la tècnica DGT. En aquesta recerca de nous materials, el polímer BTP1 va mostrar una major efectivitat en la captació i quantificació del Hg làbil, i l'eficàcia dels dispositius DGT-BTP1 va ser comparada amb la dels dispositius DGT preparats amb 3MFS en mesures in situ de Hg al riu Quito (Colòmbia). Els resultats van mostrar un bon rendiment en la quantificació de la fracció de Hg làbil i, alhora, es va

demostrar que els dispositius DGT-BTP1 són una eina útil per al monitoratge in situ de Hg biodisponible en aigües dolces.

En conclusió, els resultats obtinguts mitjançant la inclusió de nous materials en la tècnica DGT es poden considerar satisfactoris i prometedors. Així mateix, aquesta tesi proporciona una base sòlida per a futures investigacions i aplicacions en estudis de la contaminació per Hg, alhora que recolza els principis de la química verda i la valorització de residus.

Resumen

El mercurio (Hg) es uno de los contaminantes más tóxicos, complejos y persistentes en el medioambiente. A pesar de la amplia conciencia sobre los riesgos ambientales conocidos y de los numerosos efectos adversos para la salud humana, sigue siendo ampliamente utilizado en diversos sectores mineros e industriales. Principalmente se utiliza en la minería de oro artesanal y en pequeña escala (MAPE), así como en la producción de cloruro de vinilo, cloro-álcali y acetaldehído, observándose un aumento significativo en las emisiones mundiales de Hg antropogénico en las últimas décadas. A causa de esta situación y de la especial toxicodinámica del Hg, existe la necesidad de profundizar en la dinámica y biodisponibilidad del Hg ecosistemas altamente contaminados.

En esta tesis doctoral se ha priorizado la implementación in situ de la técnica de gradiente de difusión en capa fina (DGT) con el propósito de cuantificar la fracción biodisponible de Hg en medio acuático. Asimismo, se ha llevado a cabo una exhaustiva exploración y evaluación de nuevos materiales poliméricos y derivados de biomasa residual, con el objetivo de incorporarlos a esta técnica como alternativas para la captación del Hg lábil. Estos esfuerzos han sido orientados hacia el desarrollo de una estrategia eficiente y confiable para la evaluación y el monitoreo del Hg en sistemas acuáticos de áreas remotas y de difícil acceso.

En la primera parte de la tesis, se presentan los resultados de la evaluación del nivel de contaminación, el riesgo para la salud humana y el riesgo carcinogénico por consumo de alimentos contaminados con Hg y As en áreas de difícil acceso altamente impactadas por MAPE en la selva tropical colombiana. En términos generales, los resultados de los índices de peligrosidad (HI) para Hg y As a través del consumo de frutas, tubérculos y pescado superaron el nivel aceptable (HI>1) y también se muestra el riesgo

carcinogénico relacionado con As. En cuanto a la cuantificación de la fracción biodisponible de Hg, se desplegaron dispositivos DGT a lo largo del río Atrato (Colombia) y en pozas mineras abandonadas (AMPs) por la MAPE cercanas a poblaciones locales. Estos dispositivos DGT fueron manufacturados y calibrados en el laboratorio usando sílica funcionalizada con 3-mercaptopropilo (3MFS) como gl para el Hg. Además, se consideró relevante cuantificar la fracción biodisponible de otros metales traza (Pb, Cu, Zn, Cd, Ni, Mn y Cr) que podrían compartir un origen común con la contaminación por Hg. Para tal fin, se utilizaron dispositivos DGT de tipo comercial con Chelex-100 como capa de unión específica para los metales. Los resultados presentados fueron coherentes con otros estudios de Hg en el río Atrato y AMPs, y fueron comparados con otros estudios con métodos similares, lo que nos permitió concluir que la aplicación de la técnica DGT es eficiente para la cuantificación y monitoreo del Hg biodisponible en sistemas acuáticos altamente vulnerables y de difícil acceso.

La segunda parte de la tesis se enfocó en la exploración y evaluación de nuevos materiales para su incorporación en la técnica DGT mediante la revaloración de residuos agroindustriales y la aplicación de nuevos materiales poliméricos para la determinación de la fracción lábil de Hg en el medio acuático. Los materiales derivados de biomasa (biocarbón, plumas de pollo, corcho, cáscara de arroz y canola) fueron evaluados en cuanto a su capacidad de captación del Hg, la facilidad de preparación de las capas de unión (hidrogeles de agarosa y poliacrilamida), y su eficacia en la determinación de la fracción lábil de Hg. Para este fin se diseñaron experimentos de serie temporal en medio acuoso, en ausencia y presencia de otros elementos traza (Mn, Cu, Zn, Ni, Pb, Cd y As) y en condiciones controladas de laboratorio. De manera similar, se evaluaron tres polímeros sintetizados a partir de la benzoiltiourea (BTP1, BTP2 y PBTU) con demostrada afinidad con el Hg para su uso en la técnica DGT. En esta búsqueda de nuevos materiales, el polímero BTP1 demostró una mayor efectividad en la captación y cuantificación del Hg lábil, y la eficacia de los dispositivos DGT-BTP1 fue comparada con la de

dispositivos DGT preparados con 3MFS en mediciones *in situ* de Hg en el río Quito (Colombia). Los resultados mostraron un buen rendimiento en la cuantificación de la fracción de Hg lábil y, a su vez, se demostró que los dispositivos DGT-BTP1 son una herramienta útil para la monitorización *in situ* de Hg biodisponible en aguas dulces. En conclusión, los resultados obtenidos a través de la inclusión de nuevos materiales en la técnica DGT podrían considerarse satisfactorios y prometedores. Asimismo, esta tesis proporciona una base sólida para futuras investigaciones y aplicaciones en estudios de la contaminación por Hg, al tiempo que se respaldan los principios de la química verde y la valorización de residuos.

CAPÍTULO 1: Introducción

1.1. Generalidades sobre el mercurio y los elementos traza

Los procesos agroindustriales y la minería nos han permitido tener avances técnicos y tecnológicos significativos que facilitan nuestra cotidianidad, no obstante, en cada una de estas actividades se liberan al medioambiente diversos tipos de contaminantes, dentro de los que se destacan los elementos traza, principalmente metales, porque pueden llegar a tener una alta toxicidad a muy bajas concentraciones en el medioambiente (≤ 100 mg kg^{-1}).

Aunque algunos de los elementos traza tienen un rol esencial en el correcto desarrollo de los seres vivos, otros 'no esenciales' son una de las formas más peligrosas de contaminación para los ecosistemas en todo el mundo, ya que son poco o nada biodegradables, tienen una alta movilidad y tendencia a acumularse en los tejidos vivos por largos períodos de tiempo. Esta persistencia puede desencadenar procesos de *biomagnificación* dentro de las cadenas tróficas, causando alteraciones metabólicas y mutaciones, y afectando sustancialmente la biodiversidad y la salud humana.

Es por ello que el interés de la comunidad científica por estudiar los elementos traza se ha incrementado notablemente con los años. En esta introducción se hará mención únicamente a los elementos traza que podrían representar un riesgo para las comunidades, a raíz de los resultados obtenidos durante el desarrollo de este estudio: mercurio (Hg), arsénico (As) y níquel (Ni), haciendo especial énfasis en el Hg, considerado uno de los contaminantes más peligrosos.

1.1.1. Mercurio

El símbolo químico del mercurio, Hg, se origina en la palabra griega *hydrargyros*, que significa "agua plateada". Sin embargo, su nombre proviene de un símil con el dios romano Mercurio, debido a la fluidez que representaban al dios y al metal. El Hg es el único elemento químico metálico líquido a temperatura ambiente (25ºC), con una temperatura de fusión de –38,87ºC y una temperatura de ebullición de 356,58ºC. Debido a su alta densidad de 13,456 g mL^{-1} a 25°C, se considera un "metal pesado", y su brillo es similar al de la plata, de ahí que los romanos también le llamasen *Argentum Vivum*, que significa "plata líquida".

El mercurio elemental (Hg^0) tiene masa atómica promedio de 200,59 g mol^{-1} y su número atómico es 80. Su configuración electrónica (1s^2 2s^2 2p^6 3s^2 3p^6 3d^{10} 4s^2 4p^6 4d^{10} 5s^2 5p^6 4f^{14} 5d^{10} 6s^2) es la responsable de sus propiedades químicas únicas, ya que los electrones llenan todos los niveles de energía disponibles hasta 6s permitiendo un comportamiento químicamente similar los gases nobles. Dada su estabilidad energética, los electrones de valencia no son compartidos fácilmente, y es habitual la formación de enlaces débiles Hg–Hg en su propia estructura, o al unirse con otros metales. Esta característica también convierte al Hg en el metal más volátil existente con una presión de vapor de 0,261 Pa (2,58×10^{-6} atm) a 25 °C, y en efecto, el Hg es el único metal que no existe como dímero en su fase gaseosa (Fahlman, 2007; Gaffney y Marley, 2014).

1.1.1.1. Usos frecuentes del mercurio

El mercurio ha sido utilizado desde la antigüedad. Desde el Paleolítico Superior, periodo comprendido entre 33000 y 9000 a.C., el bermellón o polvo de cinabrio (HgS) fue empleado como pigmento rojo en pinturas rupestres, como se ha evidenciado en las obras encontradas en Lascaux o Altamira. Similarmente, estudios antropológicos de civilizaciones antiguas como la china, india, egipcia, maya, griega y romana han demostrado el uso de compuestos mercuriales en la elaboración de cremas, ungüentos, cosméticos, medicinas, pigmentos y ornamentos.

Se estima que alrededor del año 500 a.C., el Hg se empezó a usar para amalgamar otros metales, principalmente oro y plata. Casi dos siglos después, el filósofo y botánico griego Teofrasto documentó un método para obtener Hg líquido a partir de la molienda de cinabrio en un mortero de cobre. No obstante, no fue hasta principios del siglo XIX, que las propiedades químicas del Hg fueron reconocidas y estudiadas por Antoine Lavoisier y Joseph Priestley, al emplear el metal en sus experimentos con gases. Su papel en el descubrimiento del oxígeno fue tan relevante que incluso se concertó una unidad de medida de la presión de los gases en referencia a él (mm de Hg).

En la actualidad, el uso del Hg está prácticamente prohibido a causa de su toxicidad. Por ejemplo, una de las formas más comunes de exposición se da por la ruptura accidental de termómetros o lámparas que contienen Hg, cuyos vapores altamente tóxicos podrían saturar rápidamente la atmósfera en un ambiente cerrado y superar fácilmente el límite máximo seguro de exposición

ocupacional, el cual es 0,02 mg m^{-3} según la normativa española (INSST, 2021). Sin embargo, el Hg y algunos de sus compuestos siguen siendo considerados importantes para el desarrollo industrial, y los principales usos o aplicaciones que se le dan varían mucho dependiendo del país. De los principales usos reconocidos de este metal podríamos destacar los siguientes:

- Minería de oro y plata
- Amalgamas dentales
- Producción de cloro y álcalis
- Termómetros y manómetros
- Síntesis de pigmentos y colorantes
- Pilas y baterías (como óxido de mercurio)
- Fabricaciones de electrodos (calomelanos)
- Lámparas fluorescentes y tubos de rayos X
- Cosméticos ilegales y productos para la piel
- Interruptores eléctricos y dispositivos de relé
- Productos farmacéuticos y vacunas (como antiséptico)
- Biocidas, fungicidas y otros productos agroindustriales

Estimación mundial del uso del mercurio

Los datos globales detallados sobre el consumo de mercurio en un periodo de 10 años (2005 a 2015) fueron publicados por el Programa de las Naciones Unidas para el Medio Ambiente (PNUMA o UNEP) categorizados por sector

de aplicación (figura 1) y región geográfica (figura 2) (UNEP, 2017a). En la figura 1 se muestra la tendencia del uso del Hg en diversos sectores, siendo más notable el aumento de su uso en los sectores de la minería aurífera y la producción de monómero de cloruro de vinilo (VCM), que sumaron entre los dos más de 2000 t anuales.
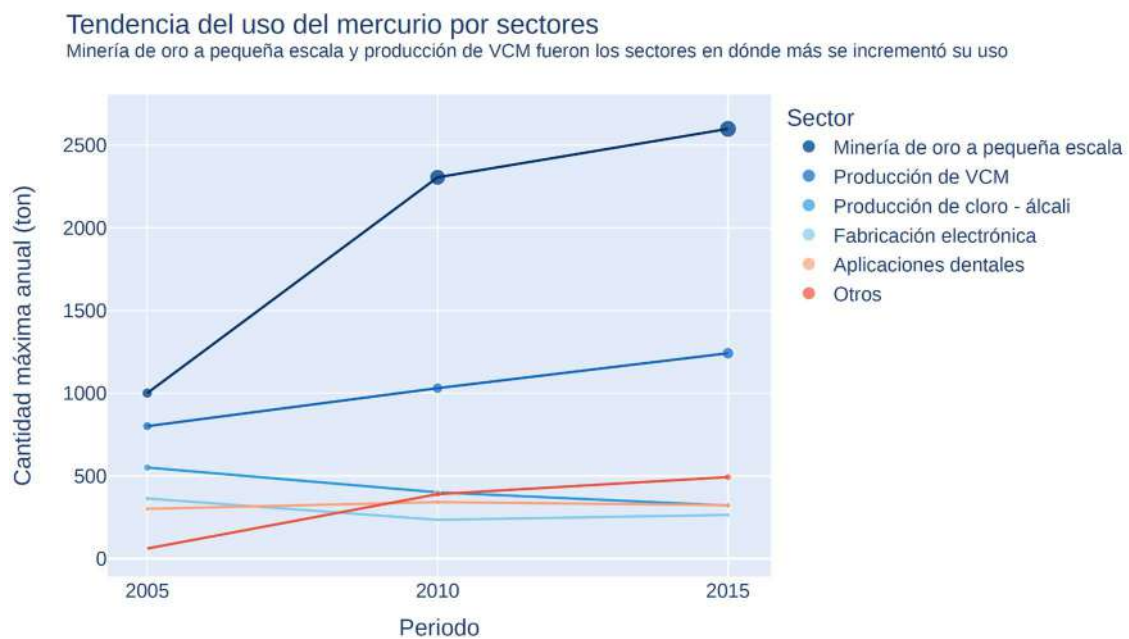
Figura 1. Uso mundial del mercurio por sector. Elaboración propia basada en datos obtenidos de UNEP (2017).

En relación al sector de la minería de oro, la minería de oro artesanal y en pequeña escala (MAPE o ASGM, por sus siglas en inglés) desempeña un papel crítico en la demanda global de este metal, especialmente desde que el precio del oro se ha ido incrementando con el tiempo (UNEP, 2017a). La sección 1.1.1.4 de esta tesis abordará la relación entre la MAPE y la contaminación por Hg. En el caso de la producción de VCM, el aumento se relaciona con la necesidad de materiales plásticos a base de cloruro de polivinilo (PVC), que

se emplean en la construcción, revestimientos de cables eléctricos, carcasas de teléfonos y computadoras, marcos de puertas y ventanas, juguetes, entre otros. En contraste, una disminución constante en el uso del Hg se observó en la fabricación de productos electrónicos, lámparas y baterías, sin embargo, el impacto de estas cantidades no es significativo en comparación con el aumento registrado.

En la figura 2 se muestra la tendencia del uso del Hg en diversas áreas geográficas. De acuerdo con el informe de las Naciones Unidas sobre la Oferta, Comercio y Demanda Mundial de Mercurio (UNEP, 2017a), la agrupación de países se realizó considerando los perfiles de uso del Hg, la ubicación geográfica, y las estadísticas de su importación y exportación para cada región, basándose en los datos proporcionados por Comtrade.
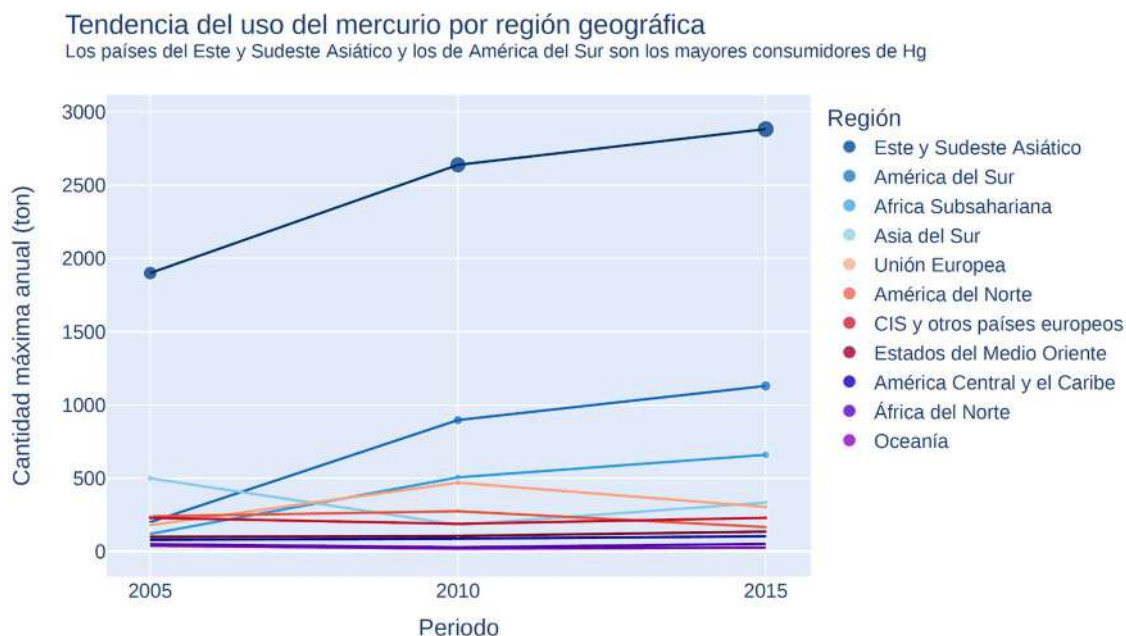
Figura 2. Uso mundial del mercurio por región geográfica. Elaboración propia basada en datos obtenidos de UNEP (2017).

Se observaron aumentos significativos en las regiones de Asia, América del Sur y África, donde la MAPE tiene un papel relevante en la economía. Sin embargo, el incremento del uso del Hg no fue tan pronunciado entre 2010 y 2015, lo que sugiere una posible transición hacia otros métodos de extracción aurífera, como las piscinas de cianuración y otros métodos gravimétricos, entre los que se incluye el lavado de oro en una bandeja o '*barequeo*'.

1.1.1.2. Toxicidad del mercurio

Desde la antigüedad hay evidencias de que los antiguos griegos y romanos estaban expuestos a niveles tóxicos de Hg a consecuencia de su uso en la minería y la producción de pigmentos. Hipócrates y Plinio, en el 370 a.C. y 77 a.C. respectivamente, describieron las enfermedades y dolencias que experimentaban los esclavos que trabajaban en minas de Hg. De igual manera, los Mayas se vieron obligados a abandonar una de sus más importantes ciudades a causa de la contaminación de sus depósitos de agua con altas concentraciones del metal (Lentz et al. 2020).

Los primeros informes de los efectos tóxicos del vapor de mercurio (Hg^0) como riesgo laboral aparecieron mucho más tarde, en el trabajo de Ulrich Ellenberg titulado *"Von der Grifftigen Bensen Terupffen von Reiichen der metal"* (1473), y en el escrito de Paracelso titulado *"Von der Bergsucht und auderen Baykrankheiten"* (1533). No obstante, uno de los casos más populares de envenenamiento se dió durante el siglo XIX, en los trabajadores expuestos a

los vapores generados por el tratamiento de fieltros con sales nítricas de mercurio, los cuales comenzaron a presentar una serie de síntomas, tales como inestabilidad emocional, depresión, irritabilidad, delirios, y alteraciones de la memoria, a los que se le denominó *eretismo mercurial* o "locura de los sombrereros", y fue representado por Lewis Carrol en su personaje del sombrerero loco del libro "*Alicia en el país de las maravillas*" (Blesa y Castro, 2015).

En la era moderna, los efectos del Hg en la salud se han estudiado de manera más detallada y rigurosa. A partir de la década de 1950, los investigadores comenzaron a estudiar los efectos del Hg en Japón, donde se observaron diversos síntomas de envenenamiento en las poblaciones cercanas a la bahía de Minamata. Más de 400 niños nacidos de madres asintomáticas presentaron graves afectaciones neurológicas, incluyendo dificultades en la coordinación de los movimientos (ataxia), alteración sensorial en manos y pies, deterioro en la capacidad auditiva y del habla, reducción del campo visual, debilidad muscular, y en casos extremos, parálisis, convulsiones y muerte. El *síndrome de Minamata*, se describió entonces como una grave enfermedad causada por la exposición crónica al metilmercurio (MeHg) en pescado de la bahía que había sido contaminado por las descargas residuales de una fábrica de cloruro de vinilo y acetaldehído local durante el período 1953–1960 (Harada, 1995).

Otro episodio de intoxicación aguda ocurrió en Iraq, dónde más de 400 personas murieron por intoxicación con MeHg debido al consumo de panes

cuyo trigo había sido tratado con un fungicida basado en este compuesto organometálico. En adultos, el síntoma más común fue la parestesia, que aparecía después de un período de latencia de entre 16 y 38 días y variaba según la dosis. Otros síntomas fueron ataxia, visión borrosa y dificultades auditivas. Sin embargo, los bebés nacidos de mujeres que ingirieron pan contaminado durante el embarazo presentaron los efectos más graves, como retraso en el habla y en el desarrollo motor, anormalidades en los reflejos y convulsiones (Greenwood, 1985). Desde entonces, la exposición al Hg y sus compuestos se convirtió en una preocupación de salud pública.

Si bien, se ha descubierto que todas las personas están expuestas a cierto nivel de Hg a lo largo de su vida, ya sea a través de alimentos, agua, aire o productos comerciales, sería un error suponer que la totalidad del metal es asimilado por los organismos vivos. A la cantidad estimada de Hg, o de cualquier otro contaminante, que es absorbida y asimilada por los organismos vivos se le denomina *fracción biodisponible*, y es un buen indicador del riesgo potencial para salud (Meyer, 2002; McGeer et al., 2004).

La fracción biodisponible del Hg también es la cantidad estimada que ingresa a las cadenas tróficas, y tiene el potencial de bioacumularse y biomagnificarse, implicando el aumento de las concentraciones de contaminante a medida que se avanza dentro de la cadena (figura 3). Por otro lado, el concepto de *"biodisponibilidad del metal"* es aún difícil de definir y varios autores han intentado dar una aproximación desde distintos enfoques (Meyer, 2002; Gochfeld, 2003; Peijnenburg y Jagger, 2003; McGeer et al.,

2004). Aún así, existe un consenso en que para su evaluación en el medioambiente se deben considerar (i) las propiedades fisicoquímicas del medio, (ii) la biota y microorganismos presentes, y (iii) las especies químicas del metal (Landner y Reuther, 2004).
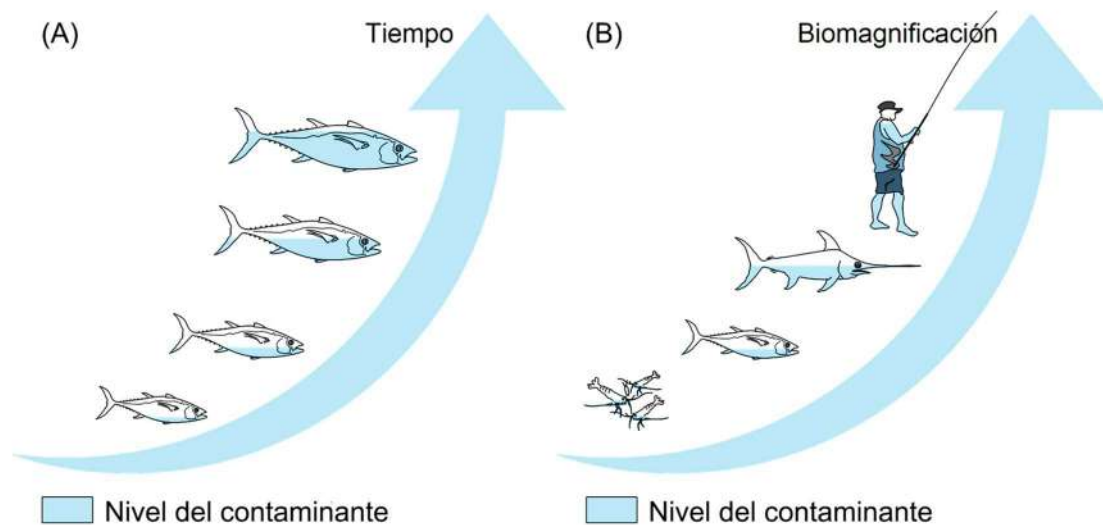
Figura 3. Representación de (A) la bioacumulación y (B) la biomagnificación del mercurio en medio acuático.

En el caso del Hg, aunque todas sus especies químicas son tóxicas, difieren en su grado de toxicidad y en su biodisponibilidad. El grado de exposición al Hg dependerá además de la duración y vías de exposición, y del estado de desarrollo de la persona expuesta, siendo los infantes y las mujeres gestantes las poblaciones más vulnerables.

Las especies químicas del Hg se clasifican en mercurio elemental o metálico, el mercurio inorgánico y el mercurio orgánico, y son detalladas en la tabla 1.

Tabla 1. Principales especies químicas del mercurio en el medioambiente.

Clasificación	Nombre de la especie	Representación química
Mercurio inorgánico	Mercurio elemental o metálico	Hg^0
	Ion mercurioso	Hg^+, Hg_2^{2+}
	Ion mercúrico	Hg^{2+}
Mercurio orgánico	Metilmercurio	CH_3Hg^+, MeHg
	Dimetilmercurio	C_2H_6Hg, Me_2Hg, DMHg
	Etilmercurio	$C_2H_5Hg^+$, EtHg

Mercurio elemental

La inhalación del vapor de mercurio elemental (Hg^0) es la forma más común de exposición, sin embargo, es importante destacar que las concentraciones atmosféricas no suelen ser lo suficientemente altas como para causar toxicidad aguda, excepto en casos de derrames o contaminación extrema. De igual manera, tenemos que considerar que el aumento de los niveles en el aire a largo plazo, sí pueden dar lugar a una exposición crónica a los vapores de Hg^0 y afectar la salud.

Cuando el Hg^0 es inhalado, alrededor del 80% es asimilado por el cuerpo, a diferencia de la exposición por vía dérmica que resulta en una absorción de menos del 1%, o por ingestión que es menor al 0,1%, no obstante, la vida media del Hg^0 en el cuerpo es de unos 60 días en la mayoría de los casos (Broussard et al., 2002; Bernhoft, 2012). Es importante destacar que el vapor de Hg^0 es soluble en lípidos, con un coeficiente de partición heptano/agua de 20, lo que

permite su rápida absorción en nuestro organismo (Clarkson et al., 1984). Una vez que pasa al torrente sanguíneo a través de los alvéolos pulmonares, el Hg^0 se oxida rápidamente a Hg^{2+} en los glóbulos rojos por la vía de la catalasa de peróxido de hidrógeno (Broussard et al., 2002), y el Hg^0 remanente se oxida lentamente a Hg^{2+} una vez que logra entrar en las células cerebrales, permaneciendo por años dentro de estas (Oliveira et al. 2018). Este proceso es coherente con las observaciones que indican que la distribución del Hg^0 en los tejidos es similar al de las especies inorgánicas (sales de Hg^{2+}).

En las actividades de la MAPE, la exposición al vapor de Hg^0 se da principalmente durante los procesos de amalgamación y su quema, que muchas veces se hacen sin la mínima protección (uso de mascarillas, guantes o '*retortas*'), inclusive en presencia de infantes o dentro del hogar. El vapor de Hg^0 también se deposita en las superficies de los alimentos, suelos y fuentes de agua locales, pudiendo provocar efectos sobre el sistema nervioso central, con síntomas como temblores, irritabilidad, insomnio, debilidad muscular y problemas de memoria y cognición. Asimismo, en personas expuestas crónicamente a vapores de Hg^0 se han observado erupciones eritematosas con pigmentación parda en las extremidades, y sensaciones de hormigueo en las plantas de los pies y las palmas de las manos (*acrodinia*). Existen casos de contaminación accidental o incluso intencional con Hg, como el de una niña de 3 meses que estuvo expuesta al Hg^0 por varias horas, presentando neumotórax e insuficiencia respiratoria (Gao et al., 2019), y varios estudios han demostrado que los mineros y poblaciones expuestas a la MAPE han

presentado concentraciones elevadas de Hg en cabello, orina y sangre, y síntomas asociados al envenenamiento progresivo con Hg (Risher et al., 2003; Noble et al., 2016; Do et al., 2017).

Mercurio inorgánico

El mercurio inorgánico comúnmente se refiere a los compuestos que contienen Hg^+ y Hg^{2+}, es decir, sales (nitratos, cloruros, sulfuros, etc.) y óxidos de mercurio. Debemos señalar que el Hg^+ se encuentra con menos frecuencia en la naturaleza, presentándose como catión Hg_2^{2+} en soluciones ácidas, y convirtiéndose en Hg^{2+} mediante una rápida oxidación al ingresar al tracto digestivo (Clarkson et al., 1984).

Los compuestos de mercurio inorgánico poseen una muy baja solubilidad en lípidos, por lo que no atraviesan fácilmente las membranas biológicas y se estima que la fracción biodisponible es solo del 15%. Sin embargo, es importante resaltar que una vez absorbido por el cuerpo humano, el Hg^{2+} podrá unirse fuertemente a la cisteína (complejos Hg–Cys), aumentando su solubilidad lipídica y su capacidad de ser transportado, atravesando fácilmente barreras protectoras como la hematoencefálica y placentaria, y acumulándose principalmente en los riñones, ocasionando daños renales irreversibles con el tiempo (Oliveira et al. 2018).

De igual manera, se ha observado que el Hg^{2+} tiene gran afinidad con el azufre (S) y el selenio (Se), en especial cuándo estos se presentan como grupos tiol o

mercapto (–SH) y selenol (–SeH). Es por ello que, el Se se ha identificado como uno de los potenciales protectores contra la toxicidad de Hg en poblaciones expuestas. Conjuntamente, la metilación del Hg^{2+} por la microbiota del tracto intestinal puede convertirlo en MeHg (Martín-Doimeadios et al. 2017). Broussard et al., (2002) han reportado que la vida media en el organismo de los compuestos inorgánicos de Hg es de aproximadamente 40 días.

Mercurio orgánico

El mercurio orgánico se considera la forma más peligrosa y frecuente de exposición. Las especies químicas principales son MeHg, Me_2Hg y EtHg, de las cuales el MeHg es el que se presenta con mayor frecuencia en el medioambiente. Aunque se han identificado otras especies orgánicas, como el fenilmercurio ($C_6H_5Hg^+$) o la merbromina ($C_{20}H_8Br_2HgNa_2O_6$), se ha demostrado que se convierten rápidamente en mercurio inorgánico, por lo que no se profundizará sobre ellas en esta tesis.

El MeHg se produce en el medioambiente principalmente por la acción de bacterias presentes en sedimentos, suelos y aguas superficiales, que utilizan el mercurio inorgánico como fuente de energía en un proceso de respiración anaerobia denominado *metilación*, del cual se hablará con más detalle en la sección 1.1.1.5. de esta tesis.

Aunque la absorción del MeHg puede darse por inhalación, la principal fuente de exposición humana es la ingestión de pescado, mariscos y mamíferos

marinos contaminados. En consecuencia, las autoridades sanitarias han establecido recomendaciones o límites legales para la cantidad máxima permitida de Hg y/o MeHg en el pescado comercial buscando proteger la salud pública. Según el criterio de la Comisión del Codex Alimentarius, la recomendación sobre las concentraciones de MeHg no debería ser mayor de 0,5 mg kg^{-1} en peces no depredadores y de 1 mg kg^{-1} en peces depredadores. La Comunidad Europea también recomienda un límite máximo de 0,5 mg kg^{-1} para el Hg total en productos de la pesca (con algunas excepciones), mientras que para la Administración de Alimentos y Medicamentos de los Estados Unidos (FDA) el límite máximo permitido es de 1 mg kg^{-1} de MeHg en peces y mariscos. Sin embargo, la Agencia de Protección Ambiental de los Estados Unidos (USEPA) recomienda que la concentración de MeHg en el tejido muscular de pescado no sea superior a 0,3 mg kg^{-1} (peso húmedo), y este mismo límite fue adoptado por Japón, que es uno de los principales países consumidores de productos marinos (USEPA, 2001; UNEP/WHO, 2008).

En estudios de campo se han reportado concentraciones de hasta 4 mg kg^{-1} de MeHg en diversas especies de peces, lo que supera significativamente los límites recomendados por las autoridades sanitarias (Díez, 2009; Marrugo-Negrete et al., 2020a; Cruz-Esquivel et al., 2023). Además, se ha observado que la concentración de MeHg en peces varía de acuerdo a factores medioambientales como el pH, el potencial redox del agua, y el tipo de cuerpo de agua, así como factores biológicos, como la especie, edad, tamaño y dieta de los peces (Díez, 2009). Los factores de bioacumulación (BAF) para el MeHg

fueron emitidos por la USEPA para estimar la medida en la que se bioacumula o biomagnifica dentro de la cadena trófica, y representan la relación entre la concentración del MeHg en el tejido y su concentración en el medio (por ejemplo, agua o suelo) en situaciones en las que el organismo está expuesto tanto directamente como a través la dieta (USEPA 1997). En sistemas acuáticos, el MeHg producido bioquímicamente por microorganismos es absorbido por plantas y se estiman que los BAF son 1×10^5 en microorganismos en el nivel trófico 2, como el zooplancton; 7×10^5 para los carnívoros primarios en el nivel trófico 3; y 3×10^6 para los carnívoros secundarios en el nivel trófico 4, incluidos los peces y las aves. Por lo tanto, los peces y mamíferos depredadores, como el tiburón, el pez espada, la barracuda, el atún, el bagre, las focas, las ballenas, entre otros, tendrán las mayores concentraciones de MeHg (USEPA 2001; Díez, 2008; Scudder Eikenberry et al. 2015).

Más del 90% de MeHg ingerido se absorbe en el tracto gastrointestinal, pasando directamente al torrente sanguíneo en dónde se une a residuos de cisteína (complejos MeHg–Cys), que se transportan fácilmente a través de las membranas celulares, debido a su alta solubilidad en lípidos y a su semejanza estructural con el aminoácido esencial metionina (figura 4), lo que conlleva a una metabolización similar a éste (Bjørklund et al. 2017). Se ha observado que el MeHg tiene una vida media de 70-80 días en el cuerpo humano, reaccionando con grupos –SH que interfieren con la estructura celular, la función enzimática y la síntesis de proteínas, y desmetilándose lentamente a

Hg^{2+}, presumiblemente por la microbiota intestinal (Bernhoft, 2012; Clarkson, 2002; Díez, 2008; Martín-Doimeadios et al. 2017). Asimismo, la interacción del MeHg con los grupos –SH puede influir significativamente en cambios epigenéticos, como la metilación del ADN, así como en las modificaciones estructurales de las proteínas ribosómicas y el ARN (Cediel-Ulloa et al. 2022; Pan et al. 2022).
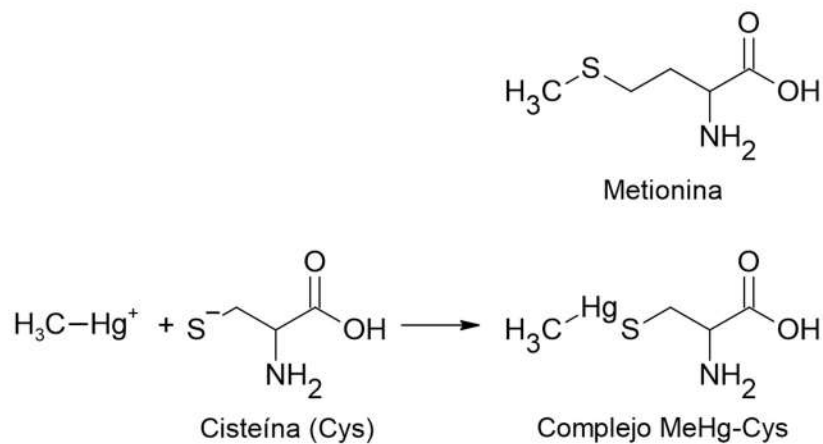
Figura 4. Comparación estructural entre el complejo formado entre el MeHg y la cisteína en el organismo, y el aminoácido esencial metionina. Elaboración propia basada en Clarkson (1987).

Aunque los efectos del MeHg en la salud varían ampliamente a nivel individual y están influenciados por factores genéticos, se ha comprobado que los alimentos ricos en Se pueden ayudar a mitigar los efectos nocivos del Hg en el organismo. Debido a la alta afinidad ente el Se y el Hg, los compuesto de Se pueden favorecer la formación de complejos estables y secuestro del Hg biodisponible, el aumento de las selenoproteínas y su actividad antioxidante, y la desmetilación del MeHg que facilita su excreción (Bjørklund et al. 2017). Asimismo, los alimentos que contienen Zn, Cu, Mg, y vitaminas C, E y B han

mostrado un efecto protector contra la toxicidad del MeHg. Los elementos esenciales Zn, Cu y Mg son cofactores de varias enzimas antioxidantes y detoxificantes que protegen al cuerpo de los radicales libres y ayudan a reducir el estrés oxidativo que puede empeorar los efectos tóxicos del MeHg. Las vitaminas C y E también son conocidos antioxidantes que protegen a las células del daño oxidativo inducido por el MeHg, y se ha demostrado que la vitamina C puede reducir las concentraciones de Hg en la sangre y los tejidos, especialmente en hígado y riñones a través de la excreción urinaria (Lee et al., 2016), mientras que las vitaminas del grupo B, como la B12 y B9 (ácido fólico), son importantes para la síntesis de glutatión, que es un antioxidante endógeno y un agente de desintoxicación que se sabe que se reduce en presencia de MeHg. Moniruzzaman et al. (2021) demostraron que una suplementación dietaria con Se, vitamina E y vitamina C no evita la bioacumulación de Hg en los tejidos y órganos de ratones, sin embargo, si reducen significativamente la peroxidación de lípidos séricos y prolongan la tasa de supervivencia acumulada en términos de exposiciones altas a MeHg. Por lo tanto, a pesar de la necesidad de mayor investigación en humanos, se sugiere que además de reducir las cantidades de alimentos contaminados con MeHg, una alimentación balanceada con una adecuada cantidad de los micronutrientes mencionados, ayudan a proteger contra los efectos tóxicos del MeHg.

El EtHg es usado como preservante en diversas aplicaciones médicas, incluyendo vacunas multidosis (Tiomersal), medicamentos tópicos nasales y

oftálmicos, y en algunas tintas para tatuajes. A diferencia del MeHg, el EtHg tiene una vida media en sangre mucho más corta (3 a 7 días) y se excreta del cuerpo sin acumularse en el sistema nervioso central. Aunque ha habido una controversia mundial por el posible vínculo entre las vacunas que contienen tiomersal y aumentos en los casos de trastornos del neurodesarrollo en infantes (autismo), la evidencia científica actual no respalda esta asociación (Gabis et al. 2022).

El Me_2Hg, también representado como DMHg, se encuentra en pequeñas cantidades en el medioambiente, principalmente como resultado de la transformación del MeHg en sistemas acuáticos. A pesar de su presencia limitada en la naturaleza, su uso como estándar es común en procedimientos analíticos. Sin embargo, actualmente se le conoce como una de las neurotoxinas más potentes conocidas.

Un triste ejemplo de su peligrosidad se registró en 1997, cuando la investigadora Karen Wetterhahn falleció después de haberse expuesto accidentalmente a unas cuantas gotas de Me_2Hg, mientras usaba guantes de látex desechables para manipular el reactivo y pese a haber seguido todas las medidas de seguridad sugeridas en la época. Las pruebas posteriores revelaron que el Me_2Hg penetra rápidamente el látex, PVC y neopreno, lo que indica que los guantes fabricados con estos materiales no ofrecen la protección adecuada, siendo ahora los guantes laminados de plástico la opción adecuada para la manipulación del Me_2Hg (OSHA, 2023). En la figura 5 se pueden apreciar las principales interconversiones entre las especies químicas del Hg

y efectos tóxicos en el cuerpo humano, teniendo en cuenta que el MeHg y el

EtHg tienen comportamientos toxicodinámicos similares.
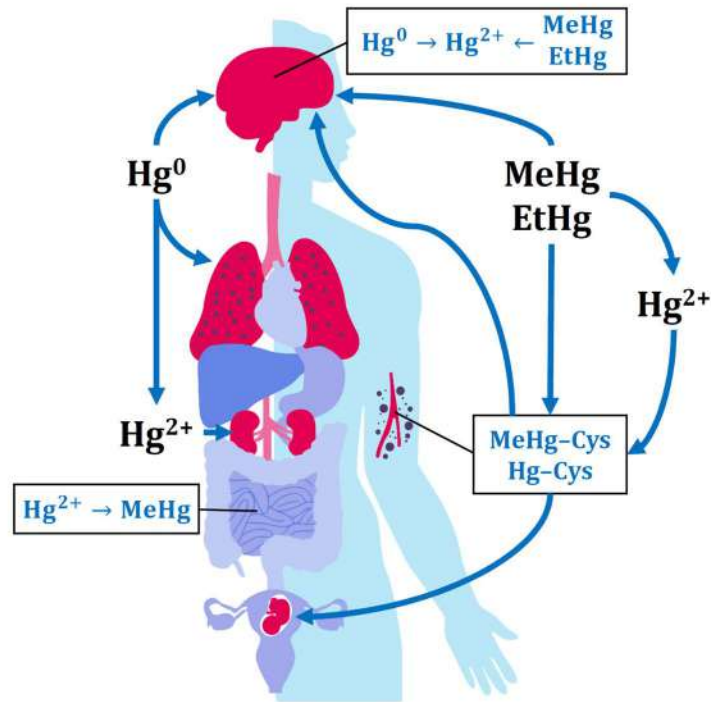
Figura 5. Toxicodinámica de las especies químicas del mercurio y efectos en el cuerpo humano. Adaptado del diseño "air pollution effects on human body infographic" de freepik.com. Fotografía: autoría propia.

1.1.1.3. Valores de referencia y aspectos legales

La expansión demográfica es bastante notoria, por lo que garantizar la seguridad alimentaria se ha convertido en una gran preocupación mundial en especial en las poblaciones cuya dieta depende mucho de la pesca. En respuesta a esta situación, la Organización Mundial de la Salud (OMS o WHO) y la Organización de las Naciones Unidas para la Alimentación y la Agricultura (FAO) han creado directrices conjuntas que instan a las

autoridades nacionales a evaluar los beneficios y riesgos del consumo de pescado, con base en la información disponible sobre sus propiedades nutricionales.

El Comité Mixto FAO/OMS de Expertos en Aditivos Alimentarios (JECFA) estableció valores para la ingesta semanal tolerable provisional (PTWI) de 4 $\mu g\ kg^{-1}$ bw (bw: peso corporal) para el Hg total, y de 1,6 $\mu g\ kg^{-1}$ bw para el MeHg (JECFA, 2011). Similarmente, la OMS estableció el valor límite de 6 $\mu g\ L^{-1}$ para el Hg total en agua potable (WHO, 2017).

Respecto a la calidad del aire, la OMS estimó que las concentraciones de Hg en exteriores, a excepción de los sitios altamente contaminados, usualmente estaban entre 0,005 y 0,010 $\mu g\ m^{-3}$, por lo que estableció el valor límite 1 $\mu g\ m^{-3}$ como promedio anual para la exposición a los vapores de Hg^0 (WHO, 2000), aunque poco tiempo después modificó este valor a 0,2 $\mu g\ m^{-3}$ (WHO, 2003). En España, el Instituto Nacional de Seguridad y Salud en el Trabajo (INSST) estimó el valor legal del límite de exposición permisible (PEL) en el aire en 0,02 $mg\ m^{-3}$ (20 $\mu g\ m^{-3}$) diarios para vapores de Hg^0 (INSST, 2021), mientras que en Estados Unidos está establecido en 0,05 $mg\ m^{-3}$ en promedio para una jornada laboral de 10 horas (OSHA, 2014).

El Convenio de Minamata sobre el Mercurio es un tratado mundial que fue adoptado por el PNUMA en 2013. El objetivo del Convenio es salvaguardar la integridad de la salud humana y el medioambiente de las emisiones antropogénicas de Hg y sus compuestos, representando el esfuerzo más relevante de los últimos 50 años en términos de alcance global en la lucha

contra la contaminación por dicho metal (UNEP, 2017b). La figura 6 muestra los 141 países que han ratificado el convenio, incluyendo los 128 firmantes que han ido implementando medidas para reducir el uso y emisiones de Hg, así como la gestión de sus desechos y la remediación de sitios contaminados (pasivos ambientales) en sus territorios, enfatizando en la regulación progresiva de las actividades de la MAPE en los países que dependen de este sector.

Figura 6. Mapa de los países que han ratificado el Convenio de Minamata sobre el Mercurio hasta el año 2021. Elaboración propia basada en mapa publicado en www.mercuryconvention.org [Consultado en: 01/05/2023].

1.1.1.4. Fuentes de emisión del mercurio

El Hg es emitido al medioambiente a través de diversas fuentes, que incluyen procesos naturales como actividades antropogénicas, y debido a la alta toxicidad del este, es importante entender y controlar sus fuentes de emisión para controlar sus impactos negativos. Con el propósito de evaluar el estado

y las tendencias globales del Hg, cada cuatro años se publica el informe *Global Mercury Assessment* (GMA). Este informe brinda una visión holística de la situación actual en relación con el Hg, incluyendo sus fuentes de emisión, cantidades, transporte y distribución en el medioambiente. Además, el GMA es ampliamente reconocido como una referencia clave para el establecimiento de estrategias eficaces y para la toma de decisiones políticas y administrativas a nivel nacional e internacional en relación con el metal.

Las fuentes de emisión del Hg pueden agruparse en tres categorías principales: naturales, antropogénicas, y de re-emisión y removilización (UNEP, 2013).

Fuentes naturales

El Hg se encuentra de manera natural en la corteza terrestre en una concentración estimada en 0,05 mg kg^{-1} y en una mezcla de siete isótopos estables, siendo el ^{202}Hg el más abundante (29,7%). Los otros isótopos son ^{196}Hg (0,16%), ^{198}Hg (10,0%), ^{199}Hg (16,9%), ^{200}Hg (23,1%), ^{201}Hg (13,2%) y ^{204}Hg (6,83%). Los isótopos ^{199}Hg, ^{200}Hg y ^{201}Hg son considerados isótopos estables altamente enriquecidos y se han utilizado ampliamente en estudios de trazabilidad y su ciclo biogeoquímico (Blum et al., 2020; Tsui et al., 2020).

Se han registrado más de 100 minerales que contienen Hg, siendo el cinabrio (HgS) el más común, así como amalgamas naturales con cloruros (calomel), oro (weishanita), plata (moschellandsbergita), cobre (belendorffita), paladio

(potarita), entre otros (Mindat, 2023). El cinabrio ha sido el mineral más explotado en la producción de Hg a nivel mundial por su alto contenido de este (~85%), y se encuentra cerca de cráteres activos, depósitos químicos de fuentes hidrotermales alcalinas y en impregnaciones de areniscas, pizarras y dolomitas relacionados con las manifestaciones volcánicas (Córdoba Sola, 2018).

La liberación del Hg de origen geológico se da por procesos naturales como la erosión del suelo, meteorización de rocas, erupciones volcánicas, y procesos biogeoquímicos en ecosistemas acuáticos. Las actividades volcánicas y geotérmicas son una fuente importante de emisiones naturales de Hg, ya que liberan Hg^0 y otros de sus compuestos de las rocas, aunque en el caso de los volcanes, estas emisiones usualmente no son constantes y dependen de la actividad del volcán.

En general, se estima que alrededor del 10% de todo el Hg emitido a la atmósfera proviene de fuentes naturales, es decir, aproximadamente de 550 − 890 t de Hg al año. Si bien, estas cantidades pueden resultar pequeñas en comparación con las cantidades de Hg emitidas de fuentes antropogénicas (2000 − 3000 t al año), debemos tener en cuenta que estos valores son imprecisos, ya que los modelos utilizados están sujetos a varias incertidumbres, entre las cuales está la dificultad de diferenciar entre la contribución meramente natural y procesos de re-emisión de Hg originado de fuentes antropogénicas del pasado (UNEP, 2013, 2019).

Fuentes antropogénicas

Las fuentes antropogénicas de Hg se refieren a aquellas relacionadas con actividades humanas industriales y comerciales. Durante más de 2500 años, las minas de Almadén (España), Monte Amiata (Italia) y Idrija (Eslovenia) fueron los principales yacimientos de Hg, aunque actualmente se encuentran agotados o cerrados. Asimismo, grandes depósitos comerciales de Hg fueron extraídos de las minas Santa Bárbara (Perú) y New Almaden (Estados Unidos), y actualmente, la mayor extracción de Hg ocurre en los yacimientos de China, con un volumen de producción minera de 2000 mtu (USGS, 2023a).

Según el reporte de GMA 2018, las fuentes antropogénicas aportan alrededor del 30% (~2220 t) de las emisiones anuales de Hg la atmósfera (UNEP, 2019), siendo la MAPE la fuente predominante al ser la responsable de casi el 38% (~838 t) de las emisiones antropogénicas de Hg al año, seguida de la combustión estacionaria de carbón con un 21%.

Aunque en menor medida, las emisiones de Hg también provienen de la eliminación de residuos, la combustión de biomasa y otros combustibles, la industria de metales no-férreos, la industria del cemento, las emisiones asociadas a la eliminación de residuos con aditivos de Hg, la producción de metales ferrosos y fuentes diversas (figura 7).

Estimaciones de los porcentajes de mercurio antropogénico emitidos por diferentes sectores

- Minería artesanal y de pequeña escala (MAPE)
- Combustión estacionaria de carbón
- Industria de metales no-férreos
- Industria del cemento
- Eliminación de residuos con aditivos de Hg
- Combustión estacionaria de otros combustibles (biomasa)
- Producción de metales ferrosos
- Otras fuentes
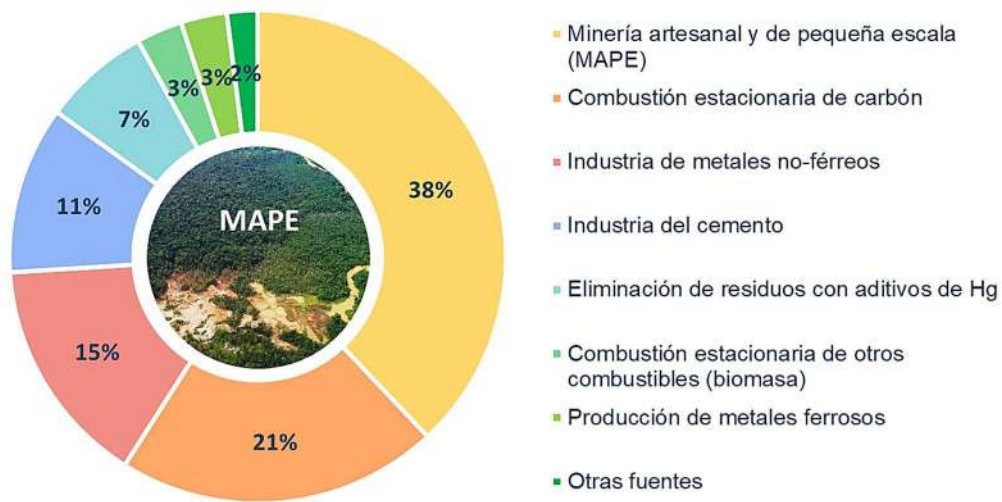
Figura 7. Porcentajes de emisiones mundiales de mercurio a la atmósfera procedentes de diferentes sectores de fuentes antropogénicas. Elaboración propia basada en datos obtenidos de UNEP (2019).

Las contribuciones de Hg antropogénico por región geográfica son muy similares a las tendencias observadas en el uso mundial del Hg. De acuerdo a los valores reportados por el GMA 2018 por regiones geográficas, la mayoría de las emisiones se produjeron en Asia (49%, de las cuales el 39% en Asia Oriental y Sudoriental), seguida de América del Sur (18%) y África Subsahariana (16%). Cabe destacar que la MAPE representa alrededor del 70% y hasta el 80% de las emisiones de África Subsahariana y América del Sur, respectivamente (figura 8).
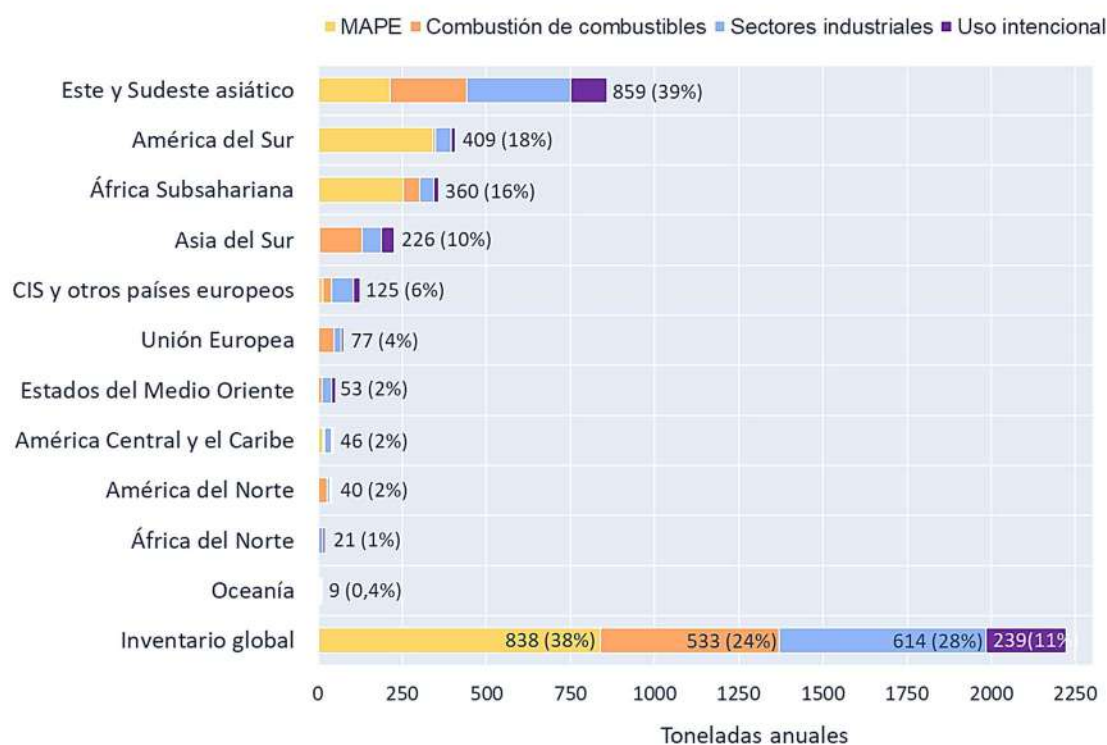
Figura 8. Cantidades de mercurio provenientes de fuentes antropogénicas, diferenciadas por sectores y región geográfica. Elaboración propia basada en datos obtenidos de UNEP (2019).

Estos datos demuestran que el Hg es un problema internacional que afecta tanto a los países desarrollados como a países en vía de desarrollo, con especial impacto en aquellos con economías extractivistas, ya que pueden enfrentar mayores desafíos en la implementación del Convenio de Minamata para la gestión de las emisiones de Hg, así como en la transición a prácticas más sostenibles y menos dependientes de la extracción de metales preciosos y otros minerales.

Aunque la extracción y uso industrial de Hg puede parecer ajeno a nuestra cotidianidad, diversos estudios han evidenciado que los picos en las emisiones de Hg al ambiente están correlacionados con momentos históricos cruciales

para el avance de la civilización, como la expansión romana en Europa, la revolución industrial, y recientemente, con el avance tecnológico exponencial que hemos venido experimentando desde el fin de la Segunda Guerra Mundial (López-Costas et al., 2020; Gębka et al., 2016; Gworek et al., 2017; Li et al., 2020). El informe de *Global Mercury Supply, Trade and Demand* presenta un interesante análisis entre los precios internacionales del oro y del Hg en una ventana de observación de 36 años desde la etapa más tensa de la guerra fría en 1980 hasta nuestros días (UNEP, 2017a).

En la actualidad, se estima que solo la industria tecnológica/electrónica consume alrededor de 265 t de oro para la fabricación de chips y microchips, y se prevé que dicha demanda continúe aumentando considerablemente en el futuro cercano. Además, en el actual sistema económico-financiero, el oro se ha consolidado como una opción segura de inversión, especialmente durante periodos de crisis caracterizados por notables fluctuaciones monetarias (World Gold Council, 2018).

Considerando que la MAPE representa la principal fuente de emisiones antropogénicas de Hg al medioambiente, y aunque aún no se ha evaluado una correlación directa entre las emisiones de Hg y el crecimiento en la demanda de oro (tanto para aplicaciones tecnológicas como comerciales), si se podría considerar que el avance acelerado de la tecnología ha impulsado indirectamente el incremento de las actividades mineras, y por consiguiente de las emisiones de Hg, especialmente en los países con economías extractivistas.

Según la información presentada por la plataforma global DELVE (https://delvedatabase.org, consultado en 30/05/2023), la MAPE constituye la mayor fuerza laboral minera del mundo, posiblemente a causa de la informalidad que la caracteriza y a varios factores que hacen de la minería una de las actividades más lucrativas. En consecuencia, se estima que actualmente hay 44,6 millones de personas dedicadas a este oficio en 80 países, de las cuales aproximadamente 30% son mujeres (a modo de contextualización, esta cifra es próxima a la población total de España).

En cuanto a los países de América del Sur, que debido a la abundancia de recursos naturales suelen basar su economía en la extracción minera, se estima que hay 1,6 millones de mineros de la MAPE, y los países con mayor actividad minera de este tipo son Brasil, Perú, Bolivia, Colombia y Ecuador (figura 9). En Colombia, la MAPE se concentra principalmente en los departamentos de Antioquia, Chocó, Bolívar, Cauca y Nariño. Es importante destacar que en ninguna de las minas de estos departamentos existe un sistema de gestión ambiental integral que cumpla con la normativa para el manejo adecuado de los vertidos, emisiones y generación de residuos peligrosos asociados al proceso de extracción de oro. Por consiguiente, junto con la práctica ilegal de utilizar Hg en la amalgamación del oro, se añaden otros impactos significativos, como la deforestación, las considerables emisiones de mercurio y cianuro derivadas de su uso inapropiado en el proceso de extracción minera, y la elevada sedimentación en cuerpos de agua (Veiga y Baker, 2004; MME/UPME/UC, 2014; Seccatore et. al., 2014).
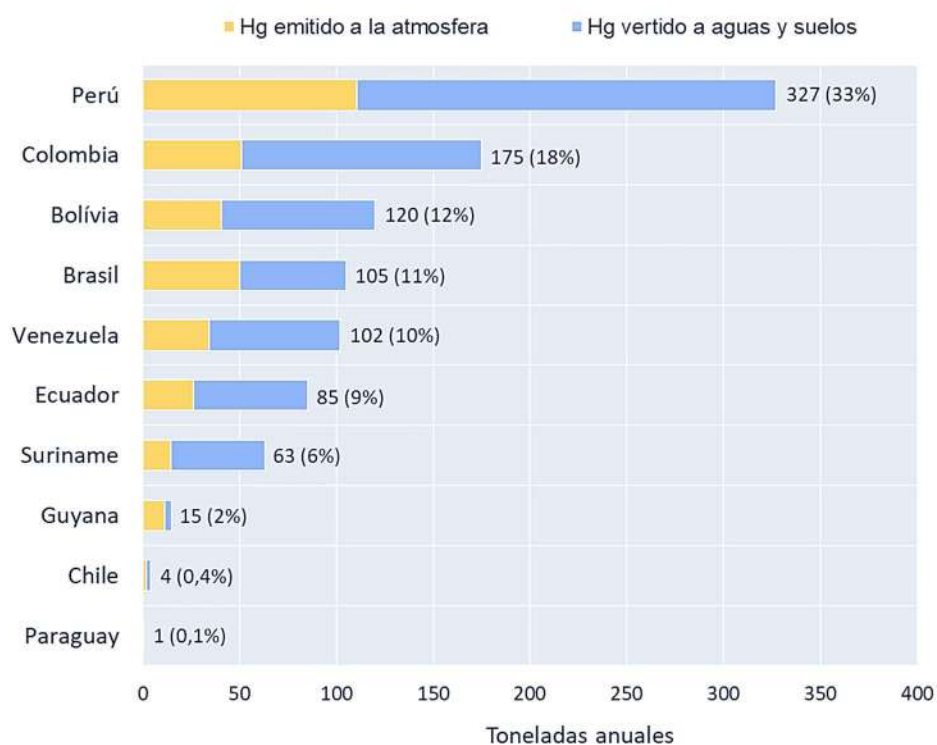
Figura 9. Emisiones de mercurio provenientes de las actividades de la MAPE en América del Sur. Elaboración propia basada en datos obtenidos de UNEP (2019).

Fuentes de re-emisión y removilización

Las fuentes de re-emisión y removilización representan la tercera categoría de fuentes de Hg y actualmente constituyen aproximadamente el 60% de las emisiones totales a la atmósfera. Estas re-emisiones ocurren cuando el Hg previamente depositado en el suelo, las aguas superficiales y la vegetación es liberado nuevamente al aire. Este proceso es resultado de procesos naturales que transforman las especies químicas orgánicas e inorgánicas (Hg^{2+}) a su forma elemental (Hg^0), el cual es volátil y, por lo tanto, se emite fácilmente hacia la atmósfera. Además, el Hg depositado en la superficie de las plantas

puede ser re-emitido durante eventos como incendios forestales o la quema de biomasa.

Es importante destacar que las re-emisiones de Hg no deben considerarse como fuentes naturales, ya que su origen inicial puede ser tanto natural como antropogénico, siendo difícil o incluso imposible determinar su origen específico una vez que se vuelve a emitir. No obstante, es un hecho que la actividad humana ha incrementado la carga ambiental de Hg, lo cual ha resultado en niveles más altos de re-emisión. A su vez, las re-emisiones también se ven influenciadas por el arado y la agricultura intensiva y por el aumento de las temperaturas asociado al cambio climático (UNEP, 2013).

La removilización ocurre cuando el Hg depositado y acumulado en suelos o sedimentos es movilizado nuevamente hacia el medio acuático, por ejemplo, a través de la lluvia, inundaciones, la acción de olas o tormentas, o durante el dragado del lecho de los ríos o creación de pozas en las prácticas de minería intensiva. La figura 10 muestra el caso de estudio del río Quito (departamento de Chocó, Colombia) en donde las actividades de minería intensiva han sido una preocupación significativa en relación con la removilización del Hg, As y otros metales, y la destrucción indiscriminada de la selva y el cauce de los ríos. Estas actividades de minería intensiva, incluidas la MAPE formal e ilegal, se caracterizan por el uso de maquinaria pesada (retroexcavadoras y dragas, también llamadas "*dragones*" por la comunidad local) para remover el suelo y el lecho de los ríos, en la búsqueda y extracción de oro y platino, conllevando a un destrucción ecológica irreversible de todo el ecosistema, que

hace parte del '*hotspot*' de biodiversidad conocido como *Chocó biogeográfico* (Lara-Rodríguez, 2018; Córdoba-Tovar et al., 2023; Marrugo-Negrete et al., 2023). Es preocupante evidenciar la existencia de numerosos casos de estudio similares al del río Quito en muchas otras localidades mineras, como el de Madre de Dios en la frontera entre Perú y Bolívia, el del delta del río Níger en Nigeria, o el de la provincia de Kalimantan en Indonesia, por poner tres ejemplos. Por lo tanto, es de suma importancia que la comunidad científica realice estudios en estos lugares con el propósito de evaluar los impactos ambientales reales que han sido generados y alertar a las autoridades correspondientes.
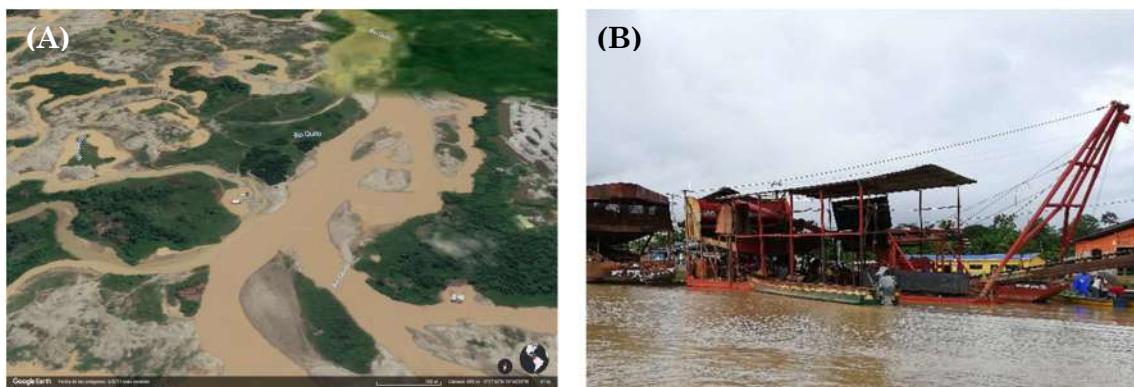
Figura 10. (A) Imagen satelital del río Quito, Colombia. El cauce del río está destruido por las operaciones de dragado intensivo en operaciones de minería de oro, re-movilizando el Hg hacia el ecosistema adyacente (Google Earth, 2023). (B) Fotografía de draga o también llamado "*dragón*", comúnmente usada en operaciones de minería ilegal para remover el lecho del río en busca de oro y platino (Fotografía: autoría propia).

La estimación de las tasas de re-emisión y re-movilización resulta difícil de calcular y se realiza frecuentemente utilizando enfoques de modelado. Estos modelos se basan en datos disponibles de Hg atmosférico, así como en el

conocimiento actual de las transformaciones químicas y la movilidad del Hg entre el aire, la tierra y el agua. El objetivo de estos modelos es establecer un balance aproximado de la cantidad de Hg circulante en la actualidad, al tiempo que son consistentes con los datos observados.

Es importante reconocer que la temperatura es un factor clave en el proceso de re-emisión del Hg, ya que las tasas más bajas de re-emisión han sido observadas a temperaturas más frías. Al mismo tiempo, la re-emisión juega un papel importante en determinar el tiempo necesario para que las reducciones en las emisiones antropogénicas se vean reflejadas en la disminución de los niveles ambientales de Hg, ya que pueden pasar varios años antes de que el metal pueda volver a emitirse o movilizarse. Por tanto, es posible que los niveles de Hg permanezcan elevados, aún después de haber reducido sustancialmente las fuentes de emisión antropogénicas. En consecuencia, seguir aumentando la reserva mundial de Hg dejará un legado cada vez más prolongado de contaminación antropogénica en todo el mundo, por lo que los esfuerzos internacionales (como el Convenio de Minamata) para reducir las emisiones de Hg han de considerarse de carácter urgente (UNEP, 2013, 2019).

1.1.1.5. Ciclo biogeoquímico del mercurio

El ciclo biogeoquímico del mercurio se refiere a su flujo continuo bidireccional de las especies químicas de Hg a través del medioambiente, incluyendo su

transformación y transporte entre la atmósfera, la tierra y el agua, lo cual es de suma importancia para entender y gestionar sus riesgos (Díez, 2018). Este ciclo está basado en el comportamiento del Hg en los diferentes medios, e implica una compleja interacción de procesos físicos, químicos y biológicos, y está influido por una serie de factores como las actividades humanas, así como los parámetros de transporte y su destino final. En cualquier punto de la Tierra, la cantidad de Hg presente dependerá de:

- El ciclo global natural
- El ciclo global perturbado por actividades antropogénicas
- Las fuentes regionales de mercurio
- Las fuentes locales de mercurio

El ciclo natural global del Hg implica que éste es liberado a la atmósfera a través de procesos naturales como las erupciones volcánicas y la meteorización de las rocas, y también puede ser transportado a largas distancias a través de la atmósfera. Una vez en la atmósfera, el Hg puede transformarse en varias formas, tal como Hg^0, MeHg, gaseoso reactivo o unirse a material particulado, y posteriormente pueden depositarse en superficies terrestres y acuáticas por precipitación o deposición seca, donde usualmente son absorbidas por plantas y animales.

A su vez, las actividades antropogénicas han alterado considerablemente el ciclo global del Hg. La minería, la quema de combustibles fósiles y la incineración de residuos han provocado un aumento significativo de los niveles de Hg en el medioambiente y en la cadena alimentaria, lo que supone

un incremento del riesgo para la salud humana y la biota. Cuando estas fuentes de Hg son catalogadas como fuentes regionales o locales, pueden influir considerablemente en la contaminación de regiones adyacentes. Por ejemplo, las zonas de cinturones volcánicos, o con presencia de centrales eléctricas de carbón o explotaciones mineras auríferas usualmente presentan niveles más altos de Hg, provocando contaminaciones puntuales importantes que pueden afectar a comunidades locales (de Paula Gutiérrez y Agudelo, 2020; Yang et al., 2022; Albanese et al., 2023).

El ciclo del Hg se inició mucho antes del comienzo de la Era Industrial. En evaluaciones anteriores, a menudo se utilizaba el año 1850 como punto de referencia para medir el impacto humano en los niveles de Hg a nivel mundial, no obstante, aún no existe consenso sobre el período previo que debería considerarse. Además, es claro que las concentraciones actuales de Hg en la atmósfera son varias veces superiores a los niveles considerados "naturales". En este aspecto, los niveles de fondo natural son <5 ng L^{-1} de Hg de acuerdo a un estudio de concentraciones históricas de Hg realizado por el Servicio Geológico de Estados Unidos (USGS) usando un testigo de profundidad del glaciar Upper Fremont en Wyoming y una datación desde el año 1700 aproximadamente (Schuster et al. 2002; Díez, 2018; UNEP, 2019). Así pues, debido a la necesidad de cuantificar el ciclo del Hg, se han reportado las cantidades estimadas de las emisiones y liberaciones de Hg total provenientes de las diferentes fuentes naturales, antropogénicas y de re-emisión en el informe GMA 2018.

La figura 11 muestra una estimación general del balance mundial de las cantidades de Hg (en toneladas), teniendo en cuenta los principales sectores y vías medioambientales. El Hg es liberado al medioambiente a partir de fuentes y procesos naturales y como resultado de las actividades humanas, y una vez ahí, la mayoría de sus especies químicas circulan entre el aire, la tierra y el agua, hasta que finalmente se entierran en sedimentos oceánicos profundos o sedimentos lacustres, o quedan atrapadas en compuestos minerales estables (UNEP, 2019).
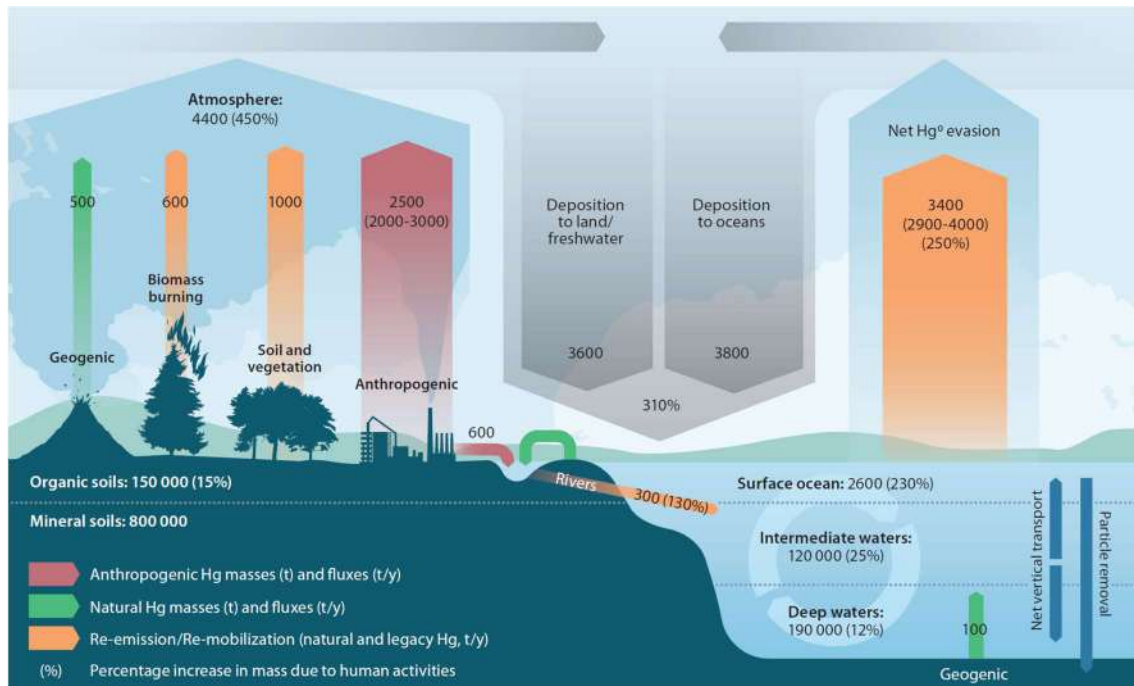
Figura 11. Estimación de las cantidades de mercurio emitidas a la atmósfera (en toneladas) de acuerdo a las principales rutas y fuentes de emisión en el ciclo global del Hg (UNEP, 2019).

El mercurio en la atmósfera

Los procesos que intervienen en el transporte y destino del Hg en nuestra atmósfera involucran principalmente sus emisiones, transformación y

transporte atmosférico, y su deposición. En el caso de las emisiones provenientes de fuentes naturales, dentro de los procesos que se dan encontramos la volatilización del Hg desde cuerpos de agua y océanos, la liberación de Hg proveniente de la vegetación, la emisión de gases de materiales geológicos y las emisiones volcánicas. Es importante destacar que las emisiones naturales de Hg ocurren principalmente en forma de Hg^0. En cuanto a las emisiones proveniente de fuentes antropogénicas, éstas son predominantemente resultado de las actividades de la MAPE, de procesos industriales y de la combustión que contienen Hg en diferentes especies químicas, ya sea en forma gaseosa (Hg^0 u otras formas oxidadas) o en forma de partículas (Hg_p). En este último caso, el Hg_p tiende a encontrarse en algunas de sus formas oxidadas debido a la alta presión de vapor del Hg^0.

Una vez que el Hg es liberado a la atmósfera, su tiempo de permanencia varía considerablemente dependiendo de su forma química. El Hg^0 tiene un tiempo de residencia promedio de hasta un año, mientras que la forma oxidada Hg^{2+} que varía desde horas a días. Esto se debe a que el Hg^{2+} puede ser depositado con relativa facilidad tanto por vía húmeda (precipitación) como por vía seca (sedimentación directa sin la intervención de la lluvia). Así pues, el impacto de Hg^{2+} es a nivel local o regional, mientras que el Hg^0 tiene un impacto a nivel global (Díez, 2018).

A diferencia del mercurio inorgánico, el Hg^0 presenta una baja solubilidad en agua y no es susceptible a los principales mecanismos de deposición seca. Sin embargo, el Hg^0 si puede ser depositado a través de diversos mecanismos que

implican su conversión a Hg^{2+} dentro de las gotas de agua presentes en las nubes. Estos mecanismos se describen mediante las ecuaciones Ec.1 a Ec.3, que reflejan los productos finales de estas reacciones (Díez, 2018).

$$Hg_{(g)} \rightarrow Hg_{(aq)} \qquad \qquad \text{Ec.1}$$

$$Hg_{(aq)} + O_3/Br/\bullet OH_{(aq)} \rightarrow Hg^{2+}_{(aq)} \qquad \text{Ec.2}$$

$$Hg^{2+}_{(aq)} + polvo/partículas \rightarrow Hg^{2+}_{(p)} \qquad \text{Ec.3}$$

$$Hg^{2+}_{(aq)} + SO_3^{2-} \rightarrow Hg^0_{(aq)} \qquad \qquad \text{Ec.4}$$
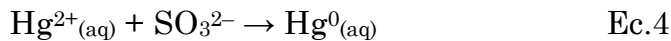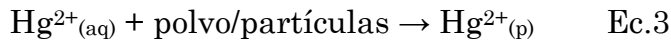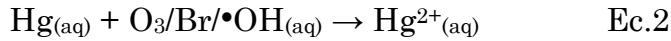
Después de que el Hg se haya depositado en cualquiera de sus formas, aunque la reacción química Ec.2 tiene una cinética muy rápida, es probable que el Hg^{2+} experimente reacciones químicas adicionales que lo transforman nuevamente en Hg^0, por ejemplo, al reaccionar con grupos sulfitos, SO_3^{2-} (Ec.4). Debido a este proceso, el Hg depositado a nivel local puede ser re-emitido a la atmósfera y viajar grandes distancias desde la fuente de emisión, distribuyéndose por el planeta, en especial, en las regiones más frías como los cascos polares (Díez, 2018).

El mercurio en suelos y sedimentos

La especie química predominante en suelos y sedimentos es el Hg^{2+}, y sus compuestos están sujetos a un amplio espectro de reacciones químicas y biológicas. Las condiciones del suelo o sedimento (pH, temperatura, materia orgánica, etc.) son normalmente favorables para la formación de compuestos inorgánicos de Hg^{2+} como $HgCl_2$, $Hg(OH)_2$, HgS y HgO. No obstante, aún no

es claro si el Hg en sedimentos se encuentra en forma de $HgCl_2$, $Hg(OH)_2$ cuando se encuentra complejado por sustancias orgánicas, o bien en las formas menos reactivas de HgS o HgO (con una menor tendencia a la metilación que las anteriores). Aunque algunos compuestos inorgánicos de Hg^{2+} son bastante solubles en agua y en principio tienen una alta movilidad, también suelen formar complejos con la materia orgánica, tal como ácidos fúlvicos y húmicos, y arcillas en los suelos y sedimentos. En consecuencia, la mayor parte del Hg (>90%) se encuentra en el suelo y se asocia con la materia orgánica, formando enlaces fuertes con grupos reducidos de azufre (S) y limitando su movilidad.

Basándonos en los rangos de concentración de Hg en suelos (20 a 70 ng g^{-1}), se estima que la carga total a nivel global para los primeros 15 cm de suelo puede alcanzar el orden de magnitud de 10^6 t aproximadamente, y se estima que la actividad humana ha incrementado esta cantidad en alrededor de un 15%, haciendo que los suelos y sedimentos actúen como grandes reservorios de Hg antropogénico (Díez, 2018).

Por otra parte, en la vegetación encontramos una pequeña fracción del Hg, el cual puede encontrarse en las partes aéreas de la planta al ser captado principalmente del aire. El Hg^{2+} se deposita sobre las hojas a través de procesos de deposición húmeda y seca, mientras que el Hg^0 se cree que es captado mediante un intercambio gaseoso en los estomas de las hojas. Asimismo, el Hg puede encontrarse en las raíces de las plantas al ser

absorbido del suelo. Por esto, el Hg contenido en la vegetación puede ser re-emitido a la atmósfera por la quema de biomasa (Díez, 2018).

Es importante mencionar que el MeHg también está presente en suelos y sedimentos, aunque en proporciones muy pequeñas. En general, la proporción de MeHg con respecto al Hg total presente en suelos y sedimentos suele ser inferior al 1%, y su formación ocurre principalmente a través de procesos microbianos que actúan sobre los compuestos de Hg^{2+} (metilación del Hg).

El mercurio en sistemas acuáticos

En los sistemas acuáticos, el Hg experimenta complejas transformaciones biogeoquímicas, incluida la metilación, que puede dar lugar a la formación de MeHg, el cual es altamente tóxico y se bioacumula. La deposición atmosférica es la principal fuente de entrada de Hg en los sistemas acuáticos, y tanto la deposición húmeda como la seca contribuyen a la carga total. Asimismo, el Hg^{2+} y el MeHg pueden ser incorporados al medio acuático por acción de la lluvia (Hg complejado a suelo/humus en suspensión, o a la materia orgánica disuelta, DOM), y por arrastre desde el suelo a través de escorrentías de las cuencas hidrográficas o de corrientes de aguas subterráneas (Mason et al., 2012; Díez, 2018).

Las especies químicas de Hg en los sistemas acuáticos son Hg^0, Hg^{2+}, MeHg, Hg_p, Hg-coloidal, y en menor medida, Me_2Hg y EtHg. Independientemente de la clasificación del sistema acuático (oceánico o continental), el Hg^{2+}

predomina en la dinámica del Hg en la columna de agua. De acuerdo a cálculos termodinámicos el Hg^{2+} en aguas superficiales no está presente como ion libre, sino que puede estar complejado en cantidades variables a hidroxilos ($Hg(OH)^+$, $Hg(OH)_2$ y $Hg(OH)_3$) y a cloruros ($HgCl^+$, $HgClOH$, $HgCl_2$, $HgCl_3$, $HgCl_4^{2-}$), dependiendo del pH y de la concentración de cloruros en el medio (Morel et al., 1998; Marins et al., 2002).

Posteriormente, este Hg^{2+} puede transformarse a Hg^0 y pasar a la atmósfera mediante volatilización, parecido a lo que ocurre en suelos y sedimentos (Ec.4), o bien puede pasar al sedimento para luego ser re-emitido mediante procesos de difusión o resuspensión. Del mismo modo, una fracción de Hg^{2+} puede metilarse convirtiéndose en MeHg, que tiene la capacidad de bioacumulación y biomagnificación en la cadena trófica acuática, lo que supone un riesgo significativo para la biota y las comunidades humanas, tal como se mencionó en la pasada sección 1.1.1.2 de esta tesis.

Asimismo, pueden producirse procesos de desmetilación, como la fotodesmetilación y la desmetilación microbiana, que convierten el MeHg de nuevo en Hg^{2+} (O'Driscoll et al., 2006). La figura 12 muestra una visión general del ciclo del Hg en sistemas acuáticos, y las interacciones y transformaciones entre las especies químicas del Hg que tienen lugar en el aire, el agua y el sedimento.
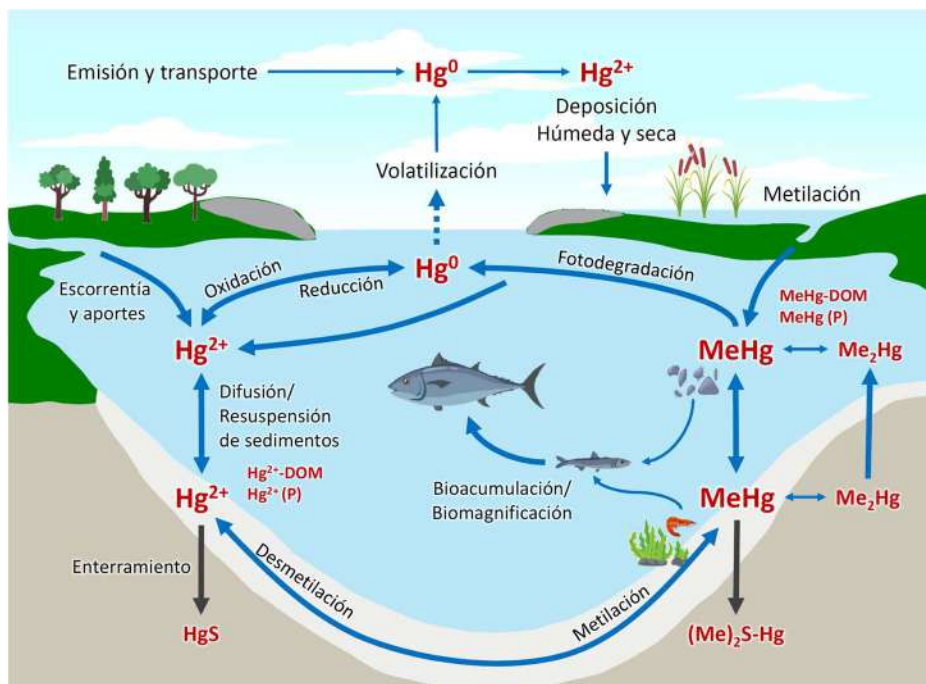
Figura 12. Ciclo biogeoquímico del mercurio en el medio acuático. Adaptado de Engstrom (2007).

Metilación del mercurio

El MeHg, la especie química más tóxica y bioacumulativa y que presenta el mayor riesgo para la salud de los seres humanos y la vida silvestre, se forma principalmente en ambientes acuáticos a través de procesos microbianos naturales.

La metilación del Hg es un proceso bioquímico en el que el Hg^{2+} se convierte en MeHg (CH_3Hg^+) por la acción de determinados microorganismos anaeróbios metilantes, como lo son las bacterias sulfato-reductoras (SRB) y bacterias ferro-reductoras (FeRB o IRB) (Benoit et al., 2003, Tang et al., 2020). Estos microorganismos poseen las enzimas necesarias, como la

metiltransferasa, para catalizar la transferencia de un grupo metilo ($-CH_3$) de co-sustrato, normalmente S-adenosilmetionina (SAM), al Hg^{2+}.

Las SRB de oxidación completa sintetizan el MeHg mediante la vía de la acetil-CoA, mientras que las cepas de oxidación incompleta lo hacen a través de otra vía que aún se desconoce. Otros microorganismos metilantes de Hg conocidos son los metanógenos que pertenecen a la clase *Methanomicrobia*, pueden utilizar CO_2, acetato y compuestos C1 como sustrato para el crecimiento y el metabolismo, y son los posibles responsables de la metilación del Hg en el perifiton (Compeau y Bartha, 1985; Hamelin et al., 2011; Tang et al., 2020).

El descubrimiento más reciente es el de los genes *hgcAB*, los cuales proporcionan una base genética para la metilación del Hg, al tiempo que su presencia es indispensable para la metilación microbiana. Específicamente, el gen *hgcA* codifica la supuesta proteína corrinoide que transfiere un grupo $-CH_3$ al Hg^{2+} para formar MeHg, mientras que el gen *hgcB* codifica [4Fe–4S] ferredoxina que es responsable de la reducción de *hgcA* (figura 13). A su vez, estos genes *hgcAB* también han sido considerados marcadores moleculares fiables para la predicción de MeHg en el medioambiente (Tang et al., 2020).

La tasa y el alcance de la metilación del Hg están influidos en general por diversas condiciones ambientales y fisicoquímicas, como la temperatura, el pH, el potencial redox, la concentración de oxígeno en el sedimento/fase acuosa, la presencia de dadores y aceptores del grupo $-CH_3$, la presencia de sulfato (SO_4^{2-}) y sulfuro (S^{2-}) en el medio, la biodisponibilidad de Hg^{2+}, y la

presencia y actividad de microorganismos metiladores (Ullrich et al., 2001; Gilmour et al., 2013; Díes, 2018; Tang et al., 2020). Las concentraciones altas de sulfuro en el medio bloquean la actividad de las SRB, al favorecer la formación de HgS mientras que se disminuye la producción *in situ* de MeHg. De igual manera, la presencia de agentes complejantes, como la DOM puede reducir la biodisponibilidad del Hg^{2+} y, por consiguiente, disminuir las tasas de metilación (Ravichandran, 2004).
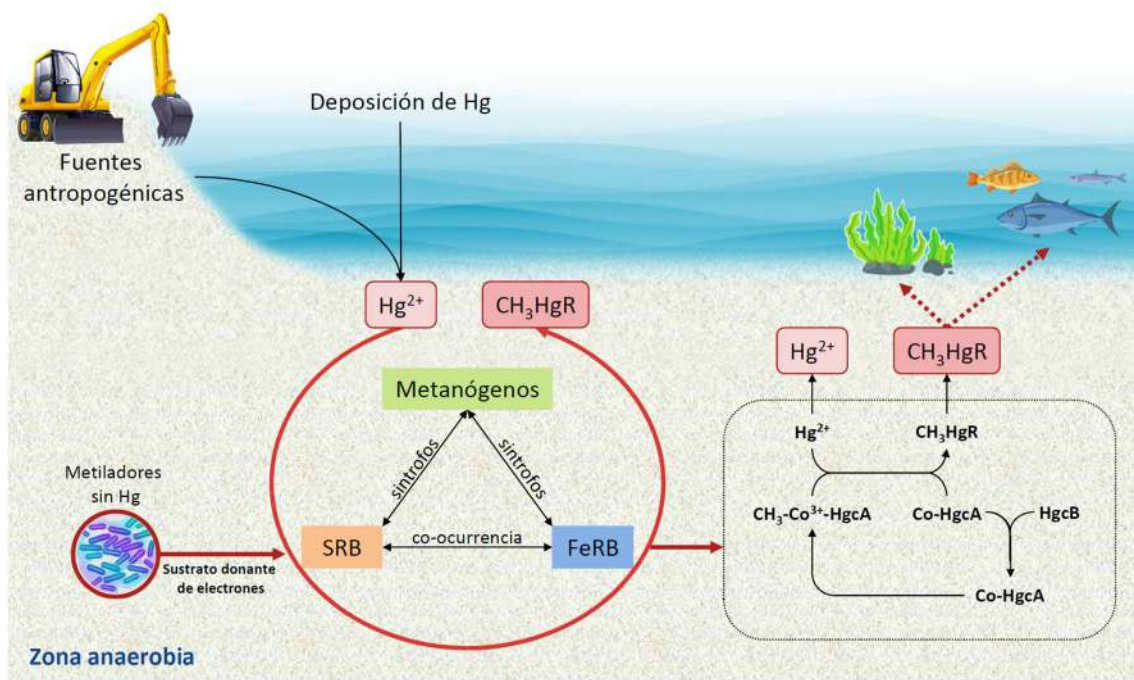
Figura 13. Posibles vías implicadas en la metilación del mercurio en medio acuático. HgcA: proteínas corrinoides putativas, codificadas por el gen *hgcA*. HgcB: ferredoxinas 2[4Fe–4S] asociadas a la proteína corrinoide putativa, codificadas por el gen *hgcB*. Co-HgcA: cobalamina-HgcA. CH_3-Co^{3+}-HgcA: formado después de pasar el metilo (–CH_3) a Co-HgcA a través de la enzima metilentetrahidrofolato (CH_3-THF). Adaptado de Tang et al., (2020).

Dado que la transformación a MeHg ocurre en el interior de las bacterias, las especies químicas del Hg que atraviesan fácilmente la pared celular favorecen la eficiencia de la metilación. Por consiguiente, las concentraciones elevadas de Hg^{2+} aumentan la fracción biodisponible y la probabilidad de metilación. Dentro de las técnicas avanzadas que han demostrado ser muy prometedoras en la evaluación cuantitativa de la fracción biodisponible del Hg^{2+} para predecir la actividad de metiladores microbianos, tenemos a la aplicación de múltiples trazadores estables de Hg enriquecidos isotópicamente, biosensores de células enteras y la técnica de gradiente de difusión en capa fina (DGT), en la cual se enfoca esta tesis (Hintelmann et al., 2000; Martín-Doimeadios et al., 2004; Tang et al., 2020).

Por otra parte, también existe un mecanismo de metilación abiótica dado principalmente por la transmetilación por parte de especies organometálicas de otros metales, tales como Pb, As o Sn (Díez, 2018).

La producción neta de MeHg se determina por la diferencia entre los procesos de metilación y desmetilación del Hg. Por lo tanto, es esencial considerar también los procesos de desmetilación, los cuales pueden ser bióticos (oxidativos o reductivos) o abióticos. En la desmetilación oxidativa, las bacterias metanogénicas intervienen en la degradación del MeHg produciendo dióxido de carbono (CO_2), metano (CH_4) y, posiblemente Hg^{2+}. En contraste, la desmetilación reductiva está relacionada con la presencia de las enzimas organomercurio liasa (MerB) y mercurio reductasa (MerA). La enzima MerB rompe el enlace C–Hg en el MeHg, generando CH_4 y Hg^{2+} como

productos. Posteriormente, el Hg^{2+} se reduce a Hg^0 por la acción de MerA. Además, los procesos abióticos de desmetilación incluyen la fotodegradación y la reacción con sulfuro, que resulta en la formación de Me_2Hg y HgS (Díez, 2018).

1.1.2. Elementos traza

Los elementos traza son elementos cuya concentración promedio es inferior a 100 mg kg^{-1}. Algunos elementos traza, como el Cu y el Zn, son esenciales en pequeñas cantidades para diversos procesos biológicos dentro de los organismos vivos, ya que desempeñan papeles cruciales en la función enzimática, la integridad estructural de las moléculas, el crecimiento de las plantas, etc. Sin embargo, otros elementos (Ni, Cd, Pb y As) pueden ser muy tóxicos en pequeñas concentraciones para la salud humana y la biota. A continuación, se presentará una breve introducción de los elementos traza cuyos resultados destacaron durante el desarrollo de esta tesis: As y Ni.

1.1.2.1. Arsénico

El arsénico (As) es un elemento químico con número atómico 33 y masa atómica 74,92 g mol^{-1}, sublima a los 616 °C (a presión atmosférica) y está clasificado como un metaloide al presentar propiedades de metales y no-metales. Usualmente se encuentra en la naturaleza combinado con elementos como oxígeno, cloro y azufre, siendo en estos casos denominado como arsénico

inorgánico, aunque también es posible encontrarle en la en asociación con hidrógeno o carbono, referido como arsénico orgánico (ATSDR, 2007). Su nombre viene del vocablo griego *arsenikon* (αρσενικόν), que era usado para nombrar un pigmento amarillo. Su descubrimiento como elemento se atribuye al obispo católico San Alberto Magno en el siglo XIII, aunque registros históricos mencionan que fue usado en el Antiguo Egipto en aplicaciones metalúrgicas y en la China del siglo XVI como plaguicida para cultivos de arroz (RSC, 2023).

Es el veinteavo componente más abundante en la corteza terrestre, por lo que se encuentra distribuido en rocas, suelos y cuerpos de agua. No obstante, es poco común hallarlo en la forma de elemento nativo, pues su presencia como mineral ocurre especialmente en la forma de sulfuros como la arsenopirita [$FeAsS$], el rejalgar [As_4S_4] o el oropimente [As_2S_3] (SME, 2022). Dichos minerales han sido usados ocasionalmente como mena de As, en especial la arsenopirita, de la cual este puede extraerse mediante tostación. Sin embargo, no existe la minería de As como elemento de interés económico principal, y en general, este es obtenido como un subproducto de la explotación del Cu, Au y Pb, estando presente en los polvos de combustión resultantes del proceso de fundición de los metales mencionados; siendo recuperado y comercializado principalmente en la forma de óxido arsenioso [As_2O_3] (USGSb, 2023).

El suministro mundial de As, según muestra el reporte World Mining Data 2023, ha oscilado en los últimos años entre las 52000 t/año y 58000 t/año.

Particularmente, para el año 2021, estuvo cerca de las 55000 t, siendo China (aprox. 24.000 t) y Perú (aprox. 21.900 t) los países líderes en producción, seguidos a una considerable distancia por Marruecos (aprox. 6.900 t); logran consolidar alrededor del 95% del total de la producción global.

Dentro de las aplicaciones industriales del As se encuentra su uso como conservante para el tratamiento de maderas y como agente fortalecedor en baterías de Pb, como insumo en la elaboración de plaguicidas e insecticidas, y también en la fabricación de vidrio. Es usado para endurecer aleaciones metálicas en municiones, soldaduras y rodamientos, e igualmente, como aditivo antifricción para cojinetes y contrapesos de ruedas para neumáticos. Asimismo, el metal de As de alta pureza se utiliza para la producción de semiconductores de arseniuro de galio e indio, que son implementados en dispositivos biomédicos, informáticos, fotovoltaicos, de telecomunicaciones, entre otros (SME, 2022; USGSb, 2023).

El As se libera de manera natural en los ecosistemas a partir de la meteorización y oxidación de rocas (en especial volcánicas), y se estima que alrededor un 25% de las emisiones totales son provenientes de fuentes naturales, sobre todo de volcanes. A su vez, la liberación con origen en actividades antrópicas ocurre en su mayoría durante el proceso de fundición del Cu, siendo esto foco de diseño de tecnologías para control de emisiones. También hay presencia de As en las cenizas resultantes de la combustión de carbón para la generación de energía eléctrica (SME, 2022).

La concentración normal de arsénico en el suelo generalmente se encuentra alrededor de 3 y 4 mg kg^{-1}, mientras que en aguas superficiales y subterráneas la presencia natural de este es alrededor de 1 µg L^{-1}. Es probable hallar valores más altos en zonas cercanas a depósitos geológicos con presencia de minerales de As, o cerca de operaciones mineras, refinerías o terrenos agrícolas donde fueron aplicados pesticidas. A su vez, el nivel de As en aire de áreas urbanas usualmente oscila entre los 20 y 30 ng-As m^{-3}, pero, dependiendo del nivel de actividad industrial, la ubicación y condiciones climáticas es posible encontrar mediciones yendo desde 1 hasta 2000 ng-As m^{-3} (ATSDR, 2007).

El As puede entrar en el cuerpo humano a través del consumo de alimentos, agua o por la respiración, siendo el As inorgánico la forma más tóxica y peligrosa para la salud de las personas, pues este es inclusive reconocido como cancerígeno cuando ocurren períodos de exposición prolongados. Beber agua contaminada con As en concentraciones alrededor de 300 a 30000 µg L^{-1} puede traer contraindicaciones como vómito, diarrea y dolor estomacal, mientras que niveles de contaminación superiores a los 60000 µg L^{-1} llegan a resultar fatales. De igual manera, la inhalación de arsénico inorgánico puede conducir a la irritación de pulmones, o a trastornos circulatorios y del sistema nervioso, aún si se da por periodos cortos, no existe certeza de los niveles mínimos a los que ocurre, pero se estima que puede ser alrededor de los 100 µg-As m^{-3} (ATSDR, 2007).

Las agencias de Naciones Unidas, OMS y FAO, recomiendan que las evaluaciones de ingesta total de arsénico consideren la exposición de alimentos y agua (incluyendo la de consumo, la de preparación de alimentos y la de riego de cultivos) junto con los hábitos dietéticos de la región en estudio. Las entidades consideraban, hasta el 2011, una PTWI de hasta 15 µg kg^{-1} bw para el As inorgánico, pero la cifra fue reevaluada y la recomendación se retiró, pues se estableció como demasiado cercana al nivel en que el riesgo de incidencia de cáncer de pulmón supera el 0,5%, y que está establecido en 2,1 µg-As/kg/semana (WHO, 2018; USEPA, 2022). La Agencia Europea para la Seguridad y la Salud en el Trabajo (OSHA) establece que el nivel límite permisible de exposición diario, en jornada de 8 horas, para el aire en el entorno de trabajo, es de hasta 10 µg-As m^{-3}, mientras que la EPA dicta que una concentración de As en 10 µg L^{-1} es el nivel máximo de contaminante permitido en suministros públicos de agua potable, y la FDA dispone un tope de 2 mg kg^{-1} en contenido de la sustancia en alimentos (ATSDR, 2023).

1.1.2.2. Níquel

El níquel (Ni) es un elemento químico con número atómico 28, masa atómica de 58,71 g mol^{-1}; con punto de fusión a 1453 °C, punto de ebullición a 2730 °C y densidad de 8,90 g cm^{-3} a temperatura ambiente (Nickel Institute, 2023a). Es un metal de color blanco-plateado, brillante, con una conductividad térmica y eléctrica relativamente baja, alta resistencia a la corrosión y

oxidación, la capacidad de magnetizarse y bastante resistente a altas temperaturas (INSG, 2023a).

Se presume que el nombre del metal viene del vocablo germano *kupfernickel*, dado por mineros del siglo XV, cuando descubrieron una mena metálica de color marrón rojizo que imaginaron contenía Cu, pero de la cual no pudieron recuperar dicho metal. El Ni fue identificado y aislado como elemento por primera vez en el año 1751 por el sueco Axel Cronstedt. Durante el siglo XIX fue común su uso para la fabricación de monedas (tanto en aleaciones y como metal puro), y finalmente, en el siglo XX, con el descubrimiento de los aceros inoxidables, se convirtió en una de las principales materias primas hasta la actualidad (Nickel Institute, 2023b).

En este orden de ideas, el consumo de níquel a nivel global ha tenido un importante aumento en la última década, pasando de alrededor de 1,4 millones de toneladas en 2010 a más 2,8 millones de toneladas al año para el 2021, siendo esto explicado por la expansión de la economía China, país que actualmente representa más de la mitad del consumo mundial del metal (Norilsk Nickel, 2023; Zhang et. al., 2023).

Actualmente, la demanda de Ni se distribuye principalmente en la elaboración de aceros inoxidables (72%), otros productos intermedios como baterías (7%), en aleaciones ferrosas y fundiciones (7%), en aleaciones no ferrosas (6%), y en otros tipos de piezas niqueladas (8%). No obstante, frente a la proyección del desarrollo de la industria de los vehículos eléctricos, y la tendencia al uso de baterías con cátodos de alto contenido de Ni, existe la

expectativa de que la fabricación de baterías aumente sustancialmente su proporción dentro de la demanda mundial de Ni hasta un 37% para el 2030 (Zhang et. al., 2023). Para ese mismo año, se espera que la demanda del Ni esté en un rango aproximado de 3,5 millones a 4,5 millones de toneladas al año, acorde con las estimaciones de la IEA (2021) sobre la electromovilidad.

Sobre la oferta primaria de Ni, los datos presentados por el Ministerio de Finanzas Austriaco en el reporte World Mining Data 2023, reflejan que para 2021 el país con el mayor registro de producción minera es Indonesia con aproximadamente un 40% del total a nivel mundial, y en una segunda instancia (con fracciones aproximadas de entre 1/3 a 1/10 del volumen de producción indonesio) aparecen estados como Filipinas, Nueva Caledonia, Rusia, Australia, Canadá y China. En este sentido, las reservas mineras mundiales se estiman en más de 100 millones de toneladas, siendo Indonesia, Australia y Brasil los países que reportan la mayor cantidad, sumando más del 50% del consolidado global.

El Ni se extrae como elemento de interés principal en depósitos lateríticos, siendo sus menas la limonita niquelífera $[(Fe,Ni)O(OH)]$ y la garnierita $[Si_4O_{13}(Ni, Mg)_2 \cdot 2H_2O]$, y asimismo, en depósitos de sulfuros magmáticos donde su mena más importante es la pentlandita $[(Ni,Fe)_9S_8]$; en algunos casos el níquel también puede obtenerse como un subproducto de la explotación minera de Cu o de elementos del grupo del platino (USGS, 2023c, 2023d).

A su vez, el suministro secundario de Ni proviene en mayor medida del reciclaje del metal contenido en chatarra de acero inoxidable, usado para producir nuevamente este tipo de productos. En Estados Unidos, el reciclaje de Ni representó alrededor del 55% de todo el consumo aparente del Mineral Commodity Summaries en 2022 (USGS, 2023c). Vale la pena mencionar, que el Ni posee una tasa de reciclaje funcional de posconsumo superior al 50%, esto es, aquel reciclaje en que las propiedades físicas y químicas deseables en la sustancia se conservan para un uso posterior al final de vida útil del bien en que se encuentra contenida (UNEP, 2011).

Por otro lado, el Ni puede liberarse en el ambiente desde las chimeneas de las siderúrgicas donde se producen aleaciones, así como de centrales eléctricas, de incineradores de residuos, o en aguas residuales industriales, donde buena parte de este termina en el suelo o en sedimentos adherido a partículas que contienen hierro (Fe), es común encontrar concentraciones de Ni en el suelo a niveles de 4 a 80 mg kg^{-1}, aunque en áreas cercanas a operaciones mineras se han identificado concentraciones de hasta 9000 mg kg^{-1}. De igual manera, las concentraciones de Ni en ríos o lagos suelen ser bastante bajas y usualmente por debajo de los 10 μg kg^{-1}, pero en cuerpos de agua cercanos a operaciones mineras o industrias en algunos casos los niveles del metal en el recurso hídrico se encuentran alrededor de los 72 μg kg^{-1}.

En este orden de ideas, una persona en promedio ingiere alrededor 170 μm-Ni/día a través del consumo de alimentos, 2 μm-Ni/día al beber agua y respira alrededor de 0,1 a 1 μm-Ni/día (sin considerar humo de tabaco), aunque la

principal exposición al metal es por la manipulación de monedas, joyería u otros objetos metálicos que han recibido procesos de niquelado, como las carcasas de algunos teléfonos móviles (ATSDR, 2005).

Sobre los efectos adversos del Ni en la salud humana, se ha reconocido que el más común es una posible reacción alérgica al contacto con la piel mostrando erupciones cutáneas (alrededor de un 10% a 20% de las personas podrían ser sensibles a este). Afectaciones graves en la salud humana pueden ocurrir en trabajadores de la industria del Ni (que laboren en minas o refinerías) pues suelen estar expuestos por períodos prolongados a niveles de concentración mucho más altos que en el entorno común, en estos se han registrado casos de bronquitis crónica, reducción de la función pulmonar, o cáncer en pulmones y en senos nasales en casos de personas expuestas a ambientes con concentraciones superiores a los 10 mg-Ni m^{-3} en presencia de compuestos de níquel que resultan difíciles de disolver (ATSDR, 2005).

1.2. Muestreo pasivo y técnica DGT

La aplicación de los muestreadores pasivos es un método innovador utilizado en la monitorización medioambiental para evaluar la presencia y concentración de diversos contaminantes en distintos medios, como el aire, el agua y el suelo. Estos dispositivos funcionan permitiendo que los analitos objetivo se pre-concentren en un material absorbente durante un periodo de tiempo específico, proporcionando una concentración media de los analitos en

función del tiempo. Este tipo de muestreadores han sido objeto de gran atención en los últimos años debido a sus numerosas ventajas, como su simplicidad en la aplicación en campo, rentabilidad y capacidad para proporcionar mediciones significativas de la exposición a los contaminantes objeto de interés.

Por otro lado, los muestreadores pasivos también presentan importantes limitaciones. Aunque algunos pueden ser adecuados para detectar concentraciones muy bajas de contaminantes, una de las principales limitaciones es que la sensibilidad de los métodos dependerá del material sorbente y del tiempo de despliegue dentro del medio. Adicionalmente, las mediciones pueden verse significativamente influidas por factores ambientales y biológicos, tal como la variación de la temperatura, la formación de biofilm o la bioincrustación, que pueden afectar a la precisión y fiabilidad de las mediciones.

A pesar de estas dificultades, los muestreadores pasivos han demostrado ser herramientas valiosas en la investigación medioambiental, especialmente en el campo del análisis de metales traza. Una de estos métodos es la técnica de gradiente de difusión en capa fina (DGT), que se ha utilizado ampliamente para la medición de especies metálicas lábiles en agua, sedimentos y suelos. En esta introducción, se presenta a continuación la revisión titulada *"Diffusive gradients in thin films for the measurement of labile metal species in water and soils: a review"*, en la que se presenta una visión completa de la técnica DGT, sus aplicaciones, ventajas y desventajas, y su potencial para

avanzar en nuestra comprensión de la especiación y biodisponibilidad de los metales en diversas matrices ambientales. Se espera que esta revisión se convierta en un punto de referencia para estudiantes, investigadores y profesionales que deseen hacer uso de los métodos de la técnica DGT para hacer frente a los retos medioambientales actuales.

1.2.1. Publicación 1: Diffusive gradients in thin films for the measurement of labile metal species in water and soils: a review

REVIEW

Diffusive gradients in thin films for the measurement of labile metal species in water and soils: a review

Siday Marrugo-Madrid[1] · Marta Turull[1] · Hao Zhang[2] · Sergi Díez[1]

Abstract

The determination of the concentration of an environmental pollutant is not sufficient to assess the related health risk because this pollutant may not be bioavailable. Therefore, methods to determine pollutant bioavailability are more relevant to assess toxicity than measuring the total concentration. For instance, the diffusive gradient in thin films (DGT) is an in situ dynamic technique used to measure the concentration of labile compounds in the environment. Here we review the latest developments achieved in speciation and bioavailability of metals and metalloids using this technique. We detail the technique, common binding agents and diffusive gels. We give laboratory procedures to prepare the gels, and we explain calculations using the DGT-induced fluxes in soils (DIFS) modeling. DIFS models can predict the resupply capacities from soils to porewater, and the uptake of trace elements by plants. Procedures for in situ field deployments, including issues of biofilm growth, are also discussed.

Keywords Passive sampling · Trace metals · Speciation · Bioavailability · Binding layer · Diffusive layer · Environmental field deployment

Abbreviations

APA	Agarose cross-linked polyacrylamide
DGT	Diffusive gradient in thin films
EtHg	Ethylmercury
MeHg	Methylmercury
RDL	Restricted diffusive layer

Introduction

Most of the inorganic chemical pollutants, e.g., trace metals and metalloids, are usually persistent on the Earth's surface and originate mainly from natural and anthropogenic sources, including volcanic eruptions, mining, industrial processes, agriculture. They can bioaccumulate and biomagnificate in organisms. Metal toxicity, including its considerable risks in the environment and human health, has been widely studied (Díez 2008; Tchounwou et al. 2012; Liu et al. 2013b; Jaishankar et al. 2014; Tóth et al. 2016; Rodríguez and Mandalunis 2018; Herrera-Herrera et al. 2019; Marrugo-Negrete et al. 2020; Pinzón-Bedoya et al. 2020). At this point, it is important to remark that there are two types of metals focusing on its toxicity: on one side metals, such as Cd, Pb and Hg, which are not essential for organisms, and could cause serious damages in neurological, renal, cardio-vascular and reproductive systems and genetic effects even at relative low concentrations. On the other hand, metals like Fe, Zn, Cu and Se, among others, have an essential role in the human health, and some of them are also important in the production and protection of DNA and damage caused by free radicals and non-essential metals. It is well known that the determination of total metal concentration is not a good indicator for metal availability for the organisms because toxicity is directly dependent on the bioavailable fraction of metal and this, in turn, of the metal speciation and its mobility in waters, soils, sediments and air.

Although with several exceptions, the free ion activity model states that the free metal ion concentration is the determining factor in metal uptake, and the competition between metal ions at this biotic surface is accounted for the biotic ligand model (Kalis 2006).

✉ Sergi Díez
   sergi.diez@idaea.csic.es

[1] Environmental Chemistry Department, Institute of Environmental Assessment and Water Research, IDÆA-CSIC, 08034 Barcelona, Spain

[2] Lancaster Environment Centre, Lancaster University, Lancaster LA1 4YQ, UK

These models have helped scientists to understand the bioavailability as the metal fraction assimilated by an organism causing a physiological response in it. Besides that, models determine (1) the physico-chemical component characterized by sorption/desorption processes, which control metal mobility in soils and determinates the "chemical availability" of metals; and (2) the biological component characterized by a physiologically driven uptake process of a specific biological receptor (Peijnenburg and Jager 2003). Total metal concentration, pH, redox, speciation, mobility and the amount of organic matter are the main factors that directly influence the bioavailability. Likewise, it is important to take into account the environmental media, since the dynamics of metals are different in aqueous media compared to soils, where other factors, such as soil type, porosity and cation exchange capacity, influence metal bioavailability (Kalis 2006).

As briefly noted above, speciation was identified years ago as one of the factors that most influences bioavailability; however, more studies are needed to understand what metal species are responsible for the final interaction with the organism. Speciation has been defined by the International Union of Pure and Applied Chemistry as the distribution of an element among chemical specific form such as isotopic composition, electronic or oxidation state and/or complex or molecular structure in a system (Feldmann et al. 2014; Templeton and Fujishiro 2017). For example, mercury (Hg) may be present in the environment in three different states: mercuric (Hg^{2+}), mercurous (Hg_2^{2+}) and elemental (Hg^0) (WHO 2000), of which the dissolved Hg^{2+} fraction is considered the most available form for subsequent biogeochemical transformations. Besides that, Hg^{2+} can be bound to one or two carbon atoms, naming alkylated forms, such as methylmercury (MeHg) and ethyl mercury as the most common species. However, bioavailability depends not only on the chemical species, but also on cellular interaction with both Hg^{2+} and MeHg, by a mechanism not yet completely understood (Bratkič et al. 2019). For this reason, chemical speciation techniques have been developed in order to measure only a certain fraction of the total metal concentration, i.e., the bioavailable fraction. Based on the free ion activity model, some of the techniques used are only focused on the determination of the free metal ion concentration, like equilibrium ion-exchange technique (Fortin and Campbell 1998), the Donnan membrane technique (Temminghoff et al. 2000), Permeation Liquid Membrane (Parthasarathy et al. 2001) and some electrochemical techniques, such as square wave anodic stripping voltammetry (Ure and Davidson 2002) or direct potentiometric measurements (Rachou et al. 2007). Nevertheless, chemical lability is considered as a proxy for bioavailability too. Labile metal fractions are often the main target, as they contain free ions and easily dissociable

complexes that may be more susceptible to interact with aquatic organisms, entering trophic chains (Fairbrother et al. 2007). Consequently, speciation techniques have been developed focused on determining the labile fractions of a metal, like gel-integrated micro-electrodes (Pei et al. 2000), stripping chronopotentiometry (Van Leeuwen and Town 2002), competing ligand exchange methods (Apte et al. 2005) and the dynamic technique diffusive gradients in thin films (DGT) (Davison and Zhang 1994). DGT is also considered as a passive sampling technique for monitoring.

According to that, passive sampling techniques are considered as an alternative method to traditional sampling techniques (Fernández-Gómez et al. 2012b), which offers high potential as a profitable monitoring tool, avoiding many of the disadvantages of active sampling, including preparation of related samples. In addition, passive sampling has some benefits, such as providing time-averaged contaminant concentrations during operation periods (hours to weeks), serving as an in situ enrichment procedure and protecting analytes from degradation during field transport to the laboratory and storage.

In this context, the DGT technique has proven to be a wide and versatile strategy to better understand the metal speciation. Its simplicity, ease of use during the in situ deployment in the field and its applicability to different environmental matrices and the capability for measuring a wide range of target compounds make this technique a good option for environmental studies. In addition, it is possible to distinguish between labile inorganic and organic species varying the diffusion gel pore size of the DGT devices (Fernández-Gómez et al. 2012b).

It is now nearly 30 years since the invention of the technique of DGT, and some reviews have already emerged. Previous reviews have been focused in different topics such as phosphorus and metals in sediments and soils (Zhang et al. 2014), organic DGT (Guibal et al. 2019), different methods used for the determination of single species (Pesavento et al. 2009), trace metals and accumulation/response by animals (Eismann et al. 2020), metals in waters (Menegário et al. 2017), theoretical approaches and numerical simulations (Galceran and Puy 2015) as well as general reviews devoted to understanding the progress on the use of DGTs (Davison and Zhang 2012; Zhang and Davison 2015; Li et al. 2019). To the best of our knowledge, this review provides a comprehensive overview of DGT passive sampler for metals in waters and soils from its first report in 1994 to the present. Theory, configurations, field deployments procedures and applications of the sampler device and advantages and challenges of DGT technique are detailed and discussed. This review is organized in an easy-to-use format to help scientists to choose the most suitable device for a particular trace element. A list with up to 400 references including all the

published studies from 1994 until 2020 for the determination of a single or multiple trace metals categorized in water and soils is given.

Concepts and theory of diffusive gradient in thin films

The diffusive gradient in thin film (DGT) technique was developed in 1994 by Hao Zhang and William Davison at the Lancaster University, UK, and was first designed for in situ determination of trace metals in water (Davison and Zhang 1994). Since then, this technique has increased its capacity to determine many other elements and compounds, including nutrients (Cai et al. 2017), radionuclides (Leermakers et al. 2016), rare earth elements (Yuan et al. 2018) as well as in further environmental matrices such as sediments and soils.

Therefore, the DGT allows in situ evaluation of labile fractions and by approximation, bioavailability of metal species in aqueous environments, including natural waters (Zhang et al. 1998; Clarisse et al. 2009; Lucas et al. 2012; Turull et al. 2017a, 2018; Bratkič et al. 2019; Gao et al. 2019c), sediments (Harper et al. 1998, 2000; Gao et al. 2009; Yin et al. 2014) and soils (Docekalová et al. 2012; Song et al. 2015; Turull et al. 2019a, b; Babalola and Zhang 2021), based on the behavior of the labile species in the diffusive layer is similar to the behavior in the proximity of biological membrane (Clarisse et al. 2012; Amirbahman et al. 2013; Fernández-Gómez et al. 2015). The DGT passive sampler houses a binding gel and a diffusive gel protected by a membrane filter, that permits the diffusion of free ions and labile complexes through the diffusive layer that are irreversibly uptake by the specific binding layer. The final objective of this technique is to accumulate the target analyte in the binding layer over time following the Fick's first law of diffusion through the diffusive layer (Davison and Zhang 1994). Thus, the speciation of metals using DGT devices depends mainly on two effects: the difference in the diffusion coefficients and the difference in the affinity of the target species with the binding agent (Fernández-Gómez et al. 2012b).

The theoretical foundations for the use of DGT technique in aqueous solutions has been extensively documented (Zhang and Davison 1995; Lehto et al. 2006; Fernández-Gómez et al. 2012b; Shiva et al. 2016; Xu et al. 2020). The DGT technique is based on Fick's first law of diffusion, which relates the diffusive flux to the gradient of the concentration. The DGT device is composed by a binding layer that consists of a selective resin usually fixed in polyacrylamide gel (Zhang et al. 1998; Österlund et al. 2010). As can be seen in Fig. 1, this binding layer is separated from the bulk solution by a diffusive layer with a specific thickness (Δg). The layer between the filter membrane and the solution where ions are transported
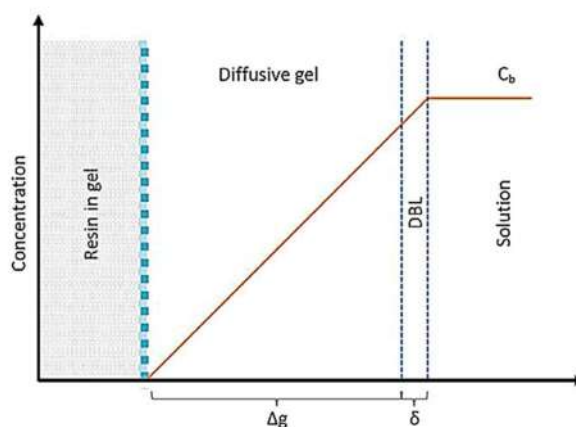
Fig. 1 Concentration of ionic species (C_b) through the diffusive layer in contact with aqueous solution. The diffusive gradients in thin film device is composed by a binding layer consisting of a selective resin embedded in a gel which is separated from the bulk solution by a diffusive layer or diffusive gel with a specific thickness (Δg). The layer between the filter membrane and the solution where ions are transported by molecular diffusion is called diffusive boundary layer (BDL). Adapted from Zhang and Davison (1995)

by molecular diffusion is called diffusive boundary layer (BDL). Since a concentration gradient is established in the diffusion layer, then the concentration is equal to the bulk concentration at the filter membrane/water interface (Fig. 1).

In an early study, Zhang and Davison (1995) established the basis to calculate concentrations of labile species using DGT devices. According to the Fick's first law, the flux goes from high concentration to low concentration, with a magnitude that is proportional to the concentration gradient (1). In this equation, J is the flux (mol cm^{-2} s^{-1}), D is the diffusion coefficient (cm^2 s^{-1}) and dC/dx (mol cm^{-4}) is the concentration gradient because C is the concentration (mol cm^{-3}) and x is the distance. This gradient induces a constant diffusion flux, which could be different depending on factors such as temperature, physical properties of the gel and concentration of labile metal in the bulk solution.

$$J = D\frac{dC}{dx} \qquad (1)$$

If dC represents the variation of free concentration of metal in the bulk solution (C_b) with respect to free concentration of metal in the resin gel layer (C'), then it could be expressed as ($C_b - C'$). If the free metal ions are in a rapid interaction with the resin, with a large binding constant, C' in effectively zero providing the resin in not saturated. In addition, the thickness of the diffusion layer (Δg) and the DBL thickness (δ) may be considered as x. If δ is negligibly small compared to Δg, the flux could be calculated as:

$$J = D \frac{C_b}{\Delta g} \quad (2)$$

According to the flux definition, the total mass of the analyte (M) diffused through an area (A), after given time (t), could be calculated as $J = M/At$. After the DGT device is deployed and retrieved, the binding layer is analyzed and the M could be determined using the most appropriate analytical techniques for each metal. Thus, from Eq. 2, the metal concentration in the bulk solution could be quantified by:

$$C_b = \frac{M\Delta g}{DAt} \quad (3)$$

In practice, DBL could include the effective δ in Eq. 4, as follows:

$$C_b = \frac{M(\Delta g + \delta)}{DAt} \quad (4)$$

The total mass of analyte accumulated on the resin gel may be extracted through elution of the gel using an appropriate volume of eluents (V_e) (e.g., HNO_3). Knowing the concentration of the analyte in the eluent (C_e), the elution factor (f_e) and the volume of the resin gel (V_g), M could be calculated by Eq. 5:

$$M = C_e \frac{(V_g + V_e)}{f_e} \quad (5)$$

Experimentally, A, t and Δg could be measured, and D is the value of the molecular diffusion coefficient in water at a given temperature. A calibration plot of M/C_b versus t could be used to calculate the value of D (Fernández-Gómez et al. 2012a, b; Turull et al. 2017a). Since the temperature influences the diffusion in the gel, D must correct the deployment temperature, T (Zhang and Davison 1995):

Fig. 2 Structure and assembly direction of a piston-type sampling device commonly used for the application of the diffusive gradients in thin film technique in aquatic and soil systems. The sampler consists in **a** the piston; **b** the binding layer; **c** the diffusive gel; **d** the membrane filter; and **e** the cap

components inside the DGT sampling device are shown in Fig. 2, including a binding layer (b), which is a resin gel supported in the base, responsible for the accumulation of the analytes; a diffusive gel (c) which has a composition up to 95% of water and allows analytes pass through by diffusion; and a filter membrane (d) to protect the gels. Different configurations of these layers are used according to the thickness of each one. Nevertheless, the most common configuration used is the configuration of binding layer (0.4 mm thick), a agarose cross-linked polyacrylamide (APA) diffusive gel (0.8 mm thick) and a 25-mm-diameter polyethersulfone membrane filter 0.45 μm pore size (0.014 mm thick), for a total thickness of 1.34 mm (Jolley et al. 2016). For other type of configurations, another diffusive gel should be placed to compensate the final thickness if is less than 1.34 mm. In this sense, it should be taken into account that the APA gel during the hydration step has an expansion factor of 1.6, and therefore the initial gel is thinner (Fernández-Gómez et al. 2011; Turull et al. 2017a).

$$\log D_T = \frac{1.37023(T - 25) + 8.36 \times 10^{-4}(T - 25)^2}{109 + T} + \log \frac{D_{25}(273 + T)}{298} \quad (6)$$

where D_{25} is the diffusion coefficient at the deployment time at 25 °C.

Device and components of diffusive gradient in thin films

In water, the type of diffusive gradient in thin film (DGT) sampler used is the piston-type device (www.dgtresearch.com) as it is shown in Fig. 2. The device consists in a DGT piston (base) (a) and a DGT cap (e) with an exposure area of 3.14 cm^2 (Jolley et al. 2016; Turull et al. 2017b). Other

Binding agents

A potential binding agent for determining an analyte should be chosen taking into consideration four key characteristics: (1) the binding strength, which is represented by an equilibrium constant for the specific analyte; (2) the intrinsic binding capacity, which relates to the number of sites able to interact with analyte species; and (3) the competition effects, due to the presence of other ions with similar binding strengths (Bennett et al. 2016a). Diverse binding agents have been used to analyze many trace metals (including cations and oxyanionic metals) and other species, such as sulfide or radionuclides (Table 1). Moreover, mixed binding layers have been developed to

Table 1 Binding agents and elements used to study some trace metals with the diffusive gradients in thin film technique

Analyte(s)	Binding agent	Eluent	References
THg/MeHg	3-Mercaptopropil functionalized silica	Direct analysis	Fernández-Gómez et al. (2011, 2014), Turull et al. (2019a)
	Spheron-Thiol	Direct analysis	Diviš et al. (2010)
	Amberlite GT73 Duolite GT73	Direct analysis	Diviš et al. (2010), Pelcová et al. (2014)
	Iontosorb AV-IM	Direct analysis	Diviš et al. (2010)
	Ambersep GT74	Direct analysis	Pelcová et al. (2014)
	Tulsion CH-95	0.1 M HCL + 2% thiourea	Ren et al. (2018)
	Saccharomyces cerevisiae	0.6 M HCl	Tafurt-Cardona et al. (2015)
Divalent and trivalent ions	Chelex-100	2 M HNO_3	Zhang and Davison (1995)
Rare earth elements	Chelex-100	2 M HCl	Yuan et al. (2018)
Cu, Cr, Cd, Mn, Ni, Pb, Zn	MMT[a]	1 M HNO_3	dos Anjos et al. (2017)
Cu, Cd, Co, Mn, Ni, Pb, Zn, Hg	Whatman P81	2 M HNO_3	Larner and Seen (2005)
Cu, Cd, Co, Ni, Zn, Pb	SPR-IDA[b]	1 M HNO_3	Gao and Lehto (2012
Cr	N-methyl-D-glucamine	1 M HNO_3	Pan et al. (2015)
Au	Activated carbon	Aqua regia	Lucas et al. (2012)
As, Sb, Mo, V, W	Ferrihydrite	1.4 M HNO_3 + 0.1 M HF	Österlund et al. (2010)
As	Amberlite IRA 910	1.2 M HCl	Rolisola et al. (2014)
As, Se	Metsorb (TiO_2)	1 M NaOH	Bennett et al. (2010)
As, Sb	3-Mercaptopropil functionalized silica	H_2O_2 + NaOH	Bennett et al. (2016b)
U	MnO_2 and Metsorb	1 M H_2O_2/HNO_3	Turner et al. (2012)
Tc	TEVA resin[c]	4 M HNO_3	French et al. (2005)

THg total mercury, *MeHg* methylmercury

[a]Natural clay mineral Montmorrilonite (MMT)

[b]Suspended particulate reagent-iminodiacetate (SPR-IDA)

[c]Trialkyl methylammonium nitrate (TEVA)

perform the determination of a wider range of analytes such as Amberlite IRP69/ferrihydrite to determine P and K (Zhang et al. 2013), Chelex–Metsorb to determine Ni, Cu, Mn, Cd, Co, Mo, Sb, Pb, As, W, V and P (Panther et al. 2014) or Chelex-100-ZrO_2 to determine P, Fe and As (Sun et al. 2015).

The binding agents are usually quasi-homogeneously incorporated into a gel matrix to form the binding layer. Chelex-100 resin was the first binding agent used to measure trace metals by DGT technique because of its advantage on determining a large amount of them, including Ni, Zn, Cu, Mn, Cd, Co, Pb, Fe and Al. This commercial resin has a high selectivity for transition metals over alkali and alkaline earth metals due to the fact that it contains functional groups of iminoacetic acid, thus avoiding analytical interferences in the measurement of trace metals in natural waters (Zhang and Davison 1995). From there, other ion-exchange binding agents have been studied alternatively for the determination of trace metals using the DGT technique, such as the cellulose phosphate-based membrane Whatman P81 (Larner and Seen 2005), the suspended particulate reagent-iminodiacetate resin (SPR-IDA) (Gao and Lehto 2012) and the natural clay mineral montmorillonite (MMT) (dos Anjos

et al. 2017). In general, ion-exchange binding agents are widely used in the DGT technique due to their easy preparation, flexibility and mechanical resistance, compared to other types of binding agents, such as liquid binding phases.

The Hg-determination by the DGT technique has been widely validated since mercury is a global pollutant that affects human and ecosystem health. Docekalová and Diviš (2005) compared the efficiencies of Chelex-100 and Spheron-thiol resins in the determination of Hg(II), finding that Spheron-thiol showed a greater and stronger affinity with mercury species that bind to the thiol (–SH) groups. Although, other thiol functionalized resins used in the binding layer have shown high affinity and selectivity with mercuric species. Later, other studies (Fernández-Gómez et al. 2011, 2014; Clarisse et al. 2012; Turull et al. 2017a, 2019a) have demonstrated the efficacy of 3-mercaptopropil functionalized silica resin as a binding agent in the Hg-determination by the DGT technique in different environmental matrices. The ion exchange resins Amberlite GT73 (also known as Duolite GT73) (Diviš et al. 2010) and Ambersep GT74 (Pelcová et al. 2014), and the functionalized

macroporous cross-linked polystyrene (Tulsion CH-95, (Ren et al. 2018) can measure several mercury species, with a high adsorption capacity and elution efficiency for Hg(II) and MeHg. In general, the effects of competition between ions with similar binding forces are more probable in binding layers that are based on adsorption or ion-exchange mechanisms compared to those that are based on complexation. In order to choose, a suitable binding agent is also important to consider the binding force, the binding sites available to interact with the analyte to be uptake, and the particle size that allows simple and uniform incorporation into the gel matrix.

Diffusive gels

The hydrogels used in the DGT technique are highly hydrophilic polymers with an intermediate structure between solid and liquid, with polar functional groups that allow them to absorb water and expand their size containing up to 95% of water. Determined by the precise composition, hydrogels can range from a viscous to a more rigid appearance, although all of them are typically flexible and elastic. Hydrogels represent the diffusion layer in the DGT device, being the transport of target analytes from the bulk solution to the binding layer by diffusion as the main function, without interfering with the determination of the target analyte by binding to it (Davison and Zhang 2016).

Various polymers have been applied as diffusion layers in the DGT technique, among which three types of gel stand out for being the most commonly used: polyacrylamide with agarose-derivative cross-linker (APA) (Zhang and Davison 1995; Fernández-Gómez et al. 2014), agarose (Docekalová and Diviš 2005) and polyacrylamide cross-linked with bis-acrylamide gels (Shiva et al. 2015; Turull et al. 2019a).

The most used diffusive layer is APA hydrogel, which has an open pore size larger than 5 nm allowing the diffusion of molecules with molecular weights $< 10^6$ (i.e., fulvic acid and some of the humic acid) as well as its advantage of retaining stability in the range of pH 2–9 after 3.2 times swelling due to hydration (Wang et al. 2016b). Some studies have been described the protocol for its preparation (Fernández-Gómez et al. 2011; Turull et al. 2017b), which consists on the addition of the cross-linker and acrylamide (or agarose derivative) to the water, followed by the addition of N,N,N',N'-tetramethylethylenediamine solution, which catalyzes the reaction and the ammonium persulfate, which plays the role of initiator of the reaction. The polymerization is carried out at 42–45 °C for 45 min approximately, resulting in a layer which contains 15% monomer and 0.3% cross-linker, although the cross-linker structure of the commercial product is still unknown. Even after an in-depth washing during the preparation, the APA gel maintains a positive charge which interacts electrostatically with the analytes, interfering with the effective diffusion of metals with low ionic strength due to the formation of the Donnan potential. This electrostatic interaction can be negligible when the ionic strength is greater than 1 mM because of the low charge density in the gel (Zhang and Davison 1999; Wang et al. 2016b). Nevertheless, although the existence of a Donnan potential is often mentioned in the results of cation diffusion through the APA gel, this effect is highly dependent on the pH at which the DGT sampling device is deployed. Negative charges for APA gel are reported in the literature, more specifically, on negatively charged acrylate functions created during the hydrolysis of acrylamide (pKa = 4.25) (Li et al. 2002a; Pommier et al. 2021).

Agarose gel is another standard diffusive layers widely used in DGT technique to determinate inorganic and organic analytes. Agarose is a polysaccharide, generally extracted from certain red seaweed of the genera *Gellidium* and *Gracillaria*. It is a linear polymer formed by repeating units of agarobiose, which is a disaccharide made up of D-galactose, 3,6-anhydro-L-galactopyranose and the lack of sulfate groups. The agarose gel has binding sites that resemble sulfonic functional groups, which are responsible of the complexation with trace metals, and negatively-charged pyruvic functional groups which represent the majority of binding sites in the gel and attractive interactions with cations and repulsive with anions, due to the formation of the Donnan potential (Wang et al. 2016b). The strength of these interactions between the gel and the ions decreases with increasing ionic strength. The lowest ionic strength capable of producing steady-state DGT flux is 0.1 mM for MeHg (Gao et al. 2014), 1.0 mM for MeHg and Hg (Hong et al. 2011) and 5.0 mM for Hg (Colaço et al. 2014). Further, in a comparison between agarose and polyacrylamide gels for the Hg determination using Chelex-100 as a binding layer, the agarose gel showed a lower absorption of Hg compared to the polyacrylamide gel. However, when diffusive polyacrylamide gel was used in DGT units in the same study, it was difficult to interpret the findings due to a possible competition for Hg ions between polyacrylamide gel and Chelex-100 (Docekalová and Diviš 2005; Gao et al. 2011). In another comparative study between agarose and APA gels, Fernández-Gómez et al. (2014) observed statistically significant differences between diffusion coefficients values of MeHg for agarose gel in DGT units in the absence and presence of dissolved organic matter (3.15×10^{-6} and 2.68×10^{-6} cm^2 s^{-1}, respectively), and also for APA gel in DGT units (2.49×10^{-6} and 1.69×10^{-6} cm^2 s^{-1}, respectively). MeHg diffusion was higher on agarose gel with and without dissolved organic matter in comparison with those observed in APA gel. Even so, DGT based on APA gel seems to be a better choice for eutrophic waters, when the monitoring is in environment with very low concentrations of MeHg, considering its slightly higher uptake capacity.

A polyacrylamide cross-linked with bis-acrylamide gel (N,N'-methylene-bis-acrylamide) is the third type of gel used in the DGT technique consisting on two acrylamide molecules linked through their aminocarbonyl groups, and in comparison with the previous two gels, this is much more fragile and its pore size is smaller (~ 1 nm), so it is usually called restricted gel or restricted diffusive layer (RDL). The smaller pore size affects the chemical species that can diffuse through the gel, allowing only free ions and small inorganic complexes to pass through and leaving out larger molecules such as organic complexes (Österlund et al. 2010; Shiva et al. 2015). According to the above mentioned, when using RDL, the difference in diffusion coefficient between the gel and the filter is larger than when using open pore (Österlund 2010), and therefore Eq. 4 can be modified to Eq. 7 as follows:

$$C_b = \frac{M}{At}\left(\frac{\Delta_{gel}}{D_{gel}} + \frac{\Delta_f}{D_f}\right) \qquad (7)$$

The main difference from Eq. 4 is that the thickness of the diffusion layer, Δg, is divided into Δ_{gel} and Δ_f, corresponding to the diffusive gel and membrane filter thickness, respectively, and D_f is the diffusion coefficient in the membrane filter.

Filter membrane

The most commonly used filter membranes have a pore size of ~ 0.45 µm. The most commonly used filter membranes are: polyvinylidene, cellulose nitrate, cellulose acetate and hydrophilic polyethersulfone filter membranes (Li et al. 2019). This filter protects the diffusion and binding layers inside the DGT device from possible contamination caused by large particles, or simply contains the gels to prevent damage or loss of these during the deployment of the DGT devices. However, they may be susceptible to biofilm formation caused by the microorganism colonization during the deployment of DGT devices in environmental matrices

(Fig. 3). This biofilm must be taken into consideration since it could absorb analytes, restricts absorption of them or act as an extension of the diffusion layer, leading to errors in the determination of analytes. Uher et al. (2012) evaluated the effect of biofilm on the determination of trace metals (Ba, Cd, Co, Cr, Cu, Mn Ni, Pb and Zn) and their results showed that the presence of biofilm in DGTs did not significantly affect diffusion of all metals. Thus, an interaction of metallic species with the biofilm in different degrees of specificity was suggested, based on the biological activity of the microorganisms that constitute the biofilm. Likewise, Díez and Giaggio (2018) showed that Hg-labile uptake in DGT devices had been reduced by up to 35% when deployment times in the field were longer, so a pretreatment of the filter membranes with a silver nanoparticle biocide was implemented. The results demonstrated the effectiveness of silver nanoparticle biocide by showing statistically significant differences between the Hg-concentration in DGT devices with and without treatment, and additionally, the Hg concentrations in treated DGT devices coincided with the theoretically calculated concentrations. However, despite the good results obtained with anti-biofilm agents, these pretreatments do not prevent the clogging of the filter membrane by suspended particulate matter (see last picture in Fig. 3), so they are not widely used, and instead, an optimization of the deployment time is chosen (Li et al. 2005a; Pichette et al. 2009; Österlund et al. 2016; Díez and Giaggio 2018). In this sense, dynamic numerical models used to understand DGT flux and explore the necessary deployment time of DGT devices have been examined in a review by Davison and Zhang (2012), as well as other basic aspects, such as geometry, competition effects and the kinetic limitations of the DGT technique.

In summary, in water and soil the most user sampler is the piston-type device composed of APA as diffusive gel and, depending on target trace metals, different ion-exchange resins as binding layer. Usually, filter membranes of 0.45 µm pore sizes are used as a protective layer to prevent contamination to hydrogels. Clogging of the filter membrane by suspended particulate matter and biofilm growth is difficult

Fig. 3 Growth of biofilm in diffusive gradients in thin film devices deployed for several days in a eutrophic river water. Last picture shows biofilm and suspended particulate matter clogging the filter

to avoid and optimization of the deployment time is the best option.

Deployment of diffusive gradient in thin films in the field

For water and soil studies, the piston-type device is the most common device used to be deployed in freshwater, seawater and agricultural and/or contaminated soils.

Deployment in water

For water, the main objective is usually obtaining time-averaged concentrations of trace metals, whereas for soil the main target has been studying plant yield response to P fertilizers (Tandy et al. 2011; Zhang et al. 2013) and prediction of trace metals in plants (Zhang et al. 2004; Turull et al. 2019b).

General operation for deployments in the field include transportation of diffusive gradient in thin films (DGT) in individual clean sealed ziplock plastic bag containing few drops of 0.01 M NaCl/NaNO$_3$ solution, to maintain the devices in adequate humid and ionic strength conditions.

Once in the field, each unit is taken out from the bag and DGT is secure inside a sampling device and submerged at each sampling point. There are several designs to hold and suspend the samplers, one consists of a double methacrylate plate with round holes where DGTs can be attached (Clarisse and Hintelmann 2006; Uher et al. 2018) (Fig. 4a). The metacrilate plate could leave it submerged or fixed to two iron sticks using nylon string and stuck on the sediment
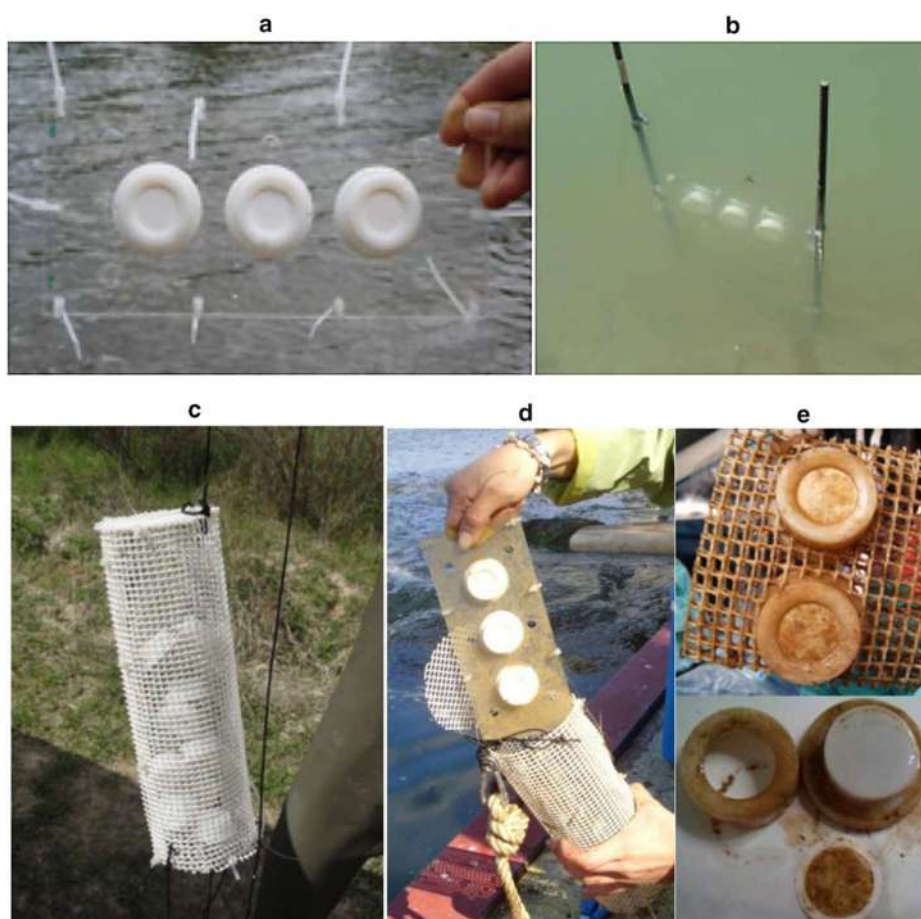
Fig. 4 Different designs for the deployment of diffusive gradients in thin films in the field. **a** Sampler in triplicate fixed in a double methacrylate plate, **b** sampling device driven into the river bed, **c** homemade baskets made of plastic mesh strips; **d** sampler in triplicate in the methacrylate plate put in a protective basket before deployment, **e** detail of the samples after 1-week deployment and dismantled device with suspended material adhered on the filter membrane

(Fernández-Gómez et al. 2012a) (Fig. 4b), or attached to plastic mesh strips with fishing line (Lucas et al. 2014). Moreover, in other studies, the DGT devices have been attached with fishing line to a buoy (Pichette et al. 2007; Clarisse et al. 2009). The most common design for DGT deployment in natural waters consist of put in the DGTs inside a homemade cylindrical basket made of a plastic net, which is anchored to a rope with a weight on one end and a buoy on the other (Turull et al. 2017b) (Fig. 4c). After retrieval, DGT units are rinsed with distilled water to stop diffusion and also to remove biofilm and suspended material adhered on the DGT filter.

Deployment in soil

For soil applications, the typical piston-type device can be deployed into soils by hand gently pressing after the soil is moistened (Zhang et al. 2004; Turull et al. 2019b). Depending on several studies, the water content could be adjusted either over 90% (Zhang et al. 2004; Turull et al. 2019a) or 70% of the maximum water holding capacity (Zhang et al. 2017a) for 48 h to ensure the equilibrium between fractions and soil (Yao et al. 2016a).

One of the most important uses of DGT devices in soil is to predict the bioavailability of metals to plants. To do that, it is the necessary concept of effective concentration (C_E), which is the concentration that should be present in the soil solution to supply the same mass of metal accumulated by DGT in the partially sustained case (Zhang et al. 2001). Only diffusion concentration is taken into consideration, which is the same process found in the rhizosphere of plants, and therefore C_E can be directly related to the uptake of the plant. To calculate C_E, a relationship between the mean interfacial concentration with the resupply solely by diffusion to the bulk concentration should be calculated as follows:

$$C_E = \frac{C_{DGT}}{R_{diff}} \tag{8}$$

R_{diff} is defined as the ratio of the concentration at the DGT interface to the concentration in the bulk soil solution and should be obtained by the numerical model DIFS (DGT-induced fluxes in sediments) (Sochaczewski et al. 2007).

The software 2D DIFS (version 1.2.3-3, 2005, Lancaster, U.K.) is available online (www.dgtresearch.com) and can be used to simulate values of R, labile distribution coefficient (Kdl) and the soil response time to depletion (Tc). Besides DGT measurements, the additional measurable parameters required for DIFS fitting are soil porosity (φ_s), diffusive gel porosity (φ_d) and thickness (Δg), the effective diffusion coefficient in the soil (D_s) and the diffusion gel (D_d) and deployment time (t).

In summary, DGT devices are normally put in cylindrical basket made of a plastic net for aquatic deployments, whereas for soil deployments, the piston-type device can be applied in the soil individually by pressing gently with the hand after wetting the soil. Moreover, DIFS models are necessary to get valuable data to know the kinetics resupply of solutes to porewater from soil, and therefore to later predict the uptake of metals to plants.

Applications in aquatic ecosystems

Natural waters show a wide variety of ions at different concentrations, as well as a wide range of physicochemical characteristics and parameters, of which it is important to consider such as pH, ionic strength, temperature, dissolved organic matter and total dissolved solids for the application of the diffusive gradient in thin film (DGT) technique. Likewise, it is also important to consider that the binding layers' effectiveness depends essentially on the environmental matrix where the DGT device is deployed. Most of the binding layers mentioned above have been applied only in freshwater, due to the high concentrations of potentially competing ions that are present in more complex matrices such as seawater. In this sense, Österlund et al. (2016) explain in detail how to design a successful DGT sampling program in freshwater, lakes, brackish and marine waters.

In this review, we aim to emphasize the huge number of trace metals that has been determined in different aquatic systems by the DGT technique, which are shown in Table 2. All these studies demonstrate the versatility of DGT passive samplers for the determination of individual trace metals as well as a simultaneous determination of several of them.

Applications in terrestrial ecosystems

Although the diffusive gradient in thin film (DGT) technique was initially developed as a passive sampling technique for water, over the years it has evolved to be applied in soils as well. The piston-type DGT device can also be deployed on wet soil, pressing it manually in such a way that the filter membrane is in contact with the soil slurry (Turull et al. 2019a). For the measurements of trace metals in terrestrial ecosystems by the DGT technique, the same influencing factors considered in aquatic systems should be considered such as the pore size of the gel, interaction between analyte-gel, effect of competition (including H^+) and the ionic strength. The principles and application of the DGT technique in soils are detailed by Lehto (2016), focusing mainly on the influence of solid phases adjacent to the DGT device in the interpretation of analyte measurement results, also considering the important morphological and biogeochemical of soils.

Table 2 Studies of the diffusive gradients in thin film technique applied in aquatic systems for the determination of different species of metals and metalloids (published works found in Web of Knowledge from its development in 1994 up to the present time in 2020)

	Studies in aquatic systems
Mercury species	
Total Hg/Labile Hg	Docekalová and Diviš (2005), Rodríguez Martín et al. (2006), Diviš et al. (2009, 2010), Roig et al. (2011), Fernández-Gómez et al. (2011, 2012a), Gao et al. (2011), Zhou et al. (2013), Colaço et al. (2014), Pelcová et al. (2014, 2017), Tafurt-Cardona et al. (2015), Senila et al. (2017a), Sierra et al. (2017), Turull et al. (2017a, b, 2018), Wu et al. (2017), Díez and Giaggio (2018), Schintu et al. (2018), Muresan et al. (2018), Noh et al. (2020), Reichstädter et al. (2020), Elias et al. (2020)
MeHg	Clarisse and Hintelmann (2006), Clarisse et al. (2009, 2012), Fernández-Gómez et al. (2014, 2015), Gao et al. (2014)
Hg(II)	Colaço et al. (2012), Wu et al. (2017), Tan et al. (2019b), Yao et al. (2020)
MeHg and Hg(II)	Cattani et al. (2009), Hong et al. (2011), Ren et al. (2018), Bratkič et al. (2019), Bretier et al. (2020)
Hg(II), MeHg, ethylmercury, phenylmercury	Pelcová et al. (2015)
Other trace elements	
1 element	
As	Panther et al. (2008a, b), Bennett et al. (2011), Österlund et al. (2012a), Sun et al. (2014b), Liu et al. (2016), Prieto et al. (2016), Senila et al. (2017b), Gorny et al. (2019), Tan et al. (2019a), Smolíková et al. (2020)
Cd	Bradac et al. (2009), Menegário et al. (2010), Fan et al. (2015)
Cr	Ernstberger et al. (2002b), Giusti and Barakat (2005), Chen et al. (2014), Guo et al. (2014), Pan et al. (2015), Devillers et al. (2016), Suárez et al. (2016), Yao et al. (2016b), Gao et al. (2019b)
Cu	Zhang and Davison (2001), Nierop et al. (2002), Luider et al. (2004), Kraal et al. (2006), Martin and Goldblatt (2007), Fan et al. (2009a), McGifford et al. (2010), Bourgeault et al. (2013), Ferreira et al. (2013), Knutsson et al. (2014), Pérez et al. (2015), Philipps et al. (2018a, b), Strivens et al. (2019, 2020), Macoustra et al. (2020)
Ni	Shafaei Arvajeh et al. (2013)
Pb	Scally et al. (2004), Van Der Veeken et al. (2008), Pescim et al. (2012), Sui et al. (2016)
Zn	Wang et al. (2009), Lourino-Cabana et al. (2011), Companys et al. (2018)
2 elements	
Al, Cu	Tonello et al. (2007, 2011)
Cd, Cu	Zhang and Davison (2000), Li et al. (2002a, b, 2005a, b), Peters et al. (2003), Warnken et al. (2005), Fan et al. (2009b), Davison et al. (2015)
Cd, Pb	Jakl et al. (2009), Reichstädter et al. (2020)
Cd, V	Mangal et al. (2016)
Cu, Ni	Österlund et al. (2012b)
Cu, Pb	Philipps et al. (2019)
Cu, Zn	Costa and Wallner-Kersanach (2013), Costa et al. (2013), Paller et al. (2019)
Ni, Zn	Zhang (2004)
Pb, Zn	Desaulty et al. (2015)
3 elements	
Al, As, Fe	Gontijo et al. (2016)
As, Sb, V	Li et al. (2020)
Cd, Co, Ni	Puy et al. (2014)
Cd, Cu, Mn	Denney et al. (1999)
Cd, Cu, Ni	Torre et al. (2000)
Cd, Cu, Pb	Fan et al. (2013), Sui et al. (2013)
Cd, Mg, Ni	Altier et al. (2019)
Cd, Ni, Zn	Uher et al. (2012)
Cu, Ni, Pb	Cleven et al. (2005)
Cu, Ni, Zn	Knutsson et al. (2013)

Table 2 (continued)

4 elements	
As, Cd, Cu, Ni	Buzier et al. (2014)
As, Mo, Sb, V	Zhang et al. (2017b)
As, P, Se, V	Price et al. (2013)
As, Se, V, Sb	Luo et al. (2010a)
Cd, Cu, Ni, Pb	Scally et al. (2006), Unsworth et al. (2006), Kawakami et al. (2008), Schintu et al. (2008), Slaveykova et al. (2009), Dakova et al. (2011), Marras et al. (2020)
Cd, Cu, Ni, Zn	Wallner-Kersanach et al. (2009), Huynh et al. (2010)
Cd, Cu, Pb, Zn	Webb and Keough (2002), Van Leeuwen et al. (2005), Balistrieri and Blank (2008), Gaabass et al. (2009), Schintu et al. (2010)
Cd, Mn, Pb, Zn	Nguyen et al. (2020)
Co, Cu, Ni, V	Hartland et al. (2011)
Cr, Cu, Ni, Zn	Smith et al. (2007)
Cu, Fe, Mn, Zn	Gimpel et al. (2003)
Cu, Mn, Ni, Zn	Forsberg et al. (2006)
Cu, Ni, Pb, Zn	Dunn et al. (2003, 2007), Han et al. (2013, 2014, 2016), Zhu and Guéguen (2016)
5 elements	
As, Cd, Cu, Mg, Mn	Colaço et al. (2012)
As, Cd, Cu, Pb, Zn	Huynh et al. (2012b)
As, Cr, Cu, Pb, V	Xu et al. (2019a)
As, Cu, Mn, Pb, Zn	Chen et al. (2013)
As, Mo, Sb, V, W	Österlund et al. (2010), Panther et al. (2013)
Cd, Co, Cu, Mn, Pb	Munksgaard and Parry (2003)
Cd, Co, Cu, Ni, Pb	Warnken et al. (2004), Garmo et al. (2008), Guéguen et al. (2011), Levy et al. (2012a), Gaulier et al. (2019), Cindrić et al. (2020)
Cd, Co, Mn, Ni, Zn	Omanović et al. (2015), Uher et al. (2017)
Cd, Cu, Fe, Ni, Zn	Stewart et al. (2016)
Cd, Cu, Ni, Pb, Zn	Rodríguez Martín et al. (2006), Sigg et al. (2006), Allan et al. (2007, 2008), Nyein Aung et al. (2008), de Souza et al. (2014), Wang et al. (2014b), Koppel et al. (2019), Yabuki et al. (2019)
6 elements	
Cd, Co, Cu, Mn, Ni, Pb	Hojaji (2012), Levy et al. (2012b), Vannuci-Silva et al. (2017)
Cd, Co, Cu, Ni, Pb, Zn	Sangi et al. (2002), Kim et al. (2016), Cindrić et al. (2017)
Cd, Cr, Cu, Ni, Pb, V	Schintu et al. (2018)
Cd, Cr, Cu, Ni, Pb, Zn	Diviš et al. (2007), Soriano-Disla et al. (2010)
Cd, Cu, Fe, Mn, Pb, Zn	Bradac et al. (2010)
Cd, Cu, Mn, Ni, Pb, Zn	Odzak et al. (2002)
Co, Cu, Mn, Ni, Pb, Zn	Almeida et al. (2012)
7 elements	
Ag, Cd, Cr, Cu, Ni, Pb, Zn	Vystavna et al. (2013)
Al, Cd, Co, Cu, Mn, Ni, Zn	Yabuki et al. (2014)
Al, Cd, Cr, Cu, Fe, Ni, Pb	Buzier et al. (2011)
As, Cd, Cr, Cu, Ni, Pb, Zn	Sierra et al. (2017)
As, Cd, Co, Mo, Ni, Sb, Zn	Schmukat et al. (2013)
As, Cu, Fe, Mn, Pb, Sr, U	Martin et al. (2019)
Cd, Co, Cr, Cu, Fe, Ni, Pb	Buzier et al. (2006)
Cd, Co, Cr, Cu, Mn, Ni, Zn	Bourgeault et al. (2010)
Cd, Co, Cr, Cu, Ni, Pb, Zn	Vystavna et al. (2012), Villanueva et al. (2013, 2015, 2016)
Cd, Co, Cu, Fe, Mn, Ni, Pb	Warnken et al. (2008), Baeyens et al. (2011)
Cd, Co, Cu, Mn, Ni, Pb, Zn	Larner and Seen (2005)
8 elements	
Al, Cd, Co, Cr, Cu, Ni, Pb, Zn	Devillers et al. (2017a)
Al, Cd, Co, Cu, Fe, Mn, Ni, Zn	Öhlander et al. (2012)

Table 2 (continued)

Al, Cd, Cu, Fe, Mn, Ni, Pb, Zn	Warnken et al. (2009)
As, Cd, Cr, Cu, Ni, Pb, Sb, Se	Devillers et al. (2017b)
Cd, Cr, Co, Cu, Mn, Ni, Pb, Zn	Uher et al. (2013, 2018), Dabrin et al. (2016)
9 elements	
Al, As, Cr, Co, Cu, Mn, Pb, Sn, Zn	Larner et al. (2006)
Al, Cd, Co, Cr, Cu, Fe, Ni, Pb, Zn	Liu et al. (2013a)
Al, Cd, Co, Cu, Fe, Mn, Ni, Pb, Zn	Warnken et al. (2007), Sherwood et al. (2009)
Al, Cr, Co, Cu, Mn, Ni, Pb, U, Zn	Agnelli et al. (2014)
Cd, Co, Cr, Cu, Fe, Mn, Ni, Pb, Zn	Dragun et al. (2008, 2015)
10+ elements	
Al, Cd, Co, Cr, Cu, Fe, Mn, Ni, Pb, Zn	Díaz et al. (2012)
	Garmo et al. (2003), Balistrieri et al. (2007), Casiot et al. (2009), Uribe et al. (2011), Roig et al. (2011), Panther et al. (2014), Shiva et al. (2016, 2017), Lucas et al. (2015), Shiva et al. (2015), Wang et al. (2016b, 2017b), dos Anjos et al. (2017), Schoyen et al. (2017), Cánovas et al. (2020)

Table 3 shows all the published studies applying DGT technique in soil for the determination of metals and metalloids. One of the most prominent applications is the comparison of the amount of metal uptake by plants vs the amount of this metal in adjacent soil by DGT devices, since understanding the metal bioavailability in agricultural soils is key for food security purposes. In this context, the studies developed in foods are outstanding, such as rice (Tian et al. 2008; Liu et al. 2012; Williams et al. 2012; Li et al. 2018; Ma et al. 2020; Peng et al. 2020; Wen et al. 2020), potatoes (Pérez and Anderson 2009a), spinach (Almås et al. 2006), onions (Yi et al. 2020) and lettuce (Koster et al. 2005; Cornu and Denaix 2006; Agbenin and Welp 2012; Turull et al. 2019b).

Studies have indicated that As, Cd, Cu, Zn and Pb are the most common trace metals and metaloids determined in soils by the DGT technique, which in some cases are determined simultaneously related to agricultural soils to predict their uptake in edible crops.

Conclusion

The diffusive gradient in thin film (DGT) technique has been continuously developed for more than 20 years, and the theoretical principles for its effective application in aquatic and terrestrial systems are well established. The development of the DGT technique has been of great importance due to the ease of application, versatility, wide range of analytes that can be determined by a single DGT deployment, even at very low concentrations (i.e., trace metals) in waters. Similarly, the great number of published studies that have been cited in this review indicates that the DGT technique is very useful for the measurement of the labile species of most elements allowing a fast, easy and relatively cost-effective detailed study of the bioavailability and speciation of metals and metalloids in waters

and soils. Later, great progress has been made in terrestrial systems, e.g., in agricultural soils, with the use of DIFS modeling that has opened the possibility of predicting the uptake of trace metals by plants, which in turn is key to the future of security food, just by analyzing the soil.

Although this technique has been developed continuously, however, significant challenges remain for the future development of DGT. Firstly, overcoming the interference to DGT measurements when applying in the field for long period of time is a big challenge since biofilms have been proved could affect analyte diffusion, as well as competition of other ions that also interfere diffusion and final adsorption performance in the binding gel. Likewise, it is necessary to unify the operating procedures for the assembly, deployment and treatment of samples of DGT devices in order to simplify comparison between different studies.

The development and implementation of new materials species-specific as binding layers is also a challenge that will let the determination of even more environmental pollutants/species, e.g., metals, nutrients or even organics. Moreover, while the process of creating a binding layer from a binding agent embedded in a gel matrix has facilitated the wide versatility of this technique, binding agents are often expensive. This could be compensated by using small quantities of them in binding layers' preparation, although not for deployment in high polluted environments as it would reduce the capacity of the DGT device. Nevertheless, it has also been presented as an obstacle for developing the DGT technique worldwide, especially in developing countries with high contamination levels and low investment in research. In addition, it should be considering the evaluation of inexpensive and easily accessible materials as possible binding agents to improve the accessibility of the DGT technique.

Finally, few studies have been conducted trying to understand the relationships between DGT determinations of trace elements and their absorption by different organisms;

Table 3 Studies of the diffusive gradients in thin film technique applied in terrestrial systems for the determination of different species of metals and metalloids (published works found in web of knowledge from its development in 1994 up to the present time in 2020)

	Studies in terrestrial systems
Mercury species	
Total Hg/Labile Hg	Liu et al. (2012), Senila et al. (2013), Hlodák et al. (2015), Ridošková et al. (2017, 2019), Ndu et al. (2018), Huu Nguyen et al. (2019), Pelcová et al. (2019)
MeHg and Hg^{2+}	Cattani et al. (2008)
Labile Hg and inorganic Hg	Turull et al. (2019a, b)
Other trace elements	
1 element	
As	Fitz et al. (2003), Mojsilovic et al. (2011), Moreno-Jiménez et al. (2013), Wang et al. (2014a, 2018a, b), Xu et al. (2014), Zhang et al. (2017a, 2019), Dai et al. (2018), Sun et al. (2018b), Zheng et al. (2019), An et al. (2020)
Cd	Pérez and Anderson (2009a), Song et al. (2015), Yao et al. (2016a, 2017), Wang et al. (2016a, 2017a), Gu et al. (2017), Dai et al. (2018), Gramlich et al. (2018), Wu et al. (2018), Li et al. (2018), Tian et al. (2018), Xu et al. (2019b), Ono et al. (2019), Wen et al. (2020), Yi et al. (2020)
Cr	Amezcua-Allieri et al. (2005a), Gao et al. (2020), Vogel et al. (2020)
Cu	Zhang et al. (2001), Ma et al. (2006), Zhao et al. (2006), Bravin et al. (2009, 2010, 2012), Amery et al. (2010), Garrido and Mendoza (2013), Le Forestier et al. (2017), Sun et al. (2018a)
Ni	Gao et al. (2018), Zhao et al. (2018)
Pb	Senila (2014), Xu et al. (2019c, d)
Zn	Degryse et al. (2003), Zhang et al. (2004), Sönmez and Pierzynski (2005), Sönmez et al. (2009, 2016), Gramlich et al. (2014), Sun et al. (2014a), Xu et al. (2018), Zhou et al. (2019), García-Gómez et al. (2020)
2 elements	
As, Sb	Ngo et al. (2016, 2020), Zhang et al. (2018)
As, Pb	Liang et al. (2014), Zhang et al. (2017c)
Cd, Cu	Cui et al. (2020)
Cd, Fe	Wang et al. (2020)
Cd, Ni	Pérez and Anderson (2009b), Luo et al. (2010b, 2014), Liu et al. (2018), Ma et al. (2020)
Cd, Pb	Zarrouk et al. (2014), Ridošková et al. (2017)
Cd, Zn	Almås et al. (2006), Cornu and Denaix (2006), Zhang et al. (2006), Muhammad et al. (2012), Williams et al. (2012), Li et al. (2014), Hoefer et al. (2015), Gramlich et al. (2017), Egene et al. (2018), Grüter et al. (2019)
Co, Ni	Gao et al. (2019a)
Cu, Pb	Fresno et al. (2017)
Cu, Zn	Nowack et al. (2004), Ahumada et al. (2011), Tella et al. (2016), Peng et al. (2020)
3 elements	
As, Cd, Pb	Tang et al. (2019)
As, Cu, Zn	Manzano et al. (2019)
As, Sb, Pb	Lomaglio et al. (2017)
Cd, Cu, Ni	Kovaríková et al. (2007), Senila et al. (2012)
Cd, Cu, Pb	Balistrieri and Blank (2008)
Cd, Ni, Zn	Ernstberger et al. (2005), Welikala et al. (2018)
Cd, Pb, Zn	Fischerová et al. (2005), Puschenreiter et al. (2013), Pavel et al. (2014), Cornu et al. (2016)
Cu, Ni, Pb	Amezcua-Allieri et al. (2005b)
Cu, P, Zn	Tandy et al. (2011)
4 elements	
As, Cd, Pb, Zn	Neu et al. (2018)
As, Cr, Cu, Zn	Hattab et al. (2014)
As, Cu, Pb, Zn	Bade et al. (2012a, b, 2013), Hattab-Hambli et al. (2016)
As, Fe, Mn, P	Chowdhury et al. (2018)
Cd, Cu, Mn, Zn	Grüter et al. (2017)
Cd, Cu, Ni, Pb	Docekalová et al. (2012)

Table 3 (continued)

Cd, Cu, Ni, Zn	Zhang et al. (1998), Ernstberger et al. (2002a), Black et al. (2011), Huynh et al. (2012a)
Cd, Cu, Pb, Zn	Nolan et al. (2005), Tian et al. (2008), Conesa et al. (2010), Agbenin and Welp (2012), Qiu et al. (2012), Bidar et al. (2019)
Cr, Cu, Ni, Zn	Ahumada et al. (2014)
Cu, Fe, Mn, Ni	Ruello et al. (2008)
5 elements	
Al, Cu, Cd, Ni, Zn	Li et al. (2015)
As, Cd, Cu, Pb, Zn	Huynh et al. (2012b)
As, Cd, Pb, Sb, Zn	Qasim et al. (2016)
Cd, Cr, Cu, Pb, Zn	Guo et al. (2016)
Cd, Cu, Ni, Pb, Zn	Hamels et al. (2014), Zhang et al. (2016), Guan et al. (2018)
6 elements	
As, Cd, Cu, Mn, Pb, Zn	Ciadamidaro et al. (2017)
As, Cd, Cu, Ni, Pb, Zn	Moreno-Jiménez et al. (2016)
As, Co, Cr, Cu, Mo, Zn	Hattab et al. (2015)
Cd, Co, Cu, Ni, Pb, Zn	Hooda et al. (1999)
Cd, Cu, Fe, Mn, Ni, Zn	Zhang and Davison (1995)
Cr, Cu, Fe, Mn, Pb, Zn	Lu et al. (2019)
9+ elements	
Al, Cd, Co, Cr, Cu, Fe, Mn, Ni, Zn	Chapman et al. (2012)
	Docekal et al. (2003), Jakl et al. (2015), Galhardi et al. (2020)

MeHg methylmercury

however, whether DGT represents the definitive bioavailable fraction in aquatic systems remains a matter of debate. Although the DGT data are very valuable to understand the biological process, many efforts should be done to link DGT values to biological responses under field conditions.

Authors' contributions SM-M writing original draft. MT helped in writing and contributing to original draft, review and editing. HZ helped in review of original draft. SD performed supervision and review of original draft, editing and revision.

Funding Not applicable.

Availability of data and material Not applicable.

Code availability Not applicable.

Declarations

Conflict of interest The authors declare that they have no conflict of interest.

Ethics approval Not applicable.

Consent to participate Not applicable.

Consent for publication Not applicable.

References

Agbenin JO, Welp G (2012) Bioavailability of copper, cadmium, zinc, and lead in tropical savanna soils assessed by diffusive gradient in thin films (DGT) and ion exchange resin membranes. Environ Monit Assess 184:2275–2284. https://doi.org/10.1007/s10661-011-2116-5

Agnelli M, Grandia F, Credoz A et al (2014) Use of diffusive gradients in thin films (DGT) as an early detection tool of low-intensity leakage from CO_2 storage. Greenh Gases Sci Technol 4:163–175. https://doi.org/10.1002/ghg

Ahumada I, Ascar L, Pedraza C et al (2011) Determination of the bioavailable fraction of Cu and Zn in soils amended with biosolids as determined by diffusive gradients in thin films (DGT), BCR sequential extraction, and ryegrass plant. Water Air Soil Pollut 219:225–237. https://doi.org/10.1007/s11270-010-0701-9

Ahumada I, Sepúlveda K, Fernández P et al (2014) Effect of biosolid application to Mollisol Chilean soils on the bioavailability of heavy metals (Cu, Cr, Ni, and Zn) as assessed by bioassays with sunflower (*Helianthus annuus*) and DGT measurements. J Soils Sediments 14:886–896. https://doi.org/10.1007/s11368-013-0842-8

Allan IJ, Knutsson J, Guigues N et al (2007) Evaluation of the Chemcatcher and DGT passive samplers for monitoring metals with highly fluctuating water concentrations. J Environ Monit 9:672–681. https://doi.org/10.1039/b701616f

Allan IJ, Knutsson J, Guigues N et al (2008) Chemcatcher® and DGT passive sampling devices for regulatory monitoring of trace metals in surface water. J Environ Monit 10:821–829. https://doi.org/10.1039/b802581a

Almås ÅR, Lombnæs P, Sogn TA, Mulder J (2006) Speciation of Cd and Zn in contaminated soils assessed by DGT–DIFS, and WHAM/Model VI in relation to uptake by spinach and ryegrass.

— 94 —

Chemosphere 62:1647–1655. https://doi.org/10.1016/j.chemo sphere.2005.06.020

Altier A, Jiménez-Piedrahita M, Uribe R et al (2019) Time weighted average concentrations measured with diffusive gradients in thin films (DGT). Anal Chim Acta 1060:114–124. https://doi.org/10.1016/j.aca.2019.01.056

Amery F, Degryse F, Van Moorleghem C et al (2010) The dissociation kinetics of Cu-dissolved organic matter complexes from soil and soil amendments. Anal Chim Acta 670:24–32. https://doi.org/10.1016/j.aca.2010.04.047

Amezcua-Allieri MA, Lead JR, Rodríguez-Vázquez R (2005a) Changes of chromium behavior in soil during phenanthrene removal by *Penicillium frequentans*. Biometals 18:23–29. https://doi.org/10.1007/s10534-004-5771-y

Amezcua-Allieri MA, Lead JR, Rodríguez-Vázquez R (2005b) Impact of microbial activity on copper, lead and nickel mobilization during the bioremediation of soil PAHs. Chemosphere 61:484–491. https://doi.org/10.1016/j.chemosphere.2005.03.002

Amirbahman A, Massey DI, Lotufo G et al (2013) Assessment of mercury bioavailability to benthic macroinvertebrates using diffusive gradients in thin films (DGT). Environ Sci Process Impacts 15:2104–2114. https://doi.org/10.1039/c3em00355h

An J, Jeong B, Jeong S, Nam K (2020) Diffusive gradients in thin films technique coupled to X-ray fluorescence spectrometry for the determination of bioavailable arsenic concentrations in soil. Spectrochim Acta Part B 164:105752. https://doi.org/10.1016/j.sab.2019.105752

Apte SC, Batley GE, Bowles KC et al (2005) A comparison of copper speciation measurements with the toxic responses of three sensitive freshwater organisms. Environ Chem 2:320–330. https://doi.org/10.1071/EN05048

Babalola B, Zhang H (2021) Diffusive gradient in thin film technique as tool for assessment of metal availability and kinetics of resupply in remediated soils. Groundw Sustain Dev 12:100493. https://doi.org/10.1016/j.gsd.2020.100493

Bade R, Oh S, Shin WS (2012a) Diffusive gradients in thin films (DGT) for the prediction of bioavailability of heavy metals in contaminated soils to earthworm (*Eisenia foetida*) and oral bioavailable concentrations. Sci Total Environ 416:127–136. https://doi.org/10.1016/j.scitotenv.2011.11.007

Bade R, Oh S, Sik Shin W (2012b) Assessment of metal bioavailability in smelter-contaminated soil before and after lime amendment. Ecotoxicol Environ Saf 80:299–307. https://doi.org/10.1016/j.ecoenv.2012.03.019

Bade R, Oh S, Shin WS, Hwang I (2013) Human health risk assessment of soils contaminated with Metal(loid)s by using DGT uptake: a case study of a former Korean metal refinery site. Hum Ecol Risk Assess 19:767–777. https://doi.org/10.1080/10807039.2012.708276

Baeyens W, Bowie AR, Buesseler K et al (2011) Size-fractionated labile trace elements in the Northwest Pacific and Southern Oceans. Mar Chem 126:108–113. https://doi.org/10.1016/j.marchem.2011.04.004

Balistrieri LS, Blank RG (2008) Dissolved and labile concentrations of Cd, Cu, Pb, and Zn in the South Fork Coeur d'Alene River, Idaho: comparisons among chemical equilibrium models and implications for biotic ligand models. Appl Geochem 23:3355–3371. https://doi.org/10.1016/j.apgeochem.2008.06.031

Balistrieri LS, Seal RR, Piatak NM, Paul B (2007) Assessing the concentration, speciation, and toxicity of dissolved metals during mixing of acid-mine drainage and ambient river water downstream of the Elizabeth Copper Mine, Vermont, USA. Appl Geochem 22:930–952. https://doi.org/10.1016/j.apgeochem.2007.02.005

Bennett WW, Teasdale PR, Panther JG et al (2010) New diffusive gradients in a thin film technique for measuring inorganic arsenic and selenium(IV) using a titanium dioxide based adsorbent. Anal Chem 82:7401–7407. https://doi.org/10.1021/ac101543p

Bennett WW, Teasdale PR, Panther JG et al (2011) Speciation of dissolved inorganic arsenic by diffusive gradients in thin films: Selective binding of As III by 3-mercaptopropyl-functionalized silica gel. Anal Chem 83:8293–8299. https://doi.org/10.1021/ac202119t

Bennett WW, Arsic M, Panther JG et al (2016a) Binding layer properties. In: Davison W (ed) Diffusive gradients in thin-films for environmental measurements. Cambridge University Press, Cambridge, pp 66–92

Bennett WW, Arsic M, Welsh DT, Teasdale PR (2016b) In situ speciation of dissolved inorganic antimony in surface waters and sediment porewaters: development of a thiol-based diffusive gradients in thin films technique for SbIII. Environ Sci Process Impacts 18:992–998. https://doi.org/10.1039/c6em00189k

Bidar G, Pelfrêne A, Louvel B et al (2019) Influence of amendments on metal environmental and toxicological availability in highly contaminated brownfield and agricultural soils. Environ Sci Pollut Res 26:33086–33108. https://doi.org/10.1007/s11356-019-06295-4

Black A, McLaren RG, Reichman SM et al (2011) Evaluation of soil metal bioavailability estimates using two plant species (*L. perenne* and *T. aestivum*) grown in a range of agricultural soils treated with biosolids and metal salts. Environ Pollut 159:1523–1535. https://doi.org/10.1016/j.envpol.2011.03.004

Bourgeault A, Gourlay-Francé C, Vincent-Hubert F et al (2010) Lessons from a transplantation of zebra mussels into a small urban river: an integrated ecotoxicological assessment. Environ Toxicol 25:468–478. https://doi.org/10.1002/tox.20591

Bourgeault A, Ciffroy P, Garnier C et al (2013) Speciation and bioavailability of dissolved copper in different freshwaters: comparison of modelling, biological and chemical responses in aquatic mosses and gammarids. Sci Total Environ 452–453:68–77. https://doi.org/10.1016/j.scitotenv.2013.01.097

Bradac P, Behra R, Sigg L (2009) Accumulation of cadmium in periphyton under various freshwater speciation conditions. Environ Sci Technol 43:7291–7296. https://doi.org/10.1021/es9013536

Bradac P, Wagner B, Kistler D et al (2010) Cadmium speciation and accumulation in periphyton in a small stream with dynamic concentration variations. Environ Pollut 158:641–648. https://doi.org/10.1016/j.envpol.2009.10.031

Bratkič A, Klun K, Gao Y (2019) Mercury speciation in various aquatic systems using passive sampling technique of diffusive gradients in thin-film. Sci Total Environ 663:297–306. https://doi.org/10.1016/j.scitotenv.2019.01.241

Bravin MN, Tentscher P, Rose J, Hinsinger P (2009) Rhizosphere pH gradient controls copper availability in a strongly acidic soil. Environ Sci Technol 43:5686–5691. https://doi.org/10.1021/es900055k

Bravin MN, Michaud AM, Larabi B, Hinsinger P (2010) RHIZOtest: a plant-based biotest to account for rhizosphere processes when assessing copper bioavailability. Environ Pollut 158:3330–3337. https://doi.org/10.1016/j.envpol.2010.07.029

Bravin MN, Garnier C, Lenoble V et al (2012) Root-induced changes in pH and dissolved organic matter binding capacity affect copper dynamic speciation in the rhizosphere. Geochim Cosmochim Acta 84:256–268. https://doi.org/10.1016/j.gca.2012.01.031

Bretier M, Dabrin A, Billon G et al (2020) To what extent can the biogeochemical cycling of mercury modulate the measurement of dissolved mercury in surface freshwaters by passive sampling? Chemosphere 248:1–10. https://doi.org/10.1016/j.chemosphere.2020.126006

Buzier R, Tusseau-Vuillemin MH, dit Meriadec CM et al (2006) Trace metal speciation and fluxes within a major French wastewater treatment plant: impact of the successive treatments stages. Chemosphere 65:2419–2426. https://doi.org/10.1016/j.chemosphere.2006.04.059

Buzier R, Tusseau-Vuillemin MH, Keirsbulck M, Mouchel JM (2011) Inputs of total and labile trace metals from wastewater treatment plants effluents to the Seine River. Phys Chem Earth 36:500–505. https://doi.org/10.1016/j.pce.2008.09.003

Buzier R, Charriau A, Corona D et al (2014) DGT-labile As, Cd, Cu and Ni monitoring in freshwater: toward a framework for interpretation of in situ deployment. Environ Pollut 192:52–58. https://doi.org/10.1016/j.envpol.2014.05.017

Cai C, Williams PN, Li H et al (2017) Development and application of the diffusive gradients in thin films technique for the measurement of nitrate in soils. Anal Chem 89:1178–1184. https://doi.org/10.1021/acs.analchem.6b03609

Cánovas CR, Basallote MD, Borrego P et al (2020) Metal partitioning and speciation in a mining-impacted estuary by traditional and passive sampling methods. Sci Total Environ 722:137905. https://doi.org/10.1016/j.scitotenv.2020.137905

Casiot C, Egal M, Elbaz-Poulichet F et al (2009) Hydrological and geochemical control of metals and arsenic in a Mediterranean river contaminated by acid mine drainage (the Amous River, France); preliminary assessment of impacts on fish (*Leuciscus cephalus*). Appl Geochem 24:787–799. https://doi.org/10.1016/j.apgeochem.2009.01.006

Cattani I, Spalla S, Beone GM et al (2008) Characterization of mercury species in soils by HPLC–ICP–MS and measurement of fraction removed by diffusive gradient in thin films. Talanta 74:1520–1526. https://doi.org/10.1016/j.talanta.2007.09.029

Cattani I, Zhang H, Beone GM et al (2009) The role of natural purified humic acids in modifying mercury accessibility in water and soil. J Environ Qual 38:493–501. https://doi.org/10.2134/jeq2008.0175

Chapman EEV, Dave G, Murimboh JD (2012) Bioavailability as a factor in risk assessment of metal-contaminated soil. Water Air Soil Pollut 223:2907–2922. https://doi.org/10.1007/s11270-012-1074-z

Chen Z, Williams PN, Zhang H (2013) Rapid and nondestructive measurement of labile Mn, Cu, Zn, Pb and As in DGT by using field portable-XRF. Environ Sci Process Impacts 15:1768–1774. https://doi.org/10.1039/c3em00250k

Chen H, Zhang YY, Zhong KL et al (2014) Selective sampling and measurement of Cr (VI) in water with polyquaternary ammonium salt as a binding agent in diffusive gradients in thin-films technique. J Hazard Mater 271:160–165. https://doi.org/10.1016/j.jhazmat.2014.02.022

Chowdhury MTA, Deacon CM, Steel E et al (2018) Physiographical variability in arsenic dynamics in Bangladeshi soils. Sci Total Environ 612:1365–1372. https://doi.org/10.1016/j.scitotenv.2017.09.030

Ciadamidaro L, Puschenreiter M, Santner J et al (2017) Assessment of trace element phytoavailability in compost amended soils using different methodologies. J Soils Sediments 17:1251–1261. https://doi.org/10.1007/s11368-015-1283-3

Cindrić AM, Cukrov N, Durrieu G et al (2017) Evaluation of discrete and passive sampling (diffusive gradients in thin-films—DGT) approach for the assessment of trace metal dynamics in marine waters—a case study in a small harbor. Croat Chem Acta 90:177–185. https://doi.org/10.5562/cca3163

Cindrić AM, Marcinek S, Garnier C et al (2020) Evaluation of diffusive gradients in thin films (DGT) technique for speciation of trace metals in estuarine waters—a multimethodological approach. Sci Total Environ 721:137784. https://doi.org/10.1016/j.scitotenv.2020.137784

Clarisse O, Hintelmann H (2006) Measurements of dissolved methylmercury in natural waters using diffusive gradients in thin film (DGT). J Environ Monit 8:1242–1247. https://doi.org/10.1039/b614560d

Clarisse O, Foucher D, Hintelmann H (2009) Methylmercury speciation in the dissolved phase of a stratified lake using the diffusive gradient in thin film technique. Environ Pollut 157:987–993. https://doi.org/10.1016/j.envpol.2008.10.012

Clarisse O, Lotufo GR, Hintelmann H, Best EPH (2012) Biomonitoring and assessment of monomethylmercury exposure in aqueous systems using the DGT technique. Sci Total Environ 416:449–454. https://doi.org/10.1016/j.scitotenv.2011.11.077

Cleven R, Nur Y, Krystek P, Van Den Berg G (2005) Monitoring metal speciation in the rivers meuse and rhine using DGT. Water Air Soil Pollut 165:249–263. https://doi.org/10.1007/s11270-005-5147-0

Colaço CD, Nozomi L, Yabuki M et al (2012) Diffusion coefficients of metals in non-conventional materials (agarose and cellulose acetate) used in the diffusive gradients in thin films technique. Quim Nova 35:1360–1364. https://doi.org/10.1590/S0100-40422012000700014

Colaço CD, Yabuki LNM, Rolisola AM et al (2014) Determination of mercury in river water by diffusive gradients in thin films using P81 membrane as binding layer. Talanta 129:417–421. https://doi.org/10.1016/j.talanta.2014.05.025

Companys E, Galceran J, Puy J et al (2018) Comparison of different speciation techniques to measure Zn availability in hydroponic media. Anal Chim Acta 1035:32–43. https://doi.org/10.1016/j.aca.2018.06.071

Conesa HM, Schulin R, Nowack B (2010) Suitability of using diffusive gradients in thin films (DGT) to study metal bioavailability in mine tailings: possibilities and constraints. Environ Sci Pollut Res 17:657–664. https://doi.org/10.1007/s11356-009-0254-x

Cornu JY, Denaix L (2006) Prediction of zinc and cadmium phytoavailability within a contaminated agricultural site using DGT. Environ Chem 3:61–64. https://doi.org/10.1071/EN05050

Cornu JY, Denaix L, Lacoste J et al (2016) Impact of temperature on the dynamics of organic matter and on the soil-to-plant transfer of Cd, Zn and Pb in a contaminated agricultural soil. Environ Sci Pollut Res 23:2997–3007. https://doi.org/10.1007/s11356-015-5432-4

Costa LDF, Wallner-Kersanach M (2013) Assessment of the labile fractions of copper and zinc in marinas and port areas in Southern Brazil. Environ Monit Assess 185:6767–6781. https://doi.org/10.1007/s10661-013-3063-0

Costa LDF, Casartelli MRO, Wallner-Kersanach M (2013) Labile copper and zinc fractions under different salinity conditions in a shipyard area in the patos lagoon estuary, south of Brazil. Quim Nova 36:1089–1095. https://doi.org/10.1590/S0100-40422013000800002

Cui H, Li H, Zhang S et al (2020) Bioavailability and mobility of copper and cadmium in polluted soil after phytostabilization using different plants aided by limestone. Chemosphere 242:125252. https://doi.org/10.1016/j.chemosphere.2019.125252

Dabrin A, Ghestem JP, Uher E et al (2016) Metal measurement in aquatic environments by passive sampling methods: lessons learning from an in situ intercomparison exercise. Environ Pollut 208:299–308. https://doi.org/10.1016/j.envpol.2015.08.049

Dai Y, Nasir M, Zhang Y et al (2018) Comparison of DGT with traditional extraction methods for assessing cadmium bioavailability to *Brassica chinensis* in different soils. Chemosphere 191:183–189. https://doi.org/10.1016/j.chemosphere.2017.10.035

Dakova I, Vasileva P, Karadjova I et al (2011) Solid phase extraction and diffusive gradients in thin films techniques for determination

of total and labile concentrations of Cd(II), Cu(II), Ni(II) and Pb(II) in black sea water. Int J Environ Anal Chem 91:62–73. https://doi.org/10.1080/03067310903195011

Davison W, Zhang H (1994) In situ speciation measurements of trace components in natural waters using thin-film gels. Nature 367:546–548. https://doi.org/10.1038/367546a0

Davison W, Zhang H (2012) Progress in understanding the use of diffusive gradients in thin films (DGT) back to basics. Environ Chem 9:1–13. https://doi.org/10.1071/EN11084

Davison W, Zhang H (2016) Diffusion layer properties. In: William D, Zhang H (eds) Diffusive gradients in thin-films for environmental measurements. Cambridge University Press, Cambridge, pp 32–65

Davison W, Lin C, Gao Y, Zhang H (2015) Effect of gel interactions with dissolved organic matter on DGT measurements of trace metals. Aquat Geochem 21:281–293. https://doi.org/10.1007/s10498-014-9244-9

De Almeida E, Do Nascimento Filho VF, Menegário AA (2012) Paper-based diffusive gradients in thin films technique coupled to energy dispersive X-ray fluorescence spectrometry for the determination of labile Mn Co, Ni, Cu, Zn and Pb in river water. Spectrochim Acta Part B 71–72:70–74. https://doi.org/10.1016/j.sab.2012.05.006

de Souza JM, Menegário AA, de Araújo Júnior MAG, Francioni E (2014) Measurements of labile Cd, Cu, Ni, Pb, and Zn levels at a northeastern Brazilian coastal area under the influence of oil production with diffusive gradients in thin films technique (DGT). Sci Total Environ 500–501:325–331. https://doi.org/10.1016/j.scitotenv.2014.08.117

Degryse F, Smolders E, Oliver I, Zhang H (2003) Relating soil solution Zn concentration to diffusive gradients in thin films measurements in contaminated soils. Environ Sci Technol 37:3958–3965. https://doi.org/10.1021/es034075p

Denney S, Sherwood J, Leyden J (1999) In situ measurements of labile Cu, Cd and Mn in river waters using DGT. Sci Total Environ 239:71–80. https://doi.org/10.1016/S0048-9697(99)00304-6

Desaulty A-M, Bodard C, Laurioux T et al (2015) Using DGT passive samplers and MC-ICPMS to determine Pb and Zn isotopic signature of natural water. Procedia Earth Planet Sci 13:76–79. https://doi.org/10.1016/j.proeps.2015.07.018

Devillers D, Buzier R, Simon S et al (2016) Simultaneous measurement of Cr(III) and Cr(VI) in freshwaters with a single diffusive gradients in thin films device. Talanta 154:533–538. https://doi.org/10.1016/j.talanta.2016.04.009

Devillers D, Buzier R, Charriau A, Guibaud G (2017a) Improving elution strategies for Chelex®-DGT passive samplers. Anal Bioanal Chem 409:7183–7189. https://doi.org/10.1007/s00216-017-0680-4

Devillers D, Buzier R, Grybos M et al (2017b) Key role of the sorption process in alteration of metal and metalloid quantification by fouling development on DGT passive samplers. Environ Pollut 230:523–529. https://doi.org/10.1016/j.envpol.2017.07.005

Díaz A, Arnedo R, Céspedes-Sánchez R et al (2012) Monitoring of (bio)available labile metal fraction in a drinking water treatment plant by diffusive gradients in thin films. Environ Monit Assess 184:539–548. https://doi.org/10.1007/s10661-011-1986-x

Díez S (2008) Human health effects of methylmercury exposure. In: Reviews of environmental contamination and toxicology. pp 111–134

Díez S, Giaggio R (2018) Do biofilms affect the measurement of mercury by the DGT technique? Microcosm and field tests to prevent biofilm growth. Chemosphere 210:692–698. https://doi.org/10.1016/j.chemosphere.2018.07.047

Diviš P, Dočekalová H, Brulík L et al (2007) Use of the diffusive gradients in thin films technique to evaluate (bio)available trace metal concentrations in river water. Anal Bioanal Chem 387:2239–2244. https://doi.org/10.1007/s00216-006-0996-y

Diviš P, Szkandera R, Brulík L et al (2009) Application of new resin gels for measuring mercury by diffusive gradients in a thin-films technique. Anal Sci 25:575–578. https://doi.org/10.2116/analsci.25.575

Diviš P, Szkandera R, Docekalová H (2010) Characterization of sorption gels used for determination of mercury in aquatic environment by diffusive gradients in thin films technique. Cent Eur J Chem 8:1103–1107. https://doi.org/10.2478/s11532-010-0090-3

Docekal B, Smetkova V, Docekalová H (2003) Characterization of Czech soils by diffusive gradients in thin films technique. Chem Pap 57:161–166. https://doi.org/10.1007/s00216-007-1628-x

Docekalová H, Diviš P (2005) Application of diffusive gradient in thin films technique (DGT) to measurement of mercury in aquatic systems. Talanta 65:1174–1178. https://doi.org/10.1016/j.talanta.2004.08.054

Docekalová H, Kovariková V, Docekal B (2012) Mobility and bioaccessibility of trace metals in soils assessed by conventional extraction procedures and passive diffusive samplers. Chem Speciat Bioavailab 24:261–265. https://doi.org/10.3184/095422912X13490131100968

dos Anjos VE, Abate G, Grassi MT (2017) Determination of labile species of As(V), Ba, Cd Co, Cr(III), Cu, Mn, Ni, Pb, Sr, V(V), and Zn in natural waters using diffusive gradients in thin-film (DGT) devices modified with montmorillonite. Anal Bioanal Chem 409:1963–1972. https://doi.org/10.1007/s00216-016-0144-2

Dragun Z, Raspor B, Roje V (2008) The labile metal concentrations in Sava River water assessed by diffusive gradients in thin films. Chem Speciat Bioavailab 20:33–46. https://doi.org/10.3184/095422908X299164

Dragun Z, Filipović Marijić V, Vuković M, Raspor B (2015) Metal bioavailability in the Sava River water. In: Handbook of environmental chemistry. pp 123–155

Dunn RJK, Teasdale PR, Warnken J, Schleich RR (2003) Evaluation of the diffusive gradient in a thin film technique for monitoring trace metal concentrations in estuarine waters. Environ Sci Technol 37:2794–2800. https://doi.org/10.1021/es026425y

Dunn RJK, Teasdale PR, Warnken J et al (2007) Evaluation of the in situ, time-integrated DGT technique by monitoring changes in heavy metal concentrations in estuarine waters. Environ Pollut 148:213–220. https://doi.org/10.1016/j.envpol.2006.10.027

Egene CE, Van Poucke R, Ok YS et al (2018) Impact of organic amendments (biochar, compost and peat) on Cd and Zn mobility and solubility in contaminated soil of the Campine region after three years. Sci Total Environ 626:195–202. https://doi.org/10.1016/j.scitotenv.2018.01.054

Eismann CE, Menegário AA, Gemeiner H, Williams PN (2020) Predicting trace metal exposure in aquatic ecosystems: evaluating DGT as a biomonitoring tool. Expo Heal 12:19–31. https://doi.org/10.1007/s12403-018-0280-3

Elias G, Díez S, Zhang H, Fontàs C (2020) Development of a new binding phase for the diffusive gradients in thin films technique based on an ionic liquid for mercury determination. Chemosphere 245:125671. https://doi.org/10.1016/j.chemosphere.2019.125671

Ernstberger H, Davison W, Zhang H et al (2002a) Measurement and dynamic modeling of trace metal mobilization in soils using DGT and DIFS. Environ Sci Technol 36:349–354. https://doi.org/10.1021/es010917d

Ernstberger H, Zhang H, Davison W (2002b) Determination of chromium speciation in natural systems using DGT. Anal Bioanal Chem 373:873–879. https://doi.org/10.1007/s00216-002-1370-3

Ernstberger H, Zhang H, Tye A et al (2005) Desorption kinetics of Cd, Zn, and Ni measured in soils by DGT. Environ Sci Technol 39:1591–1597. https://doi.org/10.1021/es048534d

Fairbrother A, Wenstel R, Sappington K, Wood W (2007) Framework for metals risk assessment. Ecotoxicol Environ Saf 68:145–227

Fan H, Bian Y, Sui D et al (2009a) Measurement of free copper(II) ions in water samples with polyvinyl alcohol as a binding phase in diffusive gradients in thin-films. Anal Sci 25:1345–1349. https://doi.org/10.2116/analsci.25.1345

Fan H, Sun T, Li W et al (2009b) Sodium polyacrylate as a binding agent in diffusive gradients in thin-films technique for the measurement of Cu^{2+} and Cd^{2+} in waters. Talanta 79:1228–1232. https://doi.org/10.1016/j.talanta.2009.04.049

Fan HT, Liu JX, Sui DP et al (2013) Use of polymer-bound Schiff base as a new liquid binding agent of diffusive gradients in thin-films for the measurement of labile Cu^{2+}, Cd^{2+} and Pb^{2+}. J Hazard Mater 260:762–769. https://doi.org/10.1016/j.jhazmat.2013.05.049

Fan HT, Lu Y, Liu AJ et al (2015) A method for measurement of free cadmium species in waters using diffusive gradients in thin films technique with an ion-imprinted sorbent. Anal Chim Acta 897:24–33. https://doi.org/10.1016/j.aca.2015.09.056

Feldmann J, Elgazali A, Ezzeldin MF et al (2014) Microwave-assisted sample preparation for element speciation. In: Microwave-assisted sample preparation for trace element determination. Elsevier, pp 281–312

Fernández-Gómez C, Dimock B, Hintelmann H, Díez S (2011) Development of the DGT technique for Hg measurement in water: comparison of three different types of samplers in laboratory assays. Chemosphere 85:1452–1457. https://doi.org/10.1016/j.chemosphere.2011.07.080

Fernández-Gómez C, Bayona JM, Díez S (2012a) Laboratory and field evaluation of diffusive gradient in thin films (DGT) for monitoring levels of dissolved mercury in natural river water. Int J Environ Anal Chem 92:1689–1698. https://doi.org/10.1080/03067319.2011.581369

Fernández-Gómez C, Hintelmann H, Díez S (2012b) Passive sampling for inorganic contaminants in water. In: Comprehensive sampling and sample preparation. pp 281–296

Fernández-Gómez C, Bayona JM, Díez S (2014) Comparison of different types of diffusive gradient in thin film samplers for measurement of dissolved methylmercury in freshwaters. Talanta 129:486–490. https://doi.org/10.1016/j.talanta.2014.06.025

Fernández-Gómez C, Bayona JM, Díez S (2015) Diffusive gradients in thin films for predicting methylmercury bioavailability in freshwaters after photodegradation. Chemosphere 131:184–191. https://doi.org/10.1016/j.chemosphere.2015.02.060

Ferreira D, Ciffroy P, Tusseau-Vuillemin MH et al (2013) DGT as surrogate of biomonitors for predicting the bioavailability of copper in freshwaters: an ex situ validation study. Chemosphere 91:241–247. https://doi.org/10.1016/j.chemosphere.2012.10.016

Fischerová Z, Száková J, Pavlíková D, Tlustos P (2005) The application of diffusive gradient technique (DGT) for assessment of changes in Cd, Pb, and Zn mobility in rhizosphere. Plant Soil Environ 51:532–538. https://doi.org/10.17221/3628-PSE

Fitz WJ, Wenzel WW, Zhang H et al (2003) Rhizosphere characteristics of the arsenic hyperaccumulator *Pteris vittata* L. and monitoring of phytoremoval efficiency. Environ Sci Technol 37:5008–5014. https://doi.org/10.1021/es0300214

Forsberg J, Dahlqvist R, Gelting-Nyström J, Ingri J (2006) Trace metal speciation in brackish water using diffusive gradients in thin films and ultrafiltration: comparison of techniques. Environ Sci Technol 40:3901–3905. https://doi.org/10.1021/es0600781

Fortin C, Campbell PGG (1998) An ion-exchange technique for free-metal ion measurements (Cd^{2+}, Zn^{2+}): applications to complex aqueous media. Int J Environ Anal Chem 72:173–194. https://doi.org/10.1080/03067319808035889

French MA, Zhang H, Pates JM et al (2005) Development and performance of the diffusive gradients in thin-films technique for the measurement of technetium-99 in seawater. Anal Chem 77:135–139. https://doi.org/10.1021/ac048774b

Fresno T, Peñalosa JM, Santner J et al (2017) Effect of *Lupinus albus* L. root activities on As and Cu mobility after addition of iron-based soil amendments. Chemosphere 182:373–381. https://doi.org/10.1016/j.chemosphere.2017.05.034

Gaabass I, Murimboh JD, Hassan NM (2009) A study of diffusive gradients in thin films for the chemical speciation of Zn(II), Cd(II), Pb(II), and Cu(II): The role of kinetics. Water Air Soil Pollut 202:131–140. https://doi.org/10.1007/s11270-008-9963-x

Galceran J, Puy J (2015) Interpretation of diffusion gradients in thin films (DGT) measurements: a systematic approach. Environ Chem 12:112–122. https://doi.org/10.1071/EN14068

Galhardi JA, Leles BP, de Mello JWV, Wilkinson KJ (2020) Bioavailability of trace metals and rare earth elements (REE) from the tropical soils of a coal mining area. Sci Total Environ 717:134484. https://doi.org/10.1016/j.scitotenv.2019.134484

Gao Y, Lehto N (2012) A simple laser ablation ICPMS method for the determination of trace metals in a resin gel. Talanta 92:78–83. https://doi.org/10.1016/j.talanta.2012.01.043

Gao Y, Lesven L, Gillan D et al (2009) Geochemical behavior of trace elements in sub-tidal marine sediments of the Belgian coast. Mar Chem 117:88–96. https://doi.org/10.1016/j.marchem.2009.05.002

Gao Y, De Canck E, Leermakers M et al (2011) Synthesized mercaptopropyl nanoporous resins in DGT probes for determining dissolved mercury concentrations. Talanta 87:262–267. https://doi.org/10.1016/j.talanta.2011.10.012

Gao Y, De Craemer S, Baeyens W (2014) A novel method for the determination of dissolved methylmercury concentrations using diffusive gradients in thin films technique. Talanta 120:470–474. https://doi.org/10.1016/j.talanta.2013.12.023

Gao L, Gao B, Yin S et al (2018) Predicting Ni dynamic mobilization in reservoir riparian soils prior to water submergence using DGT and DIFS. Chemosphere 195:390–397. https://doi.org/10.1016/j.chemosphere.2017.12.090

Gao B, Gao L, Xu D et al (2019a) A novel method for evaluating the potential release of trace metals associated with rainfall leaching/runoff from urban soils. Sci Total Environ 664:37–44. https://doi.org/10.1016/j.scitotenv.2019.01.418

Gao L, Gao B, Xu D, Sun K (2019b) In-situ measurement of labile Cr(III) and Cr(VI) in water using diffusive gradients in thin-films (DGT). Sci Total Environ 653:1161–1167. https://doi.org/10.1016/j.scitotenv.2018.10.392

Gao Y, Zhou C, Gaulier C et al (2019c) Labile trace metal concentration measurements in marine environments: from coastal to open ocean areas. TrAC Trends Anal Chem 116:92–101. https://doi.org/10.1016/j.trac.2019.04.027

Gao L, Sun K, Xu D, Gao B (2020) Kinetic process of Cr(III) in contaminated soils characterized by diffusive gradients in thin films technique. Sci Total Environ 720:137425. https://doi.org/10.1016/j.scitotenv.2020.137425

García-Gómez C, García S, Obrador A et al (2020) Effect of ageing of bare and coated nanoparticles of zinc oxide applied to soil on the Zn behaviour and toxicity to fish cells due to transfer from soil to water bodies. Sci Total Environ 706:135713. https://doi.org/10.1016/j.scitotenv.2019.135713

Garmo ØA, Røyset O, Steinnes E, Flaten TP (2003) Performance study of diffusive gradients in thin films for 55 elements. Anal Chem 75:3573–3580. https://doi.org/10.1021/ac026374n

Garmo ØA, Davison W, Zhang H (2008) Interactions of trace metals with hydrogels and filter membranes used in DET and DGT techniques. Environ Sci Technol 42:5682–5687. https://doi.org/10.1021/es800143r

Garrido RT, Mendoza CJ (2013) Application of diffusive gradient in thin film to estimate available copper in soil solution. Soil Sediment Contam 22:654–666. https://doi.org/10.1080/15320383.2013.756447

Gaulier C, Zhou C, Guo W et al (2019) Trace metal speciation in North Sea coastal waters. Sci Total Environ 692:701–712. https://doi.org/10.1016/j.scitotenv.2019.07.314

Gimpel J, Zhang H, Davison W, Edwards AC (2003) In situ trace metal speciation in lake surface waters using DGT, dialysis, and filtration. Environ Sci Technol 37:138–146. https://doi.org/10.1021/es0200995

Giusti L, Barakat S (2005) The monitoring of Cr(III) and Cr(VI) in natural water and synthetic solutions: an assessment of the performance of the DGT and DPC methods. Water Air Soil Pollut 161:313–334. https://doi.org/10.1007/s11270-005-4719-3

Gontijo ESJ, Watanabe CH, Monteiro ASC et al (2016) Distribution and bioavailability of arsenic in natural waters of a mining area studied by ultrafiltration and diffusive gradients in thin films. Chemosphere 164:290–298. https://doi.org/10.1016/j.chemosphere.2016.08.107

Gorny J, Dumoulin D, Alaimo V et al (2019) Passive sampler measurements of inorganic arsenic species in environmental waters: a comparison between 3-mercapto-silica, ferrihydrite, Metsorb®, zinc ferrite, and zirconium dioxide binding gels. Talanta 198:518–526. https://doi.org/10.1016/j.talanta.2019.01.127

Gramlich A, Tandy S, Frossard E et al (2014) Diffusion limitation of zinc fluxes into wheat roots, PLM and DGT devices in the presence of organic ligands. Environ Chem 11:41–50. https://doi.org/10.1071/EN13106

Gramlich A, Tandy S, Andres C et al (2017) Cadmium uptake by cocoa trees in agroforestry and monoculture systems under conventional and organic management. Sci Total Environ 580:677–686. https://doi.org/10.1016/j.scitotenv.2016.12.014

Gramlich A, Tandy S, Gauggel C et al (2018) Soil cadmium uptake by cocoa in Honduras. Sci Total Environ 612:370–378. https://doi.org/10.1016/j.scitotenv.2017.08.145

Grüter R, Costerousse B, Bertoni A et al (2017) Green manure and long-term fertilization effects on soil zinc and cadmium availability and uptake by wheat (*Triticum aestivum* L.) at different growth stages. Sci Total Environ 599–600:1330–1343. https://doi.org/10.1016/j.scitotenv.2017.05.070

Grüter R, Costerousse B, Mayer J et al (2019) Long-term organic matter application reduces cadmium but not zinc concentrations in wheat. Sci Total Environ 669:608–620. https://doi.org/10.1016/j.scitotenv.2019.03.112

Gu X, Liu Z, Wang X et al (2017) Coupling biological assays with diffusive gradients in thin-films technique to study the biological responses of *Eisenia fetida* to cadmium in soil. J Hazard Mater 339:340–346. https://doi.org/10.1016/j.jhazmat.2017.06.049

Guan DX, Sun FS, Yu GH et al (2018) Total and available metal concentrations in soils from six long-term fertilization sites across China. Environ Sci Pollut Res 25:31666–31678. https://doi.org/10.1007/s11356-018-3143-3

Guéguen C, Clarisse O, Perroud A, McDonald A (2011) Chemical speciation and partitioning of trace metals (Cd Co, Cu, Ni, Pb) in the lower Athabasca river and its tributaries (Alberta, Canada). J Environ Monit 13:2865–2872. https://doi.org/10.1039/c1em10563a

Guibal R, Buzier R, Lissalde S, Guibaud G (2019) Adaptation of diffusive gradients in thin films technique to sample organic pollutants in the environment: an overview of o-DGT passive samplers. Sci Total Environ 693:133537. https://doi.org/10.1016/j.scitotenv.2019.07.343

Guo L, Chen H, Zhang Y et al (2014) Determination of chromium speciation in tap water using diffusive gradients in thin film technique. Chem Lett 43:849–850. https://doi.org/10.1246/cl.140100

Guo SH, Liu ZL, Li QS et al (2016) Leaching heavy metals from the surface soil of reclaimed tidal flat by alternating seawater inundation and air drying. Chemosphere 157:262–270. https://doi.org/10.1016/j.chemosphere.2016.05.019

Hamels F, Malevé J, Sonnet P et al (2014) Phytotoxicity of trace metals in spiked and field-contaminated soils: linking soil-extractable metals with toxicity. Environ Toxicol Chem 33:2479–2487. https://doi.org/10.1002/etc.2693

Han S, Naito W, Hanai Y, Masunaga S (2013) Evaluation of trace metals bioavailability in Japanese river waters using DGT and a chemical equilibrium model. Water Res 47:4880–4892. https://doi.org/10.1016/j.watres.2013.05.025

Han S, Zhang Y, Masunaga S et al (2014) Relating metal bioavailability to risk assessment for aquatic species: Daliao River watershed, China. Environ Pollut 189:215–222. https://doi.org/10.1016/j.envpol.2014.02.023

Han S, Naito W, Masunaga S (2016) Assessing bioavailability levels of metals in effluent affected rivers: effect of Fe(III) and chelating agents on the distribution of metal speciation. Water Sci Technol 74:896–903. https://doi.org/10.2166/wst.2016.269

Harper MP, Davison W, Zhang H, Tych W (1998) Kinetics of metal exchange between solids and solutions in sediments and soils interpreted from DGT measured fluxes. Geochim Cosmochim Acta 62:2757–2770. https://doi.org/10.1016/S0016-7037(98)00186-0

Harper MP, Davison W, Tych W (2000) DIFS—a modelling and simulation tool for DGT induced trace metal remobilisation in sediments and soils. Environ Model Softw 15:55–66. https://doi.org/10.1016/S1364-8152(99)00027-4

Hartland A, Fairchild IJ, Lead JR et al (2011) Size, speciation and lability of NOM-metal complexes in hyperalkaline cave dripwater. Geochim Cosmochim Acta 75:7533–7551. https://doi.org/10.1016/j.gca.2011.09.030

Hattab N, Motelica-Heino M, Bourrat X, Mench M (2014) Mobility and phytoavailability of Cu, Cr, Zn, and As in a contaminated soil at a wood preservation site after 4 years of aided phytostabilization. Environ Sci Pollut Res 21:10307–10319. https://doi.org/10.1007/s11356-014-2938-0

Hattab N, Motelica-Heino M, Faure O, Bouchardon JL (2015) Effect of fresh and mature organic amendments on the phytoremediation of technosols contaminated with high concentrations of trace elements. J Environ Manag 159:37–47. https://doi.org/10.1016/j.jenvman.2015.05.012

Hattab-Hambli N, Motelica-Heino M, Mench M (2016) Aided phytoextraction of Cu, Pb, Zn, and As in copper-contaminated soils with tobacco and sunflower in crop rotation: mobility and phytoavailability assessment. Chemosphere 145:543–550. https://doi.org/10.1016/j.chemosphere.2015.11.051

Herrera-Herrera C, Fuentes-Gandara F, Zambrano-Arévalo A et al (2019) Health risks associated with heavy metals in imported fish in a coastal city in Colombia. Biol Trace Elem Res 190:526–534. https://doi.org/10.1007/s12011-018-1561-1

Hlodák M, Matús P, Urík M et al (2015) Evaluation of various inorganic and biological extraction techniques suitability for soil mercury phytoavailable fraction assessment. Water Air Soil Pollut 226:198–207. https://doi.org/10.1007/s11270-015-2458-7

Hoefer C, Santner J, Puschenreiter M, Wenzel WW (2015) Localized metal solubilization in the rhizosphere of *Salix smithiana* upon sulfur application. Environ Sci Technol 49:4522–4529. https://doi.org/10.1021/es505758j

Hojaji E (2012) Investigation of trace metal binding properties of lignin by diffusive gradients in thin films. Chemosphere 89:319–326. https://doi.org/10.1016/j.chemosphere.2012.04.045

Hong YS, Rifkin E, Bouwer EJ (2011) Combination of diffusive gradient in a thin film probe and IC–ICP–MS for the simultaneous determination of CH_3Hg^+ and Hg^{2+} in oxic water. Environ Sci Technol 45:6429–6436. https://doi.org/10.1021/es200398d

Hooda PS, Zhang H, Davison W, Edwards AC (1999) Measuring bioavailable trace metals by diffusive gradients in thin films (DGT): soil moisture effects on its performance in soils. Eur J Soil Sci 50:285–294. https://doi.org/10.1046/j.1365-2389.1999.00226.x

Huu Nguyen V, Yee SK, Hong Y et al (2019) Predicting mercury bioavailability in soil for earthworm *Eisenia fetida* using the diffusive gradients in thin films technique. Environ Sci Pollut Res 26:19549–19559. https://doi.org/10.1007/s11356-019-05180-4

Huynh T, Zhang H, Laidlaw WS et al (2010) Plant-induced changes in the bioavailability of heavy metals in soil and biosolids assessed by DGT measurements. J Soils Sediments 10:1131–1141. https://doi.org/10.1007/s11368-010-0228-0

Huynh T, Laidlaw WS, Singh B et al (2012a) Effect of plants on the bioavailability of metals and other chemical properties of biosolids in a column study. Int J Phytoremediation 14:878–893. https://doi.org/10.1080/15226514.2011.636400

Huynh T, Zhang H, Noller B (2012b) Evaluation and application of the diffusive gradients in thin films technique using a mixed-binding gel layer for measuring inorganic arsenic and metals in mining impacted water and soil. Anal Chem 84:9988–9995. https://doi.org/10.1021/ac302430b

Jaishankar M, Tseten T, Anbalagan N et al (2014) Toxicity, mechanism and health effects of some heavy metals. Interdiscip Toxicol 7:60–72. https://doi.org/10.2478/intox-2014-0009

Jakl M, Dytrtoavá JJ, Miholová D et al (2009) Passive diffusion assessment of cadmium and lead accumulation by plants in hydroponic systems. Chem Speciat Bioavailab 21:111–120. https://doi.org/10.3184/095422909X456870

Jakl M, Jaklová Dytrtová J, Kunes I, Balás M (2015) Effective concentration of elements in root zone of Norway spruce stand 16 years after fertilization probed with DGT. Water Air Soil Pollut 226:339–347. https://doi.org/10.1007/s11270-015-2602-4

Jolley DF, Mason S, Gao Y, Zhang H (2016) Practicalities of working with DGT. In: Davison W (ed) Diffusive gradients in thinfilms for environmental measurements. Cambridge University Press, Cambridge, pp 263–290

Kalis EJJ (2006) Chemical speciation and bioavailability of heavy metals in soil and surface water

Kawakami SK, Seidel JL, Elbaz-Poulichet F, Achterberg EP (2008) Trace-metal biogeochemistry in the Mediterranean Thau Lagoon, a shellfish farming area. J Coast Res 24:194–202. https://doi.org/10.2112/06-0808.1

Kim M, Choi M, Kim C (2016) Monitoring trace metals in seawater using a diffusive gradient in thin film probe in Ulsan Bay, East Sea, Korea: comparison with transplanted mussels. Ocean Sci J 51:169–182. https://doi.org/10.1007/s12601-016-0015-y

Knutsson J, Knutsson P, Rauch S et al (2013) Evaluation of a passive sampler for the speciation of metals in urban runoff water. Environ Sci Process Impacts 15:2233–2239. https://doi.org/10.1039/c3em00247k

Knutsson J, Rauch S, Morrison GM (2014) Estimation of measurement uncertainties for the DGT passive sampler used for determination of copper in water. Int J Anal Chem 2014:1–7. https://doi.org/10.1155/2014/389125

Koppel DJ, Adams MS, King CK, Jolley DF (2019) Diffusive gradients in thin films can predict the toxicity of metal mixtures to two microalgae: validation for environmental monitoring in Antarctic marine conditions. Environ Toxicol Chem 38:1323–1333. https://doi.org/10.1002/etc.4399

Koster M, Reijnders L, Van Oost NR, Peijnenburg WJGM (2005) Comparison of the method of diffusive gels in thin films with conventional extraction techniques for evaluating zinc accumulation in plants and isopods. Environ Pollut 133:103–116. https://doi.org/10.1016/j.envpol.2004.05.022

Kovaríková V, Docekalová H, Docekal B, Podborská M (2007) Use of the diffusive gradients in thin films technique (DGT) with various diffusive gels for characterization of sewage sludge-contaminated soils. Anal Bioanal Chem 389:2303–2311. https://doi.org/10.1007/s00216-007-1628-x

Kraal P, Jansen B, Nierop KGJ, Verstraten JM (2006) Copper complexation by tannic acid in aqueous solution. Chemosphere 65:2193–2198. https://doi.org/10.1016/j.chemosphere.2006.05.058

Larner BL, Seen AJ (2005) Evaluation of paper-based diffusive gradients in thin film samplers for trace metal sampling. Anal Chim Acta 539:349–355. https://doi.org/10.1016/j.aca.2005.03.007

Larner BL, Seen AJ, Snape I (2006) Evaluation of diffusive gradients in thin film (DGT) samplers for measuring contaminants in the Antarctic marine environment. Chemosphere 65:811–820. https://doi.org/10.1016/j.chemosphere.2006.03.028

Le Forestier L, Motelica-Heino M, Le Coustumer P, Mench M (2017) Phytostabilisation of a copper contaminated topsoil aided by basic slags: assessment of Cu mobility and phytoavailability. J Soils Sediments 17:1262–1271. https://doi.org/10.1007/s11368-015-1299-8

Leermakers M, Phrommavanh V, Drozdzak J et al (2016) DGT as a useful monitoring tool for radionuclides and trace metals in environments impacted by uranium mining: case study of the Sagnes wetland in France. Chemosphere 155:142–151. https://doi.org/10.1016/j.chemosphere.2016.03.138

Lehto NJ (2016) Principles and application in soils and sediments. Diffusive gradients in thin-films for environmental measurements. Cambridge University Press, Cambridge, pp 146–173

Lehto NJ, Davison W, Zhang H, Tych W (2006) An evaluation of DGT performance using a dynamic numerical model. Environ Sci Technol 40:6368–6376. https://doi.org/10.1021/es061215x

Levy JL, Zhang H, Davison W et al (2012a) Assessment of trace metal binding kinetics in the resin phase of diffusive gradients in thin films. Anal Chim Acta 717:143–150. https://doi.org/10.1016/j.aca.2011.12.043

Levy JL, Zhang H, Davison W et al (2012b) Kinetic signatures of metals in the presence of suwannee river fulvic acid. Environ Sci Technol 46:3335–3342. https://doi.org/10.1021/es2043068

Li W, Zhao H, Teasdale PR et al (2002a) Synthesis and characterisation of a polyacrylamide–polyacrylic acid copolymer hydrogel for environmental analysis of Cu and Cd. React Funct Polym 52:31–41. https://doi.org/10.1016/S1381-5148(02)00055-X

Li W, Zhao H, Teasdale PR et al (2002b) Application of a cellulose phosphate ion exchange membrane as a binding phase in the diffusive gradients in thin films technique for measurement of trace metals. Anal Chim Acta 464:331–339. https://doi.org/10.1016/S0003-2670(02)00492-0

Li W, Zhao H, Teasdale PR et al (2005a) Metal speciation measurement by diffusive gradients in thin films technique with different binding phases. Anal Chim Acta 533:193–202. https://doi.org/10.1016/j.aca.2004.11.019

Li W, Zhao H, Teasdale PR, Wang F (2005b) Trace metal speciation measurements in waters by the liquid binding phase DGT device. Talanta 67:571–578. https://doi.org/10.1016/j.talanta.2005.03.018

Li Z, Wu L, Hu P et al (2014) Repeated phytoextraction of four metal-contaminated soils using the cadmium/zinc hyperaccumulator Sedum plumbizincicola. Environ Pollut 189:176–183. https://doi.org/10.1016/j.envpol.2014.02.034

Li Z, Wu L, Zhang H et al (2015) Effects of soil drying and wetting-drying cycles on the availability of heavy metals and their relationship to dissolved organic matter. J Soils Sediments 15:1510–1519. https://doi.org/10.1007/s11368-015-1090-x

— 100 —

Li D, Li W, Lu Q et al (2018) Cadmium bioavailability well assessed by DGT and factors influencing cadmium accumulation in rice grains from paddy soils of three parent materials. J Soils Sediments 18:2552–2561. https://doi.org/10.1007/s11368-018-1950-2

Li C, Ding S, Yang L et al (2019) Diffusive gradients in thin films: devices, materials and applications. Environ Chem Lett 17:801–831. https://doi.org/10.1007/s10311-018-00839-9

Li K, Liu Z, Shi X et al (2020) Novel in situ method based on diffusive gradients in thin-films with lanthanum oxide nanoparticles for measuring As, Sb, and V and in waters. J Hazard Mater 383:1–10. https://doi.org/10.1016/j.jhazmat.2019.121196

Liang S, Guan DX, Ren JH et al (2014) Effect of aging on arsenic and lead fractionation and availability in soils: coupling sequential extractions with diffusive gradients in thin-films technique. J Hazard Mater 273:272–279. https://doi.org/10.1016/j.jhazmat.2014.03.024

Liu J, Feng X, Qiu G et al (2012) Prediction of methyl mercury uptake by rice plants (*Oryza sativa* L.) using the diffusive gradient in thin films technique. Environ Sci Technol 46:11013–11020. https://doi.org/10.1021/es302187t

Liu R, Lead JR, Zhang H (2013a) Combining cross flow ultrafiltration and diffusion gradients in thin-films approaches to determine trace metal speciation in freshwaters. Geochim Cosmochim Acta 109:14–26. https://doi.org/10.1016/j.gca.2013.01.030

Liu X, Song Q, Tang Y et al (2013b) Human health risk assessment of heavy metals in soil–vegetable system: a multi-medium analysis. Sci Total Environ 463–464:530–540. https://doi.org/10.1016/j.scitotenv.2013.06.064

Liu S, Qin N, Song J et al (2016) A nanoparticulate liquid binding phase based DGT device for aquatic arsenic measurement. Talanta 160:225–232. https://doi.org/10.1016/j.talanta.2016.06.064

Liu JF, Zhao YJ, Song ZT et al (2018) Characterization of the dissociation kinetics of Cd and Ni in soils based on diffusive gradients in thin films technique. Ecotoxicol Environ Saf 166:446–452. https://doi.org/10.1016/j.ecoenv.2018.09.108

Lomaglio T, Hattab-Hambli N, Bret A et al (2017) Effect of biochar amendments on the mobility and (bio) availability of As, Sb and Pb in a contaminated mine technosol. J Geochem Explor 182:138–148. https://doi.org/10.1016/j.gexplo.2016.08.007

Lourino-Cabana B, Billon G, Magnier A et al (2011) Evidence of highly dynamic geochemical behaviour of zinc in the Deûle river (northern France). J Environ Monit 13:2124–2133. https://doi.org/10.1039/c1em10244c

Lu H, Mei D, Pavao-Zuckerman M et al (2019) Combination of DGT and fluorescence spectroscopy for improved understanding of metal behaviour in mangrove wetland. Chemosphere 229:303–313. https://doi.org/10.1016/j.chemosphere.2019.05.002

Lucas A, Rate A, Zhang H et al (2012) Development of the diffusive gradients in thin films technique for the measurement of labile gold in natural waters. Anal Chem 84:6994–7000. https://doi.org/10.1021/ac301003g

Lucas AR, Reid N, Salmon SU, Rate AW (2014) Quantitative assessment of the distribution of dissolved Au, As and Sb in groundwater using the diffusive gradients in thin films technique. Environ Sci Technol 48:12141–12149. https://doi.org/10.1021/es502468d

Lucas AR, Salmon SU, Rate AW et al (2015) Spatial and temporal distribution of Au and other trace elements in an estuary using the diffusive gradients in thin films technique and grab sampling. Geochim Cosmochim Acta 171:156–173. https://doi.org/10.1016/j.gca.2015.08.025

Luider CD, Crusius J, Playle RC, Curtis PJ (2004) Influence of natural organic matter source on copper speciation as demonstrated by Cu binding to fish gills, by ion selective electrode, and by DGT Gel sampler. Environ Sci Technol 38:2865–2872. https://doi.org/10.1021/es030566y

Luo J, Zhang H, Santner J, Davison W (2010a) Performance characteristics of diffusive gradients in thin films equipped with a binding gel layer containing precipitated ferrihydrite for measuring arsenic(V), selenium(VI), vanadium(V), and antimony(V). Anal Chem 82:8903–8909. https://doi.org/10.1021/ac101676w

Luo J, Zhang H, Zhao FJ, Davison W (2010b) Distinguishing diffusional and plant control of Cd and Ni uptake by hyperaccumulator and nonhyperaccumulator plants. Environ Sci Technol 44:6636–6641. https://doi.org/10.1021/es100371d

Luo J, Cheng H, Ren J et al (2014) Mechanistic insights from DGT and soil solution measurements on the uptake of Ni and Cd by radish. Environ Sci Technol 48:7305–7313. https://doi.org/10.1021/es500173e

Ma Y, Lombi E, Oliver IW et al (2006) Long-term aging of copper added to soils. Environ Sci Technol 40:6310–6317. https://doi.org/10.1021/es060306r

Ma Q, Zhao W, Guan DX et al (2020) Comparing $CaCl_2$, EDTA and DGT methods to predict Cd and Ni accumulation in rice grains from contaminated soils. Environ Pollut 260:114042. https://doi.org/10.1016/j.envpol.2020.114042

Macoustra GK, Jolley DF, Stauber J et al (2020) Amelioration of copper toxicity to a tropical freshwater microalga: effect of natural DOM source and season. Environ Pollut 266:1–10. https://doi.org/10.1016/j.envpol.2020.115141

Mangal V, Zhu Y, Shi YX, Guéguen C (2016) Assessing cadmium and vanadium accumulation using diffusive gradient in thin-films (DGT) and phytoplankton in the Churchill River estuary, Manitoba. Chemosphere 163:90–98. https://doi.org/10.1016/j.chemosphere.2016.08.008

Manzano R, Rosende M, Leza A et al (2019) Complementary assessment of As, Cu and Zn environmental availability in a stabilised contaminated soil using large-bore column leaching, automatic microcolumn extraction and DGT analysis. Sci Total Environ 690:217–225. https://doi.org/10.1016/j.scitotenv.2019.06.523

Marras B, Montero N, Marrucci A et al (2020) Operational DGT threshold values for metals in seawater from protected coastal areas in Sardinia (Western Mediterranean). Mar Pollut Bull 150:1–8. https://doi.org/10.1016/j.marpolbul.2019.110692

Marrugo-Negrete J, Vargas-Licona S, Ruiz-Guzmán JA et al (2020) Human health risk of methylmercury from fish consumption at the largest floodplain in Colombia. Environ Res 182:109050. https://doi.org/10.1016/j.envres.2019.109050

Martin AJ, Goldblatt R (2007) Speciation, behavior, and bioavailability of copper downstream of a mine-impacted lake. Environ Toxicol Chem 26:2594–2603. https://doi.org/10.1897/07-038.1

Martin A, Landesman C, Lépinay A et al (2019) Flow period influence on uranium and trace elements release in water from the waste rock pile of the former La Commanderie uranium mine (France). J Environ Radioact 208–209:1–10. https://doi.org/10.1016/j.jenvrad.2019.106010

McGifford RW, Seen AJ, Haddad PR (2010) Direct colorimetric detection of copper(II) ions in sampling using diffusive gradients in thin-films. Anal Chim Acta 662:44–50. https://doi.org/10.1016/j.aca.2009.12.041

Menegário AA, Tonello PS, Durrant SF (2010) Use of Saccharomyces cerevisiae immobilized in agarose gel as a binding agent for diffusive gradients in thin films. Anal Chim Acta 683:107–112. https://doi.org/10.1016/j.aca.2010.10.016

Menegário AA, Yabuki LNM, Luko KS et al (2017) Use of diffusive gradient in thin films for in situ measurements: a review on the progress in chemical fractionation, speciation and bioavailability of metals in waters. Anal Chim Acta 983:54–66. https://doi.org/10.1016/j.aca.2017.06.041

Mojsilovic O, McLaren RG, Condron LM (2011) Modelling arsenic toxicity in wheat: simultaneous application of diffusive gradients in thin films to arsenic and phosphorus in soil. Environ Pollut 159:2996–3002. https://doi.org/10.1016/j.envpol.2011.04.022

Moreno-Jiménez E, Six L, Williams PN, Smolders E (2013) Inorganic species of arsenic in soil solution determined by microcartridges and ferrihydrite-based diffusive gradient in thin films (DGT). Talanta 104:83–89. https://doi.org/10.1016/j.talanta.2012.11.007

Moreno-Jiménez E, Fernández JM, Puschenreiter M et al (2016) Availability and transfer to grain of As, Cd, Cu, Ni, Pb and Zn in a barley agri-system: impact of biochar, organic and mineral fertilizers. Agric Ecosyst Environ 219:171–178. https://doi.org/10.1016/j.agee.2015.12.001

Muhammad I, Puschenreiter M, Wenzel WW (2012) Cadmium and Zn availability as affected by pH manipulation and its assessment by soil extraction, DGT and indicator plants. Sci Total Environ 416:490–500. https://doi.org/10.1016/j.scitotenv.2011.11.029

Munksgaard NC, Parry DL (2003) Monitoring of labile metals in turbid coastal seawater using diffusive gradients in thin-films. J Environ Monit 5:145–149. https://doi.org/10.1039/b209346d

Muresan B, Metzger É, Jézéquel D, Cossa D (2018) A multiscale study of mercury transformations and dynamics at the chemocline of the Petit-Saut tropical reservoir (French Guiana). Sci Total Environ 630:1401–1412. https://doi.org/10.1016/j.scitotenv.2018.02.280

Ndu U, Christensen GA, Rivera NA et al (2018) Quantification of mercury bioavailability for methylation using diffusive gradient in thin-film samplers. Environ Sci Technol 52:8521–8529. https://doi.org/10.1021/acs.est.8b00647

Neu S, Müller I, Brackhage C et al (2018) Trace elements bioavailability to Triticum aestivum and Dendrobaena veneta in a multielement-contaminated agricultural soil amended with drinking water treatment residues. J Soils Sediments 18:2259–2270. https://doi.org/10.1007/s11368-017-1741-1

Ngo LK, Pinch BM, Bennett WW et al (2016) Assessing the uptake of arsenic and antimony from contaminated soil by radish (Raphanus sativus) using DGT and selective extractions. Environ Pollut 216:104–114. https://doi.org/10.1016/j.envpol.2016.05.027

Ngo LK, Price HL, Bennett WW et al (2020) DGT and selective extractions reveal differences in arsenic and antimony uptake by the white icicle radish (Raphanus sativus). Environ Pollut 259:1–9. https://doi.org/10.1016/j.envpol.2019.113815

Nguyen HL, Phung AT, Chu THN et al (2020) Applicability of montmorillonite immobilized in hydrogel for the determination of labile Cd, Pb, Mn, and Zn in water using diffusive gradient in thin films (DGT). Water Air Soil Pollut 231:105–130. https://doi.org/10.1007/s11270-020-04474-5

Nierop KGJ, Jansen B, Vrugt JA, Verstraten JM (2002) Copper complexation by dissolved organic matter and uncertainty assessment of their stability constants. Chemosphere 49:1191–1200. https://doi.org/10.1016/S0045-6535(02)00504-0

Noh S, Kim Y, Kim H et al (2020) The performance of diffusive gradient in thin film probes for the long-term monitoring of trace level total mercury in water. Environ Monit Assess 192:66–78. https://doi.org/10.1007/s10661-019-7966-2

Nolan AL, Zhang H, Mclaughlin MJ (2005) Prediction of zinc, cadmium, lead and copper availability to wheat in contaminated soils using chemical speciation, diffusive gradient in thin films, extraction, and Isotopic dilution techniques. J Environ Qual 34:496–507. https://doi.org/10.2134/jeq2005.0496

Nowack B, Koehler S, Schulin R (2004) Use of diffusive gradients in thin films (DGT) in undisturbed field soils. Environ Sci Technol 38:1133–1138. https://doi.org/10.1021/es034867j

Nyein Aung N, Nakajima F, Furumai H (2008) Trace metal speciation during dry and wet weather flows in the Tama River, Japan, by using diffusive gradients in thin films (DGT). J Environ Monit 10:219–230. https://doi.org/10.1039/b709717d

Odzak N, Kistler D, Xue H, Sigg L (2002) In situ trace metal speciation in a eutrophic lake using the technique of diffusion gradients in thin films (DGT). Aquat Sci 64:292–299. https://doi.org/10.1007/s00027-002-8073-x

Öhlander B, Forsberg J, Österlund H et al (2012) Fractionation of trace metals in a contaminated freshwater stream using membrane filtration, ultrafiltration, DGT and transplanted aquatic moss. Geochem Explor Environ Anal 12:303–312. https://doi.org/10.1144/geochem2012-125

Omanović D, Pižeta I, Vukosav P et al (2015) Assessing element distribution and speciation in a stream at abandoned Pb–Zn mining site by combining classical, in-situ DGT and modelling approaches. Sci Total Environ 511:423–434. https://doi.org/10.1016/j.scitotenv.2014.12.076

Ono K, Yasutaka T, Hayashi TI et al (2019) Model construction for estimating potential vulnerability of Japanese soils to cadmium pollution based on intact soil properties. PLoS ONE 14:1–17. https://doi.org/10.1371/journal.pone.0218377

Österlund H (2010) Applications of the DGT technique for measurements of anions and cations in natural waters. Lulea University of Technology, Lulea

Österlund H, Chlot S, Faarinen M et al (2010) Simultaneous measurements of As, Mo, Sb, V and W using a ferrihydrite diffusive gradients in thin films (DGT) device. Anal Chim Acta 682:59–65. https://doi.org/10.1016/j.aca.2010.09.049

Österlund H, Faarinen M, Ingri J, Baxter DC (2012a) Contribution of organic arsenic species to total arsenic measurements using ferrihydrite-backed diffusive gradients in thin films (DGT). Environ Chem 9:55–62. https://doi.org/10.1071/EN11057

Österlund H, Gelting J, Nordblad F et al (2012b) Copper and nickel in ultrafiltered brackish water: Labile or non-labile? Mar Chem 132–133:34–43. https://doi.org/10.1016/j.marchem.2012.02.002

Österlund H, Widerlund A, Ingri J (2016) Applications in natural waters. In: Diffusive gradients in thin-films for environmental measurements. pp 123–145

Paller MH, Harmon SM, Knox AS et al (2019) Assessing effects of dissolved organic carbon and water hardness on metal toxicity to Ceriodaphnia dubia using diffusive gradients in thin films (DGT). Sci Total Environ 697:134107. https://doi.org/10.1016/j.scitotenv.2019.134107

Pan Y, Guan DX, Zhao D et al (2015) Novel speciation method based on diffusive gradients in thin-films for in situ measurement of CrVI in aquatic systems. Environ Sci Technol 49:14267–14273. https://doi.org/10.1021/acs.est.5b03742

Panther JG, Stillwell KP, Powell KJ, Downard AJ (2008a) Perfluorosulfonated ionomer-modified diffusive gradients in thin films: tool for inorganic arsenic speciation analysis. Anal Chem 80:9806–9811. https://doi.org/10.1021/ac801678u

Panther JG, Stillwell KP, Powell KJ, Downard AJ (2008b) Development and application of the diffusive gradients in thin films technique for the measurement of total dissolved inorganic arsenic in waters. Anal Chim Acta 622:133–142. https://doi.org/10.1016/j.aca.2008.06.004

Panther JG, Stewart RR, Teasdale PR et al (2013) Titanium dioxide-based DGT for measuring dissolved As(V), V(V), Sb(V), Mo(VI) and W(VI) in water. Talanta 105:80–86. https://doi.org/10.1016/j.talanta.2012.11.070

Panther JG, Bennett WW, Welsh DT, Teasdale PR (2014) Simultaneous measurement of trace metal and oxyanion concentrations in water using diffusive gradients in thin films with a chelex-metsorb

mixed binding layer. Anal Chem 86:427–434. https://doi.org/10.1021/ac402247j

Parthasarathy N, Pelletier M, Lou T-WM, Buffle J (2001) On-line coupling of flow through voltammetric microcell to hollow fiber permeation liquid membrane device for subnanomolar trace metal speciation measurements. Electroanalysis 13:1305–1314. https://doi.org/10.1002/1521-4109(200111)13:16%3c1305::AID-ELAN1305%3e3.0.CO;2-1

Pavel PB, Puschenreiter M, Wenzel WW et al (2014) Aided phytostabilization using *Miscanthus sinensis×giganteus* on heavy metal-contaminated soils. Sci Total Environ 479–480:125–131. https://doi.org/10.1016/j.scitotenv.2014.01.097

Pei J, Lou T-WM, Buffle J (2000) Simultaneous determination and speciation of zinc, cadmium, lead, and copper in natural water with minimum handling and artifacts, by voltammetry on a gel-integrated microelectrode array. Anal Chem 72:161–171. https://doi.org/10.1021/ac990628w

Peijnenburg WJGM, Jager T (2003) Monitoring approaches to assess bioaccessibility and bioavailability of metals: matrix issues. Ecotoxicol Environ Saf 56:63–77. https://doi.org/10.1016/S0147-6513(03)00051-4

Pelcová P, Docekalová H, Kleckerová A (2014) Development of the diffusive gradient in thin films technique for the measurement of labile mercury species in waters. Anal Chim Acta 819:42–48. https://doi.org/10.1016/j.aca.2014.02.013

Pelcová P, Docekalová H, Kleckerová A (2015) Determination of mercury species by the diffusive gradient in thin film technique and liquid chromatography—atomic fluorescence spectrometry after microwave extraction. Anal Chim Acta 866:21–26. https://doi.org/10.1016/j.aca.2015.01.043

Pelcová P, Vicarová P, Ridošková A et al (2017) Prediction of mercury bioavailability to common carp (*Cyprinus carpio* L.) using the diffusive gradient in thin film technique. Chemosphere 187:181–187. https://doi.org/10.1016/j.chemosphere.2017.08.097

Pelcová P, Zouharová I, Ridošková A, Smolíková V (2019) Evaluation of mercury availability to pea parts (*Pisum sativum* L.) in urban soils: comparison between diffusive gradients in thin films technique and plant model. Chemosphere 234:373–378. https://doi.org/10.1016/j.chemosphere.2019.06.076

Peng C, Tong H, Shen C et al (2020) Bioavailability and translocation of metal oxide nanoparticles in the soil–rice plant system. Sci Total Environ 713:136662. https://doi.org/10.1016/j.scitotenv.2020.136662

Pérez AL, Anderson KA (2009a) DGT estimates cadmium accumulation in wheat and potato from phosphate fertilizer applications. Sci Total Environ 407:5096–5103. https://doi.org/10.1016/j.scitotenv.2009.05.045

Pérez AL, Anderson KA (2009b) Soil-diffusive gradient in thin films partition coefficients estimate metal bioavailability to crops at fertilized field sites. Environ Toxicol Chem 28:2030–2037. https://doi.org/10.1897/08-637.1

Pérez M, Reynaud S, Lespes G et al (2015) Development of a new passive sampler based on diffusive milligel beads for copper analysis in water. Anal Chim Acta 890:117–123. https://doi.org/10.1016/j.aca.2015.07.037

Pesavento M, Alberti G, Biesuz R (2009) Analytical methods for determination of free metal ion concentration, labile species fraction and metal complexation capacity of environmental waters: a review. Anal Chim Acta 631:129–141. https://doi.org/10.1016/j.aca.2008.10.046

Pescim GF, Marrach G, Vannuci-Silva M et al (2012) Speciation of lead in seawater and river water by using *Saccharomyces cerevisiae* immobilized in agarose gel as a binding agent in the diffusive gradients in thin films technique. Anal Bioanal Chem 404:1581–1588. https://doi.org/10.1007/s00216-012-6248-4

Peters AJ, Zhang H, Davison W (2003) Performance of the diffusive gradients in thin films technique for measurement of trace metals in low ionic strength freshwaters. Anal Chim Acta 478:237–244. https://doi.org/10.1016/S0003-2670(02)01512-X

Philipps RR, Xu X, Mills GL, Bringolf RB (2018a) Impact of natural organic matter and increased water hardness on DGT prediction of copper bioaccumulation by yellow lampmussel (*Lampsilis cariosa*) and fathead minnow (*Pimephales promelas*). Environ Pollut 241:451–458. https://doi.org/10.1016/j.envpol.2018.05.059

Philipps RR, Xu X, Mills GL, Bringolf RB (2018b) Evaluation of diffusive gradients in thin films for prediction of copper bioaccumulation by yellow lampmussel (*Lampsilis cariosa*) and fathead minnow (*Pimephales promelas*). Environ Toxicol Chem 37:1535–1544. https://doi.org/10.1002/etc.4108

Philipps RR, Xu X, Bringolf RB, Mills GL (2019) Evaluation of the DGT technique for predicting uptake of metal mixtures by fathead minnow (*Pimephales promelas*) and yellow lampmussel (*Lampsilis cariosa*). Environ Toxicol Chem 38:61–70. https://doi.org/10.1002/etc.4289

Pichette C, Zhang H, Davison W, Sauvé S (2007) Preventing biofilm development on DGT devices using metals and antibiotics. Talanta 72:716–722. https://doi.org/10.1016/j.talanta.2006.12.014

Pichette C, Zhang H, Sauvé S (2009) Using diffusive gradients in thin-films for in situ monitoring of dissolved phosphate emissions from freshwater aquaculture. Aquaculture 286:198–202. https://doi.org/10.1016/j.aquaculture.2008.09.025

Pinzón-Bedoya CH, Pinzón-Bedoya ML, Pinedo-Hernández J et al (2020) Assessment of potential health risks associated with the intake of heavy metals in fish harvested from the largest estuary in Colombia. Int J Environ Res Public Health 17:1–13. https://doi.org/10.3390/ijerph17082921

Pommier AL, Buzier R, Simon S, Guibaud G (2021) Impact of low ionic strength on DGT sampling with standard APA gels: effect of pH and analyte. Talanta 222:1–6. https://doi.org/10.1016/j.talanta.2020.121413

Price HL, Teasdale PR, Jolley DF (2013) An evaluation of ferrihydrite- and Metsorb™-DGT techniques for measuring oxyanion species (As, Se, V, P): effective capacity, competition and diffusion coefficients. Anal Chim Acta 803:56–65. https://doi.org/10.1016/j.aca.2013.07.001

Prieto DM, Rubinos DA, Piñeiro V et al (2016) Influence of epipsammic biofilm on the biogeochemistry of arsenic in freshwater environments. Biogeochemistry 129:291–306. https://doi.org/10.1007/s10533-016-0232-6

Puschenreiter M, Wittstock F, Friesl-Hanl W, Wenzel WW (2013) Predictability of the Zn and Cd phytoextraction efficiency of a *Salix smithiana* clone by DGT and conventional bioavailability assays. Plant Soil 369:531–541. https://doi.org/10.1007/s11104-013-1597-0

Puy J, Galceran J, Cruz-González S et al (2014) Measurement of metals using DGT: impact of ionic strength and kinetics of dissociation of complexes in the resin domain. Anal Chem 86:7740–7748. https://doi.org/10.1021/ac501679m

Qasim B, Motelica-Heino M, Joussein E et al (2016) Diffusive gradients in thin films, Rhizon soil moisture samplers, and indicator plants to predict the bioavailabilities of potentially toxic elements in contaminated technosols. Environ Sci Pollut Res 23:8367–8378. https://doi.org/10.1007/s11356-015-5975-4

Qiu H, Gu HH, He EK et al (2012) Attenuation of metal bioavailability in acidic multi-metal contaminated soil treated with fly ash and steel slag. Pedosphere 22:544–553. https://doi.org/10.1016/S1002-0160(12)60039-3

Rachou J, Gagnon C, Sauvé S (2007) Use of an ion-selective electrode for free copper measurements in low salinity and low

ionic strength matrices. Environ Chem 4:90–97. https://doi.org/10.1071/EN06036

Reichstädter M, Diviš P, Abdulbur-Alfakhoury E, Gao Y (2020) Simultaneous determination of mercury, cadmium and lead in fish sauce using diffusive gradients in thin-films technique. Talanta 217:121059. https://doi.org/10.1016/j.talanta.2020.121059

Ren M, Wang Y, Ding S et al (2018) Development of a new diffusive gradient in the thin film (DGT) method for the simultaneous measurement of CH_3Hg^+ and Hg^{2+}. New J Chem 42:7976–7983. https://doi.org/10.1039/c8nj00211h

Ridošková A, Docekalová H, Pelcová P (2017) Prediction of cadmium, lead and mercury availability to plants: a comparison between diffusive gradients measured in a thin films technique and soil grown plants. J Elem 22:349–363. https://doi.org/10.5601/jelem.2016.21.2.1075

Ridošková A, Pelfrêne A, Douay F et al (2019) Bioavailability of mercury in contaminated soils assessed by the diffusive gradient in thin film technique in relation to uptake by *Miscanthus × giganteus*. Environ Toxicol Chem 38:321–328. https://doi.org/10.1002/etc.4318

Rodríguez J, Mandalunis PM (2018) A review of metal exposure and its effects on bone health. J Toxicol. https://doi.org/10.1155/2018/4854152

Rodríguez Martín JA, Arias ML, Grau Corbí JM (2006) Heavy metals contents in agricultural topsoils in the Ebro basin (Spain). Application of the multivariate geoestatistical methods to study spatial variations. Environ Pollut 144:1001–1012. https://doi.org/10.1016/j.envpol.2006.01.045

Roig N, Nadal M, Sierra J et al (2011) Novel approach for assessing heavy metal pollution and ecotoxicological status of rivers by means of passive sampling methods. Environ Int 37:671–677. https://doi.org/10.1016/j.envint.2011.01.007

Rolisola AMCM, Suárez CA, Menegário AA et al (2014) Speciation analysis of inorganic arsenic in river water by Amberlite IRA 910 resin immobilized in a polyacrylamide gel as a selective binding agent for As(v) in diffusive gradient thin film technique. Analyst 139:4373–4380. https://doi.org/10.1039/c4an00555d

Ruello ML, Sileno M, Sani D, Fava G (2008) DGT use in contaminated site characterization. The importance of heavy metal site specific behaviour. Chemosphere 70:1135–1140. https://doi.org/10.1016/j.chemosphere.2007.08.013

Sangi MR, Halstead MJ, Hunter K (2002) Use of the diffusion gradient thin film method to measure trace metals in fresh waters at low ionic strength. Anal Chim Acta 456:241–251. https://doi.org/10.1016/S0003-2670(02)00012-0

Scally S, Zhang H, Davison W (2004) Measurements of lead complexation with organic ligands using DGT. Aust J Chem 57:925–930. https://doi.org/10.1071/CH04076

Scally S, Davison W, Zhang H (2006) Diffusion coefficients of metals and metal complexes in hydrogels used in diffusive gradients in thin films. Anal Chim Acta 558:222–229. https://doi.org/10.1016/j.aca.2005.11.020

Schintu M, Durante L, Maccioni A et al (2008) Measurement of environmental trace-metal levels in Mediterranean coastal areas with transplanted mussels and DGT techniques. Mar Pollut Bull 57:832–837. https://doi.org/10.1016/j.marpolbul.2008.02.038

Schintu M, Marras B, Durante L et al (2010) Macroalgae and DGT as indicators of available trace metals in marine coastal waters near a lead-zinc smelter. Environ Monit Assess 167:653–661. https://doi.org/10.1007/s10661-009-1081-8

Schintu M, Marrucci A, Marras B et al (2018) Passive sampling monitoring of PAHs and trace metals in seawater during the salvaging of the Costa Concordia wreck (Parbuckling Project). Mar Pollut Bull 135:819–827. https://doi.org/10.1016/j.marpolbul.2018.08.011

Schmukat A, Duester L, Ecker D et al (2013) Determination of the long-term release of metal(loid)s from construction materials using DGTs. J Hazard Mater 260:725–732. https://doi.org/10.1016/j.jhazmat.2013.06.035

Schoyen M, Allan IJ, Ruus A et al (2017) Comparison of caged and native blue mussels (*Mytilus edulis* spp.) for environmental monitoring of PAH, PCB and trace metals. Mar Environ Res 130:221–232. https://doi.org/10.1016/j.marenvres.2017.07.025

Senila M (2014) Real and simulated bioavailability of lead in contaminated and uncontaminated soils. J Environ Heal Sci Eng 12:1–8. https://doi.org/10.1186/2052-336X-12-108

Senila M, Levei E, Senila LR (2012) Assessment of metals bioavailability to vegetables under field conditions using DGT, single extractions and multivariate statistics. Chem Cent J 6:119–129. https://doi.org/10.1186/1752-153X-6-119

Senila M, Senila L, Urik M, Matúš P (2013) Evaluation of mercury bioavailability in soil samples using DGT and TD-AAS techniques: case study of Baia Mare, NW Romania. Miner Slovaca 45:121–124

Senila M, Drolc A, Pintar A et al (2017a) Assessment of mercury availability in water samples using DGT and TD-AAS techniques. Environ Eng Manag J 16:1515–1520. https://doi.org/10.30638/eemj.2017.164

Senila M, Levei E, Cadar O et al (2017b) Assessment of availability and human health risk posed by arsenic contaminated well waters from Timis-Bega area, Romania. J Anal Methods Chem. https://doi.org/10.1155/2017/3037651

Shafaei Arvajeh MR, Lehto N, Garmo A, Zhang H (2013) Kinetic studies of Ni organic complexes using diffusive gradients in thin films (DGT) with double binding layers and a dynamic numerical model. Environ Sci Technol 47:463–470. https://doi.org/10.1021/es301371b

Sherwood JE, Barnett D, Barnett NW et al (2009) Deployment of DGT units in marine waters to assess the environmental risk from a deep sea tailings outfall. Anal Chim Acta 652:215–223. https://doi.org/10.1016/j.aca.2009.06.009

Shiva AH, Teasdale PR, Bennett WW, Welsh DT (2015) A systematic determination of diffusion coefficients of trace elements in open and restricted diffusive layers used by the diffusive gradients in a thin film technique. Anal Chim Acta 888:146–154. https://doi.org/10.1016/j.aca.2015.07.027

Shiva AH, Bennett WW, Welsh DT, Teasdale PR (2016) In situ evaluation of DGT techniques for measurement of trace metals in estuarine waters: a comparison of four binding layers with open and restricted diffusive layers. Environ Sci Process Impacts 18:51–63. https://doi.org/10.1039/c5em00550g

Shiva AH, Teasdale PR, Welsh DT, Bennett WW (2017) Evaluation of the DGT technique for selective measurement of aluminium and trace metal concentrations in an acid drainage-impacted coastal waterway. Environ Sci Process Impacts 19:742–751. https://doi.org/10.1039/C6EM00276E

Sierra J, Roig N, Giménez Papiol G et al (2017) Prediction of the bioavailability of potentially toxic elements in freshwaters. Comparison between speciation models and passive samplers. Sci Total Environ 605–606:211–218. https://doi.org/10.1016/j.scitotenv.2017.06.136

Sigg L, Black F, Buffle J et al (2006) Comparison of analytical techniques for dynamic trace metal speciation in natural freshwaters. Environ Sci Technol 40:1934–1941. https://doi.org/10.1021/es051245k

Slaveykova VI, Karadjova IB, Karadjov M, Tsalev DL (2009) Trace metal speciation and bioavailability in surface waters of the black sea coastal area evaluated by HF-PLM and DGT. Environ Sci Technol 43:1798–1803. https://doi.org/10.1021/es802544n

Smith IM, Hall KJ, Lavkulich LM, Schreier H (2007) Trace metal concentrations in an intensive agricultural watershed in British Columbia, Canada. J Am Water Resour Assoc 43:1455–1467. https://doi.org/10.1111/j.1752-1688.2007.00121.x

Smolíková V, Pelcová P, Ridošková A et al (2020) Development and evaluation of the iron oxide–hydroxide based resin gel for the diffusive gradient in thin films technique. Anal Chim Acta 1102:36–45. https://doi.org/10.1016/j.aca.2019.12.042

Sochaczewski Ł, Tych W, Davison B, Zhang H (2007) 2D DGT induced fluxes in sediments and soils (2D DIFS). Environ Model Softw 22:14–23. https://doi.org/10.1016/j.envsoft.2005.09.008

Song N, Wang F, Ma Y, Tang S (2015) Using DGT to assess cadmium bioavailability to ryegrass as influenced by soil properties. Pedosphere 25:825–833. https://doi.org/10.1016/S1002-0160(15)30063-1

Sönmez O, Pierzynski GM (2005) Assessment of zinc phytoavailability by diffusive gradients in thin films. Environ Toxicol Chem 24:934–941. https://doi.org/10.1897/04-350R.1

Sönmez O, Kaya C, Aydemir S (2009) Determination of zinc phytoavailability in soil by diffusive gradients in thin films. Commun Soil Sci Plant Anal 40:3435–3451. https://doi.org/10.1080/00103620903326008

Sönmez O, Pierzynski G, Kaya C, Aydemir S (2016) The effects of phosphorus addition on phytoavailability of zinc by diffusive gradients in thin films (DGT). Turk J Agric for 40:379–385. https://doi.org/10.3906/tar-1511-18

Soriano-Disla JM, Speir TW, Gómez I et al (2010) Evaluation of different extraction methods for the assessment of heavy metal bioavailability in various soils. Water Air Soil Pollut 213:471–483. https://doi.org/10.1007/s11270-010-0400-6

Stewart M, Cameron M, McMurtry M et al (2016) Development of passive sampling devices for bioavailable contaminants of current and emerging concern: Waitemata Harbour case study. N Z J Mar Freshw Res 50:526–548. https://doi.org/10.1080/00288330.2016.1181662

Strivens J, Hayman N, Johnston R, Rosen G (2019) Effects of dissolved organic carbon on copper toxicity to embryos of mytilus galloprovincialis as measured by diffusive gradient in thin films. Environ Toxicol Chem 38:1029–1034. https://doi.org/10.1002/etc.4404

Strivens J, Hayman N, Rosen G, Myers-Pigg A (2020) Toward validation of toxicological interpretation of diffusive gradients in thin films in marine waters impacted by copper. Environ Toxicol Chem 39:873–881. https://doi.org/10.1002/etc.4673

Suárez CA, De Simone TV, Menegário AA et al (2016) In situ redox speciation analysis of chromium in water by diffusive gradients in thin films using a DE81 anion exchange membrane. Talanta 154:299–303. https://doi.org/10.1016/j.talanta.2016.03.085

Sui DP, Fan HT, Li J et al (2013) Application of poly (ethyleneimine) solution as a binding agent in DGT technique for measurement of heavy metals in water. Talanta 114:276–282. https://doi.org/10.1016/j.talanta.2013.05.027

Sui DP, Chen HX, Liu L et al (2016) Ion-imprinted silica adsorbent modified diffusive gradients in thin films technique: tool for speciation analysis of free lead species. Talanta 148:285–291. https://doi.org/10.1016/j.talanta.2015.11.003

Sun Q, Chen J, Ding S et al (2014a) Comparison of diffusive gradients in thin film technique with traditional methods for evaluation of zinc bioavailability in soils. Environ Monit Assess 186:6553–6564. https://doi.org/10.1007/s10661-014-3873-8

Sun Q, Chen J, Zhang H et al (2014b) Improved diffusive gradients in thin films (DGT) measurement of total dissolved inorganic arsenic in waters and soils using a hydrous zirconium oxide binding layer. Anal Chem 86:3060–3067. https://doi.org/10.1021/ac404025e

Sun Q, Zhang L, Ding S et al (2015) Evaluation of the diffusive gradients in thin films technique using a mixed binding gel for measuring iron, phosphorus and arsenic in the environment. Environ Sci Process Impacts 17:570–577. https://doi.org/10.1039/c4em00629a

Sun H, Gao B, Gao L et al (2018a) Assessing Cu remobilization in reservoir riparian soils prior to water impoundment using DGT and geochemical fractionation. Geoderma 327:55–62. https://doi.org/10.1016/j.geoderma.2018.04.018

Sun Q, Ding S, Zhang L et al (2018b) Effect of phosphorus competition on arsenic bioavailability in dry and flooded soils: comparative study using diffusive gradients in thin films and chemical extraction methods. J Soils Sediments 19:1830–1838. https://doi.org/10.1007/s11368-018-2196-8

Tafurt-Cardona M, Eismann CE, Suárez CA et al (2015) In situ selective determination of methylmercury in river water by diffusive gradient in thin films technique (DGT) using baker's yeast (Saccharomyces cerevisiae) immobilized in agarose gel as binding phase. Anal Chim Acta 887:38–44. https://doi.org/10.1016/j.aca.2015.07.035

Tan F, Jiang X, Qiao X et al (2019a) Development of cerium oxide-based diffusive gradients in thin films technique for in-situ measurement of dissolved inorganic arsenic in waters. Anal Chim Acta 1052:65–72. https://doi.org/10.1016/j.aca.2018.11.023

Tan SY, Lee SC, Kuramitz H, Abd-Rahman F (2019b) A novel hybrid long period fiber grating-diffusive gradient in thin films sensor system for the detection of mercury (II) ions in water. Int J Light Electron Opt 194:163040. https://doi.org/10.1016/j.ijleo.2019.163040

Tandy S, Mundus S, Yngvesson J et al (2011) The use of DGT for prediction of plant available copper, zinc and phosphorus in agricultural soils. Plant Soil 346:167–180. https://doi.org/10.1007/s11104-011-0806-y

Tang J, Cao C, Gao F, Wang W (2019) Effects of biochar amendment on the availability of trace elements and the properties of dissolved organic matter in contaminated soils. Environ Technol Innov 16:100492. https://doi.org/10.1016/j.eti.2019.100492

Tchounwou PB, Yedjou CG, Patlolla AK, Sutton DJ (2012) Heavy metals toxicity and the environment. Mol Clin Environ Toxicol 101:133–164. https://doi.org/10.1007/978-3-7643-8340-4

Tella M, Bravin MN, Thuriès L et al (2016) Increased zinc and copper availability in organic waste amended soil potentially involving distinct release mechanisms. Environ Pollut 212:299–306. https://doi.org/10.1016/j.envpol.2016.01.077

Temminghoff EJM, Plette ACC, Van Eck R, Van Riemsdijk WH (2000) Determination of the chemical speciation of trace metals in aqueous systems by the Wageningen Donnan membrane technique. Anal Chim Acta 417:149–157. https://doi.org/10.1016/S0003-2670(00)00935-1

Templeton DM, Fujishiro H (2017) Terminology of elemental speciation—An IUPAC perspective. Coord Chem Rev 352:424–431. https://doi.org/10.1016/j.ccr.2017.02.002

Tian Y, Wang X, Luo J et al (2008) Evaluation of holistic approaches to predicting the concentrations of metals in field-cultivated rice. Environ Sci Technol 42:7649–7654. https://doi.org/10.1021/es7027789

Tian K, Xing Z, Liu G et al (2018) Cadmium phytoavailability under greenhouse vegetable production system measured by diffusive gradients in thin films (DGT) and its implications for the soil threshold. Environ Pollut 241:412–421. https://doi.org/10.1016/j.envpol.2018.05.086

Tonello PS, Rosa AH, Abreu CH, Menegário AA (2007) Use of diffusive gradients in thin films and tangential flow ultrafiltration for fractionation of Al(III) and Cu(II) in organic-rich river waters.

Anal Chim Acta 598:162–168. https://doi.org/10.1016/j.aca.2007.07.013

Tonello PS, Goveia D, Rosa AH et al (2011) Determination of labile inorganic and organic species of Al and Cu in river waters using the diffusive gradients in thin films technique. Anal Bioanal Chem 399:2563–2570. https://doi.org/10.1007/s00216-010-4603-x

Torre MCADL, Beaulieu PY, Tessier A (2000) In situ measurement of trace metals in lakewater using the dialysis and DGT techniques. Anal Chim Acta 418:53–68. https://doi.org/10.1016/S0003-2670(00)00946-6

Tóth G, Hermann T, Da Silva MR, Montanarella L (2016) Heavy metals in agricultural soils of the European Union with implications for food safety. Environ Int 88:299–309. https://doi.org/10.1016/j.envint.2015.12.017

Turner GSC, Mills GA, Teasdale PR et al (2012) Evaluation of DGT techniques for measuring inorganic uranium species in natural waters: Interferences, deployment time and speciation. Anal Chim Acta 739:37–46. https://doi.org/10.1016/j.aca.2012.06.011

Turull M, Elias G, Fontàs C, Díez S (2017a) Exploring new DGT samplers containing a polymer inclusion membrane for mercury monitoring. Environ Sci Pollut Res 24:10919–10928. https://doi.org/10.1007/s11356-016-6813-z

Turull M, Grmanova G, Dago À et al (2017b) Phytochelatin synthesis in response to Hg uptake in aquatic plants near a chlor-alkali factory. Chemosphere 176:74–80. https://doi.org/10.1016/j.chemosphere.2017.02.092

Turull M, Noller B, Díez S et al (2018) Evaluation of mercury in a freshwater environment impacted by an organomercury fungicide using diffusive gradient in thin films. Sci Total Environ 621:1475–1484. https://doi.org/10.1016/j.scitotenv.2017.10.081

Turull M, Fontàs C, Díez S (2019a) Diffusive gradient in thin films with open and restricted gels for predicting mercury uptake by plants. Environ Chem Lett. https://doi.org/10.1007/s10311-019-00864-2

Turull M, Fontàs C, Díez S (2019b) Conventional and novel techniques for the determination of Hg uptake by lettuce in amended agricultural peri-urban soils. Sci Total Environ 668:40–46. https://doi.org/10.1016/j.scitotenv.2019.02.244

Uher E, Zhang H, Santos S et al (2012) Impact of biofouling on diffusive gradient in thin film measurements in water. Anal Chem 84:3111–3118. https://doi.org/10.1021/ac2028535

Uher E, Tusseau-Vuillemin MH, Gourlay-France C (2013) DGT measurement in low flow conditions: diffusive boundary layer and lability considerations. Environ Sci Process Impacts 15:1351–1358. https://doi.org/10.1039/c3em00151b

Uher E, Compère C, Combe M et al (2017) In situ measurement with diffusive gradients in thin films: effect of biofouling in freshwater. Environ Sci Pollut Res 24:13797–13807. https://doi.org/10.1007/s11356-017-8972-y

Uher E, Besse JP, Delaigue O et al (2018) Comparison of the metal contamination in water measured by diffusive gradient in thin film (DGT), biomonitoring and total metal dissolved concentration at a national scale. Appl Geochem 88:247–257. https://doi.org/10.1016/j.apgeochem.2017.05.003

Unsworth ER, Warnken KW, Zhang H et al (2006) Model predictions of metal speciation in freshwaters compared to measurements by in situ techniques. Environ Sci Technol 40:1942–1949. https://doi.org/10.1021/es051246c

Ure A, Davidson C (2002) Chemical speciation in the environment, 2n edn. Blackwell Science, London

Uribe R, Mongin S, Puy J et al (2011) Contribution of partially labile complexes to the DGT metal flux. Environ Sci Technol 45:5317–5322. https://doi.org/10.1021/es200610n

Van Der Veeken PLR, Pinheiro JP, Van Leeuwen HP (2008) Metal speciation by DGT/DET in colloidal complex systems. Environ Sci Technol 42:8835–8840. https://doi.org/10.1021/es801654s

Van Leeuwen HP, Town RM (2002) Stripping chronopotentiometry for metal ion speciation analysis at a microelectrode. J Electroanal Chem 523:16–25. https://doi.org/10.1016/S0022-0728(02)00723-4

Van Leeuwen HP, Town RM, Buffle J et al (2005) Dynamic speciation analysis and bioavailability of metals in aquatic systems. Environ Sci Technol 39:8545–8556. https://doi.org/10.1021/es050404x

Vannuci-Silva M, de Souza JM, de Oliveira FF et al (2017) Bioavailability of metals at a southeastern Brazilian coastal area of high environmental concern under anthropic influence: evaluation using transplanted bivalves (Nodipecten nodosus) and the DGT technique. Water Air Soil Pollut 228:1–13. https://doi.org/10.1007/s11270-017-3387-4

Villanueva JD, Le Coustumer P, Huneau F et al (2013) Assessment of trace metals during episodic events using DGT passive sampler: a proposal for water management enhancement. Water Resour Manag 27:4163–4181. https://doi.org/10.1007/s11269-013-0401-5

Villanueva JD, Le Coustumer P, Denis A et al (2015) Trends of labile trace metals in tropical urban water under highly contrasted weather conditions. Environ Sci Pollut Res 22:13842–13857. https://doi.org/10.1007/s11356-015-4835-6

Villanueva JD, Granger D, Binet G et al (2016) Labile trace metal contribution of the runoff collector to a semi-urban river. Environ Sci Pollut Res 23:11298–11311. https://doi.org/10.1007/s11356-016-6322-0

Vogel C, Hoffmann MC, Krüger O et al (2020) Chromium (VI) in phosphorus fertilizers determined with the diffusive gradients in thin-films (DGT) technique. Environ Sci Pollut Res 27:24320–24328. https://doi.org/10.1007/s11356-020-08761-w

Vystavna Y, Huneau F, Motelica-Heino M et al (2012) Monitoring and flux determination of trace metals in rivers of the Seversky Donets basin (Ukraine) using DGT passive samplers. Environ Earth Sci 65:1715–1725. https://doi.org/10.1007/s12665-011-1151-4

Vystavna Y, Le Coustumer P, Huneau F (2013) Monitoring of trace metals and pharmaceuticals as anthropogenic and socio-economic indicators of urban and industrial impact on surface waters. Environ Monit Assess 185:3581–3601. https://doi.org/10.1007/s10661-012-2811-x

Wallner-Kersanach M, de Andrade CFF, Zhang H et al (2009) In situ measurement of trace metals in estuarine waters of Patos Lagoon using diffusive gradients in thin films (DGT). J Braz Chem Soc 20:333–340. https://doi.org/10.1590/S0103-50532009000200019

Wang P, Zhou DM, Luo XS, Li LZ (2009) Effects of Zn-complexes on zinc uptake by wheat (Triticum aestivum) roots: a comprehensive consideration of physical, chemical and biological processes on biouptake. Plant Soil 316:177–192. https://doi.org/10.1007/s11104-008-9769-z

Wang J, Bai L, Zeng X et al (2014a) Assessment of arsenic availability in soils using the diffusive gradients in thin films (DGT) technique—A comparison study of DGT and classic extraction methods. Environ Sci Process Impacts 16:2355–2361. https://doi.org/10.1039/c4em00215f

Wang Z, Zhao P, Yan C et al (2014b) Combined use of DGT and transplanted shrimp (Litopenaeus vannamei) to assess the bioavailable metals of complex contamination: Implications for implementing bioavailability-based water quality criteria. Environ Sci Pollut Res 21:4502–4515. https://doi.org/10.1007/s11356-013-2415-1

Wang P, Wang T, Yao Y et al (2016a) A diffusive gradient-in-thin-film technique for evaluation of the bioavailability of Cd in soil

contaminated with Cd and Pb. Int J Environ Res Public Health. https://doi.org/10.3390/ijerph13060556

Wang Y, Ding S, Gong M et al (2016b) Diffusion characteristics of agarose hydrogel used in diffusive gradients in thin films for measurements of cations and anions. Anal Chim Acta 945:47–56. https://doi.org/10.1016/j.aca.2016.10.003

Wang P, Liu C, Yao Y et al (2017a) Comparison of in situ DGT measurement with ex situ methods for predicting cadmium bioavailability in soils with combined pollution to biotas. Water Sci Technol 75:2171–2178. https://doi.org/10.2166/wst.2017.093

Wang Y, Ding S, Shi L et al (2017b) Simultaneous measurements of cations and anions using diffusive gradients in thin films with a ZrO–Chelex mixed binding layer. Anal Chim Acta 972:1–11. https://doi.org/10.1016/j.aca.2017.04.007

Wang J, Zeng X, Zhang H et al (2018a) Kinetic release of arsenic after exogenous inputs into two different types of soil. Environ Sci Pollut Res 25:12876–12882. https://doi.org/10.1007/s11356-018-1550-0

Wang J, Zeng X, Zhang H et al (2018b) Effect of exogenous phosphate on the lability and phytoavailability of arsenic in soils. Chemosphere 196:540–547. https://doi.org/10.1016/j.chemosphere.2017.12.191

Wang J, Li D, Lu Q et al (2020) Effect of water-driven changes in rice rhizosphere on Cd lability in three soils with different pH. J Environ Sci 87:82–92. https://doi.org/10.1016/j.jes.2019.05.020

Warnken KW, Zhang H, Davison W (2004) Performance characteristics of suspended particulate reagent- iminodiacetate as a binding agent for diffusive gradients in thin films. Anal Chim Acta 508:41–51. https://doi.org/10.1016/j.aca.2003.11.051

Warnken KW, Zhang H, Davison W (2005) Trace metal measurements in low ionic strength synthetic solutions by diffusive gradients in thin films. Anal Chem 77:5440–5446. https://doi.org/10.1021/ac050045o

Warnken KW, Davison W, Zhang H et al (2007) In situ measurements of metal complex exchange kinetics in freshwater. Environ Sci Technol 41:3179–3185. https://doi.org/10.1021/es062474p

Warnken KW, Davison W, Zhang H (2008) Interpretation of in situ speciation measurements of inorganic and organically complexed trace metals in freshwater by DGT. Environ Sci Technol 42:6903–6909. https://doi.org/10.1021/es800359n

Warnken KW, Lawlor AJ, Lofts S et al (2009) In situ speciation measurements of trace metals in headwater streams. Environ Sci Technol 43:7230–7236. https://doi.org/10.1021/es900112w

Webb JA, Keough MJ (2002) Measurement of environmental trace-metal levels with transplanted mussels and diffusive gradients in thin films (DGT): a comparison of techniques. Mar Pollut Bull 44:222–229. https://doi.org/10.1016/S0025-326X(01)00244-2

Welikala D, Hucker C, Hartland A et al (2018) Trace metal mobilization by organic soil amendments: insights gained from analyses of solid and solution phase complexation of cadmium, nickel and zinc. Chemosphere 199:684–693. https://doi.org/10.1016/j.chemosphere.2018.02.069

Wen Y, Li W, Yang Z et al (2020) Evaluation of various approaches to predict cadmium bioavailability to rice grown in soils with high geochemical background in the karst region. Southwest China Environ Pollut 258:113645. https://doi.org/10.1016/j.envpol.2019.113645

WHO (2000) Mercury. In: Air quality guidelines for Europe. Copenhagen WHO Reg. Off. Eur. https://www.euro.who.int/__data/assets/pdf_file/0004/123079/AQG2ndEd_6_9Mercury.PDF

Williams PN, Zhang H, Davison W et al (2012) Evaluation of in situ DGT measurements for predicting the concentration of Cd in Chinese field-cultivated rice: impact of soil cd: Zn ratios. Environ Sci Technol 46:8009–8016. https://doi.org/10.1021/es301195h

Wu T, Wang G, Zhang Y et al (2017) Determination of mercury in aquatic systems by DGT device using thiol-modified carbon nanoparticle suspension as the liquid binding phase. New J Chem 41:10305–10311. https://doi.org/10.1039/c7nj02007d

Wu L, Zhou J, Zhou T et al (2018) Estimating cadmium availability to the hyperaccumulator Sedum plumbizincicola in a wide range of soil types using a piecewise function. Sci Total Environ 637–638:1342–1350. https://doi.org/10.1016/j.scitotenv.2018.04.386

Xu JY, Li HB, Liang S et al (2014) Arsenic enhanced plant growth and altered rhizosphere characteristics of hyperaccumulator Pteris vittata. Environ Pollut 194:105–111. https://doi.org/10.1016/j.envpol.2014.07.017

Xu Q, Gao L, Peng W et al (2018) Assessment of labile Zn in reservoir riparian soils using DGT, DIFS, and sequential extraction. Ecotoxicol Environ Saf 160:184–190. https://doi.org/10.1016/j.ecoenv.2018.05.039

Xu D, Gao B, Chen S et al (2019a) Release risk assessment of trace metals in urban soils using in-situ DGT and DIFS model. Sci Total Environ 694:133624. https://doi.org/10.1016/j.scitotenv.2019.133624

Xu D, Gao B, Peng W et al (2019b) Application of DGT/DIFS and geochemical baseline to assess Cd release risk in reservoir riparian soils, China. Sci Total Environ 646:1546–1553. https://doi.org/10.1016/j.scitotenv.2018.07.262

Xu J, Huang L, Chen C et al (2019c) Effective lead immobilization by phosphate rock solubilization mediated by phosphate rock amendment and phosphate solubilizing bacteria. Chemosphere 237:124540. https://doi.org/10.1016/j.chemosphere.2019.124540

Xu Q, Ye B, Mou X et al (2019d) Lead was mobilized in acid silty clay loam paddy soil with potassium dihydrogen phosphate (KDP) amendment. Environ Pollut 255:113179. https://doi.org/10.1016/j.envpol.2019.113179

Xu X, Peck E, Fletcher DE et al (2020) Limitations of applying diffusive gradients in thin films to predict bioavailability of metal mixtures in aquatic systems with unstable water chemistries. Environ Toxicol Chem 39:2485–2495. https://doi.org/10.1002/etc.4860

Yabuki LNM, Colaço CD, Menegário AA et al (2014) Evaluation of diffusive gradients in thin films technique (DGT) for measuring Al, Cd Co, Cu, Mn, Ni, and Zn in Amazonian rivers. Environ Monit Assess 186:961–969. https://doi.org/10.1007/s10661-013-3430-x

Yabuki LNM, Menegário AA, Gemeiner H et al (2019) Residual biomass of coffee as a binding agent in diffusive gradients in thin-films technique for Cd, Cu, Ni, Pb and Zn measurement in waters. Talanta 205:120148. https://doi.org/10.1016/j.talanta.2019.120148

Yao Y, Sun Q, Wang C et al (2016a) The combination of DGT technique and traditional chemical methods for evaluation of cadmium bioavailability in contaminated soils with organic amendment. Int J Environ Res Public Health 13:1–14. https://doi.org/10.3390/ijerph13060595

Yao Y, Wang C, Wang P et al (2016b) Zr oxide-based coloration technique for two-dimensional imaging of labile Cr(VI) using diffusive gradients in thin films. Sci Total Environ 566–567:1632–1639. https://doi.org/10.1016/j.scitotenv.2016.06.065

Yao Y, Sun Q, Wang C et al (2017) Evaluation of organic amendment on the effect of cadmium bioavailability in contaminated soils using the DGT technique and traditional methods. Environ Sci Pollut Res 24:7959–7968. https://doi.org/10.1007/s11356-017-8868-x

Yao H, Zhao Y, Lin CJ et al (2020) Development of a novel composite resin for dissolved divalent mercury measurement using diffusive gradients in thin films. Chemosphere 251:126231. https://doi.org/10.1016/j.chemosphere.2020.126231

Yi Z, Lehto NJ, Robinson BH, Cavanagh JAE (2020) Environmental and edaphic factors affecting soil cadmium uptake by spinach, potatoes, onion and wheat. Sci Total Environ 713:1–9. https://doi.org/10.1016/j.scitotenv.2020.136694

Yin H, Cai Y, Duan H et al (2014) Use of DGT and conventional methods to predict sediment metal bioavailability to a field inhabitant freshwater snail (*Bellamya aeruginosa*) from Chinese eutrophic lakes. J Hazard Mater 264:184–194. https://doi.org/10.1016/j.jhazmat.2013.11.030

Yuan Y, Ding S, Wang Y et al (2018) Simultaneous measurement of fifteen rare earth elements using diffusive gradients in thin films. Anal Chim Acta 1031:98–107. https://doi.org/10.1016/j.aca.2018.05.067

Zarrouk S, Bermond A, Kolsi Benzina N et al (2014) Diffusive gradient in thin-film (DGT) models Cd and Pb uptake by plants growing on soils amended with sewage sludge and urban compost. Environ Chem Lett 12:191–199. https://doi.org/10.1007/s10311-013-0431-5

Zhang H (2004) In-situ speciation of Ni and Zn in freshwaters: comparison between DGT measurements and speciation models. Environ Sci Technol 38:1421–1427. https://doi.org/10.1021/es034654u

Zhang H, Davison W (1995) Performance characteristics of diffusion gradients in thin films for the in situ measurement of trace metals in aqueous solution. Anal Chem 67:3391–3400. https://doi.org/10.1021/ac00115a005

Zhang H, Davison W (1999) Diffusional characteristics of hydrogels used in DGT and DET techniques. Anal Chim Acta 398:329–340. https://doi.org/10.1016/S0003-2670(99)00458-4

Zhang H, Davison W (2000) Direct in situ measurements of labile inorganic and organically bound metal species in synthetic solutions and natural waters using diffusive gradients in thin films. Anal Chem 72:4447–4457. https://doi.org/10.1021/ac0004097

Zhang H, Davison W (2001) In situ speciation measurements. Using diffusive gradients in thin films (DGT) to determine inorganically and organically complexed metals. Pure Appl Chem 73:9–15. https://doi.org/10.1351/pac200173010009

Zhang H, Davison W (2015) Use of diffusive gradients in thin-films for studies of chemical speciation and bioavailability. Environ Chem 12:85–101. https://doi.org/10.1071/EN14105

Zhang H, Davison W, Knight B, McGrath S (1998) In situ measurements of solution concentrations and fluxes of trace metals in soils using DGT. Environ Sci Technol 32:704–710. https://doi.org/10.1021/es9704388

Zhang H, Zhao FJ, Sun B et al (2001) A new method to measure effective soil solution concentration predicts copper availability to plants. Environ Sci Technol 35:2602–2607. https://doi.org/10.1021/es000268q

Zhang H, Lombi E, Smolders E, McGrath S (2004) Kinetics of Zn release in soils and prediction of Zn concentration in plants using diffusive gradients in thin films. Environ Sci Technol 38:3608–3613. https://doi.org/10.1021/es0352597

Zhang H, Davison W, Tye AM et al (2006) Kinetics of zinc and cadmium release in freshly contaminated soils. Environ Toxicol Chem 25:664–670. https://doi.org/10.1897/04-664R.1

Zhang Y, Mason S, McNeill A, McLaughlin MJ (2013) Optimization of the diffusive gradients in thin films (DGT) method for simultaneous assay of potassium and plant-available phosphorus in soils. Talanta 113:123–129. https://doi.org/10.1016/j.talanta.2013.03.023

Zhang C, Ding S, Xu D et al (2014) Bioavailability assessment of phosphorus and metals in soils and sediments: a review of diffusive gradients in thin films (DGT). Environ Monit Assess 186:7367–7378. https://doi.org/10.1007/s10661-014-3933-0

Zhang S, Song J, Gao H et al (2016) Improving prediction of metal uptake by Chinese cabbage (*Brassica pekinensis* L.) based on a soil-plant stepwise analysis. Sci Total Environ 569–570:1595–1605. https://doi.org/10.1016/j.scitotenv.2016.07.007

Zhang L, Sun Q, Ding S et al (2017a) Characterization of arsenic availability in dry and flooded soils using sequential extraction and diffusive gradients in thin films (DGT) techniques. Environ Sci Pollut Res 24:15727–15734. https://doi.org/10.1007/s11356-017-9190-3

Zhang S, Williams PN, Zhou CY et al (2017b) Extending the functionality of the slurry ferrihydrite-DGT method: Performance evaluation for the measurement of vanadate, arsenate, antimonate and molybdate in water. Chemosphere 184:812–819. https://doi.org/10.1016/j.chemosphere.2017.06.062

Zhang W, Yang J, Li Z et al (2017c) Assessment of the availability of As and Pb in soils after in situ stabilization. Environ Sci Pollut Res 24:23153–23160. https://doi.org/10.1007/s11356-017-9877-5

Zhang S, Wang Y, Pervaiz A et al (2018) Comparison of diffusive gradients in thin-films (DGT) and chemical extraction methods for predicting bioavailability of antimony and arsenic to plants. Geoderma 332:1–9. https://doi.org/10.1016/j.geoderma.2018.06.023

Zhang T, Zeng X, Zhang H et al (2019) The effect of the ferrihydrite dissolution/transformation process on mobility of arsenic in soils: investigated by coupling a two-step sequential extraction with the diffusive gradient in the thin films (DGT) technique. Geoderma 352:22–32. https://doi.org/10.1016/j.geoderma.2019.05.042

Zhao F-J, Rooney CP, Zhang H, Mcgrath SP (2006) Comparison of soil solution speciation and diffusive gradients in thin-films measurement As an indicator of copper bioavailability to plants. Environ Toxicol Chem 25:733–742. https://doi.org/10.1897/04-603r.1

Zhao X, Jiang Y, Gu X et al (2018) Multisurface modeling of Ni bioavailability to wheat (*Triticum aestivum* L.) in various soils. Environ Pollut 238:590–598. https://doi.org/10.1016/j.envpol.2018.03.064

Zheng C, Wang X, Liu J et al (2019) Biochar-assisted phytoextraction of arsenic in soil using *Pteris vittata* L. Environ Sci Pollut Res 26:36688–36697. https://doi.org/10.1007/s11356-019-06688-5

Zhou Y, Stotesbury T, Dimock B et al (2013) Novel silica sol–gel passive sampler for mercury monitoring in aqueous systems. Chemosphere 90:323–328. https://doi.org/10.1016/j.chemosphere.2012.07.022

Zhou JW, Wu LH, Zhou T et al (2019) Comparing chemical extraction and a piecewise function with diffusive gradients in thin films for accurate estimation of soil zinc bioavailability to Sedum plumbizincicola. Eur J Soil Sci 70:1141–1152. https://doi.org/10.1111/ejss.12810

Zhu Y, Guéguen C (2016) Evaluation of free/labile concentrations of trace metals in Athabasca oil sands region streams (Alberta, Canada) using diffusive gradient in thin films and a thermodynamic equilibrium model. Environ Pollut 219:1140–1147. https://doi.org/10.1016/j.envpol.2016.09.018

CAPÍTULO 2: Objetivos y estructura de la tesis

2.1. Objetivos

La minería de oro artesanal y en pequeña escala (MAPE) es una actividad humana que conlleva una intensa demanda de recursos y que, por su naturaleza, es una de las principales fuentes de emisión de elementos tóxicos, como el Hg, y representa un alto riesgo ambiental y afectación a la salud humana.

Los efectos del Hg, As y otros metales originados por la MAPE se ha investigado ampliamente, no obstante, se dispone de poca información sobre las dinámicas ambientales y la biodisponibilidad de estos contaminantes en ecosistemas únicos, como lo son los bosques y selvas tropicales, y en especial las pozas mineras abandonadas (AMPs) por la MAPE. Asimismo, la exposición al Hg en estas zonas puede ser aún más crítica para las poblaciones locales, que a menudo dependen de la pesca y la agricultura local para su sustento.

Es necesario seguir investigando y evaluando los riesgos ambientales y de salud asociados con la exposición al Hg en zonas remotas y de difícil acceso, y desarrollar estrategias efectivas para monitorear y minimizar su impacto en estos ecosistemas únicos y vulnerables. Por este motivo, los objetivos generales de esta tesis son:

- Evaluar el riesgo para la salud humana y riesgo carcinogénico por consumo de alimentos contaminados por elementos traza debido al impacto de la MAPE

- Evaluar la eficiencia de la técnica de gradiente de difusión en capa fina (diffusive gradients in thin-films, DGT) mediante la aplicación de dispositivos manufacturados con resinas comerciales y nuevos materiales, para el análisis cuantitativo del Hg lábil en condiciones controladas de laboratorio.

- Estudiar la biodisponibilidad del Hg en la dinámica de la contaminación por minería aurífera, mediante la aplicación *in situ* de muestreadores pasivos tipo DGT en aguas naturales en áreas de difícil acceso impactadas por la MAPE.

Para desarrollarlos, se establecieron los siguientes los objetivos específicos:

1. Determinar las concentraciones de Hg y As en aguas y alimentos locales, y MeHg en peces en zonas afectadas por la minería.

2. Evaluar el riesgo para la salud humana por exposición a especies de Hg y As a través del consumo de alimentos locales.

3. Estudiar la capacidad de captación de Hg y de inclusión dentro del dispositivo DGT de nuevos materiales poliméricos derivados de la benzoiltiourea y de biomasa residual de actividades agroindustriales.

4. Realizar ensayos de modificación de un material derivado de la biomasa (biochar) para mejorar su capacidad y selectividad para captar Hg.

5. Preparar hidrogeles como capas de difusión y unión, a partir de agarosa, poliacrilamida, sílica funcionalizada con 3-mercaptopropilo (3MFS), nuevos polímeros derivados de la benzoiltiourea y materiales derivados de biomasa.

6. Manufacturar muestreadores DGT con hidrogeles de 3MFS y con nuevos materiales poliméricos y derivados de biomasa.

7. Utilizar muestreadores DGT comerciales con resina de Chelex-100 para la cuantificación *in situ* de otros metales traza (Pb, Cu, Zn, Cd, Ni, Mn y Cr).

8. Calibrar muestreadores DGT comerciales y manufacturados en el laboratorio con nuevos materiales para la captación de Hg lábil en condiciones de laboratorio.

9. Desplegar los muestreadores DGT comerciales y manufacturados en el laboratorio en el río Atrato y AMPs en el departamento de Chocó, Colombia, para el análisis cuantitativo y monitoreo de la biodisponibilidad de Hg y otros metales.

10. Relacionar la biodisponibilidad del Hg con el tiempo de abandono de las pozas mineras y con su proximidad a las zonas de mayor actividad de extracción de oro.

2.2. Estructura de la tesis

La estructura de esta tesis se compone de cinco capítulos principales. En el Capítulo 1 se presenta una introducción sobre el Hg en la dinámica de la contaminación por minería de oro. En este capítulo, se hace énfasis en la importancia del estudio de estos elementos tóxicos en zonas afectadas por la minería de oro, también se incluye una breve introducción de dos elementos traza (As y Ni) cuyos resultados fueron significativos y requieren atención, y

se incluye la publicación de una revisión detallada de los fundamentos y aplicabilidad de la técnica de gradiente de difusión en capa fina (DGT), así como se establece la necesidad de estudiar nuevos materiales como capas de unión. La publicación incluida es:

- Publicación 1: **Marrugo-Madrid, S.**, Turull, M., Zhang, H., & Díez, S. (2021). Diffusive gradients in thin films for the measurement of labile metal species in water and soils: a review. Environmental Chemistry Letters, 19(5), 3761-3788. DOI: 10.1007/s10311-021-01246-3

En el Capítulo 2 se presentan los objetivos generales y específicos de la tesis, así como la estructura de la misma. Este capítulo es crucial para entender el enfoque de la investigación y cómo se abordarán los temas a lo largo de la tesis.

En el Capítulo 3 se presentan dos publicaciones relacionadas con la evaluación de la contaminación por Hg y otros elementos traza en zonas afectadas por la MAPE. Una primera publicación está enfocada en los resultados obtenidos en una evaluación de riesgo para la salud humana por exposición a Hg y As a través del consumo de alimentos locales en un área minera de oro en Colombia. La segunda publicación se centra en la determinación de la biodisponibilidad del Hg mediante DGT en el río Atrato

y en AMPs, lugares donde los habitantes pescan el pescado que consumen. Las publicaciones incluidas son:

- Publicación 2: **Marrugo-Madrid, S.**, Pinedo-Hernández, J., Paternina-Uribe, R., Marrugo-Negrete, J., & Díez, S. (2022). Health risk assessment for human exposure to mercury species and arsenic via consumption of local food in a gold mining area in Colombia. Environmental Research, 215, 113950. DOI: 10.1016/j.envres.2022.113950

- Publicación 3: **Marrugo-Madrid, S.**, Salas-Moreno, M., Gutiérrez-Mosquera, H., Salazar-Camacho, C., Marrugo-Negrete, J., & Díez, S. (2022). Assessment of dissolved mercury by diffusive gradients in thin films devices in abandoned ponds impacted by small scale gold mining. Environmental Research, 208, 112633. DOI: 10.1016/j.envres.2021.112633

El Capítulo 4 muestra los resultados obtenidos en los diferentes estudios realizados para lograr la inclusión de nuevos materiales poliméricos derivados de la benzoiltiourea y de biomasa residual de actividades agroindustriales en la técnica DGT en condiciones de laboratorio, y se desarrolla una discusión general al respecto. Las publicaciones incluidas en este capítulo son:

- Publicación 4: **Marrugo-Madrid, S.**; Marrugo-Negrete, J.; Queralt, I.; Palet, C.; & Díez, S. (2023). Evaluation of novel biomass-derived materials as binding layers for determining labile mercury in water by diffusive

gradient in thin-film technique. [submitted to the journal: Environmental Technology & Innovation]

- Publicación 5: **Marrugo-Madrid, S.**, Fontàs, C., Kurt, G., Salazar-Camacho, C., Salas-Moreno, M., Gutierrez-Mosquera, H., Marrugo-Negrete, J. & Díez, S. (2022). Benzoylthiourea based polymers as new binding agents for diffusive gradients in thin films technique in labile mercury determination in freshwaters. Environmental Technology & Innovation, 28, 102911. DOI: 10.1016/j.eti.2022.102911

Finalmente, en el Capítulo 5 se presentan las conclusiones de esta tesis en base a los objetivos planteados y los resultados obtenidos a lo largo del estudio, de igual manera, se establecen las recomendaciones para futuras investigaciones.

CAPÍTULO 3: Evaluación de la contaminación por Hg en zonas afectadas por la MAPE

3.1. Introducción

Conforme se ha expuesto en la introducción general de esta tesis doctoral, la contaminación ambiental por mercurio constituye una problemática de alcance mundial debido a la capacidad de algunas especies químicas del Hg de transportarse a largas distancias y transformarse en otras formas más tóxicas para la salud humana. Este riesgo se ve incrementado por la complejidad de la toxicología del Hg, los múltiples factores no controlables que influyen sobre el ciclo del Hg y la insuficiencia de sistemas adecuados de información y vigilancia sanitaria que permitan valorar el impacto real de la contaminación.

Del mismo modo, es relevante recordar que, aunque la minería ha sido de indiscutible importancia para nuestro desarrollo económico y tecnológico como sociedad, una de sus principales consecuencias negativas es la generación de grandes emisiones de contaminantes a la atmósfera, la deforestación y el impacto negativo sobre ecosistemas y poblaciones cercanas a zonas en donde se implementa. En este contexto, cabe destacar la relevancia de la minería de oro artesanal y en pequeña escala (MAPE) dentro del panorama minero, dado que es la fuente antropogénica que más cantidad de Hg emite a la atmósfera actualmente, por tanto, este capítulo se enfoca principalmente en la evaluación de la contaminación por Hg en zonas afectadas por la MAPE, no obstante, otros elementos traza potencialmente tóxicos (Pb, Cu, Zn, Cd, Ni, Mn, Cr y As) también fueron medidos y discutidos en las publicaciones incluidas.

3.2. Metodología

3.2.1. Consideraciones del área de estudio

Los estudios presentados en este capítulo fueron llevados a cabo en la cuenca hidrográfica del río Atrato, situada en el departamento de Chocó al noroeste de Colombia (figura 14). El departamento de Chocó forma parte de uno de los *hotspot* de biodiversidad del planeta conocido como el *Chocó biogeográfico*, y el 90% de su territorio es considerado zona especial de conservación. Una característica particular del departamento de Chocó es la extrema pluviosidad, con alrededor de 11700 mm anuales, por lo que se le considera también uno de los lugares más húmedos del planeta.

Estos factores ambientales favorecen la existencia de un ecosistema selvático que alberga más de 10000 especies endémicas, y es el hábitat de un gran número de resguardos indígenas y comunidades vulnerables que subsisten principalmente de la pesca y la minería. Adicionalmente, por su condición de selva tropical, singular geografía e intensas precipitaciones, las vías terrestres son escasas en el departamento. Esto resulta en un acceso sumamente desafiante a las zonas rurales y poca presencia estatal en el departamento, lo que a su vez propicia la presencia de grupos al margen de la ley que alteran el orden público (Medina-Rivas et al., 2016; Pérez-Escobar et al., 2019).

Ahora bien, las adversas condiciones ambientales características del departamento de Chocó, no han sido obstáculo para el establecimiento de más

de 500 unidades de beneficio minero (denominadas *entables mineros)* dedicadas a la MAPE, de las cuales un considerable número operan en la ilegalidad. Como resultado de estas actividades de minería intensiva, el departamento es el segundo mayor productor de oro en Colombia (MME/UPME/UC, 2014).

La MAPE en este departamento es predominantemente de aluvión, ya que la recuperación del mineral se hace principalmente mediante el lavado de oro en bandejas (barequeo), y el uso de dragas y retroexcavadoras. Mientras tanto, el Hg es utilizado con telas o placas en los canalones, o la amalgamación de los concentrados que se generan durante el proceso. El uso de éste se ve reflejado en las elevadas concentraciones de Hg encontradas en los suelos y sedimentos de los ríos de la región (MME/UPME/UC, 2014; MME/UPME/UC, 2015; Palacios-Torres et. al., 2018).

En este mismo contexto, otra de las problemáticas causadas por la MAPE en la cuenca del río Atrato, es la gran cantidad de sitios y pozas mineras abandonadas contaminadas con Hg (considerados pasivos ambientales). Muchas de las actividades de MAPE se llevan a cabo en los propios ríos y en áreas adyacentes a humedales naturales que forman parte de esta cuenca hidrográfica.

Estos cuerpos de agua son fundamentales para las comunidades locales, ya que proporcionan recursos vitales como el pescado, agua para consumo y riego de cultivos, espacios recreativos, entre otros. En consecuencia, los efectos de la MAPE en esta región derivan en la deforestación, la sedimentación, las

altas concentraciones de Hg y otros elementos traza, así como de residuos aceitosos de la maquinaria empleada, generando un riesgo potencialmente alto para la salud de estas comunidades (Palacios-Torres et. al., 2018; Salazar-Camacho et. al., 2017).

Figura 14. Ubicación del área de estudio y áreas rurales en la Cuenca del río Atrato. Fotografías: autoría propia.

3.2.2. Generalidades sobre los muestreos

Los muestreos realizados en el marco de esta tesis se integraron dentro de un macroestudio de tipo descriptivo transversal cuyo objetivo principal fue obtener información sustancial y representativa de los municipios que forman parte de la cuenca del río Atrato (Colombia) afectados por actividades mineras. Este proyecto se llevó a cabo con la colaboración de las entidades

gubernamentales presentes en la zona, en especial con las secretarías municipales de salud y representantes de las comunidades, con el fin de informar a las personas sobre la realización del estudio y facilitar la recolección de muestras. Aunque los detalles de cada muestreo están contenidos en los apartados de *"Materiales y métodos"* de ambas publicaciones, a continuación se presentan algunos aspectos generales sobre su realización:

Aplicación de encuestas

A los participantes del estudio se les aplicó una encuesta para recopilar información relacionada con condiciones sociodemográficas, ambientales, sanitarias, hábitos alimentarios, entre otras variables. En el marco de esta encuesta, se incluyó un cuestionario de dieta que se utilizó de forma aleatoria a 178 personas del área de estudio.

Los alimentos mencionados incluyeron las principales frutas, tubérculos y pescados de origen local y comercial. Mediante el cuestionario, se obtuvo información sobre la edad, el sexo, el peso y el consumo de alimentos (por ejemplo, número de comidas diarias y semanales, así como tamaño de las porciones), lo que permitió dividir la muestra poblacional en tres grupos categorizados de la siguiente manera: niños (CHD: 1-15 años), mujeres en edad fértil (WCBA: 16-45 años), y el resto de la población (RP).

Recolección de peces y alimentos

Se recolectaron muestras de pescado en los ecosistemas acuáticos del área de estudio, asegurando la inclusión de diversas especies y niveles tróficos. Estas muestras de pescado se embolsaron de manera individual en bolsas de polietileno debidamente etiquetadas y se transportaron refrigeradas al laboratorio. Una vez en el laboratorio, se llevó a cabo la extracción de muestras de tejido muscular, siguiendo el procedimiento descrito por UNEP/IOC/IAEA/FAO (1990), que implica la sustracción de la aleta pectoral izquierda junto con la piel, y el corte de una porción de 3 cm de ancho utilizando un cuchillo de plástico. Estas muestras de tejido muscular fueron guardadas individualmente en bolsas de polietileno y se preservaron en nevera a una temperatura constante de 4 ºC hasta su posterior análisis.

Por otro lado, los frutos y tubérculos se recolectaron tanto de huertas y cultivos locales como de las casas de las personas encuestadas, considerando la información dietética obtenida de las encuestas. Al igual que las muestras de pescado, estos alimentos fueron envasados individualmente en bolsas de polietileno etiquetadas y se transportaron refrigerados al laboratorio para su posterior análisis.

Muestreadores DGT

En términos generales, los hidrogeles y dispositivos DGT utilizados para la determinación de la fracción biodisponible de Hg disuelto en el río Atrato y

AMPs fueron manufacturados en el laboratorio del IDAEA-CSIC a partir de la resina de sílice funcionalizada con 3-mercaptopropilo (3MFS), la cual fue incorporada en un gel de poliacrilamida dando como resultado el gel de resina donde se espera que el Hg sea retenido debido a su alta afinidad con el grupo mercapto (–SH) del 3MFS. En cuanto a la capa de difusión, los hidrogeles se prepararon utilizando solución de poliacrilamida, persulfato de amonio y N,N,N´,N´-tetrametiletilendiamina (TEMED) introducida entre dos placas de vidrio con un espaciador de 0,5 mm de grosor (figura 15). Posteriormente, fueron calentados a 45ºC, y una vez que fueron hidratados, los geles de poliacrilamida resultantes fueron capaces de expandirse hasta 0,8 mm de grosor.

Los hidrogeles fueron cortados circularmente con 2 cm de diámetro, y montados sobre los moldes de plástico adquiridos de DGT® Research Ltd. para garantizar la estandarización del diseño. Para proteger los hidrogeles del exterior, se utilizaron membranas de filtro de Nylon con un tamaño de poro de 0,45 µm y con un grosor aproximado de 0,1 mm. Los dispositivos DGT fueron guardados individualmente en bolsas de polietileno para su refrigeración y transporte, al tiempo que la hidratación de los hidrogeles dentro de las bolsas se aseguró con gotas de agua ultrapura Milli-Q (figura 15).

De cada lote de dispositivos DGT preparados, se seleccionaron aleatoriamente hasta 15 dispositivos para llevar a cabo experimentos de serie temporal en condiciones controladas de concentración de Hg en el medio, fuerza iónica y

temperatura. Estos experimentos fueron necesarios para la calibración y cálculo de los coeficientes de difusión (D) de los dispositivos DGT con 3MFS. Asimismo, se seleccionaron dispositivos DGT para realizar controles de blancos tanto de la manufacturación como del muestreo. En la figura 15 se ilustra el proceso de preparación, calibración y despliegue de los dispositivos DGT en los sitios de muestreo.

Figura 15. (A) Materiales para la preparación de hidrogeles, montaje de dispositivos DGT y calibración mediante ensayo de serie temporal en condiciones de laboratorio. (B) Muestreo en el río Atrato y AMPs.

3.3. Resultados

Los resultados obtenidos se encuentran recopilados en dos artículos científicos publicados en la revista Environmental Research (Q1). Estos artículos abordan el análisis de las concentraciones de Hg, MeHg y los elementos potencialmente tóxicos presentes en muestras de pescado, frutas, tubérculos y muestreadores DGT provenientes de la cuenca hidrográfica del río Atrato, ubicada en el departamento de Chocó, Colombia. Las publicaciones correspondientes son:

- Publicación 2: **Marrugo-Madrid, S.**, Pinedo-Hernández, J., Paternina-Uribe, R., Marrugo-Negrete, J., & Díez, S. (2022). Health risk assessment for human exposure to mercury species and arsenic via consumption of local food in a gold mining area in Colombia. Environmental Research, 215, 113950. DOI: 10.1016/j.envres.2022.113950

- Publicación 3: **Marrugo-Madrid, S.**, Salas-Moreno, M., Gutiérrez-Mosquera, H., Salazar-Camacho, C., Marrugo-Negrete, J., & Díez, S. (2022). Assessment of dissolved mercury by diffusive gradients in thin films devices in abandoned ponds impacted by small scale gold mining. Environmental Research, 208, 112633. DOI: 10.1016/j.envres.2021.112633

3.3.1. Publicación 2: Health risk assessment for human exposure to mercury species and arsenic via consumption of local food in a gold mining area in Colombia

Marrugo-Madrid, S., Pinedo-Hernández, J., Paternina-Uribe, R., Marrugo-Negrete, J., Díez, S. Environmental Research, 215 (2022): 113950.

Health risk assessment for human exposure to mercury species and arsenic via consumption of local food in a gold mining area in Colombia

Siday Marrugo-Madrid [a,b], José Pinedo-Hernández [b], Roberth Paternina-Uribe [b], José Marrugo-Negrete [b,**], Sergi Díez [a,*]

[a] Environmental Chemistry Department, Institute of Environmental Assessment and Water Research, IDÆA-CSIC, E-08034 Barcelona, Spain
[b] University of Córdoba, Faculty of Basic Sciences, Department of Chemistry, Water, Applied and Environmental Chemistry Group, Monteria, Colombia

ARTICLE INFO

ABSTRACT

The risk to human health from exposure to certain pollutants through the consumption of fruits, tubers, and fish were evaluated in a settlement located in a Colombian area highly impacted by gold mining activities. The concentrations of mercury (Hg) and arsenic (As) in edible food tissues and methylmercury (MeHg) in fish were determined for risk assessment. A questionnaire-based dietary survey was answered by 178 residents of three population groups: children (CHD), women of childbearing age (WCBA), and the rest of the population (RP). The estimated weekly intake (EWI) of MeHg presented values of 1.9 and 2.4 times higher than the provisional tolerable weekly intake (1.6 µg/kg BW/week) recommended by the FAO/WHO for CH and WCBA, respectively. The results of the HQ values of As and Hg for different food were above the safety level (HQ < 1) for most of the groups. For Hg, the highest HQ values correspond to fish, whereas for As in most of the food, but specially in fruits. The total target hazard quotients (HI) were higher than 1, in all the groups (except for CHD that consume tubers) indicating potential non-carcinogenic health risks. The values of carcinogenic risk (CR) for As through exposure to food ranged from $1.2 \cdot 10^{-4}$ to $7.7 \cdot 10^{-4}$, well above than the safety level of US EPA risk (10^{-4}–10^{-6}), suggesting the probability of carcinogenic risk for the entire population via ingestion. Therefore, safety control mechanisms and environmental education strategies should be applied to address food intake, associated with good agricultural practices to provide solutions to protect the health of the residents in areas affected by gold mining activities.

1. Introduction

Food is an essential source of nutrients for the human body. However, it can also contain unwanted elements that can cause acute and chronic poisoning if ingested. This is why food security is a global concern, given the demographic expansion, the decrease in food resources availability, and contamination by different chemical substances (FAO, 2016, 2017). The presence of some metals (e.g. Pb, Hg, Cd ...) and metalloids (e.g. As) in food is a current issue due to their biomagnification in the trophic chain (Córdoba-Tovar et al., 2021) and the evidence of adversely affecting public health (Wei et al., 2019). Due to its high toxicity, the effect on health caused by prolonged pollutant exposure is alarming. Depending on the type of metal or metalloid, conditions ranging from damage to vital organs to the development of cancer might occur. Among the most important potentially toxic elements due to their effects on human health, mercury (Hg) and arsenic (As) are highlighted, and considered toxic and dangerous (Dryzalowska and Falandysz, 2014; Liu et al., 2017). Mercury causes a variety of neurological problems, including uncontrollable tremors, loss of balance and neurotoxicity, congenital malformations, and perinatal mortality (Oken et al., 2008; Choi et al., 2014). Arsenic is a known carcinogen related with skin, lung, bladder, kidney, and liver cancer (Naujokas et al., 2013) with proved dermatological, cardiovascular, nervous, renal, hepatobiliary, gastrointestinal, and respiratory effects (IARC International Agency for Research on Cancer, 2012; ATSDR, 2012a). Besides, non-cancer health effects include cognitive deficits in children and adults, skin disorders, induction of thrombosis, and fetus disturbances during pregnancy (Ahsan et al., 2000; Lee et al., 2002; Chattopadhyay et al., 2002; Tsai et al., 2003; Tyler and Allan, 2014; Saha et al., 2016). Consequently, it is essential to guarantee food quality to maintain and

improve health conditions and to avoid potential risks in the population due to metal and metalloid intake through food consumption.

Colombia offers an immense potential in various natural resources, and the department of Chocó is considered the richest province in resources in the country (Gallego Rios et al., 2018). This department has 30 municipalities, underlining the municipality of Lloró in the Atrato River basin as one of the areas with the highest population density and where economic activities include mining (gold and platinum), agriculture, and forest exploitation. In other words, this municipality depends exclusively on natural resources (CODECHOCÓ, 2012; CGP, 2013). Mining, as a rural and central economic activity, is developed traditionally by artisanal and small-scale gold mining, using Hg for the recovery of gold by amalgamation (Gutiérrez-Mosquera et al., 2020). Furthermore, As appears as a pollutant associated with mining wastes, since in many deposits, it is associated with gold-containing deposits such as galena and arsenopyrite (Lightfoot et al., 2010; UPME-MME-UC, 2014; UPME-MME-UC, 2016). However, this artisanal and small-scale gold mining activity is carried out without any type of environmental control in areas where agricultural products such as banana, sugar cane, borojó, pineapple, cassava, cocoa, chontaduro, and other fruits are cultivated in self-consumption crops. This problem of contamination by Hg has been reported in different environmental matrices (e.g. fish, sediments, hair, blood, and urine) in sites affected by gold mining near the study area in the department of Chocó (Quibdó, Paimadó, San Juan, Tadó, Unión Panamericana, and Atrato River) (Medina Mosquera et al., 2011; Salazar-Camacho et al., 2017; Lara-Rodríguez, 2018; Arias Espana et al., 2018; Palacios-Torres et al., 2018; Gallego Rios et al., 2018; Gutiérrez-Mosquera et al., 2018). Nevertheless, studies on the contamination of local food that are essential in the diet of the population are scarce.

Consequently, in this study, the concentrations of Hg and As in different kind of local food (i.e. fruits, tubers, and fish) and MeHg in fish were determined, with the aim to evaluate the risk to human health in a gold mining area in Chocó, considered one of the leading gold and platinum producer departments in Colombia (SIMCO, 2017). In addition, this study would constitute a starting point to comply with Article 19b of the Minamata Convention (Uddh-Söderberg et al., 2015) and Sentence T-622 of the Constitutional Court of Colombia of 2016 (Constitutional Court of Colombia, Judgment T-622-2016), which granted the Atrato River basin the "Subject of Law" status and ordered carrying out environmental and public health studies to evaluate the impacts that gold mining activities cause in the basin.

2. Materials and methods

2.1. Study area

The study was carried out in the municipality of Lloró, located in the western region of the Department of Chocó, northwestern Colombia (Fig. 1). The area has a tropical rainforest type climate, and rainfall occurs throughout the year. According to estimates based on the records of a meteorological station installed in the area, this zone has the highest average annual precipitation worldwide, equivalent to 13,300 mm (Ramírez, 1992). It has a total area of 905 km^2 and 10,248 inhabitants (urban: 20% - rural: 80%). Human settlements are distributed mainly along four rivers, the Atrato River being of greatest importance,
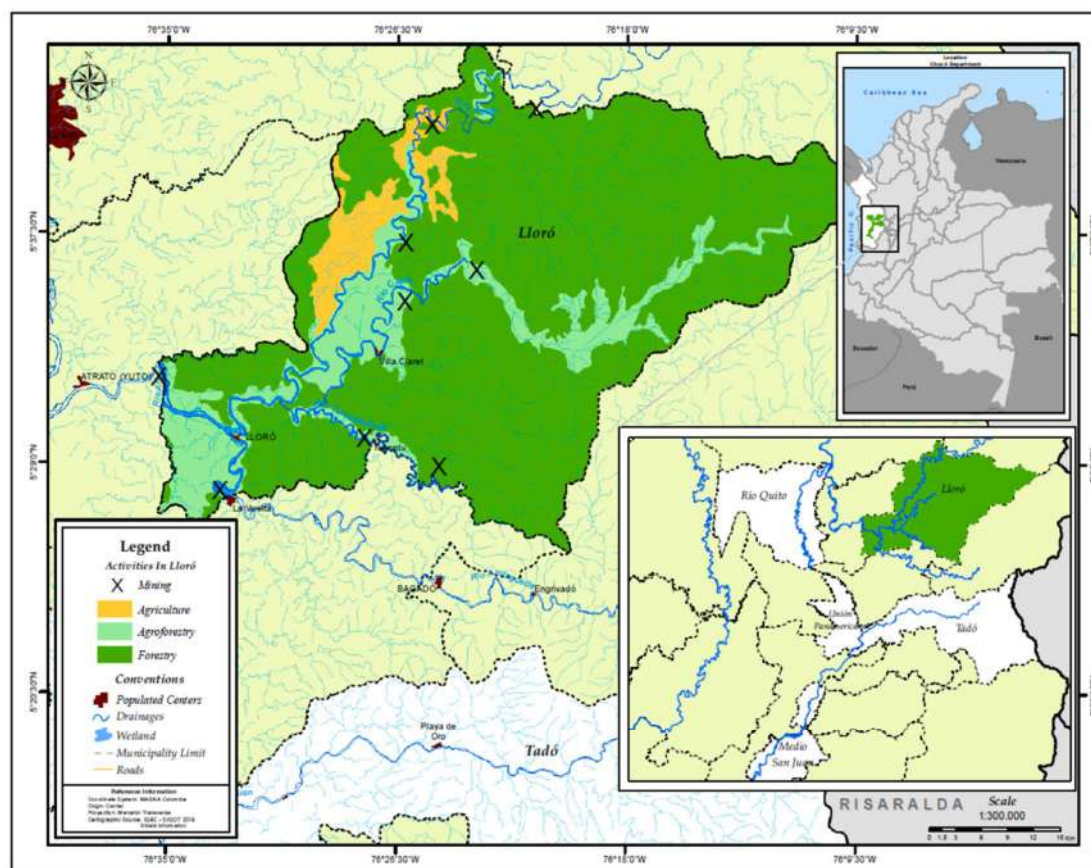

Fig. 1. Location of the study area. Municipality of Lloró, department of Chocó, Colombia.

followed by Andagueda, Capa, and Tumutumbudo rivers, all of them with the presence of mining (gold and platinum), agriculture, and forestry activities. The eating habits of the inhabitants of these regions have a marked preference for the consumption of fish and self-consumption crop products (CODECHOCÓ, 2012), especially fruits.

2.2. Questionnaire survey

A diet questionnaire was answered by 178 residents in the study area. All participants were residents, mainly from the rural area, consuming local food, and dietary data were collected during detailed face-to-face interviews in a sampling period between May and June 2019. The reported foods included the main fruits, tubers, and fish of local and commercial interest. With the questionnaire, basic demographic information was acquired, including age, sex, weight, and food consumption (i.e., meal composition, number of meals per day, and size). The population sample was divided into three groups categorized as follows: children, CHD (1–15 years), women of childbearing age, WCBA (16–45 years), and the rest of the population, RP.

2.3. Sample collection and analysis

Eight species of cultivated fruits (N = 26) (i.e. pineapple, guava, lulo, custard apple, passion fruit, and three different varieties of banana) and two tubers (N = 6) (i.e. cassava and yam) were collected from the orchards or cultivation areas near the houses of the local inhabitants. Four species of fish (N = 28) (*Astyanax fasciatus*, *Hypostomus hondae*, *Pimelodus blochii*, and *Pinguipes chilensis*) from different trophic levels were caught in the aquatic ecosystems of the study area. The samples were individually packed in labeled polyethylene bags, refrigerated, and transported to the laboratory for analysis. Once in the lab, crop samples (fruits and tubers) were washed with running and deionized water to remove soil particles, and a proportion of 50 g of the inner edible part (pulp) was extracted. For the fish samples, the skin and pectoral fin were removed from the left side, and with a knife, a portion of 3 cm wide was cut (UNEP/IOC/IAEA/FAO, 1990). For the analysis of Hg in fruits, tubers, and fish, and MeHg in fish, a Hg analyzer (DMA 80 Tricell Milestone, Italy) was used according to the EPA method 7473 for THg (EPA, United States Environmental Protection Agency Method 7473) and the one described by Cordeiro et al. (2013) for MeHg. Arsenic analysis was carried out by atomic absorption spectrophotometry using hydride generation in a Thermo Scientific model iCE series 3500 equipment after calcination of 1 g of sample mixed with $Mg(NO_3)_2$ at 550 °C with the addition of 1 mL of concentrated HNO_3, and heating to dryness. Re-dissolution was carried out with HCl 4.5 N, filtration through a 0.45 μm membrane, and gauging to 25 mL with distilled water (Szkoda et al., 2006). The analytical quality control of the method was evaluated in triplicate with the certified reference material (CRM) DORM-2 (THg: 4.640 ± 14.4 μg/kg; MeHg: 4.470 ± 18.9 μg/kg; As: 18.0 ± 1.7 μg/kg). The different metal concentrations in the CRM were found in good agreement with the certified value, with a recovery percentage from 94% to 97%. The detection limits for the different metals were: 14 μg/kg for Hg, 23 μg/kg for MeHg, and 16 μg/kg for As.

2.4. Human health risk assessment

The potential risk for human health was estimated, considering the concentrations of Hg and As (Table S1), and dietary information on food consumption obtained from interviews (fruits, tubers, and fish) (Table S2). The calculation of the estimated dietary intake (EDI), the non-carcinogenic risk ratios (target hazard quotient, THQ, and total target hazard quotients, HI), and the carcinogenic risk (CR) were determined as reported by Muñoz et al. (2017) (see equations in Supplemental material). The risk to human health from MeHg due to the consumption of fish was calculated as described by Marrugo-Negrete et al. (2020).

2.5. Statistical analysis

An exploratory analysis using the Kolmogorov-Smirnov test showed a non-normal distribution. Therefore, values in figures are presented as the geometric mean (GM) ± standard deviation, and calculations for risk analysis were performed with GM. Values of the geometric mean, median, and interquartile range for Hg, As and MeHg are presented in Table S1. Differences between food categories were evaluated using nonparametric tests (Mann–Whitney U and Kruskal–Wallis). The criterion for significance was set at < 0.05. Statistical analyses were performed employing the Statgraphics Centurion XV. II software.

3. Results and discussion

The results of the questionnaire indicated that of the 178 people surveyed, 84 are male, and 94 are female. Forty percent are CHD (N = 71), 10% are WCBA (N = 18), and 50% are RP (N = 89). For the surveyed population, fruits are the food with the highest average consumption rate (1118 g/day), followed by fish (441 g/day) and tubers (234 g/day). Moreover, the total daily intake of each food by group are presented in Fig. 2. As can be seen, the three varieties of banana are the fruit, by far, most consumed by the inhabitants. The fish species with the highest collection frequency were non-carnivorous, representing 68% of the fish samples collected. However, according to the daily intake, the order in which individual fish species consumption contributes to the accumulation of metal(loid)s in the exposed population is the following: *Pinguipes chilensis* > *Pimelodus brochii* > *Astyanax fasciatus* > *Hypostomus hondae*. On the other hand, for fruit and tuber species, the contribution of metal(loid)s accumulation in the population can be ordered as follows: *Musa paradisiaca* > *Musa acuminata* cv. *Sucrier* > *Musa balbisiana* > *Manihot esculenta* > *Dioscorea trifida* > other varieties of fruits.

3.1. Metal(loid)s concentrations in food

Fig. 3 shows the concentration of metal(loid)s in food samples. The GM values of concentration of As and Hg varied between 28.2 and 288 μg/kg and from 0.70 to 88.5 μg/kg, respectively. Fruits and tubers do not present statistically significant differences ($p > 0.05$) between the concentration of metal(loid)s; however, significant differences were found in fish. The order based on the average concentration of As by food category was: fruits > tubers > fish, whereas for Hg the order is: fish > tubers > fruits. The concentrations of Hg and As do not show any relationship with respect to fruit or tuber species, showing that plant species have different metal(loid)s absorption and accumulation capacities, possibly associated with factors such as different characteristics of the soil (Li et al., 2004; Xiao et al., 2009; You et al., 2020; Margenat et al., 2020) or to the growth period of each plant (Saha and Zaman, 2013). Conversely, there is a relationship based on the fish trophic level, where the highest Hg and As concentrations occur for carnivorous species. Similar results for Hg were reported by Palacios-Torres et al. (2018) and Gallego et al. (2018) in the Atrato River basin in Colombia, a tributary of the water drainage network of aquatic ecosystems in the study area. These results are also consistent with those reported for numerous aquatic ecosystems around the world (Ikemoto et al., 2008; Tadiso et al., 2011; Ouédraogo and Amyot, 2013; Fuentes-Gandara et al., 2018; Marrugo-Negrete et al., 2020).

The Hg/As ratio in fish is approximately 2; meanwhile, the As/Hg in fruits and tubers was 80 and 70 times, respectively. The above indicates the bioaccumulation capacity of Hg with respect to As, or vice versa, depending on the type of food and the possible public health problem through the consumption of fruits, tubers, and fish species, where 78% of the THg content in fish corresponds to MeHg, a neurotoxic compound capable of being easily concentrated in the body (Marrugo-Negrete et al., 2020).

The GM concentration of Hg in tubers (2.2 ± 0.1 μg/kg) was a little bit higher than the one registered in fruits (1.9 ± 0.7 μg/kg), whereas
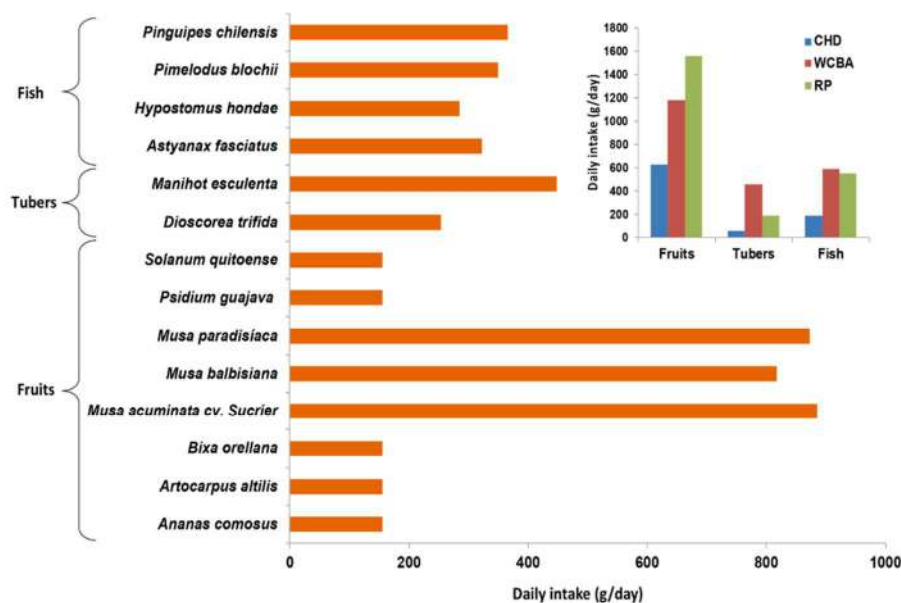
3

Fig. 2. Daily intake of different species and by food category and population group. CHD: children (1–15 years), WCBA: women of childbearing age (16–45 years), and RP: the rest of the population.

values for As are similar in tubers and fruits (149 ± 74 μg/kg) (Table 1). Different studies indicate that the plant organ that can accumulate the highest proportion of Hg is the root (Moreno et al., 2005; Cargnelutti et al., 2006; Marrugo-Negrete et al., 2015); this could explain the Hg content in tubers, which is related to the high Hg in the soil associated with the gold mining activities (Medina Mosquera et al., 2011; UPME-MME-UC, 2016; Salazar-Camacho et al., 2017; Lara-Rodríguez, 2018; Arias Espana et al., 2018; Gallego Rios et al., 2018). Arsenic contamination could be derived from the parent material of the soil (Lightfoot et al., 2010), although the application of fertilizers and pesticides still used in agricultural activities, which are enriched with As, could also increase this amount (Renner, 2004; Islam et al., 2014). Moreover, Palacios-Torres et al. (2020) reported As concentrations in sediments and fish collected in the Atrato River (downstream of the municipality of Lloró) presumably originating in gold mining activities in the area.

The results obtained show that the concentrations of Hg and As are related to cropping conditions. In crops cultivated in the open air (e.g. fruits), low Hg and high As concentrations were found. For Hg, this is congruent with mining processes, where atmospheric deposition would not have a significant influence due to the high precipitation in the area, causing Hg to be deposited in the soil and, due to runoff or leaching, may contaminate other ecosystems such as freshwaters; nonetheless, low translocation factors prevail. This is unlike As, where high translocation factors occur possibly from the concentrations that could be found as natural sources from the crust of the Earth or linked to mining residues from the removal of soils in the gold extraction activities in this region, which could reach water bodies used for irrigation, and causing accumulation in crops.

When comparing the results, although this is the first report in Colombia regarding metal(loid)s in fruits and tubers, these values were lower to the ones found in other countries for Hg (Table 1), however for As, values in some cases, were higher (Fang et al., 2014; Cheng et al., 2017; Filippini et al., 2018). The Hg concentrations in fish were found in the range of those reported at national (Fuentes-Gandara et al., 2018; Palacios-Torres et al., 2018; Gutiérrez-Mosquera et al., 2018; Marrugo-Negrete et al., 2020; Salazar-Camacho et al., 2020; Pinzón-Bedoya et al., 2020) and international levels (Filippini et al., 2018; Costa et al.,

2020). In contrast, the concentration of As was lower for studies at the international level, and also in national reports such as those related to the Atrato River (Gallego et al., 2018; Palacios-Torres et al., 2020) and the Santa Marta swamp (Pinzón-Bedoya et al., 2020). It should be noted that As and Hg concentrations in all food samples were below the established permissible limits for these elements according to FAO/WHO (2007), the Codex Alimentarius Commission (CAC), and the Chinese maximum allowable concentrations (MAC) (Table 1), suggesting that these foods do not appear to pose a health threat. However, if the consumption of these foods is high, then it could constitute a potential risk since these metals have no physiological function and can bioaccumulate, causing chronic diseases and potential harm to the population, so their human risk must be determined.

3.2. Potential human risk assessment

The estimated daily intake (EDI) rates of fruits, tubers, and fish by population group are shown in Table 2, as well as data on the average body weight per population group, the intake per food category, the reference dose (RfD) for As (USEPA, 2000) and the provisional tolerable weekly intake (PTWI) established by the JECFA (FAO/WHO, 2007).

The increasing order of EDI for Hg according to the population group, was WCBA > RP > CHD with EDI values ranged from 0.005 μg/kg/day for tubers in CHD to 0.646 μg/kg/day for fish in WCBA. For As, EDI values increasing following CHD > RP > WCBA, ranged between 0.271 μg/kg/day for tubers in CHD to 4.090 μg/kg/day for fruits in CHD.

Fish contributes to the highest Hg intake in the different population groups, with values approximately 2 times higher in comparison with As. On the other hand, fruits contribute, by far, with the highest daily intake of As in all the groups, with values about 100 times higher related the EDI of Hg per fruit. Furthermore, the exposure of As through consumption of fruits could represents a threat to health for all population groups since calculated EDI values exceed (i.e. 10 times higher) the reference dose of tolerable consumption (RfD: 0.3 μg As/kg/day) (USEPA, 2022). In fact, the EDI value of As for CHD in tubers is the only one below the RfD, even though the value is very close (0.27 vs 0.3 μg/kg/week), which suggest a health risk in all population groups. On the other hand, Hg represents a low potential health risk compared to
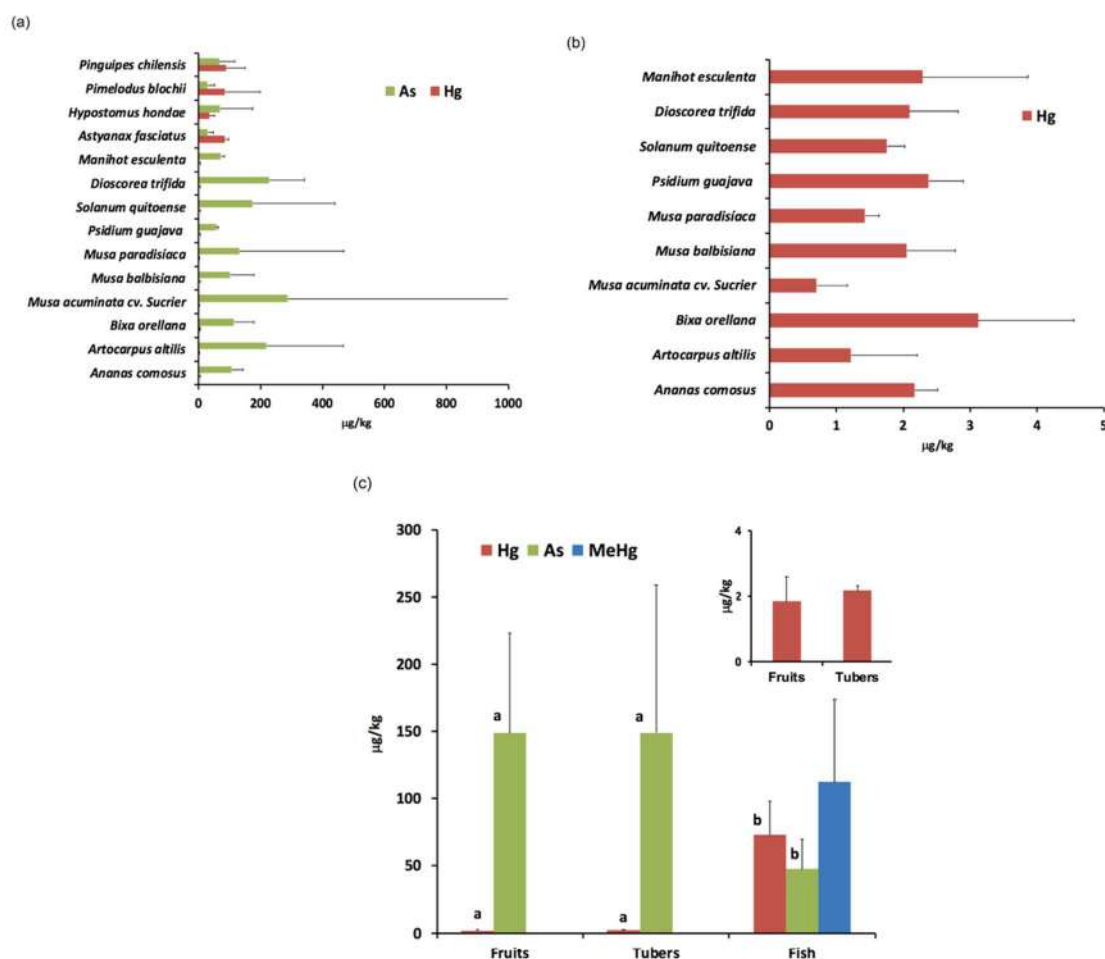
Fig. 3. Hg and As concentrations (μg/kg) in food shown by (a) individual species, (b) fruits and tubers for Hg, and (c) food category.

As, since none of the EDI values exceed the provisional tolerable weekly intake (PTWI) value of 1.6 μg/kg BW/week for CHD and WCBA or 3.3 μg/kg BW/week for RP.

It is widely known that the main route of exposure of MeHg is through fish consumption, and in this study, it represents 78% of the THg. For this reason, the potential risk for MeHg in the population was evaluated from the estimated weekly intake (EWI), i.e., the maximum amount of fish that can be consumed weekly (MFW) per person without harmful effects on health, and the permissible safety level (PSL) concentration of MeHg (MeHg$_{PSL}$) in fish for human consumption.

Table 3 shows that the highest EWI corresponds to the WCBA group (3.76 μg/kg/week). The EWI values were approximately 1.9 (CHD) and 2.4 (WCBA) times higher than the provisional tolerable weekly intake (PTWI) value. According to the survey, the amounts of fish consumed weekly were 1.31 kg for the CHD group, 4.12 kg for WCBA, and 3.84 kg for RP, and these values were higher than the results obtained for the estimation of MFW. For WCBA and RP groups, the estimated [MeHg]$_{PSL}$ in fish was lower than the MeHg concentrations in the analyzed samples (55 μg/kg), suggesting a risk for those groups. Consequently, given that EWI and WI values are higher than the reference (PTWI) and the estimated values (MFW), respectively, there exists a potential health risk in all population groups, with the following risk pattern: WCBA > CHD > RP.

Health risk were also assessed based on THQ; where if THQ <1, then the exposed population should not experience any adverse risk, and if THQ >1, it means that the population may experience non-cancer health risks; as the value increases, the risk rises. Table 4 showed that most of the THQ values were higher than 1, indicating that people would experience significant health risks if they only ingest individual meta (loid)s through food consumption. Moreover, the cumulative risk for the different population groups was HI > 1 in all the cases except for CHD consuming tubers, indicating that people have a high potential non-carcinogenic health risk due to exposure to the combination of Hg and As (HI$_{CHD}$ = 18; HI$_{WCBA}$ = 17; HI$_{RP}$ = 16). A non-carcinogenic risk of Hg and As from fish consumption, has been recently reported in mining activity areas downstream of the current study area (Palacios-Torres et al., 2020; Gutiérrez-Mosquera et al., 2021). It should be highlighted that As represents most of the potential cumulative risk (98–99%) in fruits and tubers, whereas Hg represents a lower percentage, with a significant contribution (50–69%) due to fish intake (Table 4).

The range of carcinogenic risks acceptable or tolerable by the US EPA is $1\ 10^{-6}$ to $1\ 10^{-4}$ for As. Therefore, risks surpassing $1\ 10^{-4}$ are unacceptable while the risks below $1\ 10^{-6}$ are not likely to pose significant health hazards. Our results showed (Table 5) that CR values through As exposure from fruits, tubers and fish consumption were well above $1\ 10^{-4}$ for all the groups, especially in fruits (CR: $5.5\ 10^{-4}$ – $7.7\ 10^{-4}$), meaning that local population should reduce the intake of fruits.

In general, children are usually more vulnerable than adults in exposure to metal(loid)s through the diet (Wang et al., 2015). In our case study, a similar trend was found since the CHD group has the highest CR

Table 1
Comparison of geometric mean concentrations of Hg and As in foods sampled in different regions around the world.

Reference/country	Food category	Hg (μg/kg)	As (μg/kg)
Current study	Fruits	1.9	149
	Tubers	2.2	149
	Fish	55 (78%)*	48
Fang et al. (2014)/China	Fish	–	10–20
	Vegetables	–	ND-50
Uddh-Söderberg et al. (2015)/Sweden	Vegetables	–	2.2–4300
Bentley and Soebandrio (2017)/Indonesia	Fish	110–114	1710–2120
Zhou et al. (2017)/China	Vegetables	4.0	–
Cheng et al. (2017)/China	Fruits	184-1530	2–21
Palacios et al. (2018)/ Colombia	Fish	60–950	–
Filippini et al. (2018)/Italy	Fish	55.03	1346.9
	Vegetables - Fresh fruits	0.63–0.28	2.51–1.20
Fuentes-Gandara et al. (2018)/Colombia	Fish	40–220	–
Gallego et al.(2018)/ Colombia	Fish	ND-6303	ND- 133
Li et al. (2018)/China	Vegetables	4.0	–
Ahmeda et al. (2019)/India	Fish	–	1080
Marrugo-Negrete et al. (2020)/Colombia	Fish	220–580	–
Costa et al. (2020)/Portugal	Fish	3–200	–
Pinzón-Bedoya et al. (2020)/Colombia	Fish	13.1–36.6	94.2–141.5
Palacios-Torres et al. (2018)/Colombia	Fish	–	ND-430
Salazar-Camacho et al. (2020)/Colombia	Fish	5.48–3112.62	–
Gutiérrez-Mosquera et al. (2021)/Colombia	Fish	250 ± 0.25	–
Permissible limits	Fish	FAO/ WHO[a]	500	1000
	Vegetables	CAC[b]	–	1000
	Vegetables	MAC[c]	10	500

ND: Not detectable.

* Represents the % of MeHg in fish.

[a] FAO/WHO (2017)FAO/WHO (1995).

[b] CAC Codex Alimentarius Commission (2011)

[c] MAC, Chinese maximum allowable concentrations of each heavy metal in food (GB 2762–2012) (Cheng et al., 2017).

values vs. WCBA and RP, derived primarily from the exposure of As though fruits intake. This is why exposure to metal(loid)s in children during vulnerability windows of organogenesis and histogenesis or neurodevelopment of the brain can cause brain function alterations with consequences, profound and permanent changes, as well as lasting disabilities with high family, social and economic costs (Tellerías and Paris,

2008). Therefore, the establishment of continuous metal(loid)s monitoring and strategies to address food consumption are recommended, to guarantee human health security for the inhabitants who depend mainly on the aquatic and vegetables resources of the area, as well as the general population due to the commercialization of these foods in the country. Since the RfD value is based on inorganic As, the determination of As species and selenium content in fish is recommended to avoid an overestimation of health risk because a large part of the As in fish muscle is arsenobetaine, a non-toxic organic compound (Rahman et al., 2012). On the other hand, selenium in the form of seleno-organic compounds or selenoenzymes, or both, coexists with Hg in the muscle tissue of fish and other foods, which could be exerting protective effects in the diet against MeHg toxicity (Ralston and Raymond, 2010).

4. Conclusions

The concentrations of Hg and As varied depending on the type of food, with values below the permissible limits established internationally for contaminated food and those reported in other regions worldwide. The estimation of food consumption is of interest to public health, because the intake of fish and fruits represent a threat to health in the entire population by exceeding the reference dose (RfD) established by the FAO/WHO and the US EPA for Hg and As, respectively. The cumulative risks (HI) of Hg and As through the consumption of fruits, tubers and fish exceeded the acceptable level (HI > 1), indicating a potential non-carcinogenic risk to the health of highly exposed consumers. For all the food (i.e. fruits, tubers and fish) carcinogenic risk due to As was higher than the acceptable range indicating a potential risk of cancer due to exposure to As through food consumption. The consumption of certain fruits is not fully recommended, specifically bananas, considering the high amounts of consumption (around 500 g/day) and its high As concentration (around 174 μg/kg). Given that increasing the intake of Hg and As in the diet can contribute to the development of various disorders, there is a need to control these pollutants in the human diet in a balanced and healthy way, associated with good agricultural practices and based on a clear policy to support and guide food security and nutrition actions. Therefore, the availability of recent and accurate food consumption data plays a fundamental role in risk assessment, since it allows the calculation of consumer exposure to potential hazards.

Table 3
Potential risk due to methylmercury (MeHg) in fish.

	WI	BW	EWI[a]	MFW	[MeHg]$_{PSL}$
CHD	1.31	26.1	3.03	0.69	65.4
WCBA	4.12	70.0	3.76	1.76	20.8
RP	3.84	68.2	3.36	3.76	47

WI: weekly intake (kg/week); BW: body weight (kg); EWI; estimated weekly intake of MeHg (μg/kg BW/week), MeHg$_{PSL}$: permissible safety level for MeHg (μg/kg).

Table 2
The estimated daily intake (EDI) rates of fruits, tubers, and fish by population group: children (CHD), women of childbearing age (WCBA), and the rest of the population (RP).

Food category	Consumption rate (g/day)			EDI (μg/kg/day)					
				Hg			As		
	CHD	WCBA	RP	CHD	WCBA	RP	CHD	WCBA	RP
Fruits	625	1176	1553	0.035	0.024	0.038	4.090	2.911	3.625
Tubers	56	457	188	0.005	0.014	0.006	0.271	0.837	0.351
Fish	187	589	548	0.529	0.646	0.588	0.329	0.384	0.398

PTWI = 1.6 μg Hg/kg BW/week for children (CHD) and women of childbearing age (WCBA); PTWI = 3.3 μg Hg/kg BW/week for the rest of the population (RP) (FAO/WHO, 2007); RfD = 0.3 μg As/kg BW/day (USEPA, 2000).

Table 4
Target hazard quotients (THQs) and total target hazard quotients (HI) of Hg and As through food consumption for different groups: CHD (children), WCBA (women of childbearing age), and RP (the rest of the population).

Food category	Hg			As			HI		
	THQ			THQ					
	CHD	WCBA	RP	CHD	WCBA	RP	CHD	WCBA	RP
Fruits	0.15	0.10	0.08	13.63	9.70	12.08	13.78	9.8	12.16
Tubers	0.02	0.06	0.01	0.90	2.79	1.17	0.92	2.85	1.18
Fish	2.30	2.81	1.25	1.10	1.28	1.33	3.4	4.09	2.58

Table 5
Carcinogenic risk (CR) for As.

Food category	CR (As)		
	CHD	WCBA	RP
Fruits	7.7×10^{-4}	5.5×10^{-4}	6.8×10^{-4}
Tubers	2.0×10^{-4}	6.3×10^{-4}	2.6×10^{-4}
Fish	1.2×10^{-4}	1.4×10^{-4}	1.5×10^{-4}

Individual author contributions

Siday Marrugo-Madrid: Formal analysis, Sampling campaign. José Pinedo-Hernández: Writing – original draft, Methodology, Sampling campaign. Roberth Paternina-Uribe: Methodology. José Marrugo-Negrete: Conceptualization, Project administration, Funding acquisition. Sergi Díez: Supervision, Formal analysis, Writing – review & editing

Declaration of competing interest

The authors declare that they have no known competing financial interests or personal relationships that could have appeared to influence the work reported in this paper.

Data availability

Data will be made available on request.

Appendix A. Supplementary data

Supplementary data to this article can be found online at https://doi.org/10.1016/j.envres.2022.113950.

References

Ahmeda, A.S., Rahmanc, M., Sultanab, S., Faruque Babua, S.M., Shafiqul Islam Sarkerd, Md, 2019. Bioaccumulation and heavy metal concentration in tissues of some commercial fishes from the Meghna River Estuary in Bangladesh and human health implications. Mar. Pollut. Bull. 145, 436–447.

Ahsan, H., Perrin, M., Rahman, A., Parvez, F., Stute, M., Zheng, Y., et al., 2000. Associations between drinking water and urinary arsenic levels and skin lesions in Bangladesh. J. Occup. Environ. Med. 42 (12), 1195–1201.

Arias Espana, V.A., Rodriguez Pinilla, A.R., Bardos, P., Naidu, R., 2018. Contaminated land in Colombia: a critical review of current status and future approach for the management of contaminated sites. Sci. Total Environ. 618, 199–209.

ATSDR, 2012a. Toxicological profile for arsenic. In: U.S. Department of Health and Human Services - Public Health Service. Agency for Toxic Substances and Disease Registry, Atlanta, GA.

Bentley, K., Soebandrio, A., 2017. Arsenic and mercury concentrations in marine fish sourced from local fishermen and fish markets in mine-impacted communities in Ratatotok Subdistrict, North Sulawesi, Indonesia. Mar. Pollut. Bull. 120, 75–81.

CAC Codex Alimentarius Commission, 2011. Joint FAO/WHO Food Standards Programme Codex Committee on Contaminants in Foods. Codex Alimentarius Commission, The Hague, NL, 5th Session.

Cargnelutti, D., Tabaldi, L.A., Spanevello, R.M., Jucoski, G.O., Battisti, V., Redin, M., Linares, C.E.B., Dressler, V.L., Flores, E.M.M., Nicoloso, F.T., Morsch, V.M., Schetinger, M.R.C., 2006. Mercury toxicity induces oxidative stress in growing cucumber seedlings. Chemosphere 65, 999–1006.

CGP - Contraloría General de la Republica, 2013. La explotación ilícita de recursos minerales en Colombia Casos Valle del Cauca (Río Dagua) – Chocó (Río San Juan) Efectos sociales y ambientales. Informe espacial minería ilegal. Colombia.

Chattopadhyay, S., Bhaumik, S., Purkayastha, M., Basu, S., Nag Chaudhuri, A., Das Gupta, S., 2002. Apoptosis and necrosis in developing brain cells due to arsenic toxicity and protection with antioxidants. Toxicol. Lett. 136 (1), 65–76.

Cheng, J., Zhang, X., Tang, Z., Yang, Y., Nie, Z., Huang, Q., 2017. Concentrations and human health implications of heavy metals in market foods from a Chinese coal-mining city. Environ. Toxicol. Pharmacol. 50, 37–44.

Choi, A.L., Mogensen, U.B., Bjerve, K.S., Debes, F., Weihe, P., Grandjean, P., Budtz Jørgensen, E., 2014. Negative confounding by essential fatty acids in methylmercury neurotoxicity associations. Neurotoxicol. Teratol. 42, 85–92.

CODECHOCÓ, 2012. Corporación Autónoma Regional del Chocó (Plan de Acción Institucional 2012–2015). Quibdó, Chocó, Colombia.

Cordeiro, F., Gonçalves, S., Caldéron, J., Robouch, P., Emteborg, H., Coneely, P., de la Calle, B., 2013. IMEP-115: Determination of Methylmercury in Seafood. https://doi.org/10.2787/76278.

Córdoba-Tovar, L., Marrugo-Negrete, J., Ramos Barón, P., Díez, S., 2021. Drivers of biomagnification of Hg, as and Se in aquatic food webs. A rev. Environ. Res., 112226 https://doi.org/10.1016/j.envres.2021.112226.

Costa, F., Coelho, J.P., Baptista, J., Martinho, F., Pereira, M.E., Pardal, M.A., 2020. Mercury accumulation in fish species along the Portuguese coast: are there potential risks to human health? Mar. Pollut. Bull. 150, 110740.

Dryzalowska, A., Falandysz, J., 2014. Bioconcentration of mercury by mushroom Xerocomuschrysenteron from the spatially distinct locations: levels, possible intake and safety. Ecotoxicol. Environ. Saf. 107, 97–102.

EPA, United States Environmental Protection Agency Method 7473 (SW-846), 1998. Mercury in Solids and Solutions by Thermal Decomposition. Amalgamation, and Atomic Absortion Spectrophotometry, Washington DC).

Fang, Y., Nie, Z., Liu, F., Die, Q., He, J., Huang, Q., 2014. Concentration and health risk evaluation of heavy metals in market-sold vegetables and fishes based on questionnaires in Beijing, China. Environ. Sci. Pollut. Res. 21, 11401–11408. https://doi.org/10.1007/s11356-014-3127-x.

FAO, 2016. The State of World Fisheries and Aquaculture 2016 (Contributing to food security and nutrition for all. Rome). http://www.fao.org/3/a-i5555s.pdf.

FAO, 2017. Food and Agriculture Organization. The State of Food Security and Nutrition in the World 2017. http://www.fao.org/3/a-I7695s.pdf.

FAO/WHO, 2017. Codex Committee on Food Additives and Contaminants. The Hague, Netherlands Adopted in 1995 Revised in 1997, 2006, 2008, 2009 Amended in 2010, 2012, 2013, 2014, 2015, 2016, 2017. http://www.fao.org/fao-who-codexalimentarius/.

FAO/WHO, 2007. Evaluation of Certain Food Additives and Contaminants. Sixty-Seventh Report of the Joint FAO/WHO Expert Committee on Food Additives.WHO Technical Report Series 940.

Filippini, T., Malavolti, M., Cilloni, S., Wise, L.A., Violi, F., Malagoli, C., et al., 2018. Intake of arsenic and mercury in a northern Italy community from fish and seafood. Food Chem. Toxicol. 116, 20–26.

Fuentes-Gandara, F., Pinedo-Hernández, J., Marrugo-Negrete, J., Díez, S., 2018. Human health impacts of exposure to metals through extreme consumption of fish from the Colombian Caribbean Sea. Environ. Geochem. Health 40 (1), 229–242.

Gallego Rios, S.E., Ramírez, C.M., López, B.E., Macías, S.M., Leal, J., Velásquez, C.M., 2018. Evaluation of Mercury, Lead, Arsenic, and Cadmium in Some Species of Fish in the Atrato River Delta, Gulf of Urabá, Colombian Caribbean. Water Air Soil Pollut, pp. 229–275.

Gutiérrez-Mosquera, H., Sujitha, S.B., Jonathan, M.P., Sarkar, S.K., Medina-Mosquera, F., Ayala-Mosquera, H., Morales-Mira, G., Arreola-Mendoza, L., 2018. Mercury levels in human population from a mining district in Western Colombia. J. Environ. Sci. 68, 83–90.

Gutiérrez-Mosquera, H., Marrugo-Negrete, J., Díez, S., Morales-Mira, G., Montoya-Jaramillo, L.J., Jhonatan, M.P., 2020. Distribution of chemical forms of mercury in

sediments from abandoned ponds created during former gold mining operations in Colombia. Chemosphere 68, 83–90.

Gutiérrez-Mosquera, H., Marrugo-Negrete, J., Díez, S., Morales-Mira, G., Montoya-Jaramillo, L.J., Jhonatan, M.P., 2021. Mercury distribution in different environmental matrices in aquatic systems of abandoned gold mines, Western Colombia: focus on human health. J. Hazard Mater. 404, 124080.

IARC International Agency for Research on Cancer, 2012. IARC Monographs on the Evaluation of Carcinogenic Risks to Humans. Arsenic, Metals, Fibres, and Dusts, Volume 100 C. A Review of Human Carcinogens. International Agency for Research on Cancer, Lyon, France. http://monographs.iarc.fr/ENG/Monographs/vol100C/.

Ikemoto, T., Tu, N., Okuda, N., Iwata, A., Omori, K., Tanabe, S., Tuyen, B., Takeuchi, I., 2008. Biomagnification of trace elements in the aquatic food web in the Mekong Delta, South Vietnam using stable carbon and nitrogen isotope analysis. Arch. Environ. Contam. Toxicol. 54, 504–515.

Islam, M.S., Ahmed, M.K., Al-mamun, M.H., Masunaga, S., 2014. Trace metals in soil and vegetables and associated health risk assessment. Environ. Monit. Assess. 186, 8727–8739.

Lara-Rodríguez, J.S., 2018. All that glitters is not gold or platinum: institutions and the use of mercury in mining in Chocó, Colombia. Extr. Ind. Soc. 5, 308–318.

Lee, M., Bae, O.N., Chung, S.M., Kang, K.T., Lee, J.Y., Chung, J.H., 2002. Enhancement of platelet aggregation and thrombus formation by arsenic in drinking water: a contributing factor to cardiovascular disease. Toxicol. Appl. Pharmacol. 179 (2), 83–88.

Li, X.-D., Hua, R.-M., Yue, Y.-D., Cao, D.-J., Yuan, L.-Z., Shen, W.-W., 2004. Pollution and assessment of metal Chromium, lead, cadmium and copper in vegetables in Hefei, China. J. Anhui Agric. Univ. 31, 143–147 (in Chinese).

Li, X., Li, Z., Lin, C., Bi, X., Liu, J., Zhang, H., Chen, J., Wu, T., Feng, X., 2018. Health risks of heavy metal exposure through vegetable consumption near a large-scale Pb/Zn smelter in central China. Ecotoxicol. Environ. Saf. 161, 99–110.

Lightfoot, N.E., Pacey, M.A., Darling, S., 2010. Gold, nickel and copper mining and processing. Chron. Dis Can [Internet] 29 (Suppl. 2), 101–124. Disponible en: https://www.ncbi.nlm.nih.gov/pubmed/21199602.

Liu, Y., Liu, G., Yuan, Z., et al., 2017. Heavy metals (As, Hg and V) and stable isotope ratios (σ^{13} C and σ^{15} N) in fish from Yellow River Estuary, China. Sci. Total Environ. 613–614, 462–471.

Margenat, A., You, R., Cañameras, N., Carazo, N., Díez, S., Bayona, J.M., Matamoros, V., 2020. Occurrence and human health risk assessment of antibiotics and trace elements in Lactuca sativa amended with different organic fertilizers. Environ. Res. 190, 109946 https://doi.org/10.1016/j.envres.2020.109946.

Marrugo-Negrete, J., Durango-Hernández, J., Pinedo-Hernández, J., Díez, S., 2015. Phytoremediation of mercury-contaminated soils by Jatropha curcas. Chemosphere 127 (2015), 58–63.

Marrugo-Negrete, J., Vargas-Licona, S., Ruiz-Guzmán, J., Marrugo-Madrid, S., Bravo, A., Díez, S., 2020. Human health risk of methylmercury from fish consumption at the largest floodplain in Colombia. Environ. Res. 182, 109050.

Medina Mosquera, F.M., Ayala Mosquera, H.J., Perea, J.D., 2011. Determinación de la contaminación mercurial en personas vinculadas con la minería de oro en el Distrito Minero del San Juan departamento del Chocó, Colombia. Bioetnia 8, 195–206.

Moreno, E., Gamarra, R., Carpena, R., Millan, R., Penalosa, J., Esteban, E., 2005. Mercury bioaccumulation and phytotoxicity in two wild plant species of Almaden area. Chemosphere 63, 1969–1973.

Muñoz, O., Zamorano, P., Garcia, O., Miguel Bastías, J., 2017. Arsenic, cadmium, mercury, sodium, and potassium concentrations in common foods and estimated daily intake of the population in Valdivia (Chile) using a total diet study. Food Chem. Toxicol. 109, 1125–1134.

Naujokas, M.F., Anderson, B., Ahsan, H., Aposhian, H.V., Graziano, J.H., Thompson, C., et al., 2013. The broad scope of health effects from chronic arsenic exposure: update on a worldwide public health problem. Environ. Health Perspect. 121, 295–302.

Oken, E., Radesky, J., Wright, R., Bellinger, D., Amarasiriwardena, C., Kleinman, P., 2008. Maternal fish intake during pregnancy, blood mercury levels, and child cognition at age 3 years in a US cohort. Am. J. Epidemiol. 167, 1171–1181.

Ouédraogo, O., Amyot, M., 2013. Mercury, arsenic and selenium concentrations in water and fish from sub-Saharan semi-arid freshwater reservoirs (Burkina Faso). Sci. Total Environ. 444, 243–254.

Palacios-Torres, Y., Caballero-Gallardo, K., Olivero-Verbel, J., 2018. Mercury pollution by gold mining in a global biodiversity hotspot, the Choco biogeographic region, Colombia. Chemosphere 193, 421–430.

Palacios-Torres, Y., Caballero-Gallardo, K., Olivero-Verbel, J., 2020. Trace elements in sediments and fish from Atrato River: an ecosystem with legal rights impacted by gold mining at the Colombian Pacific. Environ. Pollut. 256, 113290.

Pinzón-Bedoya, C., Pinzón-Bedoya, M., Pinedo-Hernández, J., Urango-Cardenas, I., Marrugo-Negrete, J., 2020. Assessment of potential health risks associated with the intake of heavy metals in fish harvested from the largest estuary in Colombia. Int. J. Environ. Res. Publ. Health 17, 2921.

Rahman, M., Molla, A., Saha, N., Rahman, A., 2012. Study on heavy metals levels and its risk assessment in some edible fishes from Bangshi River, Savar, Dhaka, Bangladesh. Food Chem. 134, 1847–1854.

Ralston, N.V.C., Raymond, L.J., 2010. Dietary selenium's protective effects against methylmercury toxicity. Toxicology 278, 112–123. https://doi.org/10.1016/j.tox.2010.06.004PMID: 20561558.

Renner, R., 2004. Arsenic and lead leach out of popular fertilizer. Environ. Sci. Technol. 38, 382A.

Saha, N., Zaman, M.R., 2013. Evaluation of possible health risks of heavy metals by consumption of foodstuffs available in the central market of Rajshahi City, Bangladesh. Environ. Monit. Assess. 185, 3867e3878.

Saha, N., Molla, M.Z.I., Alam, M.F., Rahman, M.S., 2016. Seasonal investigation of heavy metals in marine fishes captured from the Bay of Bengal and the implications for human health risk assessment. Food Control 70, 110–118.

Salazar-Camacho, C., Salas-Moreno, M., Marrugo-Madrid, S., Marrugo-Negrete, J., Díez, S., 2017. Dietary human exposure to mercury in two artisanal small-scale gold mining communities of northwestern Colombia. Environ. Int. 107 (May), 47–54. https://doi.org/10.1016/j.envint.2017.06.011.

Salazar-Camacho, C., Salas-Moreno, M., Paternina – Uribe, R., Marrugo-Negrete, J., Díez, S., 2020. Dataset of Concentrations of Mercury and Methylmercury in FIsh from a Tropical River Impacted by Gold Mining in the Colombian Pacific. https://doi.org/10.1016/j.chemosphere.2020.128478.

SIMCO, 2017. Volumen por departamento anual, producción de oro y platino. Bogotá D.C.

Szkoda, J., Żmudzki, J., Grzebalska, A., 2006. Determination of arsenic in biological material by hydride generation atomic absorption spectrometry method. Bull. Vet. Inst. Pulawy 50 (2), 269–272.

Tadiso, T., Borgstrom, R., Rosseland, B., 2011. Mercury concentrations are low in commercial fish species of Lake Ziway, Ethiopia, but stable isotope data indicated biomagnification. Ecotoxicol. Environ. Saf. 74, 953–959.

Tellerías, L., Paris, E., 2008. Impacto de los tóxicos en el neurodesarrollo. Rev. Chil. Pediatr. 79 Supl (1), 55–63.

Tsai, S., Chou, H.Y., The, H.W., Chen, C.M., Chen, C.J., 2003. The effects of chronic arsenic exposure from drinking water on the neurobehavioral development in adolescence. Neurotoxicology 24 (4–5), 747–753.

Tyler, C.R., Allan, A.M., 2014. The effects of arsenic exposure on neurological and cognitive dysfunction in human and rodent studies: a review. Curr. Environ. Health Rep. 1 (2), 132–147.

Uddh-Söderberg, T.E., Gunnarsson, S.J., Hogmalm, K.J., Lindegård, M.I., Augustsson, A., 2015. An assessment of health risks associated with arsenic exposure via consumption of homegrown vegetables near contaminated glassworks sites. Sci. Total Environ. 536, 189–197.

UNEP/IOC/IAEA/FAO, 1990. Contaminant monitoring programmes using marine organisms: quality assurance and good laboratory practice. Ref. Meth. Marin. Pollut. Stud. N°57.

UPME-MME-UC, 2014. Unidad de Planeación Minero Energética, Ministerio de Minas y Energía, Universidad de Córdoba. Incidencia real de la minería del carbón, del oro y del uso de mercurio en la calidad ambiental con énfasis especial en el recurso hídrico - Diseño de herramientas para la planeación sectorial. Informe Técnico (Reporte Final), Bogotá D.C.

UPME-MME-UC, 2016. Unidad de Planeación Minero Energética, Ministerio de Minas y Energía, Universidad de Córdoba. Identificación y caracterización de Unidades Básicas de Beneficio Aurífero en 261 Municipios de Colombia. Informe Técnico (Reporte Final), Bogotá D.C.

USEPA, 2022. Risk-based concentration table. Available from: https://cfpub.epa.gov/ncea/iris2/chemicallanding.cfm?substance_nmbr=278.

Wang, B.H., Ma, Z.H., Feng, X.Y., Wang, J.H., 2015. Concentrations and health risk evaluation of heavy metals in vegetables in Beijing. J. Food Saf. Qual 7, 2736–2745.

Wei, J., Gao, J., Cen, K., 2019. Levels of eight heavy metals and health risk assessment considering food consumption by China's residents based on the 5th China total diet study. Sci. Total Environ. 689, 1141–1148.

Xiao, X.-Y., Chen, T.-B., Liao, X.-Y., Yan, X.-L., Xie, H., Wu, B., Wang, L.-X., 2009. Comparison of concentrations and bioconcentration factors of arsenic in vegetables, grain and oil crops in China. J. Environ. Sci. 29, 291–296.

Zhou, Y., Bi, C.J., Zhou, X.X., Zhang, H.H., Chen, Z.L., Bao, X.Y., 2017. Distribution characteristics and health risk of heavy metals in vegetables near the industrial area in shanghai. Environ. Sci. 38, 5292–5298 (In Chinese with English abstract.

8

Publicación 2: *Supplementary information*

Health risk assessment for human exposure to mercury species and arsenic via consumption of local food in a gold mining area in Colombia

Health risk assessment for human exposure to mercury species and arsenic via consumption of local food in a gold mining area in Colombia

Table S1. Values of Hg and As (mg/kg) in fish, fruits and tubers, and MeHg (mg/kg) in fish

Hg	GM	Median	25th percentile	75th percentile	IQR
Fish					
Astyanax fasciatus	83.77	89.43	83.26	91.06	7.80
Hypostomus hondae	35.31	44.27	21.14	49.61	28.47
Pimelodus blochii	84.71	57.80	50.96	213.65	162.69
Pinguipes chilensis	88.51	117.94	77.70	137.42	59.72
Fruits					
Ananas comosus	2.17	2.21	2.07	2.33	0.26
Artocarpus altilis	1.21	2.11	1.25	2.12	0.86
Bixa orellana	3.12	2.66	2.61	3.36	0.76
Musa acuminata cv. Sucrier	0.70	0.73	0.43	1.11	0.67
Musa balbisiana	2.05	1.76	1.71	2.36	0.65
Musa paradisíaca	1.43	1.50	1.34	1.59	0.25
Psidium guajava	2.38	2.54	2.20	2.71	0.51
Solanum quitoense	1.75	1.77	1.56	1.98	0.42
Tubers					
Dioscorea trifida	2.09	1.75	1.74	2.38	0.64
Manihot esculenta	2.28	1.78	1.66	3.08	1.42

As	GM	median	25th percentile	75th percentile	IQR
Fish					
Astyanax fasciatus	28.22	24.38	16.40	51.46	35.06
Hypostomus hondae	68.81	52.82	38.72	124.09	85.37
Pimelodus blochii	28.68	25.46	16.40	50.85	34.45
Pinguipes chilensis	65.15	85.53	55.54	106.04	50.50
Fruits					
Ananas comosus	106.48	125.28	107.79	130.02	22.23
Artocarpus altilis	218.58	468.39	257.29	475.57	218.29
Bixa orellana	113.03	111.10	92.39	143.79	51.39
Musa acuminata cv. Sucrier	287.70	283.88	156.24	820.59	664.35
Musa balbisiana	102.61	77.20	72.97	140.39	67.42
Musa paradisíaca	131.79	91.95	79.24	257.81	178.57
Psidium guajava	56.89	58.13	54.60	60.08	5.47
Solanum quitoense	174.08	282.13	63.13	507.66	444.53
Tubers					
Dioscorea trifida	226.78	306.98	211.98	315.87	103.89
Manihot esculenta	71.40	76.73	67.87	78.55	10.68

Table S1 (cont.)

Fish	MeHg GM	median	25th percentile	75th percentile	IQR
Astyanax fasciatus	73.77	66.29	65.20	81.32	16.12
Hypostomus hondae	21.40	23.58	13.38	33.76	20.38
Pimelodus blochii	68.40	49.53	40.40	166.54	126.15
Pinguipes chilensis	75.85	122.80	75.04	126.52	51.48

Table S2. Frequency intake of fruits, tubers, and fish by different population groups

Food items	Scientific name	N	CHD Fi	WCBA Fi	RP Fi
Fruits	Ananas comosus	3	12	21	122
	Artocarpus altilis	3	12	21	122
	Bixa orellana	3	12	21	122
	Musa acuminata cv. Sucrier	4	190	376	320
	Musa balbisiana	3	182	346	289
	Musa paradisíaca	4	194	347	332
	Psidium guajava	3	12	21	122
	Solanum quitoense	3	12	21	122
Tubers	Dioscorea trifida	3	20	167	68
	Manihot esculenta	3	36	291	121
Fish	Astyanax fasciatus	5	46	173	104
	Hypostomus hondae	14	43	104	138
	Pimelodus blochii	6	57	151	142
	Pinguipes chilensis	3	41	161	163

Frequency intake (Fi): g/day; CHD (children), WCBA (women of childbearing age), and RP (the rest of the population).

Equations for human health risk assessment:

The potential human health risk assessment was conducted by considering the estimated daily intake (EDI) (µg/kg bw/day), calculated using the following equation:

EDI= (Cm x Fi)/BW

where Cm is the mean metal concentration in edible muscle tissue (µg/g), Fi is the intake of fish consumed per day (g/day), and BW is the mean body weight (bw) of the participants (kg).

Risk may be characterised using a hazard quotient (HQ). This is the ratio of the EDI of a chemical to a reference dose (RfD, µg/kg bw/day) defined as the maximum tolerable daily intake of a specific metal that does not result in any deleterious health effects:

HQ =EDI/RfD

There would be no obvious hazard if the value of HQ was less than 1. If HQ [1, then the EDI of a particular metal exceeds the RfD, indicating that there is a potential risk associated with that metal. The RfDs used in this study for As is 0.3 µg/kg bw/day, whereas for Hg and MeHg is the PTWI = 1.6 µg/kg bw/week for children (CHD) and women of childbearing age (WCBA) and PTWI = 3.3 µg/kg bw/week for the rest of the population (RP).

It has been reported that exposure to two or more pollutants can result in additive and/or interactive effects. Thus, in the present study, cumulative health risk was evaluated by summing the THQ value of individual metals and expressed as total THQ (HI) as follows:

HI = Σ THQ

When the value of HI is greater, the level of concern is greater. The HI value greater than 1 generally indicates a potential for adverse human health effects and suggests the need to undertake a higher level of research or possibly remedial action.

The equation used to estimate cancer risk is as follows:

CR= CSF x EDI

where CSF is the carcinogenic slope factor of 1.5 (mg/kg/ day)$^{-1}$ for i-As set by USEPA (USEPA, 2000, 2010), and EDI is the estimated daily intake of heavy metals (USEPA, 2000, 2010). The acceptable lifetime CR considered by USEPA (2000) is $10^{-4} - 10^{-6}$ (average risk of developing cancer over a human lifetime is 1 in 100 000).

The maximum amount of fish that can be consumed weekly per person (MFW), without harmful effects to health, was calculated using the following equation:

MFW=(PTWI×WI)/EWI

The permissible safety level (MeHg$_{PSL}$), which is the allowable concentration of MeHg in fish consumed by humans, was calculated using the following equation:

MeHg$_{PSL}$ = (Cm x PTWI)/WI

WI is the intake of fish consumed per week (g/week)

3.3.2. Publicación 3: Assessment of dissolved mercury by diffusive gradients in thin films devices in abandoned ponds impacted by small scale gold mining

Marrugo-Madrid, S., Salas-Moreno, M., Gutiérrez-Mosquera, H., Salazar-Camacho, C., Marrugo-Negrete, J., Díez, S. Environmental Research, 208 (2022): 112633.

Assessment of dissolved mercury by diffusive gradients in thin films devices in abandoned ponds impacted by small scale gold mining

Siday Marrugo-Madrid [a], Manuel Salas-Moreno [b], Harry Gutiérrez-Mosquera [b], Carlos Salazar-Camacho [b], José Marrugo-Negrete [c], Sergi Díez [a,*]

[a] Environmental Chemistry Department, Institute of Environmental Assessment and Water Research, IDAEA-CSIC, E-08034, Barcelona, Spain
[b] Faculty of Natural Sciences, Department of Biology, Universidad Tecnológica del Chocó, Quibdó, Colombia
[c] University of Córdoba, Carrera 6 No. 76-103, Montería, Colombia

ARTICLE INFO

ABSTRACT

In order to fulfil the Minamata Convention on Mercury, it is necessary to monitor the Hg contamination in freshwater ecosystems nearby artisanal and small scale gold mining (ASGM) areas. Since most of these ASGM communities are located in remote areas, a convenient method for sampling, preserving and transporting samples is needed. In this study we evaluated the feasibility of the diffusive gradient in thin-films (DGT) technique to detect and quantify the labile fraction of Hg and other metals (Pb, Cu, Zn, Cd, Ni, Mn and Cr) in a hard-to-reach gold mining district in the state of Chocó, Colombia. We deployed DGT at sampling sites along the Atrato river and abandoned mining ponds (AMPs) which were deserted in different periods since 1997 to 2019 (6–15 years). In average, the labile THg concentrations in AMPs (148.9 $\pm$ 43.2 ng L^{-1}) were a 50% higher than in the river water (99.9 $\pm$ 37.4 ng L^{-1}). In the ponds, no significant differences were found in labile Hg with respect abandonment period. Labile Ni (0.9–493.1), Mn (1.33–11.48), Cu (0.030–2.233), and Zn (0.67–10.29) (in µg L^{-1}) were found in higher amounts than for the rest of metals. Labile concentrations of metals are related with their downstream proximity to gold mining activities, being higher in devices deployed close to ASGM sites. Moreover, this study demonstrates the feasibility of the DGT technique to sample, transport, storage, and preserve labile Hg from hard-to-reach ASGM areas.

1. Introduction

Mercury (Hg) is a toxic metal with a high potential for neurotoxicity and teratogenicity, that could severely harm human health and aquatic biota (USEPA, 2001), affecting mainly to mining communities. In consequence, one of the key pieces of the Minamata Convention on Mercury, the global environmental agreement to reduce mercury pollution, is its focus on reducing and eventually eliminating the use of Hg in the artisanal and small scale gold mining (ASGM) sector. The Annex C of the treaty addresses the development of national plans for ASGM including strategies for promoting the reduction of emissions and releases of Hg, to address the potential illegal trade of Hg, and a public health strategy on the exposure of ASGM miners and their communities (UNEP, 2019). To fulfil the objectives of this treaty, there is a need to perform sampling campaigns to monitor Hg contamination in ASGM communities, especially in water and fish, which is the primary source of animal protein to riverine communities. Furthermore, these communities are often located in remote areas, and therefore, the main drawbacks that could arise in Hg monitoring are related to the high amount of samples to carry on, deterioration of samples and costly transport to laboratory (Fernández-Gómez et al., 2012a). Various techniques have been developed in order to overcome these drawbacks, such as advanced colorimetric-based sensors (Hossain and Brennan, 2011), on-site analytical system with a coupled peristaltic pump and mercury vapor analyzer (Amyot et al., 2001), portable x-ray fluorescence (pXRF) spectrometer (Zhou et al., 2018), optical chemical sensors nanomaterial-based (Ding et al., 2016), or screen-printed electrodes (SPEs) for environmental monitoring of metals (Bernalte et al., 2020). Nevertheless, these techniques are often costly to manufacture, or present additional drawbacks under extreme conditions (high temperatures, high humidity or long periods of time). For these reasons, it should be appropriate to use of non-heavy sampling devices to minimize these disadvantages, especially during extreme conditions until the appropriate analysis can be done.
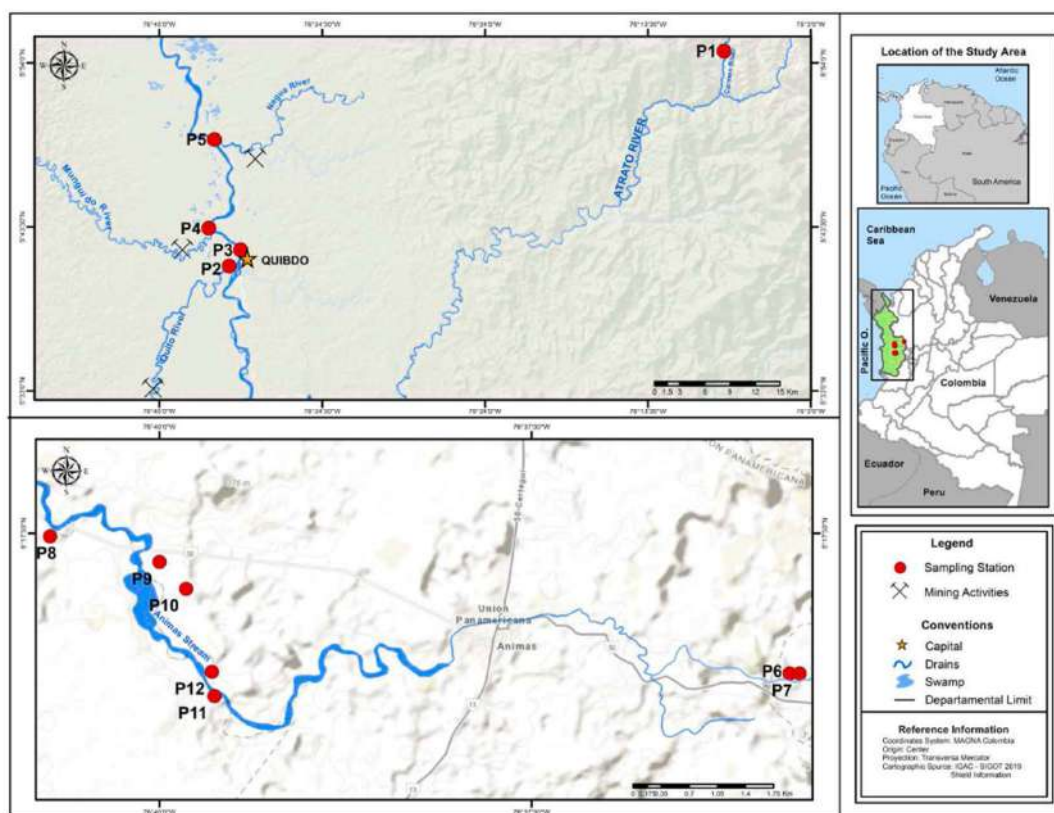

Fig. 1. Location of the department of Chocó, and distribution of sampling sites in the Atrato river basin.

Passive samplers could represent a good option to monitor Hg concentrations in hard-to-reach areas, due to the advantages they offer in terms of transportation, deployment at the sampling sites and preserving them once recovered. Many studies have demostrated the effectivity of the diffusive gradient in thin-films (DGT) technique since its development (Davison and Zhang, 1994) for on-site evaluation of labile metals in aqueous environments (Dočekalová and Diviš, 2005; Fernández-Gómez et al., 2011; Turull et al., 2018; Bratkič et al., 2019; Marrugo-Madrid et al., 2021), sediments (Divis et al., 2005; Wang et al., 2016; Lin et al., 2017; Liu et al., 2019; Sun et al., 2019; Valero et al., 2020) and soils (Bade et al., 2012; Zarrouk et al., 2014; Huynh et al., 2015; Zhang and Davison, 2015; Zhang et al., 2017; Guan, 2019; Turull et al., 2019a, 2019b). For labile-Hg determination, one of the most used binding layers is 3-mercaptopropyl functionalized silica gel (3MFS), due to the affinity existing between thiol groups and Hg (Fernández-Gómez et al., 2014; Turull et al., 2017, 2019a; Bratkič et al., 2019). For other metals determination, DGT with Chelex-100 resin in the binding layer has been proven successfully (Davison and Zhang, 1994; Gao et al., 2019; Marrugo-Madrid et al., 2021).

The main objective of the present study was to evaluate the feasibility of DGT technique in order to detect and quantify Hg in a hard-to-reach ASGM area (i.e. locations along the Atrato River and several abandoned mining ponds, AMPs). Furthermore, this is the first time that DGT samplers were deployed in AMPs to determine the Hg bioavailable concentrations, and to verify if availability will depend from the time of abandoment. Finally, other types of DGT were deployed in order to determine the concentration of trace metals such as Pb, Cu, Zn, Cd, Ni, Mn and Cr, to know the impact of the machinery employed during ASGM operations. Moreover, generated information could be used to develop potential restoration strategies in the areas and to get relevant information on the impact on the biota, human health and food web.

2. Materials and methods

2.1. Study area and sampling sites

This study was conducted in the Atrato River basin and in widely dispersed AMPs in areas of difficult access in the Chocó department, Colombia (Fig. 1). The department of Chocó is one of the most biodiverse regions on the planet known as the biogeographic Chocó or the Tumbes-Chocó-Magdalena biodiversity hotspot, it has a great natural and ethnic diversity, and where 90% of its territory is considered a special zone of conservation (Medina-Rivas et al., 2016). A particular feature of Chocó is the extreme rainfall, with around 11,700 mm per year; therefore, it is included among the wettest places on earth. Likewise, due to its condition of tropical forest, geographical location, and low development of land routes in the region, it is also considered a remote area with very difficult access (Medina-Rivas et al., 2016; Pérez-Escobar et al., 2019). Despite being a region with high indices of poverty and difficult access, Chocó is the second department in the country with a greater presence of gold mining, and annually produces almost 15 tons of this precious metal (MME, 2015, 2016; Veiga and Marshall, 2019). Mechanized mining and ASGM affects to upper and middle basin of the main river in Chocó, the Atrato River, as well as, its principal tributaries. In addition, the riverbed and natural course of the river have been affected by the creation of mining ponds, which contribute greatly to the contamination by Hg and other metals in the area (MME, 2014, 2015, 2016).

The Atrato River is considered the most flowing river in Colombia, it receives the waters of more than 15 rivers and 30 streams during its

Table 1
Physicochemical parameters measured by sampling site: temperature (°C), dissolved oxygen (DO, mg L^{-1}), conductivity (mS cm^{-1}) and total dissolved solids (TDS, mg L^{-1}), and estimated abandonment years in AMPs. Values as average $\pm$ SD (n = 3).

Sampling site	Abandonment time[a]	pH	Temperature	DO	Conductivity	TDS
P1	–	7.0	17.4 $\pm$ 0.5	6.2 $\pm$ 0.1	20.6 $\pm$ 2.9	13.1 $\pm$ 1.6
P2	–	6.3	26.7 $\pm$ 0.2	5.3 $\pm$ 0.3	16.2 $\pm$ 0.0	10.3 $\pm$ 0.1
P3	–	6.0	24.9 $\pm$ 0.4	7.2 $\pm$ 0.9	12.5 $\pm$ 2.3	8.2 $\pm$ 1.6
P4	–	6.2	25.7 $\pm$ 0.2	5.6 $\pm$ 0.6	35.0 $\pm$ 5.7	21.7 $\pm$ 2.4
P5	–	6.1	24.7 $\pm$ 0.0	6.8 $\pm$ 0.1	18.5 $\pm$ 3.8	12.2 $\pm$ 2.5
P6	11	5.6	28.4 $\pm$ 0.4	5.0 $\pm$ 0.1	5.0 $\pm$ 0.1	7.4 $\pm$ 1.3
P7	11	5.6	27.5 $\pm$ 0.4	5.3 $\pm$ 0.1	14.8 $\pm$ 0.0	9.8 $\pm$ 1.1
P8	8	5.4	26.7 $\pm$ 0.1	4.1 $\pm$ 0.9	14.0 $\pm$ 0.5	8.8 $\pm$ 0.4
P9	11	5.9	26.0 $\pm$ 0.7	5.3 $\pm$ 0.7	22.8 $\pm$ 1.4	14.5 $\pm$ 1.1
P10	15	5.6	27.2 $\pm$ 0.1	1.5 $\pm$ 1.0	35.6 $\pm$ 1.6	22.1 $\pm$ 0.7
P11	6	5.5	27.1 $\pm$ 0.4	1.6 $\pm$ 0.7	25.8 $\pm$ 6.9	16.2 $\pm$ 4.4
P12	9	5.6	27.5 $\pm$ 0.5	2.5 $\pm$ 0.1	20.8 $\pm$ 0.0	13.4 $\pm$ 1.2

[a] Estimated time until sampling year in 2019.

trajectory, which is approximately 750 km from its source in the western Andes mountains, in Carmen de Atrato, until its mouth into the Gulf of Urabá, in the Caribbean Sea (Poveda et al., 2004). The Constitutional Court of Colombia issued the judgment T-622 of 2016 as a legal framework for the protection, conservation, maintenance and restoration of the Atrato River, its basin and tributaries, against the serious consequences caused by ASGM activities. The mining ponds are water reservoirs formed during gold mining operations in the area, and then, they have been abandoned without restoration. These reservoirs have served as sinks for drains of organic and inorganic material, including Hg from previous mining. Likewise, the high organic load, the abundant adjacent vegetation and the low level of dissolved oxygen in water are characteristic of these ponds, and in turn, provide favourable conditions for Hg methylation (Gutiérrez-Mosquera et al., 2020, 2021).

For the river campaign, a boat was used to reach the five sampling sites (P1 to P5) along the Atrato River (Fig. 1). A sampling site at the source of the river in Carmen de Atrato (P1) was chosen as a control site, due to the absence of gold mining exploitation. Sampling sites downstream (P2 to P5) were chosen according to their proximity to riverine communities or mining activities, including a sampling site close to the city of Quibdó (P3), which is the main urban area of the department of Chocó.

The AMPs have become wetlands that provide ecosystem services to the surrounding rural population and fauna, therefore, seven sampling sites (P6 to P12) were chosen according to the years of abandonment and use of the ponds. The mining ponds chosen as sampling sites have a period of abandonment between 8 and 15 years, and are located within the San Juan mining district, in the middle of the basin and near small urbanized areas. Figure S1 displays pictures of motorcycle cars and motorcycles used to enter to abandoned gold mines, whereas Figure S2 shows pictures of DGT deployments at some sites.

2.2. Gel preparation and mounting of DGT devices

The reagents and preparation of the DGT gels and mounting are described in previous works (Fernández-Gómez et al., 2011, 2014; Turull et al., 2017, 2019b). In-house manufactured polyacrylamide DGT devices (DGT-P) were made with a resin gel of 3MFS embedded in a polyacrylamide gel as the binding layer, a 0.5 mm thick polyacrylamide gel as the diffusive layer, and a 0.45-μm pore size Nylon filter membrane to protect the diffusive gel. A plastic mold based on a simple tight-fitting piston and cap design with a 2 cm diameter window (DGT Research Ltd., UK) was used to support and enclose all the layers, keeping the layers wet during assembly to avoid the inclusion of air bubbles between them, and ensuring that only a known surface of the DGT device (area = 3.14 cm^2) was in contact with the solution.

Commercial DGT devices were obtained from DGT® Research, and used for the uptake of cationic species of metals (i.e. Pb, Cu, Zn, Cd, Ni, Mn and Cr), with a 0.8 mm APA diffusive gel, a polyethersulphone filter
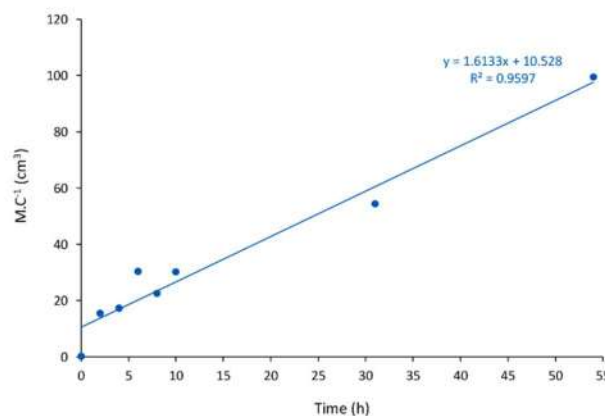

Fig. 2. Time-series experiment. Mass of mercury accumulated in the resin (M) normalized by the Hg(II) concentration in the solution for various periods of time.

membrane and Chelex-100 as binding layer (DGT-Chelex).

2.3. General sampling procedures of DGT devices

All DGT devices were preserved inside ziplock polyethylene bags until deployment at the field. Cylindrical baskets made of a plastic net were used for the DGT deployment at each sampling site, where 4 DGT-P and 2 DGT-Chelex were introduced inside the basket and submerged at 1–2 m depth in the water column (Figure S2). The deployment time was between 3 and 4 days, and temperature, pH, dissolved oxygen (DO), conductivity and total dissolved solids (TDS) were measured in water using a multiparameter YSI Pro 2030 (Table 1). After retrieval, the DGT devices were rinsed with Milli-Q water and put it back to the polyethylene bags for transport to the laboratory. Finally, some DGT-P and DGT-Chelex devices from the same batch were chosen as travelling blank or control.

2.4. Dissolved Hg in water with DGT

For the determination of the labile THg fraction in water, we used the following equation:

$$C = \frac{M \, \Delta g}{D \, A \, t}$$

where M is the mass of Hg accumulated on binding layer, t is the time of deployment, A is the area of exposed surface and Δg is the diffusive layer thickness. The diffusion coefficient of the labile Hg (D) can be calculated
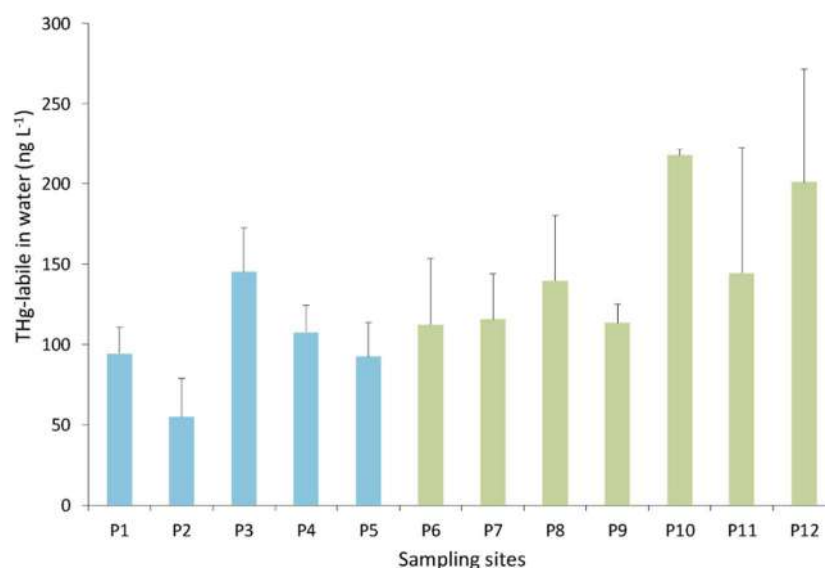
3

Fig. 3. Labile-THg concentrations in Atrato River (blue bars, P1 to P5) and AMPs (green bars, P6 to P12) measured by DGT-P devices. (For interpretation of the references to color in this figure legend, the reader is referred to the Web version of this article.)

from the slope of the relationship between the amount of Hg accumulated by the DGT units (normalized for the concentration of Hg in solution) and the deployment time (Fig. 2).

2.5. Mercury analysis

Prior to analysis, all DGT devices were dismantled and the resin gels were extracted (Figure S2). Total mercury (THg) analysis in resin gels and solutions were made using a direct mercury analyzer DMA-80 Tri-cell Milestone, that uses catalytic combustion of the sample, pre-concentration by gold amalgamation, thermal desorption and atomic absorption spectrometry (AAS), according to the EPA method 7473 (USEPA, 1998). The entire analytical procedure was validated by analysis of certified reference material (DORM-2, dogfish-muscle) samples from the National Research Council of Canada (NRCC), with Hg certified value of 4.64 ± 0.26 mg kg^{-1}. This reference material was analyzed in triplicate at the beginning and ends of each set of (usually 10) samples, to ensure the calibration of the instrument during the study. The detection limit (LOD) and the limit of quantification (LOQ) (0.1 and 0.2 ng g^{-1} ww of Hg, respectively) were calculated based a series of blank samples.

2.6. Statistical analysis

Analysis of the labile THg in all DGT binding layers was reported as the average $\pm$ standard deviation (SD). Normal distribution was tested based on the Shapiro-Wilk test for DGT-P and DGT-Chelex (N < 50). T-test was used with p value of 0.05 to indicate statistical differences. A principal component analysis (PCA) and a Pearson correlation coefficient were used with the aim of identifying sources among metals, and possible correlations between physicochemical parameters and metals. Statistical analysis was performed with IBM-SPSS statistics 25 (SPSS Inc., Chicago, IL, USA).

3. Results and discussion

3.1. Labile Hg in waters by DGT-P

The diffusion coefficient (D) of the labile Hg in DGT-P was calculated according to the procedure described by Fernández-Gómez et al. (2011),

with a value of 7.23×10^{-6} cm^2 s^{-1} (Fig. 2) which is close to the magnitude order 10^{-6} shown in other studies for the same labile species (Dočekalová and Diviš, 2005; Fernández-Gómez et al., 2011). Studies of Dočekalová and Diviš (2005) stated that the agarose is the best diffusive gel for low THg concentrations, however, since we did not found THg-sorption onto the polyacrylamide gel, it can be used as diffusive gel (Clarisse and Hintelmann, 2006; Fernández-Gómez et al., 2011).

Table 1 shows the average $\pm$ standard deviation (SD) values of different physicochemical parameters measured during the DGT deployment period in the Atrato River and AMPs, two aquatic environments with dissimilar dynamics. Values in Atrato River were pH: 6.3 $\pm$ 0.4, temperature: 23.8 ± 3.7 °C, DO: 6.2 ± 0.8 mg L^{-1}, conductivity: 20.6 ± 8.6 mS cm^{-1}, and TDS: 13.1 ± 5.2 mg L^{-1}. In the AMPs, values were pH: 5.6 ± 0.2, temperature: 27.2 ± 0.7 °C, DO: 3.6 ± 1.7 mg L^{-1}, conductivity: 19.8 ± 9.8 mS cm^{-1}, and TDS: 13.2 ± 5.1 mg L^{-1}. The pH and DO in the AMPs are lower than in the Atrato River, which could directly influence the presence and development of more aquatic biota in the Atrato River (Null et al., 2017; Post et al., 2018).

Labile THg concentrations measured by DGT-P are show in Fig. 3. Values in the Atrato River were between 54.7 ± 24.1 and 145.0 ± 27.1 ng L^{-1}, while in the AMPs the values were higher, from 112.2 ± 41.0 to 217.4 ± 3.8 ng L^{-1}. In average, the labile THg concentrations in AMPs (148.9 ± 43.2 ng L^{-1}) were a 50% higher than in the river water (99.9 ± 37.4 ng L^{-1}); however, the variability was higher in AMP.

The Atrato River and the AMPs represent two different and significant impacted freshwater ecosystems in terms of Hg contamination dynamics derived from ASGM. As can be seen in Fig. 3, P3 was the sampling site with the highest labile Hg concentration in the Atrato River. The values in P1, P3, P4 and P5 did not show significant differences between them (p > 0.05), however, a difference was observed between P2 and P1 (p < 0.05). We hypothesize that constant flow from the main river upstream gold mining sites increases Hg loads in P3. Our hypothesis agrees with the behaviour also observed in P4 and P5. Both sampling sites are located in the confluence of the Atrato River with Munguidó (P4) and Neguá (P5) rivers (Fig. 1), where gold mining activities are relatively close to deployed DGTs. In contrast with P2, where DGTs were deployed 1 km upstream minor ASGM operations (e.g. use of machinery such as dredgers and dragons), and about 8 km downstream large gold mining activities that take place in the Quito River. Likewise, P3 is also the sampling site with the higher DGT values for other metals
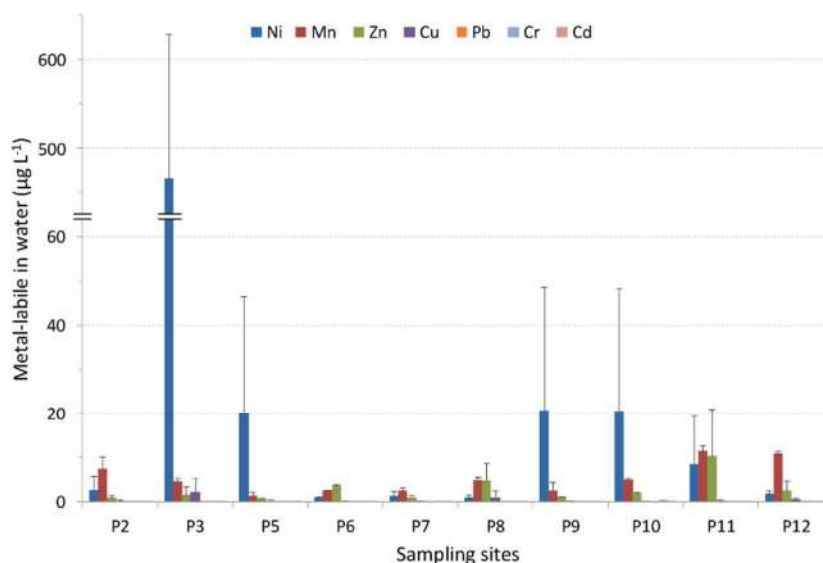
4

Fig. 4. Labile-metal concentrations in Atrato River (P2 to P5) and AMPs (P6 to P12) measured by DGT-Chelex devices.

as can be observed in Fig. 4. Concentrations of labile metals in P3 are about 2-times, 10-times and between 25 and 150-times higher than in P2 and P5, for Zn, Cu and Ni, respectively. Unfortunately, DGT-Chelex devices in P4 were lost, and no data can be shown.

Besides being the first data of labile Hg obtained by the DGT technique in the region, results displays certain human risk since the highest levels found in P3 could be related with higher Hg levels in fish caught and consumed by inhabitants of this urban community. In fact, in a previous study carried out in the Atrato River (Palacios-Torres et al., 2018), the median THg concentration in hair from inhabitants of Quibdó was 1.26 $\mu g\ g^{-1}$, exceeded the USEPA threshold dose of 1 $\mu g\ g^{-1}$ (USEPA, 2001).

Labile THg concentrations in AMPs were statistically significantly higher ($p > 0.05$) than in the Atrato River (Fig. 3). The AMPs were formed in the past as water reservoirs or sinks for drains of organic and inorganic material that flow from mining areas, including Hg derived from the gold amalgamation process (Gutiérrez-Mosquera et al., 2020, 2021). Due to a lack of environmental liability policy, most of these ponds were abandoned and turned into wetlands that people use for different activities (i.e. swimming, fishing, collecting water for domestic activities). The AMPs chosen for this study have an estimated time of abandonment between 6 and 15 years (since 1997). Statistical analyses show that there are no significant differences ($p > 0.05$) for labile Hg concentration measured for the ponds when years of abandonment were matched, which suggests that the labile Hg content is not related to time that former mercury remains in the pond. Studies on the distribution of chemical forms of Hg in sediments from AMPs (Gutiérrez-Mosquera et al., 2020) suggested high organic matter from erosion of the surrounding soil, and the low levels of dissolved oxygen provide favourable conditions that promotes Hg methylation, particularly at the water-sediment interface, which would imply a possible impact on the health of the local population by fish consumption (Salazar-Camacho et al., 2017, 2021; Palacios-Torres et al., 2018; Gutiérrez-Mosquera et al., 2020).

Recent studies carried out in 36 AMPs (Gutiérrez-Mosquera et al., 2020, 2021) of the same gold mining district, showed average concentrations for THg in fish muscles (250 ng/g ww), sediments (210 ng/g ww) and three different macrophytes (i.e. *Eliocharis elegans, Becquerelia cymosa,* and *Tripogandra serrulate*) (range 50–250 ng/g ww). In a couple of AMPs common with our study, e.g. P8 and P9, Hg concentrations in fish (P8: 220 ng/g ww and P9: 1430 ng/g ww), sediments (P8: 156 ng/g

Table 2
Labile THg concentrations (ng L^{-1}) obtained by the DGT technique in different studies in freshwaters.

Freshwater environment	Hg-labile	Binding layer	Source
Svitava river, Czech Republic	11.6 ± 0.9	SH-Thiol[a] resin	Dočekalová and Diviš (2005)
Vrije Universiteit Brussel (VUB) campus pond, Belgium	17.6 ± 3.6	SH-PMO[b] resin	Gao et al. (2011)
Gállego river, Spain	9–36	SH-Thiol[a] resin	Fernández-Gómez et al. (2012b)
Ribeirão Claro, Brazil	0.62–1.80	P81	Colaço et al. (2014)
Negro river, Brazil	13	Whatman	
Tien river, Vietnam	4.75 ± 2.61	3MFS[c] resin	Hong et al. (2014)
Nanfei river, China	71 ± 0.6	SH-CNP[d] suspension	Wu et al. (2017)
Ebro river basin, Spain	0.0–19	3MFS[c] resin	Sierra et al. (2017)
Tully river, Australia	106–170	SH-Thiol[a] resin	Turull et al. (2018)
Costa Concordia wreck, Italy	1.0–2.1	SH-Thiol[a] resin	Schintu et al. (2018)
Zenne river, Belgium	4.7–5.9	3MFS[c] resin	Bratkič et al. (2019)
Gulf of Trieste, Northern Adriatic	1.7		
Deûle river, France	3.22–16.4	3MFS[c] resin	Bretier et al. (2020)
Gier river, France	0.37–3.99		
Andong lake, South Korea	0.8–1.0	3MFS[c] resin	Noh et al. (2020)
Baihua reservoir, China	3.19 ± 0.06	TM-MDH[e] resin	Yao et al. (2020)
Atrato river, Colombia	54.7–145	3MFS[c] resin	This study
AMPs in Chocó, Colombia	112–217		

[a] SH-Thiol: Spheron thiol.

[b] SH-PMO: 3-mercaptopropyl functionalized ethenylene bridged periodic mesoporous organosilica.

[c] 3MFS: 3-mercaptopropyl functionalized silica gel.

[d] SH-CNP: Thiol-modified carbon nanoparticle.

[e] TM-MDH: Thiol-modified metal double hydroxide.

dw and P9: 135 ng/g dw), and macrophytes (P8: 540 ng/g dw and P9: 320 ng/g dw) showed a similar trend with the labile Hg-DGT concentrations in water (P8: 0.140 ng/g and P9: 0.113 ng/g), which could be suggest than higher values of labile Hg are more bioavailable to biota. Furthermore, the highest bioavailable Hg found in AMPs could give a

5

Table 3

Labile metal concentrations (µg L^{-1}) obtained by the DGT technique in different freshwater studies.

| Freshwater environment	Metal-labile (µg L^{-1})							Source
	Ni	Mn	Zn	Cu	Pb	Cr	Cd	
Headwater streams, England	0.12–96.90	0.0–0.5	0.7–9079.3	0.04–11.23	0.0–10.83	–	0.003–17.455	Warnken et al. (2009)
Orge river, France	0.17–0.46	12.47–26.36	0.88–2.82	0.06–0.42	–	0.04–0.09	0.001–0.002	Bourgeault et al. (2010)
Amazon river, Brazil	2.6 ± 0.6	–	13.7 ± 0.2	2.3 ± 1.0	–	–	0.021	Yabuki et al. (2014)
Seine river, France	0.19	1.6	0.68	0.15	0.034	0.058	0.002	Uher et al. (2017)
Estuary Ria of Huelva, Spain	–	4.8–61.0	–	4.6–23.0	0.3–8.0	–	0.1–2.3	Cánovas et al. (2020)
Atrato river, Colombia	2.6–493.1	1.33–7.44	0.67–1.52	0.204–2.233	0.003–0.159	0.028–0.075	0.003–0.026	This study
AMPs in Chocó, Colombia	0.9–20.6	2.41–11.48	0.99–10.29	0.030–1.040	0.0–0.125	0.016–0.382	0.001–0.004	
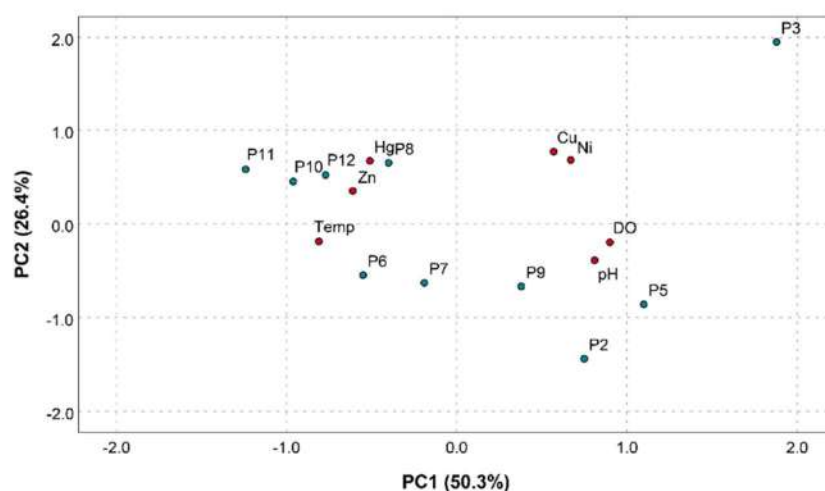
Fig. 5. PCA biplot showing the loading of metals and physicochemical parameters (red circles) and the scores of each sampling station (green circles) in the Atrato River (P1–P5) and AMPs (P6–P12). (For interpretation of the references to color in this figure legend, the reader is referred to the Web version of this article.)

better explanation to the results obtained by Salazar-Camacho et al. (2017) in THg concentrations in hair from the inhabitants of Tadó and Unión Panamericana municipalities, who use these reservoirs as a water and fishes source. In fact, the average concentration in the whole group was 1.16 µg g^{-1} and nearly 60% of subjects having THg levels that exceeded the USEPA reference dose of 1.0 µg g^{-1}.

The labile Hg concentrations of the Atrato River were notably higher than values in other areas worldwide (Table 2), because Chocó is the second Colombian department with high ASGM activities, and hence, representing a high emission of Hg to the environment (MME, 2015; Veiga and Marshall, 2019). Values are comparable with those detected in the Australian Tully River after a flood event, receiving runoff from soil polluted by an organomercury based fungicide. Compared with other rivers worldwide, concentrations in the Atrato River were one order of magnitude higher than in the Sinú River basin, whereas values found in AMPs are not comparable since this is the first study performed in mining ponds. On the other hand, the labile concentrations for the others metals in our study were similar to those found in other studies in freshwater, with the exception of Ni, that shows a high labile fraction in the Atrato River (Table 3). Recently, high Ni concentrations were found in sediments (Palacios-Torres et al., 2020), mainly associated with extensive mining activities and deforestation in the Atrato River basin.

The relationship between physicochemical parameters and metals were further analyzed by PCA, as shown in the biplot (Fig. 5). Two principal components explained 76.7% of data variation. The biplot indicates a strong correlation between Ni and Cu, indicating that they were derived from the same anthropogenic sources (i.e. the use of excavation dredges in the river bed). Hg have a strong correlation with the sampling sites P8, P10, P11 and P12, which were the AMPs with the highest concentration of labile Hg. The temperature, pH, DO,

conductivity and TDS could not be significantly affecting (p > 0.05) the uptake of the labile Hg and other metals by DGT devices, with the exception of Cr, which shows a strong correlation with conductivity and TDS (Table S1). However, the amounts of labile Cr found in the Atrato River and AMPs were minimal and do not represent an hazard for human health. Finally, Zn may not be associated with a specific anthropogenic source and can be attributed to residues from other activities in the area.

4. Conclusions

In this study, the labile Hg concentration in waters of the Atrato River and abandoned mining ponds (AMPs) impacted by artisanal and small scale gold mining was assessed using in house manufactured DGT. Other types of DGT were used to assess the concentrations of several labile metals in waters such as Pb, Cu, Zn, Mn, Cd, Ni and Cr. The impact of mining in AMPs has been evaluated for the first time by DGT. In the river, labile Hg-DGT samples show higher Hg levels in sampling sites (e. g. P3 and P4) close to downstream mining operations in comparison with sampling sites that are at least 1 km downstream far from ASGM activities (e.g. P2). Nevertheless, labile Ni, Cu and Zn concentrations were found in higher amounts than for the rest of metals.

In average, the labile THg concentrations in AMPs were a 50% higher than in the river water; however, the variability of the values was higher in each AMP. In sum, metal concentrations in the Atrato River are related with their downstream proximity to gold mining activities, being higher in devices deployed close to ASGM sites. Therefore, our results on bioavailability match with other studies that showed that Hg accumulated in fish is higher close to ASGM. Finally, it seems that bioavailability is not associated with the abandonment period, because no significant differences were found in labile Hg at the different ponds.

Declaration of competing interest

The authors declare that they have no known competing financial interests or personal relationships that could have appeared to influence the work reported in this paper.

Acknowledgments

Appendix A. Supplementary data

Supplementary data to this article can be found online at https://doi.org/10.1016/j.envres.2021.112633.

References

Amyot, M., Auclair, J.C., Poissant, L., 2001. In situ high temporal resolution analysis of elemental mercury in natural waters. Anal. Chim. Acta 447, 153–159. https://doi.org/10.1016/S0003-2670(01)01287-9.

Bade, R., Oh, S., Shin, W.S., 2012. Diffusive gradients in thin films (DGT) for the prediction of bioavailability of heavy metals in contaminated soils to earthworm (Eisenia foetida) and oral bioavailable concentrations. Sci. Total Environ. 416, 127–136. https://doi.org/10.1016/j.scitotenv.2011.11.007.

Bernalte, E., Arévalo, S., Pérez-Taborda, J., Wenk, J., Estrela, P., Avila, A., Di Lorenzo, M., 2020. Rapid and on-site simultaneous electrochemical detection of copper, lead and mercury in the Amazon river. Sensor. Actuator. B Chem. 307, 127620 https://doi.org/10.1016/J.SNB.2019.127620.

Bourgeault, A., Gourlay-France, C., Vincent-Hubert, F., Palais, F., Geffard, A., Biagianti-Risbourg, S., Pain-Devin, S., Cemagref, M.-H.T.-V., 2010. Lessons from a transplantation of zebra mussels into a small urban river: an integrated ecotoxicological assessment. Env. Toxicology 25, 468–478. https://doi.org/10.1002/tox.

Bratkič, A., Klun, K., Gao, Y., 2019. Mercury speciation in various aquatic systems using passive sampling technique of diffusive gradients in thin-film. Sci. Total Environ. 663, 297–306. https://doi.org/10.1016/j.scitotenv.2019.01.241.

Bretier, M., Dabrin, A., Billon, G., Mathon, B., Miège, C., Coquery, M., 2020. To what extent can the biogeochemical cycling of mercury modulate the measurement of dissolved mercury in surface freshwaters by passive sampling? Chemosphere 248. https://doi.org/10.1016/j.chemosphere.2020.126006.

Cánovas, C.R., Basallote, M.D., Borrego, P., Millán-Becerro, R., Pérez-López, R., 2020. Metal partitioning and speciation in a mining-impacted estuary by traditional and passive sampling methods. Sci. Total Environ. 722, 137905 https://doi.org/10.1016/j.scitotenv.2020.137905.

Clarisse, O., Hintelmann, H., 2006. Measurements of dissolved methylmercury in natural waters using diffusive gradients in thin film (DGT). J. Environ. Monit. 8, 1242–1247. https://doi.org/10.1039/b614560d.

Colaço, C.D., Yabuki, L.N., Rolisola, A.M., Menegário, A.A., De Almeida, E., Suárez, C., Gao, Y., Corns, W.T., Do Nascimento Filho, V.F., 2014. Determination of mercury in river water by diffusive gradients in thin films using P81 membrane as binding layer. Talanta 129, 417–421. https://doi.org/10.1016/j.talanta.2014.05.025.

Davison, W., Zhang, H., 1994. In situ speciation measurements of trace components in natural waters using thin-film gels. Nature 367, 546–548.

Ding, Y., Wang, S., Li, J., Chen, L., 2016. Nanomaterial-based optical sensors for mercury ions. TrAC Trends Anal. Chem. (Reference Ed.) 82, 175–190. https://doi.org/10.1016/J.TRAC.2016.05.015.

Divis, P., Leermakers, M., Dočekalová, H., Gao, Y., 2005. Mercury depth profiles in river and marine sediments measured by the diffusive gradients in thin films technique with two different specific resins. Anal. Bioanal. Chem. 382, 1715–1719. https://doi.org/10.1007/s00216-005-3360-8.

Dočekalová, H., Diviš, P., 2005. Application of diffusive gradient in thin films technique (DGT) to measurement of mercury in aquatic systems. Talanta 65, 1174–1178. https://doi.org/10.1016/j.talanta.2004.08.054.

Fernández-Gómez, C., Bayona, J.M., Díez, S., 2014. Comparison of different types of diffusive gradient in thin film samplers for measurement of dissolved methylmercury in freshwaters. Talanta 129, 486–490. https://doi.org/10.1016/j.talanta.2014.06.025.

Fernández-Gómez, C., Dimock, B., Hintelmann, H., Díez, S., 2011. Development of the DGT technique for Hg measurement in water: comparison of three different types of samplers in laboratory assays. Chemosphere 85, 1452–1457. https://doi.org/10.1016/j.chemosphere.2011.07.080.

Fernández-Gómez, C., Hintelmann, H., Díez, S., 2012a. Passive sampling for inorganic contaminants in water. In: Comprehensive Sampling and Sample Preparation, vol. 1, pp. 281–296. https://doi.org/10.1016/B978-0-12-381373-2.10015-8.

Fernández-Gómez, C., Bayona, J.M., Díez, S., 2012b. Laboratory and field evaluation of diffusive gradient in thin films (DGT) for monitoring levels of dissolved mercury in natural river water. Int. J. Environ. Anal. Chem. 92, 1689–1698. https://doi.org/10.1080/03067319.2011.581369.

Gao, Y., De Canck, E., Leermakers, M., Baeyens, W., Van Der Voort, P., 2011. Synthesized mercaptopropyl nanoporous resins in DGT probes for determining dissolved mercury concentrations. Talanta 87, 262–267. https://doi.org/10.1016/j.talanta.2011.10.012.

Gao, Y., Zhou, C., Gaulier, C., Bratkic, A., Galceran, J., Puy, J., Zhang, H., Leermakers, M., Baeyens, W., 2019. Labile trace metal concentration measurements in marine environments: from coastal to open ocean areas. TrAC Trends Anal. Chem. (Reference Ed.) 116, 92–101. https://doi.org/10.1016/j.trac.2019.04.027.

Guan, D.X., 2019. Diffusive gradients in thin-films (DGT): an effective and simple tool for assessing contaminant bioavailability in waters, soils and sediments. In: Encyclopedia of Environmental Health, second ed. Elsevier. https://doi.org/10.1016/B978-0-12-409548-9.11403-4.

Gutiérrez-Mosquera, H., Marrugo-Negrete, J., Díez, S., Morales-Mira, G., Montoya-Jaramillo, L.J., Jonathan, M.P., 2021. Mercury distribution in different environmental matrices in aquatic systems of abandoned gold mines, Western Colombia: focus on human health. J. Hazard Mater. 404 https://doi.org/10.1016/j.jhazmat.2020.124080.

Gutiérrez-Mosquera, H., Marrugo-Negrete, J., Díez, S., Morales-Mira, G., Montoya-Jaramillo, L.J., Jonathan, M.P., 2020. Distribution of chemical forms of mercury in sediments from abandoned ponds created during former gold mining operations in Colombia. Chemosphere 258. https://doi.org/10.1016/j.chemosphere.2020.127319.

Hong, Y., Dan, N.P., Kim, E., Choi, H.J., Han, S., 2014. Application of diffusive gel-type probes for assessing redox zonation and mercury methylation in the Mekong Delta sediment. Environ. Sci. Process. Impacts 16, 1799–1808. https://doi.org/10.1039/c3em00728f.

Hossain, S.M.Z., Brennan, J.D., 2011. β-Galactosidase-based colorimetric paper sensor for determination of heavy metals. Anal. Chem. 83, 8772–8778. https://doi.org/10.1021/ac202290d.

Huynh, T., Harris, H.H., Zhang, H., Noller, B.N., 2015. Measurement of labile arsenic speciation in water and soil using diffusive gradients in thin films (DGT) and X-ray absorption near edge spectroscopy (XANES). Environ. Chem. 12, 102–111. https://doi.org/10.1071/EN14047.

Lin, J., Sun, Q., Ding, S., Wang, D., Wang, Y., Tsang, D.C.W., 2017. First observation of labile arsenic stratification in aluminum sulfate-amended sediments using high resolution Zr-oxide DGT. Sci. Total Environ. 609, 304–310. https://doi.org/10.1016/j.scitotenv.2017.07.165.

Liu, J.J., Diao, Z.H., Xu, X.R., Xie, Q., Ni, Z.X., 2019. In situ arsenic speciation and the release kinetics in coastal sediments: a case study in Daya Bay, South China Sea. Sci. Total Environ. 2221–2230. https://doi.org/10.1016/j.scitotenv.2018.09.389.

Marrugo-Madrid, S., Turull, M., Zhang, H., Díez, S., 2021. Diffusive gradients in thin films for the measurement of labile metal species in water and soils: a review. Environ. Chem. Lett. 3761–3788. https://doi.org/10.1007/s10311-021-01246-3.

Medina-Rivas, M.A., Norris, E.T., Rishishwar, L., Conley, A.B., Medrano-Trochez, C., Valderrama-Aguirre, A., Vannberg, F.O., Mariño-Ramiírez, L., Jordan, I.K., 2016. Chocó, Colómbia: a hotspot of human biodiversity. Rev Biodivers Neotrop 6, 45–54. https://doi.org/10.18636/bioneotropical.v6i1.341.Choc.

MME, 2014. Estudio de la cadena del mercurio en Colombia con énfasis en la actividad minera de oro. UPME. Tomo 3 [WWW Document]. URL. http://www.upme.gov.co/SeccionMineria_sp/cadena_de_mercurio/Cadena_Mercurio_Tomo_III.pdf.

MME, 2015. Incidencia real de la minería del carbón, del oro y del uso del mercurio en la calidad ambiental con énfasis especial en el recurso hídrico-diseño de herramientas para la planeación [WWW Document]. URL. https://www1.upme.gov.co/simco/Cifras-Sectoriales/EstudiosPublicaciones/Incidencia_real_de_la_mineria_sobre_el_recurso_hidrico.pdf.

MME, 2016. Identificación y caracterización de las unidades básicas de beneficio aurífero en 261 municipios. UPME [WWW Document]. URL. http://www1.upme.gov.co/simco/Cifras-Sectoriales/EstudiosPublicaciones/Identificacion_Caracterizacion_Unidades_Basicas.pdf.

Noh, S., Kim, Y., hee, Kim, H., Seok, K. seol, Park, M., Bailon, M.X., Hong, Y., 2020. The performance of diffusive gradient in thin film probes for the long-term monitoring of trace level total mercury in water. Environ. Monit. Assess. 192 https://doi.org/10.1007/s10661-019-7966-2.

Null, S.E., Mouzon, N.R., Elmore, L.R., 2017. Dissolved oxygen, stream temperature, and fish habitat response to environmental water purchases. J. Environ. Manag. 197, 559–570. https://doi.org/10.1016/J.JENVMAN.2017.04.016.

Palacios-Torres, Y., Caballero-Gallardo, K., Olivero-Verbel, J., 2018. Mercury pollution by gold mining in a global biodiversity hotspot, the Choco biogeographic region, Colombia. Chemosphere 193, 421–430. https://doi.org/10.1016/j.chemosphere.2017.10.160.

Palacios-Torres, Y., de la Rosa, J.D., Olivero-Verbel, J., 2020. Trace elements in sediments and fish from Atrato River: an ecosystem with legal rights impacted by gold mining at the Colombian Pacific. Environ. Pollut. 256, 113290 https://doi.org/10.1016/j.envpol.2019.113290.

Pérez-Escobar, O.A., Lucas, E., Jaramillo, C., Monro, A., Morris, S.K., Bogarín, D., Greer, D., Dodsworth, S., Aguilar-Cano, J., Sanchez Meseguer, A., Antonelli, A., 2019. The origin and diversification of the hyperdiverse flora in the Chocó biogeographic region. Front. Plant Sci. 10, 1–9. https://doi.org/10.3389/fpls.2019.01328.

Post, C.J., Cope, M.P., Gerard, P.D., Masto, N.M., Vine, J.R., Stiglitz, R.Y., Hallstrom, J. O., Newman, J.C., Mikhailova, E.A., 2018. Monitoring spatial and temporal variation of dissolved oxygen and water temperature in the Savannah River using a sensor network, 2018 1905 Environ. Monit. Assess. 190, 1–14. https://doi.org/10.1007/S10661-018-6646-Y.

Poveda, I., Rojas, C., Rudas, A., Rangel, J.O., 2004. El Chocó biogeográfico: ambiente físico. In: Colombia Diversidad Biótica IV, El Chocó Biogeográfico/Costa Pacífica. Universidad Nacional de Colombia, Sede Bogotá, Bogotá, pp. 1–21.

Salazar-Camacho, C., Salas-Moreno, M., Marrugo-Madrid, S., Marrugo-Negrete, J., Díez, S., 2017. Dietary human exposure to mercury in two artisanal small-scale gold mining communities of northwestern Colombia. Environ. Int. https://doi.org/10.1016/j.envint.2017.06.011.

Salazar-Camacho, C., Salas-Moreno, M., Paternina-Uribe, R., Marrugo-Negrete, J., Díez, S., 2021. Mercury species in fish from a tropical river highly impacted by gold mining at the Colombian Pacific region. Chemosphere 264, 128478. https://doi.org/10.1016/j.chemosphere.2020.128478.

Schintu, M., Marrucci, A., Marras, B., Atzori, M., Pellegrini, D., 2018. Passive sampling monitoring of PAHs and trace metals in seawater during the salvaging of the Costa Concordia wreck (Parbuckling Project). Mar. Pollut. Bull. 135, 819–827. https://doi.org/10.1016/j.marpolbul.2018.08.011.

Sierra, J., Roig, N., Giménez Papiol, G., Pérez-Gallego, E., Schuhmacher, M., 2017. Prediction of the bioavailability of potentially toxic elements in freshwaters. Comparison between speciation models and passive samplers. Sci. Total Environ. 605–606, 211–218. https://doi.org/10.1016/j.scitotenv.2017.06.136.

Sun, H., Gao, B., Gao, L., Xu, D., Sun, K., 2019. Using diffusive gradients in thin films (DGT) and DGT-induced fluxes in sediments model to assess the dynamic release of copper in sediment cores from the Three Gorges Reservoir, China. Sci. Total Environ. 672, 192–200. https://doi.org/10.1016/j.scitotenv.2019.03.400.

Turull, M., Elias, G., Fontàs, C., Díez, S., 2017. Exploring new DGT samplers containing a polymer inclusion membrane for mercury monitoring. Environ. Sci. Pollut. Res. 24, 10919–10928. https://doi.org/10.1007/s11356-016-6813-z.

Turull, M., Fontàs, C., Díez, S., 2019a. Diffusive gradient in thin films with open and restricted gels for predicting mercury uptake by plants. Environ. Chem. Lett. https://doi.org/10.1007/s10311-019-00864-2.

Turull, M., Fontàs, C., Díez, S., 2019b. Conventional and novel techniques for the determination of Hg uptake by lettuce in amended agricultural peri-urban soils. Sci. Total Environ. 668, 40–46. https://doi.org/10.1016/j.scitotenv.2019.02.244.

Turull, M., Komarova, T., Noller, B., Fontàs, C., Díez, S., 2018. Evaluation of mercury in a freshwater environment impacted by an organomercury fungicide using diffusive gradient in thin films. Sci. Total Environ. 621, 1475–1484. https://doi.org/10.1016/j.scitotenv.2017.10.081.

Uher, E., Compère, C., Combe, M., Mazeas, F., Gourlay-Francé, C., 2017. In situ measurement with diffusive gradients in thin films: effect of biofouling in freshwater. Environ. Sci. Pollut. Res. 24, 13797–13807. https://doi.org/10.1007/s11356-017-8972-y.

UNEP, 2019. Minamata Convention on Mercury 1–67.

USEPA, 2001. Water Quality Criterion for the Protection of Human Health : Methylmercury Final. US Environ. Prot. Agency, Washington, DC.

USEPA, 1998. Mercury in Solids and Solutions by Thermal Decomposition. Amalgamation and Atomic Absorption Spectrophotometry. Method 7473).

Valero, A., Umbría-Salinas, K., Wallner-Kersanach, M., Andrade, C.F. de, Yabe, M.J.S., Contreira-Pereira, L., Wasserman, J.C., Kuroshima, K.N., Zhang, H., 2020. Potential availability of trace metals in sediments in southeastern and southern Brazilian shipyard areas using the DGT technique and chemical extraction methods. Sci. Total Environ. 710, 136216 https://doi.org/10.1016/j.scitotenv.2019.136216.

Veiga, M.M., Marshall, B.G., 2019. The Colombian artisanal mining sector: formalization is a heavy burden. Extr. Ind. Soc. 6, 223–228. https://doi.org/10.1016/j.exis.2018.11.001.

Wang, C., Yao, Y., Wang, P., Hou, J., Qian, J., Yuan, Y., Fan, X., 2016. In situ high-resolution evaluation of labile arsenic and mercury in sediment of a large shallow lake. Sci. Total Environ. 541, 83–91. https://doi.org/10.1016/j.scitotenv.2015.09.037.

Warnken, K.W., Lawlor, A.J., Lofts, S., Tipping, E., Davison, W., Zhang, H., 2009. In situ speciation measurements of trace metals in headwater streams. Environ. Sci. Technol. 43, 7230–7236. https://doi.org/10.1021/es900112w.

Wu, T., Wang, G., Zhang, Y., Kong, M., Zhao, H., 2017. Determination of mercury in aquatic systems by DGT device using thiol-modified carbon nanoparticle suspension as the liquid binding phase. New J. Chem. 41, 10305–10311. https://doi.org/10.1039/c7nj02007d.

Yabuki, L.N.M., Colaço, C.D., Menegário, A.A., Domingos, R.N., Kiang, C.H., Pascoaloto, D., 2014. Evaluation of diffusive gradients in thin films technique (DGT) for measuring Al, Cd, Co, Cu, Mn, Ni, and Zn in Amazonian rivers. Environ. Monit. Assess. 186, 961–969. https://doi.org/10.1007/s10661-013-3430-x.

Yao, H., Zhao, Y., Lin, C.J., Yi, F., Liang, X., Feng, X., 2020. Development of a novel composite resin for dissolved divalent mercury measurement using diffusive gradients in thin films. Chemosphere 251, 126231. https://doi.org/10.1016/j.chemosphere.2020.126231.

Zarrouk, S., Bermond, A., Kolsi Benzina, N., Sappin-Didier, V., Denaix, L., 2014. Diffusive gradient in thin-film (DGT) models Cd and Pb uptake by plants growing on soils amended with sewage sludge and urban compost. Environ. Chem. Lett. 12, 191–199. https://doi.org/10.1007/s10311-013-0431-5.

Zhang, H., Davison, W., 2015. Use of diffusive gradients in thin-films for studies of chemical speciation and bioavailability. Environ. Chem. 12, 85–101. https://doi.org/10.1071/EN14105.

Zhang, W., Yang, J., Li, Z., Zhou, D., Dang, F., 2017. Assessment of the availability of as and Pb in soils after in situ stabilization. Environ. Sci. Pollut. Res. 24, 23153–23160. https://doi.org/10.1007/s11356-017-9877-5.

Zhou, S., Yuan, Z., Cheng, Q., Zhang, Z., Yang, J., 2018. Rapid in situ determination of heavy metal concentrations in polluted water via portable XRF: using Cu and Pb as example. Environ. Pollut. 243, 1325–1333. https://doi.org/10.1016/J.ENVPOL.2018.09.087.

Publicación 3: *Supplementary information*

Assessment of dissolved mercury by diffusive gradients in thin films devices in abandoned ponds impacted by small scale gold mining

Marrugo-Madrid, S., Salas-Moreno, M., Gutiérrez-Mosquera, H., Salazar-Camacho, C., Marrugo-Negrete, J., Díez, S. Environmental Research, 208 (2022): 112633.

Figure S1. Pictures of motorcycle cars and motorcycles to enter to abandoned gold mines located at remote sites that are difficult to reach with 4-wheel vehicles

Figure S2. Sampling sites in Atrato River and abandoned ponds. Pictures of DGTs before and after deployment at river and ponds.

Table S1. Pearson correlation coefficients.

	pH	Temperature	DO	Conductivity	TDS	Hg	Ni	Mn	Zn	Cu	Pb	Cr	Cd
pH	1												
Temperature	-0.866**	1											
DO	0.598*	-0.459	1										
Conductivity	0.098	-0.084	-0.435	1									
TDS	0.067	-0.033	-0.459	0.982**	1								
Hg	-0.572	0.319	-0.700*	0.362	0.374	1							
Ni	0.302	-0.569	0.475	-0.220	-0.281	0.092	1						
Mn	-0.229	0.271	-0.680*	0.336	0.293	0.369	-0.085	1					
Zn	-0.598	0.319	-0.599	0.138	0.165	0.219	-0.167	0.599	1				
Cu	0.118	-0.532	0.400	-0.319	-0.423	0.132	0.886**	0.043	-0.041	1			
Pb	-0.161	-0.298	0.112	-0.248	-0.355	0.339	0.646*	0.291	0.117	0.904**	1		
Cr	-0.220	0.165	-0.626	0.727*	0.761*	0.843**	-0.048	0.336	-0.094	-0.109	0.037	1	
Cd	0.297	-0.549	0.509	-0.344	-0.401	-0.015	0.980**	-0.064	-0.071	0.910**	0.674*	-0.186	1

**The correlation is significant at the 0.01 level (bilateral).
*The correlation is significant at the 0.05 level (bilateral).

3.4. Discusión

Es esencial reconocer que el notable avance industrial y tecnológico de nuestra civilización ha estado estrechamente ligado al descubrimiento y explotación de recursos minerales, lo que confiere a la minería un papel indispensable en el sector industrial. Sin embargo, la problemática asociada a la MAPE, puede ser considerablemente más compleja de lo que se percibe inicialmente. Además de los impactos ambientales que esta actividad puede generar, también implica una serie de dinámicas sociales y económicas de alta complejidad, lo que dificulta en gran medida la implementación de soluciones efectivas. Por lo tanto, considero que los estudios ambientales en las áreas afectadas por la MAPE no cuentan con soluciones simples, y resulta fundamental adoptar una visión holística que aborde la realidad vivida por las comunidades afectadas.

Considerando lo anterior, en los artículos que conforman este capítulo se presentan las discusiones detalladas desde una perspectiva analítica y ambiental acerca de los resultados obtenidos sobre la ingesta de alimentos contaminados con Hg, MeHg y As, y sus riesgos, así como de la fracción biodisponible de Hg, Pb, Cu, Zn, Cd, Ni, Mn y Cr disueltos en algunos sistemas acuáticos (ríos y AMPs) cercanos a zonas de minería y que ofrecen diversos servicios ecosistémicos a las comunidades de la cuenca del río Atrato, en el departamento de Chocó (Colombia). Por tanto, en esta sección se complementará la discusión científica con un análisis del contexto

sociopolítico que rodea a la región, identificando los desafíos para la protección de la salud y el ecosistema.

3.4.1. Enfoque socioeconómico y político

En el caso de Colombia, un país reconocido por su riqueza en recursos minerales y una economía que aún se basa en gran medida en la extracción de dichos recursos, la contribución del sector minero sigue siendo de vital importancia para el país. La minería en Colombia representa aproximadamente un tercio de las exportaciones (de las cuales el 33% corresponden a las exportaciones de oro), generando ingresos anuales cercanos a los US$10,2 billones de manera directa e indirecta por los sectores asociados. No obstante, las cifras oficiales reportan que, mientras el aporte del sector minero al Producto Interno Bruto (PIB) ha decrecido en los últimos 5 años, la tendencia en la producción de oro nacional es ascendente, llegando hasta las 50 t anuales en 2021 según el último reporte del Servicio Geológico de Estados Unidos en 2022, y alcanzando el cuarto puesto dentro de los países productores de oro en América del Sur (SIMCO, 2021; ANM, 2022).

Las cifras mencionadas anteriormente plantean una reflexión acerca del origen y la legalidad del oro en el país. Si bien es cierto que no toda la actividad de la MAPE es ilegal, la gran mayoría de la minería ilegal se encuentra en esta categoría, lo cual representa un importante desafío para la implementación de regulaciones ambientales y la adopción de leyes y

convenios orientados a reducir las emisiones de Hg. En Colombia se encontró que cerca del 87% de las actividades de minería aurífera son ilegales, es decir, que no cuentan con una licencia o título minero, ni están obligadas a cumplir con los requisitos legales y regulaciones ambientales sobre desechos y vertidos establecidas por las autoridades competentes. En este contexto, la cuenca hidrográfica del río Atrato es una de las áreas más afectadas por la MAPE, debido a su intensa actividad de extracción de minerales, particularmente oro y platino. Sin embargo, esta región cuenta con menos del 2% de las licencias mineras otorgadas en el país, lo que sugiere que una gran parte de la producción de oro proviene de actividades de minería ilegal y de mineros informales independientes (Minenergía, 2012; EConcept, 2020).

Esta situación plantea un desafío considerable, ya que la informalidad que caracteriza a las actividades de la MAPE en combinación con la poca presencia del Estado en esta zona, derivan en problemas sociales más profundos que trascienden la problemática ambiental, tales como el lavado de dinero, actividades ilícitas, alteración del orden público y del bienestar social, aparición de grupos armados al margen de la ley, incremento de la prostitución, explotación laboral, trabajo infantil, entre otros (Science for Environment Policy, 2017). A diferencia de lo que se podría suponer dada la abundancia de oro, el departamento de Chocó enfrenta altos índices de pobreza y analfabetismo, particularmente en sus zonas rurales, que son también las más vulnerables y donde la actividad minera ilegal está más presente (DANE, 2014).

Así pues, este panorama refleja la complejidad de los impactos sociales y económicos asociados a la minería ilegal y refuerza la necesidad de abordar de manera integral los desafíos sociales que surgen a raíz de la MAPE. Consciente de la complejidad de este panorama, el gobierno de Colombia ha venido haciendo esfuerzos importantes para el abordaje de estos desafíos mediante la financiación de macroestudios enmarcados y la aprobación de leyes y sentencias que buscan proteger a la población y al medioambiente en situación de vulnerabilidad.

Con la aprobación de la Ley 1658 de 2013 se marcó un punto de partida significativo en la gestión de la problemática. Esta ley tiene como objetivo principal prohibir el uso y la comercialización de Hg en todas las actividades extractivas, principalmente en la minería aurífera, con la visión de eliminar completamente su uso de todas las operaciones mineras para el año 2023. Además, Colombia firmó el Convenio de Minamata sobre el Mercurio en 2013, y posteriormente, se aprobó su implementación en el país a través de la Ley 1892 de 2018, con la posterior ratificación internacional en agosto de 2019.

En el mismo contexto, en 2014 se formuló el Plan Único Nacional de Mercurio (PUNHg), el cual ha sido actualizado en 2018. A partir del PUNHg se desarrolló el Plan de Acción Sectorial Ambiental de Mercurio (PASAHg), y más adelante, la Corte Constitucional colombiana emitió la Sentencia T-622 de 2016, la cual instó a atender de manera urgente la problemática ambiental en la cuenca del río Atrato, respaldada por los derechos fundamentales a la vida, la salud, el agua, la seguridad alimentaria, el medioambiente sano, la

cultura y el territorio de las comunidades que habitan la región (Minambiente, 2023).

Estos esfuerzos realizados por el gobierno colombiano están alineados con los Objetivos de Desarrollo Sostenible (ODS) establecidos por las Naciones Unidas, en especial con los objetivos (1) fin de la pobreza, (3) salud y bienestar, (6) agua limpia y saneamiento, (8) trabajo decente y crecimiento económico, y (15) vida de ecosistemas terrestres. De esta manera, se busca no solo abordar los impactos ambientales y de salud asociados a la MAPE y la contaminación por Hg, sino también contribuir a la consecución de metas más amplias relacionadas con la sostenibilidad, la protección de los derechos humanos y el desarrollo integral (UN, 2023).

3.4.2. Enfoque en la salud pública

La minería aurífera aluvial que se practica en la cuenca del río Atrato es desarrollada a cielo abierto de forma artesanal, forma artesanal, semi tecnificada y tecnificada, de las cuales la última es la que emite mayor cantidad de carga contaminantes y destruye el medioambiente (figura 16). Entre las consecuencias ambientales podemos destacar las afectaciones a la calidad fisicoquímica y ecológica de los cuerpos de agua, debido en gran medida por el aporte de grandes volúmenes de sedimentos, cargas orgánicas, metales pesados, grasas, aceites y combustibles, limitando el uso del recurso agua, entre otros. Desde el punto de vista ecológico, también hay

consecuencias importantes como la pérdida de la cobertura vegetal, reducción del hábitat y de conectividad entre la fauna, la erosión y destrucción de cauces de ríos, y la disminución del caudal debido a la gran demanda de agua que requiere la minería. La falta de regulación y control de la MAPE, especialmente la de carácter ilegal, también dificulta la implementación de estrategias para el manejo adecuado de pasivos ambientales de minería, lo que a su vez resulta en una marcada afectación a la agricultura, la pesca y la salud de la población local.

Figura 16. MAPE aurífera aluvial artesanal y mecanizada desarrolladas a cielo abierto en la cuenca del río Atrato y aplicación de dispositivos DGT para la captación de metales traza derivados de la minería. Fotografías: Banco de imágenes de la Universidad de Córdoba (Colombia) y autoría propia.

Dentro de las grandes cantidades de residuos y contaminantes emitidos a la biosfera debido al uso intensivo de maquinaria pesada en la MAPE, se destacan los metaloides (As) y varios metales (Cd, Cr, Co, Cu, Fe, Hg, Mn, Ni,

Pb y Zn). Por consiguiente, los riesgos para la salud provienen principalmente de la presencia de estos elementos potencialmente tóxicos en las fuentes hídricas de la zona.

Las emisiones de dichos metales se vieron reflejadas en los resultados obtenidos mediante la implementación de los dispositivos DGT a lo largo del río Atrato y en las AMPs. Aunque a través de los dispositivos DGT podemos calcular exclusivamente la fracción lábil de los metales disueltos en el medio acuático y no sus concentraciones totales, es importante recordar que la importancia de determinar estas fracciones está directamente vinculada con su capacidad de ser absorbidos por los organismos y su potencial para causar enfermedades asociadas que se han mencionado en el capítulo de Introducción. Según los resultados, podemos destacar los obtenidos para las fracciones biodisponibles de Hg y Ni, ya que en general estuvieron muy por encima de los reportados en otros estudios que aplicaron la técnica DGT en sitios contaminados.

Respecto al Ni, podríamos considerar alarmantes las concentraciones de Ni lábil encontradas en los puntos cercanos a la ciudad de Quibdó, capital del departamento de Chocó, que estuvieron alrededor de 493 µg L^{-1} (P3) y alrededor de 20 µg L^{-1} aguas abajo (P5). Estas concentraciones las cuales son significativamente mayores a las encontradas habitualmente en sitios afectados por la minería. Las concentraciones de Hg total lábil captadas por los dispositivos DGT-3MFS en el río Atrato estuvieron entre 54,7 y 145 ng L^{-1}, mientras que en las AMPs los valores fueron superiores entre 112,2 y 217,4

ng L^{-1}. Este resultado era de esperarse, ya que se trata de dos ecosistemas acuáticos con dinámicas significativamente diferentes. Aunque ambos sistemas acuáticos están afectados por la MAPE, el río Atrato se distingue por tener uno de los cursos fluviales más caudalosos del país y sus características fisicoquímicas podrían ser más variables a lo largo de su curso, mientras que las AMPs son consideradas pasivos ambientales de minería lo cual ha permitido que durante varios años se produzca la deposición del Hg usado anteriormente en sus sedimentos y los suelos adyacentes.

Debido a que algunas de estas pozas ofrecen servicios ecosistémicos a las comunidades locales y se encuentran en proximidad a áreas de cultivo, es posible que las altas concentraciones de Hg total lábil encontradas sean las responsables de que los valores del cociente de riesgo (HQ) del Hg estén por encima del nivel de seguridad (HQ < 1) en niños (CHD) y mujeres en edad fértil (WCBA) que viven en la parte alta de la cuenca del río Atrato. Asimismo, la remoción del suelo durante las intensas actividades de excavación podría ser la causa de la movilización del As hacia estos cuerpos de agua, que son usados posteriormente para el riego de cultivos. Esto se ve reflejado esto en los resultados obtenidos de HQ > 1 para el As y un riesgo carcinogénico (CR) alto para la mayoría de la población en dicha región (intervalo de 1,2×10^{-4} a 7,7×10^{-4}) como consecuencia de la ingesta frecuente de frutas. Entre ellas, destacan las distintas variedades de plátanos, que contienen altas concentraciones del metaloide y que son alimentos base de la dieta de la región (Berkowitz et. al., 2008).

Además de los estudios analizados previamente en los artículos de este capítulo, se han llevado a cabo recientemente otro estudio en la zona que también revelan el riesgo para la salud humana debido al consumo de pescado contaminado con Hg, As, Pb y Cd en la cuenca del río Atrato (Salazar-Camacho et al. 2022). Dicha evaluación del riesgo para la salud se realizó en 13 municipios de la zona y 47 especies de pescados. Similar a los resultados presentados en este capítulo, los resultados también sugirieron que la población podría experimentar efectos adversos para la salud no cancerígenos a través del consumo de pescado, especialmente de Hg y As. Los valores de EDI y el THQ individual seguían el orden: Hg > As > Pb ≈ Cd. En cuanto al CR por consumo de pescado, también fue considerado elevado ya que una gran parte de las especies más consumidas presentaron valores entre $1,074\times10^{-4}$ y $9,675\times10^{-3}$, que superaron en aproximadamente dos órdenes de magnitud los valores de referencia (1×10^{-6} a 1×10^{-4}). Las concentraciones más altas de MeHg se midieron en especies de peces carnívoros, particularmente en *H. malabaricus*, *A. pardalis*, *P. schultzi*, *R. quelen* y *C. kraussii*, demostrando que existe un riesgo significativo para la población por el consumo de estas especies.

Otros estudios desarrollados en la zona han evidenciado la bioacumulación de Hg y otros metales en la población. Se destaca el estudio de Gutiérrez-Mosquera et al. (2018), en el cual se analizaron las concentraciones de Hg total en matrices biológicas (cabello, sangre y orina) de habitantes de un distrito minero de la zona del alto Atrato. Al comparar los resultados entre

hombres y mujeres, las concentraciones medias de Hg total fueron: 16 y 9 µg g^{-1} en cabello, 24 y 6 µg L^{-1} en sangre, y 11 y 9 µg L^{-1} en orina, respectivamente. Estos valores alarmantes reflejan períodos prolongados de exposición al Hg, generando preocupación en cuanto a la salud pública.

Lamentablemente, el consumo de alimentos contaminados como pescado y frutas no puede ser reemplazado rápidamente en la dieta de los habitantes de la cuenca del río Atrato. Por lo tanto, es fundamental establecer una evaluación de estrategias en relación con la continuación del consumo de estos alimentos, de modo que el análisis de riesgo para la salud realizado en este capítulo pueda proporcionar información relevante para formalizar recomendaciones adecuadas. En relación al control de la actividad minera en el Chocó, actualmente se están desarrollando campañas de capacitación en la región, involucrando especialmente a los mineros. Estos esfuerzos buscan mejorar las condiciones laborales y humanas de estas comunidades afectadas por la MAPE y fomentar la transición hacia una actividad minera formal.

Por otro lado, los resultados aquí mostrados sugieren que se deben programar charlas divulgativas en estas comunidades para informar a la población de los peligros que conlleva el consumo de algunos tipos de pescados y frutas. El consumo de ciertas frutas como el plátano, no se debe consumir en las cantidades actuales, que son muy elevadas (cerca de 500 g al día). Igualmente, se debe reducir la ingesta diaria de ciertas especies de pescado, que en algunos casos llega a ser de cerca de 600 g al día en mujeres embarazadas.

CAPÍTULO 4: Inclusión de nuevos materiales en la técnica DGT

4.1. Introducción

La química analítica desempeña un papel fundamental en la comprensión y el abordaje de diversos desafíos contemporáneos, que van desde la contaminación ambiental hasta los problemas de salud pública. Entre las técnicas destacadas en este campo se encuentra la técnica DGT, ampliamente empleada en la medición de especies metálicas lábiles en agua, sedimentos y suelos (Marrugo-Negrete et al. 2020b). Además, el muestreo pasivo con DGT tiene algunas ventajas, como proporcionar valores de concentración de la fracción disuelta de contaminantes promediadas en el tiempo (figura 17). También sirve como un procedimiento de enriquecimiento *in situ* y protege los analitos de la degradación durante el transporte de campo al laboratorio y almacenamiento.
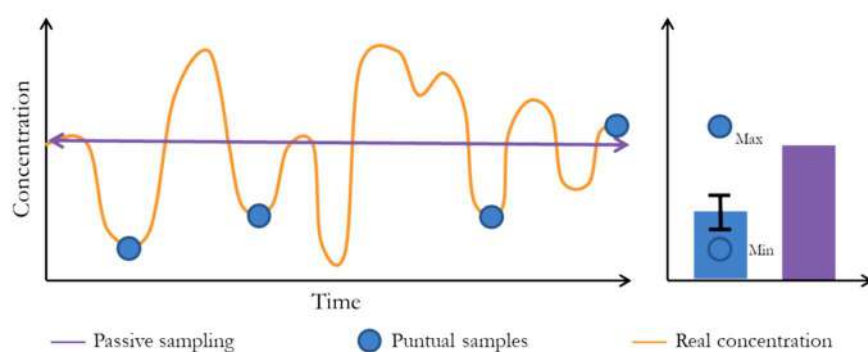
Figura 17. Comparación entre el muestreo puntual y el muestreo pasivo (Turull, 2019).

Por otro lado, el campo de la química verde ha surgido como un enfoque esencial para el diseño de productos y procesos químicos que minimicen o eliminen el uso y generación de elementos potencialmente tóxicos. Este

enfoque está alineado con los ODS según las aspiraciones y prioridades de la agenda internacional de las Naciones Unidas para 2030, que buscan proteger el medioambiente y promover el crecimiento social y económico. Por lo tanto, la utilización de biomasa residual proveniente de actividades agroindustriales, su posterior pirolización y modificación estructural, ejemplifica los principios de la química verde en acción. Además, los polímeros derivados de benzoiltiourea destacan por su alta afinidad por el Hg podrían convertirse en buenos candidatos para su inclusión en dispositivos DGT. Este enfoque no solo provee una fuente sostenible de materiales para la manufacturación de dispositivos DGT, sino que también podría ofrecer una solución para la gestión de residuos agroindustriales, el cual es otro importante problema medioambiental, y que enlaza en cierta forma con la economía circular.

En este marco, la incorporación de nuevos materiales poliméricos derivados de benzoiltiourea y biomasa residual de actividades agroindustriales a la técnica DGT representa un avance integral y significativo en los campos de la química analítica y la química verde, creando un valor añadido. Con estos estudios, además de evaluar la eficiencia de estos nuevos materiales en la técnica DGT, también buscamos contribuir al uso sostenible de recursos y a la reducción o valorización de residuos.

4.2. Metodología

Los materiales y métodos empleados para la inclusión y análisis de los nuevos materiales en la técnica DGT están contenidos en las publicaciones incluidas en este capítulo. Cabe aclarar que los métodos usados para la incorporación de los materiales de biomasa residual (plumas, biocarbón, corcho, cáscara de canola y cáscara de arroz) y de los polímeros derivados de benzoiltiourea (PBTU, BTP1 y BTP2) fueron muy similares a los usados para la manufacturación de hidrogeles con 3MFS. Las figuras 18 y 19 muestran los diagramas de flujo de las metodologías que se siguieron en condiciones controladas de laboratorio.
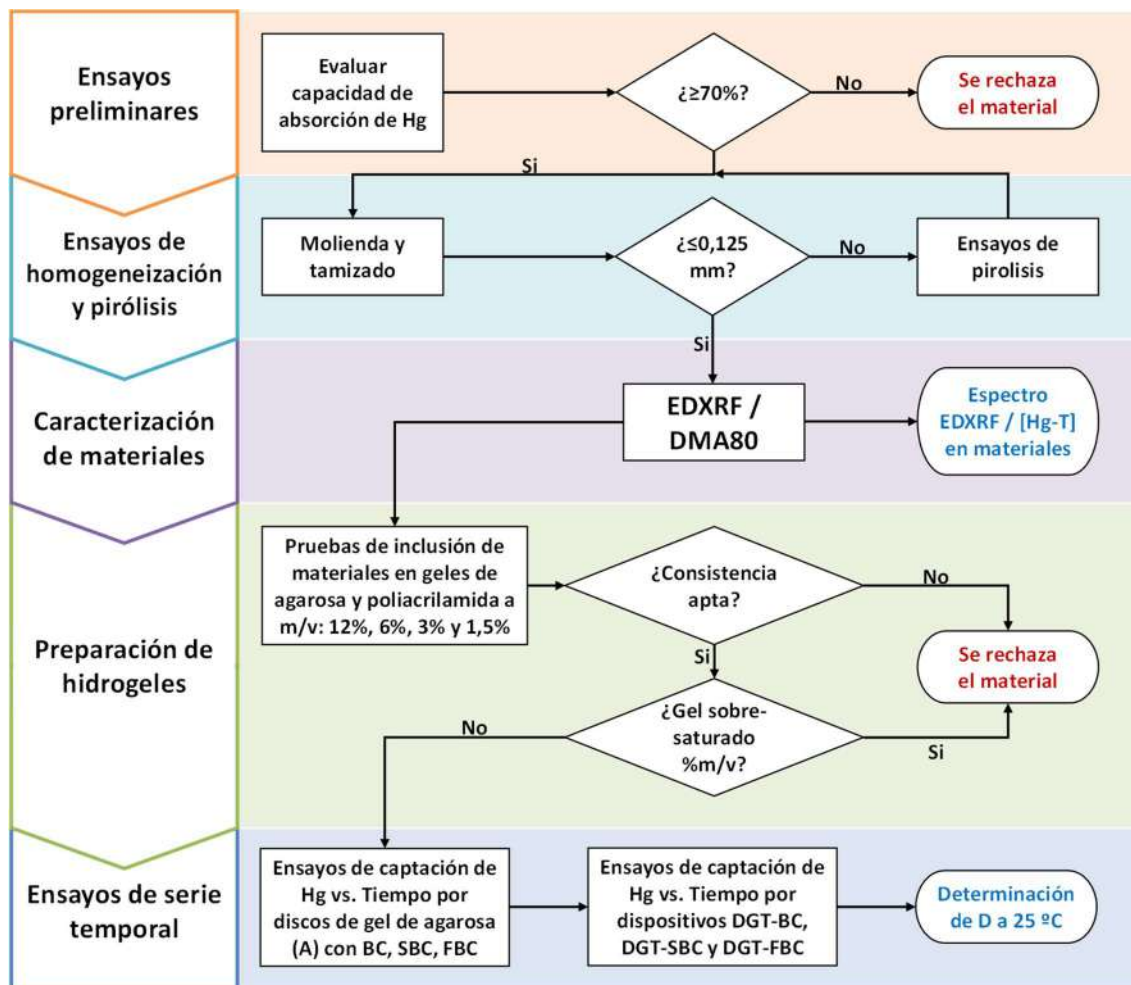
Figura 18. Metodología para evaluar nuevos materiales derivados de la biomasa (plumas, biocarbón, corcho, cáscara de canola y cáscara de arroz) como posibles geles de unión en la técnica DGT para la determinación de Hg lábil. BC: Biocarbón base, SBC: Biocarbón sulfurado, FBC: Biocarbón de plumas.
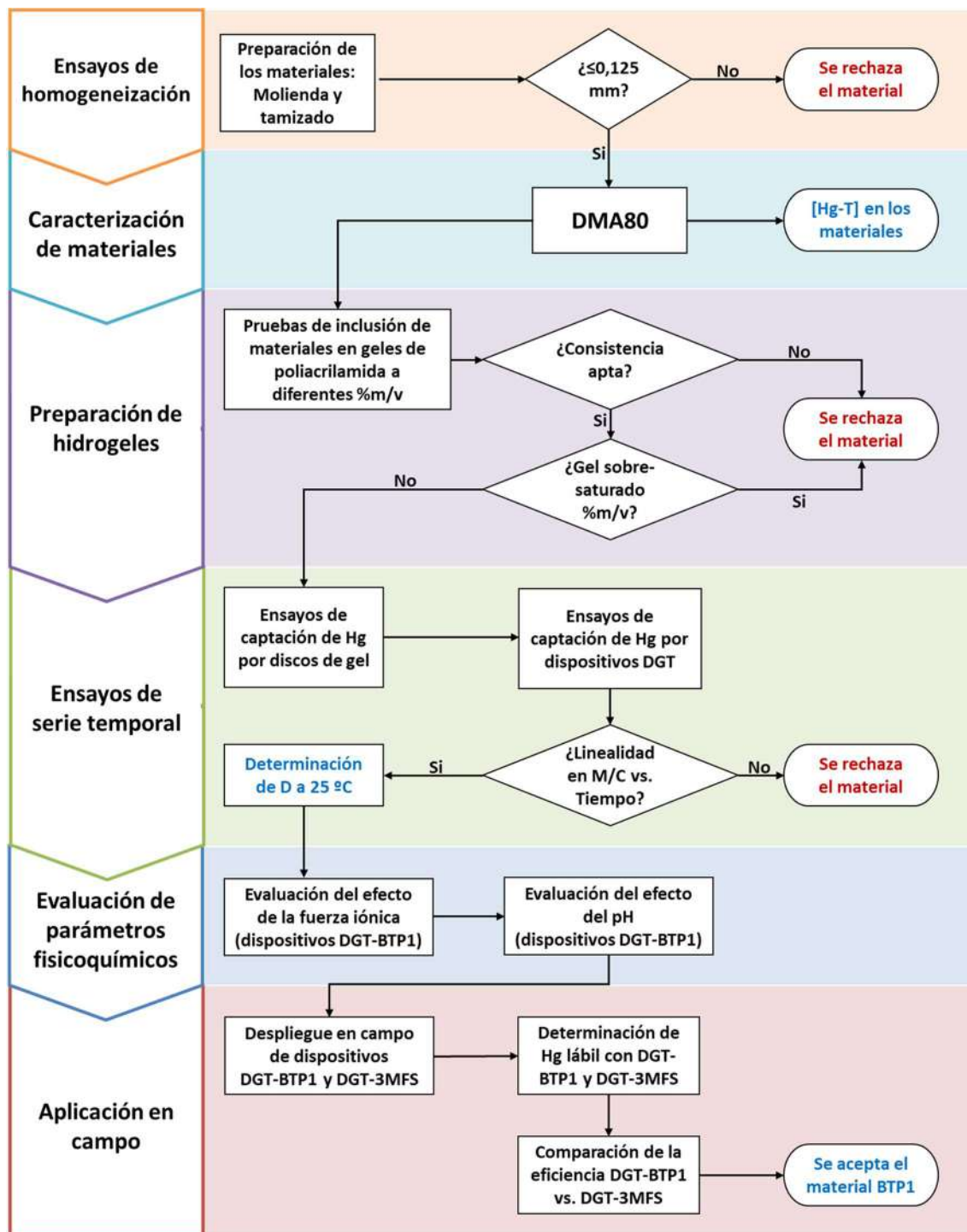
Figura 19. Metodología para evaluar polímeros basados en benzoiltiourea (PBTU, BTP1 y BTP2) como posibles geles de unión en la técnica DGT para la determinación de Hg lábil.

4.3. Resultados

Los resultados obtenidos se encuentran recopilados en dos artículos científicos, uno de los cuales ya ha sido publicado, mientras que el otro ha sido enviado para su revisión y posible publicación.

En estos artículos se evaluaron materiales derivados de biomasa residual y polímeros derivados de la benzoiltiourea como capas de unión en la técnica DGT en su efectividad para la determinación de Hg lábil en medio acuoso y en condiciones de laboratorio. Las publicaciones correspondientes son:

11. Publicación 4: **Marrugo-Madrid, S.**; Marrugo-Negrete, J.; Queralt, I.; Palet, C.; & Díez, S. (2023). Evaluation of novel biomass-derived materials as binding layers for determining labile mercury in water by diffusive gradient in thin-film technique. [submitted to the journal Environmental Technology & Innovation, on May 30, 2023]

12. Publicación 5: **Marrugo-Madrid, S.**, Fontàs, C., Kurt, G., Salazar-Camacho, C., Salas-Moreno, M., Gutierrez-Mosquera, H., Marrugo-Negrete, J. & Díez, S. (2022). Benzoylthiourea based polymers as new binding agents for diffusive gradients in thin films technique in labile mercury determination in freshwaters. Environmental Technology & Innovation, 28, 102911. DOI: 10.1016/j.eti.2022.102911

4.3.1. Publicación 4: Evaluation of novel biomass-derived materials as binding layers for determining labile mercury in water by diffusive gradient in thin-film technique.

Marrugo-Madrid, S.; Marrugo-Negrete, J.; Queralt, I.; Palet, C.; & Díez, S.

Evaluation of novel biomass-derived materials as binding layers for determining labile mercury in water by diffusive gradient in thin-films technique

Siday Marrugo-Madrid[a,b], Jose Marrugo-Negrete[b], Ignasi Queralt[c], Cristina Palet[d] and Sergi Díez[a,*]

[a]Department of Environmental Chemistry, Institute of Environmental Assessment and Water Research, IDAEA-CSIC, E-08034, Barcelona, Spain
[b]Department of Chemistry, Faculty of Sciences, University of Cordoba, Montería, Colombia
[c]Department of Geosciences, Institute of Environmental Assessment and Water Research, IDAEA-CSIC, E-08034, Barcelona, Spain
[d]GTS-UAB Research Group, Department of Chemistry, Faculty of Sciences, Universitat Autònoma de Barcelona, Bellaterra, 08193, Spain

*Corresponding author
ORCID. 0000-0002-9870-2179
E-mail: sergi.diez@idaea.csic.es

Abstract

In this work, several binding gels were successfully prepared in Diffusive Gradient in Thin-film (DGT) that targeted the inclusion of novel biomass-derived materials for the determination of the labile fraction of total Hg (THg) in water. First, five biomass-derived materials were tested and the descending order as a function of the average percentage of THg removal in

solution was feathers>biochar>cork>canola meal>rice husk. The best two materials were treated and pulverized into powder to be embedded in a hydrogel; and so, feathers were pyrolyzed preserving the sulfur contained in their keratin structure (FBC), and biochar (BC) was modified and pyrolyzed with sublimated sulfur (SBC) to increase the Hg sorption sites in its structure. Analysis by Energy Dispersive X-ray fluorescence (EDXRF) spectrometry confirmed that the different pyrolysis procedures increased sulfur absorption successfully. The efficiency of the obtained gels (BC, SBC and FBC) in agarose was evaluated by comparative Hg uptake tests, showing a larger efficacy in the following order: SBC>BC>FBC. To test its feasibility for freshwater deployments, DGTs were also evaluated to determine their diffusion coefficients (D) in the presence/absence of other trace elements (Mn, Cu, Zn, Ni, Pb, Cd and As) at controlled conditions in the lab. Good linear correlations were obtained between the amount of Hg uptake and the deployment time only for the DGT devices prepared with BC and SBC (R^2 = 0.907 and 0.942), respectively. Therefore, D obtained for the labile species of Hg were 2.8×10^{-6} for DGT-BC and 5.2×10^{-6} cm^2 s^{-1} for DGT-SBC devices at 25 ºC, both into the order of magnitude reported by previous studies. The good performance obtained by BC and SBC DGT devices is a promising result and indicates the potential for valorization of waste materials in the DGT technique.

Keywords: Diffusive gradients in thin films; labile mercury; biomass-derived material; feathers; biochar; pyrolysis; binding gel

1. Introduction

Mercury (Hg) has been identified as one of the most hazardous pollutants worldwide as a consequence of its high levels of emissions into the environment, mainly from anthropogenic sources such as gold mining, chlor-alkali industry, waste disposal, and others (UNEP, 2018). The concern around Hg arises from its capacity for biomagnification along foodwebs, and the proven harmful health effects in humans, affecting the nervous, respiratory, renal and immune systems (Bjørklund et al., 2017; Calao-Ramos et al., 2021). More than two million tons of Hg per year are emitted into the atmosphere from anthropogenic sources (UNEP, 2018). As a result, the Minamata Convention (i.e. the global treaty to protect human health and the environment from the adverse effects of Hg) has focused mainly on the reduction of Hg emissions and on public health strategies, but also in monitoring the Hg species already present in the different aquatic ecosystems, especially those that may represent the bioavailable fraction of the metal (UNEP, 2017b).

Diffusive Gradients in Thin films (DGT) technique was established in the 90's by Davison and Zhang (1994) for the metal speciation in aqueous solutions. Since then, it has been widely studied and its efficiency has been proven in monitoring the Hg bioavailable fraction in complex matrices, such as natural waters, soils and sediments (Bratkič et al., 2019; Clarisse and Hintelmann, 2006; Divis et al., 2005; Marrugo-Madrid et al., 2022b, 2021; Turull et al., 2019). The DGT devices consist of three layers: two kinds of hydrogels,

diffusive and binding gels, protected by a membrane filter. The Hg bioavailable fraction present in the aqueous medium passes by diffusion through the filter membrane and the diffusion gel, until it is immobilized on the binding gel. This diffusion makes it possible to apply the Fick's first law to relate the amount of Hg uptake by the binding layer (M) and its concentration in solution (C_{DGT}). The diffusive layer thickness (Δg), the diffusion coefficient of the labile Hg (D), the area of exposed surface (A) and the deployment time (t) can be determined experimentally (Eq.1).

$$C_{DGT} = \frac{M \, \Delta g}{D \, A \, t} \qquad \text{(Eq. 1)}$$

The effectiveness of the DGT technique is highly dependent on the capacity of the resin gel to retain the analyte; hence the importance of exploring materials with an affinity for Hg as binding layers. Initially, the Chelex-100 cation exchange resin was used as binding layer in the determination of Hg and others trace metals in aqueous media (Davison and Zhang, 1994; Dočekalová and Diviš, 2005), however, its iminodiacetic functional groups only showed affinity with ionic Hg and weak Hg-complexes (Divis et al., 2005). Afterwards, this resin was substituted by others with thiol groups (–SH), which improved the Hg uptake in DGT devices, such as Spheron-Thiol, 3-mercaptopropyl functionalized silica or thiol-modified carbon nanoparticles (Clarisse and Hintelmann, 2006; Diviš et al., 2010; Dočekalová and Diviš, 2005; Gao et al., 2011; Shade and Hudson, 2005; Wu et al., 2017). Nevertheless, most of the resins included in the binding layers are relatively expensive and represent an important part of the manufacturing of DGT

devices. Therefore, there has been a need to study alternative materials as possible binding layers in an attempt to reduce costs. Three alternative materials successfully embedded in DGT binding layers, showing good performance and linearity in Hg uptake, were i) the cellulose phosphate-based Whatman P81 membrane (Colaço et al., 2014; Larner and Seen, 2005; Li et al., 2002), ii) the biological substrate *Saccharomyces cerevisiae* (Tafurt-Cardona et al., 2015), and more recently iii) a polymer derived from benzoylthiourea, BTP1 (Marrugo-Madrid et al., 2022a), of which only *Saccharomyces cerevisiae* is currently commercially available. An alternative source of materials with potential for use in the DGT technique could be biomass derived from agro-industrial residues. This type of residual biomass has also been studied as materials for the possible treatment of water and soil contaminated with Hg and other trace metals, in order to develop environmentally friendly methodologies and the attempt to improve the cost-efficiency ratio. The main applications of this type of residual biomass have been as biosorbents or amendments, obtaining good results in studies carried out with materials such as rice husks, feathers, cork, and others (Arsenie et al., 2022; Chakraborty et al., 2020; El-Said et al., 2018; Feizi and Jalali, 2015; Lopes et al., 2014; Wang et al., 2020). Furthermore, different types of biochar obtained from the pyrolysis of this residual biomass have been shown to be successful in the immobilization of Hg, especially in contaminated soils in mining areas (de Souza et al., 2019; Gamboa-Herrera et al., 2021). To improve the Hg uptake capacity of biochar, modifications to their structure have been implemented by combining sulfur-containing functional groups with the base

structure of the biochar, based on the demonstrated affinity of these two elements (Huang et al., 2019; Park et al., 2019; Shi et al., 2022; Zhao et al., 2022).

The aim of the research was to assess the potential for valorization of waste materials in the use as binding gels in DGT devices for the determination of the dissolved-bioavailable fraction of Hg in water. Therefore, the Hg removal capacity of various types of biomass derived from agro-industrial residues was evaluated. The ease of handling the material, hydrogel manufacture, Hg affinity and possible competition with other metals usually present in mining-contaminated waters were considered. In addition, the efficiency of these novel DGT devices was evaluated through the diffusion constants calculated experimentally in controlled conditions in the laboratory.

2. Materials and methods

2.1. Uptake capacity of biomass-derived materials

Five types of biomass-derived materials (biochar, canola meal, chicken feathers, cork and rice husk) were chosen to evaluate their Hg uptake capacity and to explore the possibility of including them as binding layers in the DGT technique. The materials were initially washed with milliQ water, dried at 40 °C for three days and stored in polyethylene bags, and afterwards, THg concentrations were determined to get background values. Then, 30 mg of each material was submerged in a solution with Hg(II) (12 mL, 0.01M

NaCl) at different concentrations (1.8 to 13 μg L^{-1}) and pH values (4.8 and 6.8)) in a container of 15 mL of capacity. The stirring was constant for the entire 24 h of the experiment at room temperature. Subsequently, the materials were centrifuged, filtered, washed and dried. The THg were determined both in the materials and in the containing solutions, before and after the experiment. Based on the values of the initial concentration (C_i) and final concentration (C_f) in each of the solutions, we can calculate the Hg removal percent (%R) according to the equation: *%R = [(C_i – C_f) / C_i] x 100.*

2.2. Evaluation and modification of biomass materials

Homogenization of the biomass-derived materials was carried out to evaluate their possible inclusion within the binding gels. The materials were ground and sieved to < 0.121 mm, which was chosen considering the thickness of binding gels plastic spacers used in the manufacture of DGTs. For those that could not be ground, diminished its particle size or did not offer ease of handling during the assay were either further treated to improve their inclusion within the binding gel or discarded.

Biochar was produced by Bodegas Torres (Vilafranca del Penedès, Barcelona, Spain) from vineyards by pyrolysis at 400-600 °C. In order to improve the Hg affinity of our base biochar (BC), this BC was modified it by adding sublimated sulfur (S) according to the methodology proposed by Park et al. (2019). The BC was ground and sieved to < 0.121 mm and mixed with S in a

1:1 mass ratio. The mixture was placed in porcelain crucibles with covers and pyrolyzed at 600 °C in a Carbolite CWF1300 furnace with nitrogen atmosphere for 240 min, obtaining a sulfurized biochar (SBC). BC and SBC were stored in sealed glass vials until experiments. Likewise, a pyrolysis with feathers was carried out according to the thermogravimetric analysis shown by Senoz et al., (2012). Briefly, the feathers were weighed and washed with Milli-Q water, dried for 180 min at 60 °C and pyrolyzed in an oven with nitrogen gas purged, first to 210 °C at a heating rate of 4 °C min^{-1} for 180 min, and subsequently to 450 °C by doubling the heating rate to 8 °C min^{-1} until completing 270 min of the experiment, obtaining a biochar based on feathers (FBC). Similar to previous biochars, the FBC was also ground and sieved to < 0.121 mm, and stored in a sealed glass vial.

2.3. EDXRF characterization

The effectiveness of the biochar modification was verified by chemical characterization. The S content in the BC, SBC and FBC biomass derivatives was evaluated by small-spot energy dispersive X-ray fluorescence (EDXRF) in a FISCHERSCOPE® X-RAY XDV®-SDD analyser with 3 mm of focal spot, 10 KV, 1000 μA and 300 s of counting time, as parameters. Samples of the certified reference material CRM/Coal SARM-18 (Mintek, SA) liver) were measured by triplicate. The S concentration found was 5655 ± 80 mg kg^{-1} (certified value is 5600 mg kg^{-1}). Finally, graphite Merck and graphite Merck

doped with 25% of elemental S were used for comparisons between measurements during the analysis.

2.4. Gel preparation and mounting of DGT devices

The reagents, the inclusion of new materials in polyacrylamide gels and the assembly of the in-house fabricated DGT devices have been described in previous studies (Fernández-Gómez et al., 2011; Marrugo-Madrid et al., 2022b; Turull et al., 2017). The diffusive gels were made with polyacrylamide (0.80 mm thickness after hydration), and were cut into 2.5 cm diameter discs. Similarly, biochar-polyacrylamide binding layers were prepared at 6.0, 3.0 and 1.5% w/v ratio.

Diffusion and binding gels with agarose were also prepared. The diffusion gels were prepared by diluting agarose in Milli-Q water at 1.5% w/v ratio. The mixture was heated and stirred gently until completely homogenized, and the resulting solution was immediately pipetted onto two glass plates with a plastic spacer (0.75 mm thickness) and preheated to 45 °C. After cooling, the agarose gel was cut into 2.5 cm diameter discs and stored in a refrigerator at 4 ºC (Fernández-Gómez et al., 2011; Gao et al., 2011). In a similar procedure, the binding gels were prepared by immobilizing BC, SBC and FBC materials into the agarose gel at 1.5% w/v ratio.

A plastic mold based on a simple tight-fitting piston design with an exposure area of 3.14 cm² (DGT Research Ltd., UK) was used to support the gels that

were protected by a nylon filter membrane (0.45 µm pore size and 0.11 mm thickness) as an outer layer.

2.5. Mercury uptake capacity by binding gels

The Hg uptake capacity was evaluated by deployments of biomass-derived materials/agarose discs gels in 10 µg L^{-1} $HgNO_3$ solutions with pH adjusted around 6. The solutions were continuously stirred at 25 ºC, and the gel discs were removed at different periods of time (0, 1, 2, 3, and 6 h).

2.6. Determination of the diffusion coefficient for labile Hg

A time series experiment was performed with the aim of obtaining the diffusion coefficient of mercury. Three of DGT devices from each were submerged in 4 L of a solution ($NaNO_3$ 0.01M and pH 6.6) with the following concentrations: 40 µg L^{-1} of Hg, 100 µg L^{-1} of Mn, Cu, Zn and Ni; 10 µg L^{-1} of Pb and As, and 5 µg L^{-1} of Cd. Metal standards in 2% HNO_3 were used for the preparation of the deployment solution and the concentrations were chosen considering studies carried out in rivers affected by mining activities (Enamorado-Montes et al., 2021). Sets of DGT devices were retrieved after 2, 4, 6, 8, 10, 24 and 32 h. Controls consisted of units that were not deployed at all (DGT blank) and units, which were deployed for 32 h in 0.01 M $NaNO_3$

(experimental blank). At each sampling interval, 5 mL of Hg solution were also sampled in order to monitor the Hg concentration remaining in solution.

2.7. Mercury analysis

A direct mercury analyzer DMA80 Evo Milestone was used to determine Hg concentrations in subsamples of the deployed solution and in the biomass-derived material/agarose gel discs. The relationship between Hg masses in the binding layers, Hg concentrations in solution and the deployment time allow us to apply Fick's law (Eq. 1) to calculate D, that could be modified for different temperatures with the Stoke-Einstein equation (Zhang and Davison, 1995). Samples of the certified reference material DOLT-5 (dogfish liver), from the National Research Council of Canada (NRCC), were measured by triplicate to validate all analytical procedures. The Hg concentration found was 0.49 ± 0.07 mg kg^{-1} (n = 5, average recovery 110%), which agrees with the reference value (0.38 ± 0.10 mg kg^{-1}). Finally, blank samples were used to calculate the limit of detection (LOD) (0.2 μg L^{-1} of Hg).

3. Results and discussion

3.1. Comparison of biomass-derived materials

The Hg uptake capacity was evaluated in biomass-derived materials (biochar, canola meal, chicken feathers, cork and rice husk), at different concentrations

and pH values, and considering the Hg removal percent as the response variable. Initial Hg concentrations measured in solution were 1.8, 3.0, 10 and 13 µg L^{-1}, at the same time that the pH was adjusted to values around 4.8 and 6.7. The combinations between the controllable variables and the results of the percentage of THg removal for each material are shown in Figure S1.

The percentage of THg removal values were 84-99% for feathers, 56-94% for biochar, 38-90% for cork, 11-84% for canola meal, and 3-80% for rice husk. Thereby, the descending order as a function of the average total-Hg removal percent in solutions was feathers>biochar>cork>canola meal>rice husk (Figure 1). A normal distribution in the results for all materials was shown by applying a Shapiro-Wilk test ($p > 0.05$). Statistically significant differences were found between the Hg removal results of each material at different combinations of pH and initial concentration of Hg in solution; nevertheless, no statistical differences were found in the percentages of Hg removal in relation to pH using feathers, therefore, the Hg removal in solution for this material is independent of the pH values in water. For all the materials, the highest percentage of Hg removal (80-100%) in solution was obtained at pH 6.7 and Hg initial concentration of 13 µg L^{-1} (Figure S1).
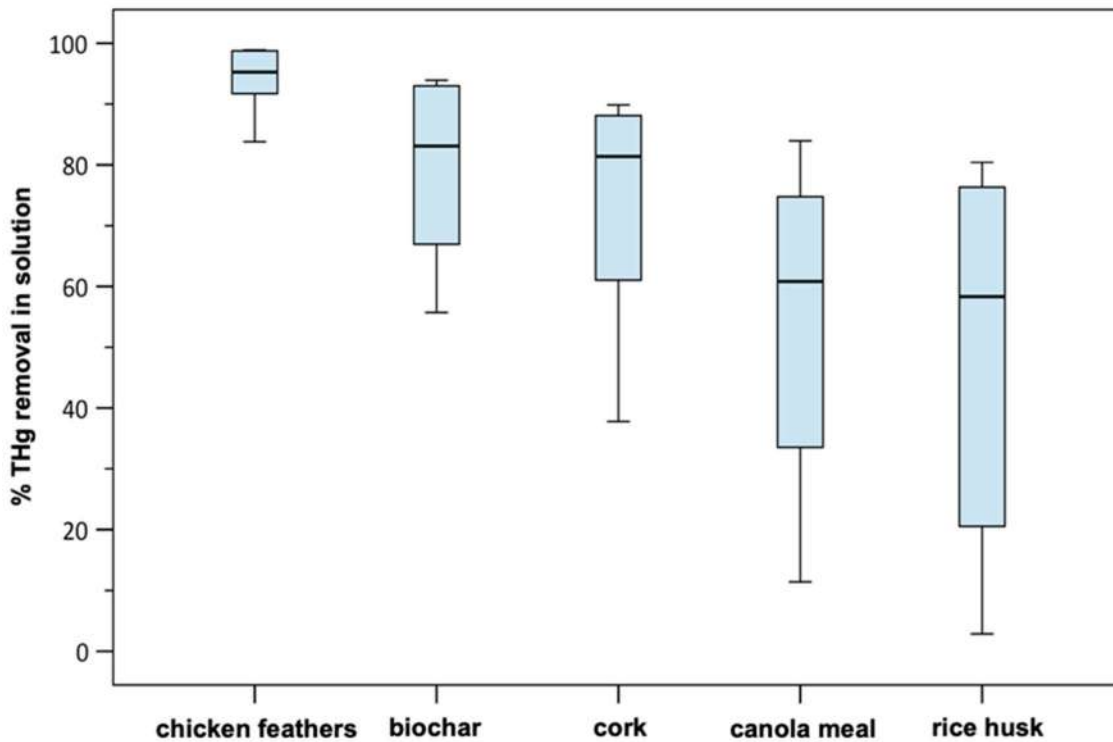
Figure 1. Percentages of THg removal in solution by different biomass-derived materials

Based on the above results of Hg removal in solution, feathers, biochar and cork were chosen as materials for particle size homogenization tests and preparation of binding gels. Cork was discarded due to its low density and difficulty of handling, since it was not possible to weigh and sieve it properly, or to manufacture gels, because the material floats on the hydrogel surface.

3.2. Preparation of sulfurized biochar (SBC)

The modification of surface group structure in the BC could increase the sorption sites for Hg (Shi et al., 2022), therefore, once the BC was modified by

pyrolysis, both the BC and the obtained SBC were analyzed in triplicate by EDXRF with parameters of 3 mm of focal spot, 10 KV, 1000 μA and 300 s of counting time. Figure 2 shows the spectrum of BC, SBC and an unpyrolyzed 1:1 mixture of BC and S. The peak of binding energy of 2.3 keV is assigned to S, and it could be observed a clear increasing signal of the peak, which means a successful absorption of S in the SBC samples in comparison with BC.
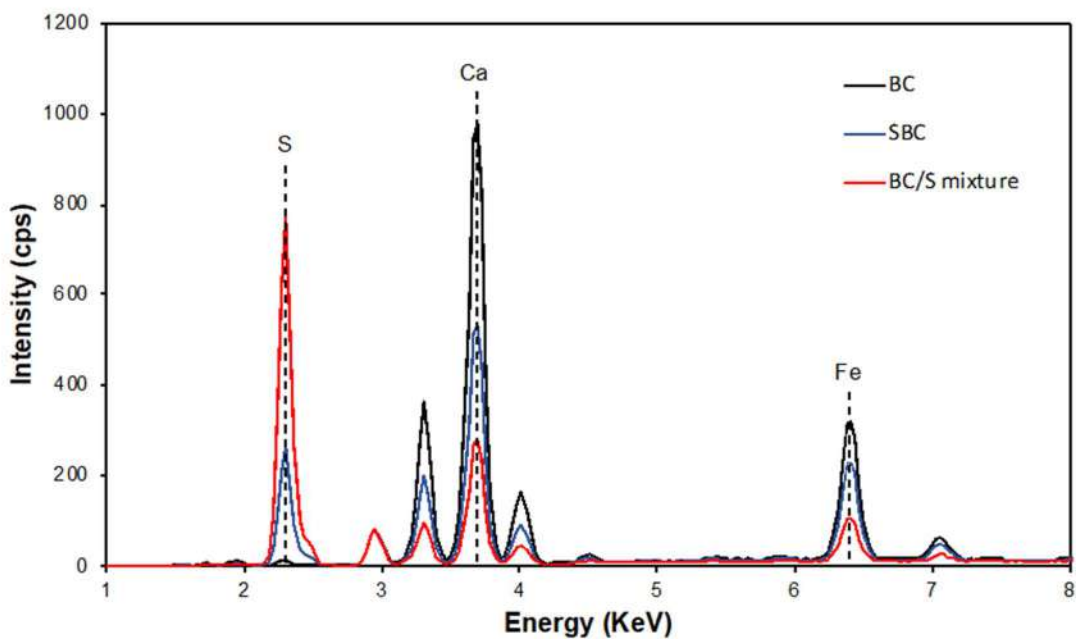
Figure 2. EDXRF analysis spectra comparing samples of BC, SBC and a unpyrolyzed mixture of BC and S (1:1).

The S content in the BC and SBC samples was 0.71 ± 0.03% and 18.56 ± 0.23%, respectively, indicating a strong increase of S content, that is much higher than the increment of 8.7% obtained by Park et al. (2019). Finally, the SBC was successfully homogenized to a particle size of < 0.121 mm prior to be incorporated into the binding gel.

3.3 Preparation of biochar based on feathers (FBC)

The feathers are a material very difficult to handle and could not be reduced mechanically or homogenized, however, it is an interesting material to be used as binding because it was the material that exhibited the best percentage of Hg removal in solution, probably due to the sulfhydryl groups of keratin that form strong bonds to metals. Therefore, a modification by pyrolysis was made trying to maintain the S associated with thiol groups (–SH) in the keratin structure of feathers. Keratin pyrolysis is complex due to the large number of possible combinations between the sequences and molar ratios of the amino acids (Senoz et al., 2012). During the pyrolysis of feathers, the preservation and formation of disulfide bonds was enhanced by applying a short isothermal heat treatment below the melting point (215 °C) at a slow heating rate (4 °C min^{-1}) (Senoz et al., 2012). The FBC obtained was ground and homogenized to a particle size of < 0.121 mm, and its S content was 2.77 ± 0.21% by EDXRF analysis, which is higher than BC and lower than SBC.

3.4. Mercury uptake capacity by biochar-binding gels

The binding gels with BC-polyacrylamide (BC-P) were manufactured following a similar procedure using 3-mercaptopropyl functionalized silica gel (3MFS) as resin (Fernández-Gómez et al., 2011). In the original procedure, the 3MFS ratio with respect to the polyacrylamide gel solution was 12% w/v, however, it was not possible to obtain stable gels by keeping the same ratio

or even reducing to 6% the amount of BC in the gel solution. Satisfactory results were obtained with the ratios of 3% and 1.5% w/v of BC, even so, gels prepared with a 3% w/v ratio could be considered saturated.

A short explorative Hg uptake test was carried on using DGT devices assembled with BC-P gels as binding layer and polyacrylamide gel as diffusive layer (Figure S2). No statistically significant differences ($p > 0.05$) were found between the results obtained for both types of DGT-BC-P at the first 10 hours of experiment. Therefore, since no major differences were observed and the amount of BC used for manufacturing is lower, the ratio 1.5% w/v of BC-P gel was chosen for the rest of the tests. Unlike the BC and FBC, it was not possible to obtain appropriate gels using SCB with polyacrylamide at any ratio. We obtained binding gels without a proper consistency for subsequent handling and inclusion in the DGT device, hence, a procedure with agarose was chosen for manufacturing all the diffusive and binding gels (Figure S3) (Fernández-Gómez et al., 2011; Gao et al., 2011).

The Hg uptake capacity was evaluated by immersing discs of biochar-agarose binding gels (BC-A, SBC-A and FBC-A) in solutions prepared at 10 µg L^{-1} of $HgNO_3$ and neutral pH. Figure 3 shows the Hg uptake by the three types of binding gels during a 6 h of times series experiment. The maximum Hg masses uptake by BC-A, SBC-A and FBC-A were 35.3, 36.8 and 19.0 ng, respectively. Although the Hg mass uptake was higher in BC-A gels during most of the experiment, differences were not statistically significant ($p > 0.05$) with the Hg values obtained with SBC-A gels. Moreover, a better linear

— 189 —

correlation with Hg mass in solution of SBC-A gels was obtained ($R^2 = 0.950$), in comparison with those obtained for BC-A ($R^2 = 0.785$) and FBC-A gels ($R^2 = 0.836$).
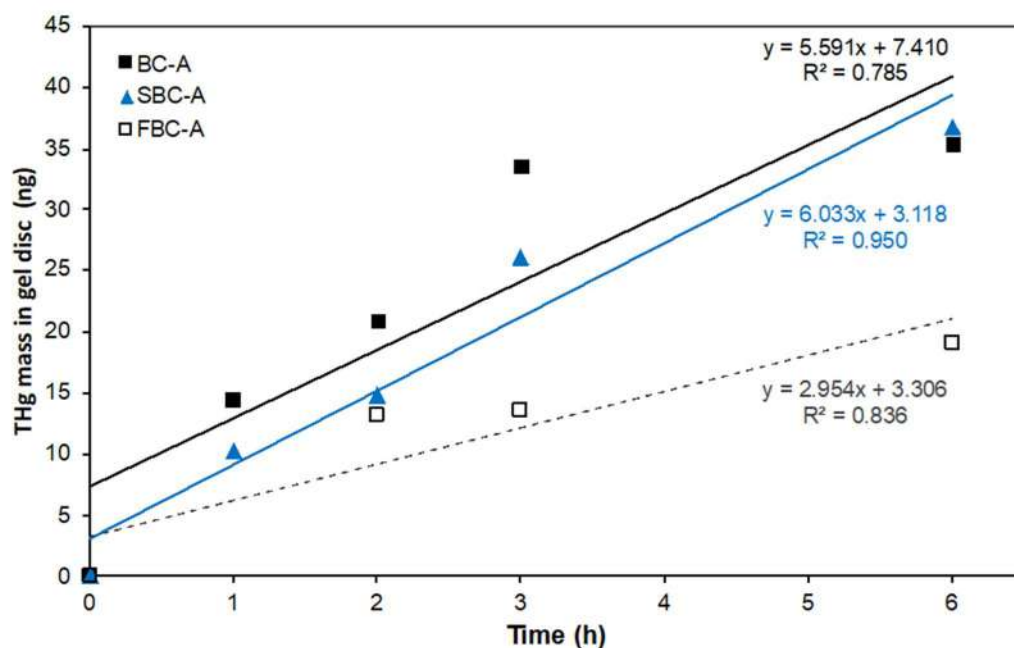

Figure 3. Comparison between Hg mass uptake by the BC-A, SBC-A and FBC-A binding gels discs vs. deployment time in solution with Hg only at 25 ºC.

As previous studies claim (Haider et al., 2022; Li et al., 2017; Nkoh et al., 2022), biochars are not specific for Hg uptake and may also have affinities for other trace metals, which could compete with Hg for sorption sites on the surface of their structure. To check its selectivity, a times series experiment was conducted in a solution prepared at 40 µg L^{-1} of Hg, 100 µg L^{-1} of Mn, Cu, Zn and Ni, 10 µg L^{-1} of Pb and As, and 5 µg L^{-1} of Cd, where the three types of DGT devices (DGT-BC, DGT-SBC and DGT-FBC) were deployed in triplicate. The comparison between the three types of DGT devices is shown

in Figure 4. As can be seen, results for DGT-FBC devices showed that Hg uptake increased linearly with the time but only during the first 4 h of the experiment, and later on, Hg accumulation in the DGT reaches a plateau. This weak positive correlation (R^2= 0.551) in the DGT-FBC devices indicates that, although both variables (i.e. Hg vs. time) tend to go up in response to one another, there is a lower affinity for Hg in comparison with the other two types of devices. Thus, the Fick's first law cannot be applied to estimate the diffusion coefficient for Hg, and therefore, the performance for FBC as a resin to be used in binding gels for the DGT technique is not suitable. This result agrees with our previous findings in Figure 3, where FCB gels uptake was about 47% less of Hg per unit of disc with respect BC and SBC.
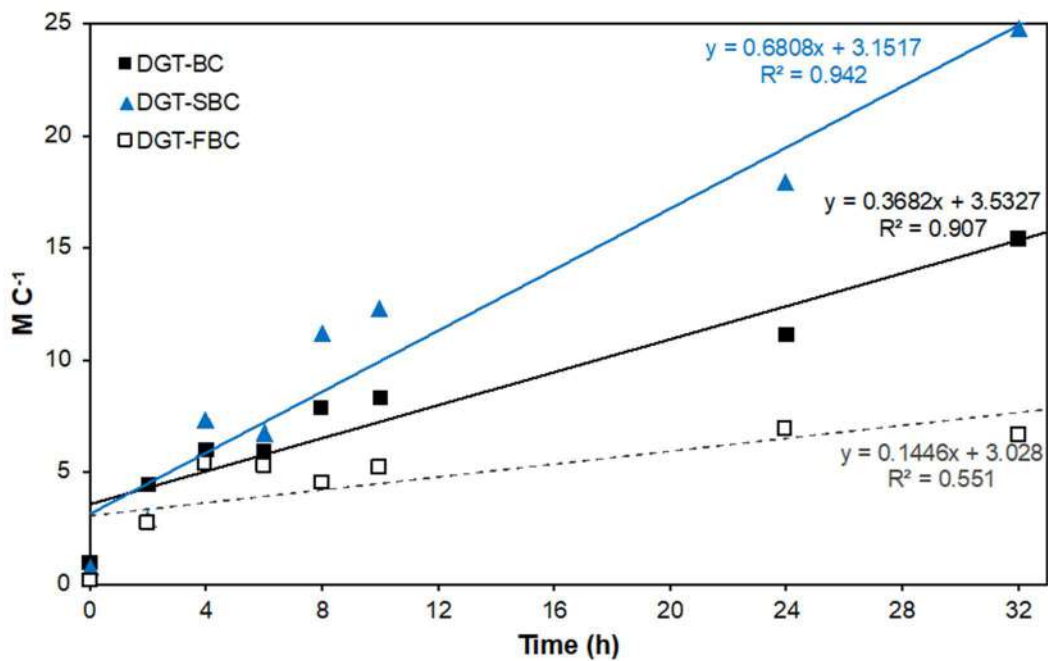
Figure 4. Comparison between the relations of Hg masses in the binding gel (M) and measured Hg concentration in the solution (C) vs. deployment time for DGT-BC, DGT-SBC and DGT-FBC devices (all based on agarose gels) in a solution containing Hg, Mn, Cu, Zn, Ni, Pb, Cd and As, at 25.1 ± 0.6 ºC.

In contrast, two remarkable linear correlations between Hg uptake and deployment time were observed for the DGT-BC (R^2 = 0.907) and DGT-SBC (R^2 = 0.942) devices (Figure 4). The D obtained at 25 ºC for the labile species of Hg in solution were 2.8×10^{-6} for DGT-BC devices and almost two-fold for DGT-SBC devices (5.2×10^{-6} cm^2 s^{-1}). A comparison of the D values reported in previous studies to assess the labile Hg by DGT technique in water are shown in Table 1. While the D obtained with DGT-BC devices is the lowest, the D obtained with DGT-SBC could be considered similar to others reported for resins that have a well proven high affinity for Hg, such as 3MFS and Spheron-Thiol (Fernández-Gómez et al., 2011; Hong et al., 2011).

Table 1. Diffusion coefficients (D) reported for labile Hg determination in water.

Binding gel	Diffusive gel	D ($\times 10^{-6}$; cm^2 s^{-1})	T (ºC)	pH	Ionic strength	Reference
BC-A	Agarose	2.79	25	6.6	0.01M NaNO$_3$	This study
SBC-A	Agarose	5.16	25	6.6	0.01 M NaNO$_3$	
Chelex-100	Agarose	8.97	-	5.0	0.01 M NaNO$_3$	Dočekalová and Diviš, (2005)
Spheron-Thiol	Agarose	9.13	-	5.0	0.01 M NaNO$_3$	
Spheron-Thiol	Agarose	4.41	21.5	7.0	0.01 M NaCl	Fernández-Gómez et al., (2011)
3MFS	Agarose	3.86	21.5	7.0	0.01 M NaCl	
Mercaptopropyl Nanoporous resins	Agarose	8.44	20	5.0	0.01 M NaNO$_3$	Gao et al., (2011)
3MFS	Agarose	4.48	-	7.0	0.01 M NaNO$_3$	Hong et al., (2011)
Ambersep GT74	Agarose	9.07	25	5.0	0.01 M NaNO3	Pelcová et al., (2014)
3MFS	Polyacrylamide	3.08	20	7.0	0.01 M NaCl	Turull et al., (2019)
BTP1	Polyacrylamide	3.95	25	6.8	0.01 M NaCl	Marrugo-Madrid et al., (2022a)

BTP1: Poly (4-((2-aminonaphthalene-6-carbonothioyl) carbamoyl) benzoyl isothiocyanate)
3MFS: 3-mercaptopropil functionalized silica gel

Moreover, our findings could be considered a promising result considering that Hg uptake was determined in a deployment solution containing high concentrations of trace elements such as Mn, Cu, Zn, Ni, Pb, Cd and As.

Values of D for both DGT-BC and DGT-SBC devices are in the same order of magnitude (10^{-6}) than those obtained in previous studies. Moreover, the higher affinity and more stable bonds between S and Hg were probably the main factors for the higher D of DGT-SBC in comparison with DGT-BC devices (Gao et al., 2011; Pearson, 1963; Shi et al., 2022).

Conclusions

The biochar, feathers and cork were the biomass-derived materials that exhibited an optimal Hg removal capacity in water with maximum percentages of 99%, 94% and 90%, respectively. In order to improve their affinity for Hg, the biochar was pyrolyzed with S (i.e. preparation of SBC) and feathers were pyrolyzed under controlled conditions to preserve the thiol groups of its structure (i.e. preparation of FBC). The suggested DGT method using BC and SBC agarose-based binding gels and agarose gels as diffusion layers was successful for the labile Hg determination under controlled experimental conditions, showing a satisfactory linearity correlation between Hg uptake and deployment time. The diffusion coefficients in agarose for labile Hg at 25 ºC were 2.8 x10^{-6} and 5.2 x10^{-6} cm^2 s^{-1} for DGT-BC and DGT-SBC devices, respectively, fitting the same order of magnitude reported in the literature. Considering that the deployment solution contained high concentrations of trace elements (Mn, Cu, Zn, Ni, Pb, Cd and As) in competition with Hg for sorption sites on the surface of BC and SBC, the very

good performance found is a promising result in the use of these biomass-derived materials in the DGT technique.

Acknowledgements

References

Arsenie, T., Cara, I.G., Popescu, M.C., Motrescu, I., Bulgariu, L., 2022. Evaluation of the Adsorptive Performances of Rapeseed Waste in the Removal of Toxic Metal Ions in Aqueous Media. Water (Switzerland) 14. https://doi.org/10.3390/w14244108

Bjørklund, G., Dadar, M., Mutter, J., Aaseth, J., 2017. The toxicology of mercury: Current research and emerging trends. Environ. Res. 159, 545–554. https://doi.org/10.1016/j.envres.2017.08.051

Bratkič, A., Klun, K., Gao, Y., 2019. Mercury speciation in various aquatic systems using passive sampling technique of diffusive gradients in thin-film. Sci. Total Environ. 663, 297–306. https://doi.org/10.1016/j.scitotenv.2019.01.241

Calao-Ramos, C., Bravo, A.G., Paternina-Uribe, R., Marrugo-Negrete, J., Díez, S., 2021. Occupational human exposure to mercury in artisanal small-scale gold mining communities of Colombia. Environ. Int. 146. https://doi.org/10.1016/j.envint.2020.106216

Chakraborty, R., Asthana, A., Singh, A.K., Yadav, S., Susan, M.A.B.H., Carabineiro, S.A.C., 2020. Intensified elimination of aqueous heavy metal ions using chicken feathers chemically modified by a batch method. J. Mol. Liq. 312, 113475. https://doi.org/10.1016/j.molliq.2020.113475

Clarisse, O., Hintelmann, H., 2006. Measurements of dissolved methylmercury in natural waters using diffusive gradients in thin film (DGT). J. Environ. Monit. 8, 1242–1247. https://doi.org/10.1039/b614560d

Colaço, C., Yabuki, L., Rolisola, A., Menegário, A., De Almeida, E., Suárez, C., Gao, Y., Corns, W.T., Do Nascimento Filho, V.F., 2014. Determination of mercury in river water by diffusive gradients in thin films using P81

membrane as binding layer. Talanta 129, 417–421. https://doi.org/10.1016/j.talanta.2014.05.025

Davison, W., Zhang, H., 1994. In situ speciation measurements of trace components in natural waters using thin-film gels. Nature 367, 546–548.

de Souza, E.S., Dias, Y.N., da Costa, H.S.C., Pinto, D.A., de Oliveira, D.M., de Souza Falção, N.P., Teixeira, R.A., Fernandes, A.R., 2019. Organic residues and biochar to immobilize potentially toxic elements in soil from a gold mine in the Amazon. Ecotoxicol. Environ. Saf. 169, 425–434. https://doi.org/10.1016/j.ecoenv.2018.11.032

Divis, P., Leermakers, M., Dočekalová, H., Gao, Y., 2005. Mercury depth profiles in river and marine sediments measured by the diffusive gradients in thin films technique with two different specific resins. Anal Bioanal Chem 382, 1715–1719. https://doi.org/10.1007/s00216-005-3360-8

Diviš, P., Szkandera, R., Dočekalová, H., 2010. Characterization of sorption gels used for determination of mercury in aquatic environment by diffusive gradients in thin films technique. Cent. Eur. J. Chem. 8, 1103–1107. https://doi.org/10.2478/s11532-010-0090-3

Dočekalová, H., Diviš, P., 2005. Application of diffusive gradient in thin films technique (DGT) to measurement of mercury in aquatic systems. Talanta 65, 1174–1178. https://doi.org/10.1016/j.talanta.2004.08.054

El-Said, A., Badawy, N., Garamon, S., 2018. Adsorption of Heavy Metal Ions from Aqueous Solutions onto Rice Husk Ash Low Cost Adsorbent. J.

Environ. Anal. Toxicol. 08, 10–15. https://doi.org/10.4172/2161-0525.1000543

Enamorado-Montes, G., Tirado-Montoya, J., Marrugo-Negrete, J., 2021. Metales pesados (Hg, As, Cd, Zn, Pb, Cu, Mn) en un trayecto del río Cauca impactado por la minería de oro. Rev. EIA 19, 1–15. https://doi.org/10.24050/reia.v19i37.1481

Feizi, M., Jalali, M., 2015. Removal of heavy metals from aqueous solutions using sunflower, potato, canola and walnut shell residues. J. Taiwan Inst. Chem. Eng. 54, 125–136. https://doi.org/10.1016/j.jtice.2015.03.027

Fernández-Gómez, C., Dimock, B., Hintelmann, H., Díez, S., 2011. Development of the DGT technique for Hg measurement in water: Comparison of three different types of samplers in laboratory assays. Chemosphere 85, 1452–1457. https://doi.org/10.1016/j.chemosphere.2011.07.080

Gamboa-Herrera, J.A., Ríos-Reyes, C.A., Vargas-Fiallo, L.Y., 2021. Mercury speciation in mine tailings amended with biochar: Effects on mercury bioavailability, methylation potential and mobility. Sci. Total Environ. 760, 143959. https://doi.org/10.1016/j.scitotenv.2020.143959

Gao, Y., De Canck, E., Leermakers, M., Baeyens, W., Van Der Voort, P., 2011. Synthesized mercaptopropyl nanoporous resins in DGT probes for determining dissolved mercury concentrations. Talanta 87, 262–267. https://doi.org/10.1016/j.talanta.2011.10.012

Haider, F.U., Wang, X., Farooq, M., Hussain, S., Cheema, S.A., Ain, N. ul, Virk, A.L., Ejaz, M., Janyshova, U., Liqun, C., 2022. Biochar application for the remediation of trace metals in contaminated soils: Implications for stress tolerance and crop production. Ecotoxicol. Environ. Saf. 230, 113165. https://doi.org/10.1016/j.ecoenv.2022.113165

Hong, Y.S., Rifkin, E., Bouwer, E.J., 2011. Combination of diffusive gradient in a thin film probe and IC-ICP-MS for the simultaneous determination of CH 3Hg + and Hg 2+ in oxic water. Environ. Sci. Technol. 45, 6429–6436. https://doi.org/10.1021/es200398d

Huang, S., Liang, Q., Geng, J., Luo, H., Wei, Q., 2019. Sulfurized biochar prepared by simplified technic with superior adsorption property towards aqueous Hg(II) and adsorption mechanisms. Mater. Chem. Phys. 238, 121919. https://doi.org/10.1016/j.matchemphys.2019.121919

Larner, B.L., Seen, A.J., 2005. Evaluation of paper-based diffusive gradients in thin film samplers for trace metal sampling. Anal. Chim. Acta 539, 349–355. https://doi.org/10.1016/j.aca.2005.03.007

Li, H., Dong, X., da Silva, E.B., de Oliveira, L.M., Chen, Y., Ma, L.Q., 2017. Mechanisms of metal sorption by biochars: Biochar characteristics and modifications. Chemosphere 178, 466–478. https://doi.org/10.1016/j.chemosphere.2017.03.072

Li, W., Zhao, H., Teasdale, P.R., John, R., Zhang, S., 2002. Application of a cellulose phosphate ion exchange membrane as a binding phase in the

diffusive gradients in thin films technique for measurement of trace metals. Anal. Chim. Acta 464, 331–339. https://doi.org/10.1016/S0003-2670(02)00492-0

Lopes, C.B., Oliveira, J.R., Rocha, L.S., Tavares, D.S., Silva, C.M., Silva, S.P., Hartog, N., Duarte, A.C., Pereira, E., 2014. Cork stoppers as an effective sorbent for water treatment: The removal of mercury at environmentally relevant concentrations and conditions. Environ. Sci. Pollut. Res. 21, 2108–2121. https://doi.org/10.1007/s11356-013-2104-0

Marrugo-Madrid, S., Fontàs, C., Kurt, G., Salazar-Camacho, C., Salas-Moreno, M., Gutierrez-Mosquera, H., Marrugo-Negrete, J., Díez, S., 2022a. Benzoylthiourea based polymers as new binding agents for diffusive gradients in thin films technique in labile mercury determination in freshwaters. Environ. Technol. Innov. 28, 102911. https://doi.org/10.1016/j.eti.2022.102911

Marrugo-Madrid, S., Salas-Moreno, M., Gutiérrez-Mosquera, H., Salazar-Camacho, C., Marrugo-Negrete, J., Díez, S., 2022b. Assessment of dissolved mercury by diffusive gradients in thin films devices in abandoned ponds impacted by small scale gold mining. Environ. Res. 208. https://doi.org/10.1016/j.envres.2021.112633

Marrugo-Madrid, S., Turull, M., Zhang, H., Díez, S., 2021. Diffusive gradients in thin films for the measurement of labile metal species in water and soils: a review. Environ. Chem. Lett. https://doi.org/10.1007/s10311-021-01246-3

Nkoh, J.N., Ajibade, F.O., Atakpa, E.O., Abdulaha-Al Baquy, M., Mia, S., Odii, E.C., Xu, R., 2022. Reduction of heavy metal uptake from polluted soils and associated health risks through biochar amendment: A critical synthesis. J. Hazard. Mater. Adv. 6, 100086. https://doi.org/10.1016/j.hazadv.2022.100086

Park, J.H., Wang, J.J., Zhou, B., Mikhael, J.E.R., DeLaune, R.D., 2019. Removing mercury from aqueous solution using sulfurized biochar and associated mechanisms. Environ. Pollut. 244, 627–635. https://doi.org/10.1016/j.envpol.2018.10.069

Pearson, R.G., 1963. Hard and Soft Acids and Bases. J. Am. Chem. Soc. 85, 3533–3539. https://doi.org/10.1021/ja00905a001

Pelcová, P., Dočekalová, H., Kleckerová, A., 2014. Development of the diffusive gradient in thin films technique for the measurement of labile mercury species in waters. Anal. Chim. Acta 819, 42–48. https://doi.org/10.1016/j.aca.2014.02.013

Senoz, E., Wool, R.P., McChalicher, C.W.J., Hong, C.K., 2012. Physical and chemical changes in feather keratin during pyrolysis. Polym. Degrad. Stab. 97, 297–307. https://doi.org/10.1016/j.polymdegradstab.2011.12.018

Shade, C.W., Hudson, R.J.M., 2005. Determination of MeHg in environmental sample matrices using Hg - Thiourea complex ion chromatography with on-line cold vapor generation and atomic fluorescence spectrometric detection. Environ. Sci. Technol. 39, 4974–4982. https://doi.org/10.1021/es0483645

Shi, Y., Ma, W., Wang, D., 2022. Study on Mercury Adsorption and Desorption on Different Modified Biochars. Bull. Environ. Contam. Toxicol. 108, 629–634. https://doi.org/10.1007/s00128-021-03381-7

Tafurt-Cardona, M., Eismann, C.E., Suárez, C.A., Menegário, A.A., Silva Luko, K., Sargentini Junior, É., 2015. In situ selective determination of methylmercury in river water by diffusive gradient in thin films technique (DGT) using baker's yeast (Saccharomyces cerevisiae) immobilized in agarose gel as binding phase. Anal. Chim. Acta 887, 38–44. https://doi.org/10.1016/j.aca.2015.07.035

Turull, M., Elias, G., Fontàs, C., Díez, S., 2017. Exploring new DGT samplers containing a polymer inclusion membrane for mercury monitoring. Environ. Sci. Pollut. Res. 24, 10919–10928. https://doi.org/10.1007/s11356-016-6813-z

Turull, M., Fontàs, C., Díez, S., 2019. Conventional and novel techniques for the determination of Hg uptake by lettuce in amended agricultural peri-urban soils. Sci. Total Environ. 668, 40–46. https://doi.org/10.1016/j.scitotenv.2019.02.244

UNEP, 2018. Global Mercury Assessment [WWW Document]. URL https://www.unep.org/resources/publication/global-mercury-assessment-2018

UNEP, 2017. Minamata Convention on Mercury [WWW Document]. URL https://www.mercuryconvention.org/en/resources/minamata-convention-mercury-text-and-annexes

Wang, L., Hou, D., Cao, Y., Ok, Y.S., Tack, F.M.G., Rinklebe, J., O'Connor, D., 2020. Remediation of mercury contaminated soil, water, and air: A review of emerging materials and innovative technologies. Environ. Int. 134, 105281. https://doi.org/10.1016/j.envint.2019.105281

Wu, T., Wang, G., Zhang, Y., Kong, M., Zhao, H., 2017. Determination of mercury in aquatic systems by DGT device using thiol-modified carbon nanoparticle suspension as the liquid binding phase. New J. Chem. 41, 10305–10311. https://doi.org/10.1039/c7nj02007d

Zhang, H., Davison, W., 1995. Performance Characteristics of Diffusion Gradients in Thin Films for the in Situ Measurement of Trace Metals in Aqueous Solution. Anal. Chem. 67, 3391–3400. https://doi.org/10.1021/ac00115a005

Zhao, L., Zhang, Y., Wang, L., Lyu, H., Xia, S., Tang, J., 2022. Effective removal of Hg(II) and MeHg from aqueous environment by ball milling aided thiol-modification of biochars: Effect of different pyrolysis temperatures. Chemosphere 294. https://doi.org/10.1016/j.chemosphere.2022.133820

Publicación 4: *Supplementary information*

Evaluation of novel biomass-derived materials as binding layers for determining labile mercury in water by diffusive gradient in thin-film technique

Marrugo-Madrid, S.; Marrugo-Negrete, J.; Queralt, I.; Palet, C.; & Díez, S.

Enviado a la revista: Environmental Technology & Innovation,
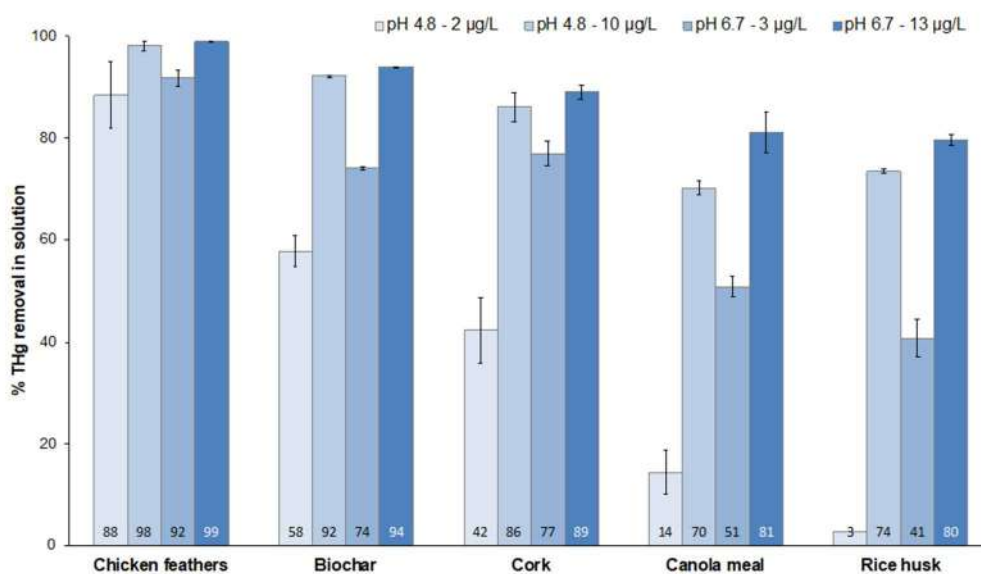
el 30 de mayo de 2023.

Figure S1. Total-Hg removal percentages in solution by biomass-derived materials (biochar, canola meal, chicken feathers, cork and rice husk) at different combination of pH (4.8 and 6.7) and initial Hg concentration in solution (2, 3, 10 and 13 μg L^{-1}).
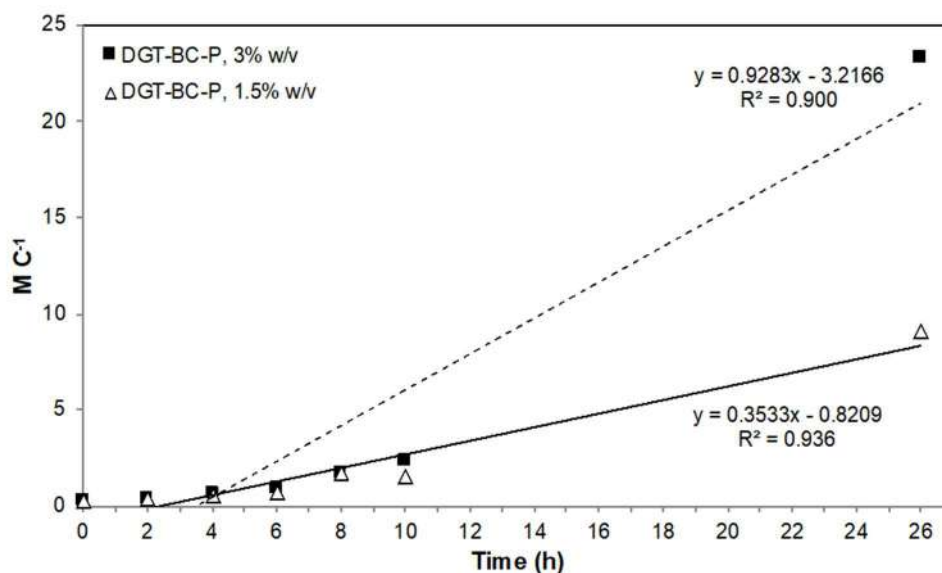

Figure S2. Comparison between the relations of Hg masses in the binding gel (M) and measured total Hg concentration in the solution (C) vs. deployment time for DGT devices assembled with biochar-polyacrylamide gels (BC-P) as binding layer and polyacrylamide gel as diffusive layer at 24.3 ± 0.5 °C. The DGT-BC-P devices were prepared at two ratios of 3% and 1.5% w/v of BC.
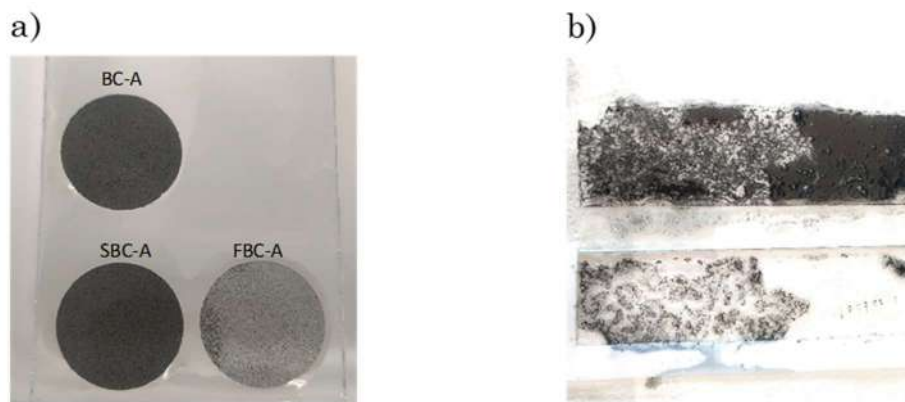
Figure S3. Photos of (a) binding gels made from BC, SBC and FBC with agarose gel solution at 1.5 w/v; and (b) the result of SBC with polyacrylamide gel solution at 1.5% w/v.

4.3.2. Publicación 5: Benzoylthiourea based polymers as new binding agents for diffusive gradients in thin films technique in labile mercury determination in freshwaters

Marrugo-Madrid, S., Fontàs, C., Kurt, G., Salazar-Camacho, C., Salas-Moreno, M., Gutiérrez-Mosquera, H., Marrugo-Negrete, J. Díez, S.

Benzoylthiourea based polymers as new binding agents for diffusive gradients in thin films technique in labile mercury determination in freshwaters

Siday Marrugo-Madrid [a], Clàudia Fontàs [b], Gülşah Kurt [c],
Carlos Salazar-Camacho [d], Manuel Salas-Moreno [d],
Harry Gutierrez-Mosquera [d], Jose Marrugo-Negrete [e], Sergi Díez [a,*]

[a] Environmental Chemistry Department, Institute of Environmental Assessment and Water Research,
IDAEA-CSIC, E-08034, Barcelona, Spain
[b] Department of Chemistry, University of Girona, C/Maria Aurèlia Capmany 69, 17003 Girona, Spain
[c] Department of Chemistry, Faculty of Arts and Sciences, Aksaray University, Aksaray, Turkey
[d] Faculty of Natural Sciences, Department of Biology, Technological University of Chocó, Quibdó, Colombia
[e] Department of Chemistry, Faculty of Sciences, University of Córdoba, Montería, Colombia

ARTICLE INFO

ABSTRACT

In this study, the diffusive gradient in thin film (DGT) has been developed using three new materials derived from benzoylthiourea (PBTU, BTP1 and BTP2) for the determination of bioavailable mercury (Hg). The efficiency of these DGT devices was compared with the well-established 3-mercaptopropyl functionalized silica gel (3MFS) in laboratory and field conditions. It was found that PBTU lacked of consistency for handling and assembling in the DGT device, whereas the other two polymers provided mechanically stable binding gels and extracted satisfactorily Hg. However, BTP2 showed no correlation between Hg uptake and Hg present in the aqueous solution, and therefore, BTP1 gels was chosen as the binding layer used for DGT technique. The calculated diffusion coefficient of DGT-BTP1 was 4.0×10^{-6} cm^2 s^{-1} at 25 °C in 0.8 mm thick diffusion layer and 2.3% w/v of material in gel, whereas for DGT-3MFS, the D value was 9.1×10^{-6} cm^2 s^{-1}. Moreover, it was found that neither the pH (range 4.5 – 9.5) nor the ionic strength (range 0.005–0.1 mol L^{-1}) significantly affected the binding behavior of Hg (p > 0.05). Finally, the DGT-BTP1 devices were successfully used for in-situ measurements of Hg in Quito River (Colombia), impacted by artisanal gold mining, and were compared with DGT-3MFS. Results showed a good performance with values of the labile Hg concentration between 5 to 8% of the total Hg in water. This study demonstrates that benzoylthiourea based DGT is a useful tool for in situ monitoring of Hg in freshwaters.

1. Introduction

Despite the fact that mercury (Hg) is one of the main pollutants in the world and its use has been discouraged since the Minamata Convention on Mercury (UNEP, 2017), this toxic metal is still widely used in artisanal and small-scale gold
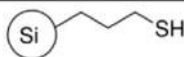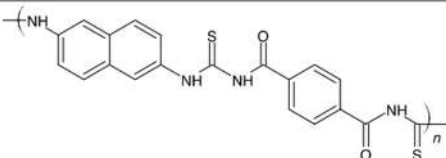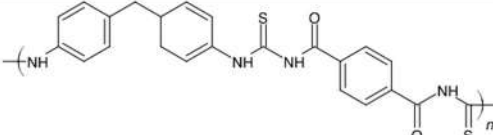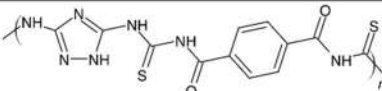
* Corresponding author.
  E-mail address: sergi.diez@idaea.csic.es (S. Díez).

S. Marrugo-Madrid, C. Fontàs, G. Kurt et al.

Environmental Technology & Innovation 28 (2022) 102911

Table 1
Chemical structures of the materials used in this study.

Name	Acronym	Chemical structure	Binding gel composition (% w/v)
3-Mercaptopropyl functionalized silica	3MFS		12
Poly(4-((2-aminonaphthalene-6-carbonothioyl) carbamoyl) benzoyl isothiocyanate)	BTP1		2.3
Poly(4-((4-(4-aminobenzyl) phenylcarbonothioyl) carbamoyl) benzoyl isothiocyanate)	BTP2		2.3
Polybenzoylthiourea polymer	PBTU		–

mining (ASGM) in which Hg amalgamation is used to extract gold from ore. As it has been reported recently (Marrugo-Madrid et al., 2022), to fulfill the objectives of this treaty, there is a need to perform sampling campaigns to monitor Hg contamination in remote ASGM areas (Palacios-Torres et al., 2018; Gutiérrez-Mosquera et al., 2021; Salazar-Camacho et al., 2021, 2017) where the diffusive gradient in thin-films (DGT) technique (Davison and Zhang, 1994) is useful.

The total concentration of Hg is the value commonly used to regulate contamination; however, measuring only the total concentration does not give a useful basis for the assessment of risks because toxicity is related to the concentration of bioavailable metal rather than the total concentration (Marrugo-Negrete et al., 2017; Turull et al., 2019).

The effectiveness of the application of the DGT technique as an analytical method for the determination of bioavailable Hg has been widely demonstrated in previous studies (Clarisse and Hintelmann, 2006; Diviš et al., 2010; Colaço et al., 2014; Fernández-Gómez et al., 2014; Turull et al., 2018; Bratkič et al., 2019; Elias et al., 2020; Marrugo-Madrid et al., 2022). This is based on the use of easily transportable passive sampling devices, which contain a binding layer (resin gel), a diffusion gel and a filter membrane, which protects the gels from the outside. Hg ions, due to a concentration gradient, diffuse through the filter membrane and diffusion gel, until they reach the binding layer, where they accumulate during a certain deployment time.

The 3-mercaptopropyl functionalized silica gel (3MFS) has been one of the most used resins for the preparation of binding layers, because its thiol groups have a high affinity towards Hg (Shade and Hudson, 2005; Clarisse and Hintelmann, 2006; Gao et al., 2011). However, it is important to continue evaluating the selective capacity of other materials with a high affinity for Hg, which could be less expensive and easily incorporated into the DGT technique, such as those derived from thiourea. Kurt (2021, 2019) synthesized polymeric compounds derived from benzoylthiourea that proved to have high thermal stability, resistance to external physical effects and capacity to Hg uptake.

Benzoylthioureas, due to their strong donor groups (carbonyl and thioamide), are promising as coordinating agents. Their ability to coordinate oxygen and sulfur atoms with metal has made them effective in analytical and environmental applications (Fontàs et al., 2005) (Table 1). When we compare the synthesized benzoylthiourea polymers, we observe that the naphthalene structure in BTP1 increases the stability of the complex and the acidity of the ligand, and the triazole heterocycle in PBTU increases the solubility of the polymer. The surfaces of all three polymers are homogeneous and dense (Kurt, 2021, 2019).

For the first time, this study evaluates the possible inclusion of different compounds derived from benzoylthiourea in a DGT passive sampling device. Therefore, the efficiency of DGT devices made of new polymeric materials was compared with 3MFS binding gels in laboratory conditions and in the field. Likewise, an evaluation of the effects of ionic strength and pH on the Hg uptake capacity of the binding layers obtained with the new materials was also carried out. Moreover, since there is a great interest to determine Hg bioavailability in rivers impacted by ASGM, we also evaluated their efficiency in the field.

2. Materials and methods

2.1. Reagents, gel preparation and mounting of DGT devices

The reagents, gel preparation and mounting of in-house manufactured DGT devices with 3MFS have been described in previous studies (Fernández-Gómez et al., 2011; Turull et al., 2017; Marrugo-Madrid et al., 2022). The different polymers

2

investigated as binding phase were: Poly (4-((2-aminonaphthalene-6-carbonothioyl) carbamoyl) benzoyl isothiocyanate) (BTP1), Poly (4-((4-(4-aminobenzyl) phenylcarbonothioyl) carbamoyl) benzoyl isothiocyanate) (BTP2) and a polybenzoylthiourea polymer (PBTU). These polymers were synthesized as described by Kurt (2021, 2019). Prior to their used, they were sieved at 0.125 mm. Table 1 shows the chemical characteristics and the binding gel composition for each compound. The diffusive gels were made with polyacrylamide (0.8 mm thickness). Finally, a nylon filter membrane (0.45 μm pore size) was used as the outer layer to protect the gels. The piston types with an exposure area of 3.14 cm^2 were used (DGT Research Ltd., UK) for assembling the DGT devices. All reagents used were of analytical grade and the solutions were prepared with Milli-Q water (18.25 MΩ cm).

2.2. Determination of the diffusion coefficient

The general procedure used to calculate the diffusion coefficients is described by Fernández-Gómez et al. (2011). In laboratory experiments, 16 DGT devices were deployed in 4 L of a Hg(II) solution at 2 μg L^{-1} in 0.01 M NaCl, in order to guarantee a constant ionic strength, and two DGTs were retrieved at different times (2 h, 4 h, 8 h, 10 h, 20 h, 30 h, 60 h and 72 h). The initial pH of the solution was 6.8, the temperature was 27 ± 0.5 °C, and the stir was constant throughout the experiment. Subsequently, the DGT devices were removed and dismantled to extract the binding layers and to determine the mass of Hg on a direct Hg analyzer DMA-80 Evo Milestone. Similarly, the concentrations of Hg(II) solution subsamples, withdrawn at the same time as each DGT device, were also determined with the DMA-80 Evo Milestone.

According Fick's law, the Hg(II) concentration in the solution (C_{DGT}) is equivalent to the relationship between the mass of Hg accumulated on binding layer (M), the diffusive layer thickness (Δg), the diffusion coefficient of the labile Hg (D), the area of exposed surface (A) and the deployment time (t):

$$C_{DGT} = \frac{M \Delta g}{DAt} \tag{1}$$

D can be calculated from the slope of the relationship between Hg accumulated by the DGT devices and the deployment time by Eq. (1). At different temperatures, it is possible to determine D using Stoke-Einstein's equation (Zhang and Davison, 1995).

The entire analytical procedure was validated by analysis of certified reference material (DOLT-5, dogfish liver) samples from the National Research Council of Canada (NRCC). The Hg concentration found in the DOLT-5 was 0.38 ± 0.10 mg kg^{-1} ($n = 5$), which was in good agreement to the certified value (0.44 ± 0.18 mg kg^{-1}) (mean recovery 86%). This reference material was analyzed in triplicate at the beginning and ends of each set of (usually 10) samples, to ensure the calibration of the instrument during the study. The detection limit (LOD) (0.2 ng mL^{-1} of Hg) was calculated based a series of blank samples.

2.3. Effect of ionic strength and pH on the Hg uptake

DGT devices were deployed in triplicate in Hg(II) solutions at 3 μg L^{-1} with NaCl at different concentrations: 0.005, 0.01 and 0.1 M, in order to evaluate the effect of ionic strength on Hg(II) uptake. The mean initial pH of the solutions was 4.50 ± 0.03, and the mean temperature was 21.5 ± 0.5 °C. Constant stirring was maintained during the 6 h that DGTs were immersed in the solutions.

To evaluate the effect of pH, the DGT devices were again deployed in triplicate in Hg(II) solutions at 3 μg L^{-1} with 0.01M NaCl, and different initial pH (4.5, 6.5, 8.0 and 9.5) previously adjusted with NaOH or HNO$_3$, with a pH-meter GLP 22 Crison. The mean temperature of the solutions was 21.5 ± 0.5 °C, and constant stirring was maintained during 6 h. All DGT devices were removed and dismantled to extract the binding layers and determine the mass of Hg on a direct Hg analyzer DMA-80 Evo Milestone.

2.4. Deployment of the DGT devices in field

The DGT devices manufactured with either 3MFS or BTP1 binding layers were deployed in triplicate at 6 stations in Quito River, tributary of the Atrato River, Colombia (Marrugo-Madrid et al., 2022). Field deployment time was around 92 h, and temperature, pH, dissolved oxygen (DO), conductivity, total dissolved solids (TDS), turbidity, and total mercury concentration in water were determined at the start and end of each deployment with an YSI Pro2030 multiparameter. Furthermore, at each sampling site, a freshwater sample was taken, and 3 DGT devices from the same batch were chosen as traveling blank or "control".

After recovering the DGT devices, they were rinsed with Milli-Q water and returned to individual polythene bags for its conservation. All samples were preserved, transported to the laboratory and refrigerated at 4 °C until analyzed. In Colombia, also a DMA-80 Evo Milestone was used for the determination of the Hg concentration in binding layers from DGT devices and a certified reference material from International Atomic Energy Agency (IAEA-336 Lichen Hg: 0.16–0.24 mg kg^{-1}), and a Liquid Mercury Analyzer RA-915M/RP92 Lumex was used in the measurement of Hg in freshwater samples.
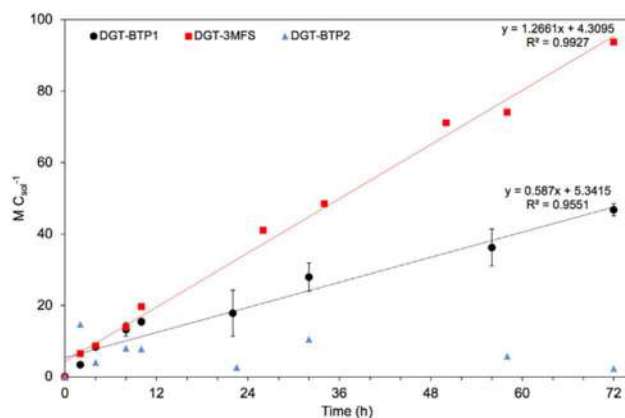
3

Fig. 1. Comparison between the relations of mass of Hg in the binding gel (M) and concentration in the solution (C_{sol}) vs. the time for BTP1, BTP2 and 3MFS DGT devices.

3. Results and discussion

3.1. Comparison of different benzoylthiourea derivative materials

Three different benzoylthiourea derivative materials were tested to prepare stable binding layers. The main difference between PBTU, BTP1, and BTP2 polymers (Table 1) is the triazole unit in the chemical structure of PBTU, which makes it soluble in polar organic solvents, including DMSO and DMF, in contrast with BTP1 and BTP2, which are insoluble in any organic solvent (Kurt, 2021).

The manufacture of the binding gels with three new polymeric materials BTP1, BTP2 and PBTU was done in a similar manner as for DGT-3MFS, according to Fernández-Gómez et al. (2011). In the original procedure, the binding gel of DGT-3MFS is mixed with a polyacrylamide gel solution at a ratio of 12% w/v. Nevertheless, applying the same w/v ratio to the new polymeric materials, it was not possible to obtain stable gels with a similar shape to those of DGT-3MFS. Then, we reduced the amount of mass from the new polymeric materials until we found satisfactory results with the ratio of 2.3% w/v for BTP1 and BTP2. For PBTU, possibly due to its high solubility in organic solvents (Kurt, 2021), it was not possible to obtain a gel with an adequate texture and thickness for its subsequent handling and inclusion in the DGT device, so it was discarded for the following tests (Figure S1).

3.2. Diffusion coefficient of Hg in benzoylthiourea derivative gels discs

Manufactured DGT devices must be calibrated under controlled conditions of temperature, pH and concentration of both Hg(II) and NaCl in solution, in order to determine their diffusion coefficients by applying Fick's Law (Eq. (1)). According the Stoke-Einstein's equation (Zhang and Davison, 1995), D values at 25 °C for DGT-BTP1 and DGT-3MFS devices were 4.0×10^{-6} and 9.1×10^{-6} cm^2 s^{-1}, respectively. Moreover, calibration test for DGT-BTP2 was also performed, however no correlation was obtained between the Hg amount uptake and deployment time, confirming that BTP2 binding gels are not able to be used as binding gels (Fig. 1).

Even though the D of DGT-BTP1 is about 2-times lower than for DGT-3MFS devices, they are at the same order of magnitude (10^{-6}), which are closer to reported D values (Dočekalová and Diviš, 2005; Clarisse and Hintelmann, 2006; Fernández-Gómez et al., 2011; Gao et al., 2011; Pelcová et al., 2014; Turull et al., 2017). Furthermore, it is possible that the difference in D between DGT-BTP1 and DGT-3MFS devices may be due to the w/v ratio of BTP1 binding gels that is almost fivefold lower than the w/v ratio used to prepare the 3MFS binding gels. Fig. 1 shows the comparison between both calibrations for DGT-BTP1 and DGT-3MFS devices. A linear relationship was observed in both DGT devices, with very good R^2 correlation coefficients (0.993 for DGT-3MFS and 0.955 for DGT-BTP1). The difference between the D values may indicate that 3MFS has a higher affinity/selectivity for Hg than the BTP1 material, which may, in turn, be influenced by the simplicity of its chemical structure compared to that of BTP1 (Table 1). A comparison of the recently found D values for 3MFS and BTP1 with values already reported in the literature is shown in Table 2.

3.3. Effect of ionic strength and pH on Hg uptake

Fig. 2 shows the average values of the ratio between the concentrations in solution, calculated from the mass of Hg in the binding gels of DGT-BTP1 devices (C_{DGT}), and the Hg concentration in solution after 6 h (C_{sol}). The C_{DGT}/C_{sol} range was between 0.80–1.12 in the evaluated range, at different ionic strengths, with a good performance and a little dispersion at

4

Table 2
Comparison between diffusion coefficients (D) reported for Hg(II) in BTP1 vs. resins based on thiol groups.

Binding gel	Diffusive gel	Medium	pH	T (C)	D ($\times 10^{-6}$; cm^2 s^{-1})	
BTP1	Polyacrylamide	0.01 M NaCl	6.8	25	3.95	This study
3MFS	Polyacrylamide	0.01 M NaCl	6.8	25	9.08	This study
Spheron-Thiol	Agarose	0.01 M NaNO$_3$	5.0	–	9.13	Dočekalová and Diviš (2005)
Spheron-Thiol	Agarose	0.01 M NaCl	7.0	21.5	4.41	Fernández-Gómez et al. (2011)
3MFS	Agarose	0.01 M NaCl	7.0	21.5	3.86	
3MFS	Polyacrylamide	0.01 M NaCl	7.0	21.5	2.84	
	Agarose	0.01 M NaNO$_3$	5.0	20	8.44	Gao et al. (2011)
3MFS	Agarose	0.01 M NaNO$_3$	7.0	–	4.48	Hong et al. (2011)
3MFS	Agarose	0.01 M NaCl	7.7	–	4.04	
Ambersep GT74	Agarose	0.01 M NaNO$_3$	5.0	25	9.07	Pelcová et al. (2014)
3MFS	Polyacrylamide	0.01 M NaCl	–	20.5	1.59	Turull et al. (2017)
3MFS	Polyacrylamide	0.01 M NaCl	7.0	20	3.08	Turull et al. (2019)

BTP1: Poly (4-((2-aminonaphthalene-6-carbonothioyl) carbamoyl) benzoyl isothiocyanate)
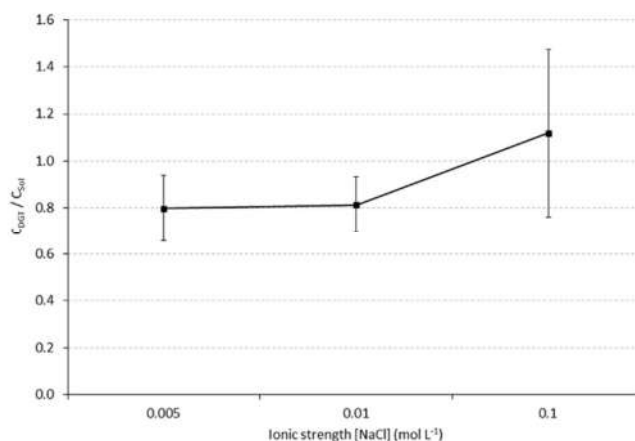3MFS: 3-mercaptopropyl functionalized silica gel.

Fig. 2. Effect of ionic strength on Hg uptake by DGT-BPT1 devices. Deployment solution: 3.0 μg L^{-1} of Hg(II) at 21.5 °C and initial pH: 4.5.

ionic strength $\leq$ 0.01M. Although at an ionic strength of 0.1 M, the average performance could also be considered suitable, there is a greater dispersion between the measurements, which could reduce the efficiency of the DGT-BTP1 devices in water bodies with a high ionic strength, such as seawater.

The pH is one of the factors that influence the formation of mercuric species in natural waters, so it is also very important to evaluate its influence in the application of DGT devices. The effect of pH on Hg uptake was also tested in triplicate in solutions of 3.0 μg L^{-1} of Hg(II) and 0.01 M of NaCl. Fig. 3 shows the average values of the ratio between C_{DGT} and C_{sol}, obtained after 6 h. The C_{DGT}/C_{sol} range was between 0.72–0.96, at different pH, evidencing that DGT-BPT1 devices are not sensitive to variations in pH ($p > 0.05$). The Hg uptake results were better at acidic pH (4.5) and good at slightly acidic pH (6.5), and, therefore, this binding phase is suitable for Hg uptake at the typical pH of natural waters. Moreover, the dispersion between the measurements was minimal in all cases, which could be interpreted as a good efficiency of the devices in the absorption of labile Hg.

3.4. Deployment of the DGT devices in field

According to the previous results obtained in the laboratory for the DGT-BTP1 devices, we also evaluated their efficiency in the field, making a comparison with the DGT-3MFS devices under equal deployment conditions. Sampling was carried out in the Quito River, at 6 stations impacted by gold mining activities, for approximately 92 h. The mean values $\pm$ SD of temperature, pH, DO, conductivity, TDS, turbidity, and total mercury concentration in water (THg) are shown in Table S1. Labile Hg concentrations calculated from DGT-3MFS and DGT-BTP1 devices and THg in freshwater are shown in Fig. 4. Labile Hg concentrations calculated from both types of DGT devices were similar in most stations, with no statistically significant differences between them ($p > 0.05$). In turn, these values of labile mercury represented between 5 to 8% of the total Hg in water. The results showed a good performance of the DGT-BTP1 devices, which makes them a useful tool for in situ monitoring of Hg in freshwater.
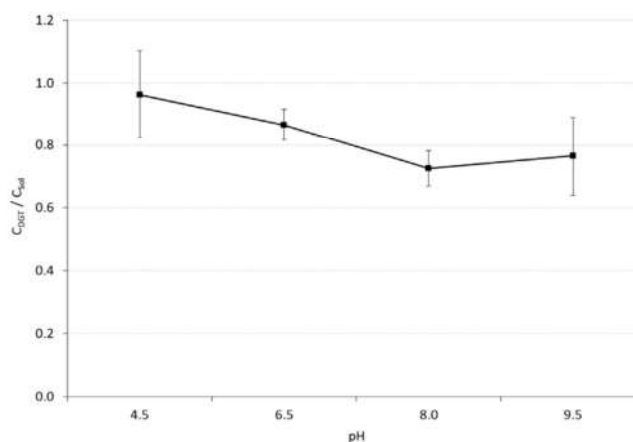
5

Fig. 3. Effect of pH on Hg uptake by DGT-BPT1 devices. Deployment solution: 3.0 μg L^{-1} of Hg(II) and 0.01M of NaCl at 21 °C.
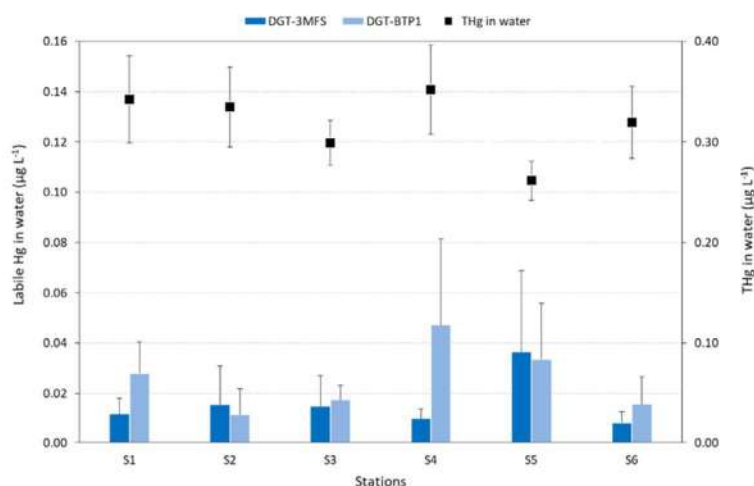

Fig. 4. Comparison between labile Hg concentrations calculated from DGT-3MFS, DGT-BTP1 devices and the total mercury concentration in freshwater (THg).

4. Conclusions

The proposed DGT method using benzoylthiourea as a binding agent and polyacrylamide gel as a diffusive layer was effective for the determination of labile Hg species, showing a strong linear correlation between the accumulated Hg mass and the deployment time. The polyacrylamide DGT-BTP1 was suitable for aqueous solutions with a wide pH range (4.5–7.5), and ionic strength in the range between 0.005 M and 0.01 M; however, it may not be suitable at aqueous solutions with ionic strength close to 0.1 mol L^{-1}, due to the dispersion of measured accumulations Regarding the field deployment, this new DGT showed as a useful tool for bioavailable Hg determination in river water, with matching results with other devices assembled with 3-mercaptopropyl, that have already been proved a high performance in freshwater deployments.

CRediT authorship contribution statement

Siday Marrugo-Madrid: Writing – original draft, Investigation, Formal analysis, Methodology. **Clàudia Fontàs:** Conceptualization, Funding acquisition, Review. **Gülşah Kurt:** Synthesis of new resins. **Carlos Salazar-Camacho:** Support during sampling campaign. **Manuel Salas-Moreno:** Transport and support during sampling campaign. **Harry Gutierrez-Mosquera:** Transport and support during sampling campaign, Contact to local sites. **Jose Marrugo-Negrete:** Conceptualization, Funding acquisition. **Sergi Díez:** Supervision, Conceptualization, Funding acquisition, Writing – review & editing.

Declaration of competing interest

The authors declare that they have no known competing financial interests or personal relationships that could have appeared to influence the work reported in this paper.

Data availability

Data will be made available on request.

Acknowledgments

Appendix A. Supplementary data

Supplementary material related to this article can be found online at https://doi.org/10.1016/j.eti.2022.102911.

References

Bratkič, A., Klun, K., Gao, Y., 2019. Mercury speciation in various aquatic systems using passive sampling technique of diffusive gradients in thin-film. Sci. Total Environ. 663, 297–306. http://dx.doi.org/10.1016/j.scitotenv.2019.01.241.

Clarisse, O., Hintelmann, H., 2006. Measurements of dissolved methylmercury in natural waters using diffusive gradients in thin film (DGT). J. Environ. Monit 8, 1242–1247. http://dx.doi.org/10.1039/b614560d.

Colaço, C.D., Yabuki, L.N., Rolisola, A.M., Menegário, A.A., de Almeida, E., Suárez, C.A., Gao, Y., Corns, W.T., do Nascimento Filho, V.F., 2014. Determination of mercury in river water by diffusive gradients in thin films using P81 membrane as binding layer. Talanta 129, 417–421. http://dx.doi.org/10.1016/j.talanta.2014.05.025.

Davison, W., Zhang, H., 1994. In situ speciation measurements of trace components in natural waters using thin-film gels. Nature 367, 546–548.

Diviš, P., Szkandera, R., Dočekalová, H., 2010. Characterization of sorption gels used for determination of mercury in aquatic environment by diffusive gradients in thin films technique. Cent. Eur. J. Chem. 8, 1103–1107. http://dx.doi.org/10.2478/s11532-010-0090-3.

Dočekalová, H., Diviš, P., 2005. Application of diffusive gradient in thin films technique (DGT) to measurement of mercury in aquatic systems. Talanta 65, 1174–1178. http://dx.doi.org/10.1016/j.talanta.2004.08.054.

Elias, G., Díez, S., Zhang, H., Fontàs, C., 2020. Development of a new binding phase for the diffusive gradients in thin films technique based on an ionic liquid for mercury determination. Chemosphere 245, http://dx.doi.org/10.1016/j.chemosphere.2019.125671.

Fernández-Gómez, C., Bayona, J.M., Díez, S., 2014. Comparison of different types of diffusive gradient in thin film samplers for measurement of dissolved methylmercury in freshwaters. Talanta 129, 486–490. http://dx.doi.org/10.1016/j.talanta.2014.06.025.

Fernández-Gómez, C., Dimock, B., Hintelmann, H., Díez, S., 2011. Development of the DGT technique for Hg measurement in water: Comparison of three different types of samplers in laboratory assays. Chemosphere 85, 1452–1457. http://dx.doi.org/10.1016/j.chemosphere.2011.07.080.

Fontàs, C., Hidalgo, M., Salvadó, V., Anticó, E., 2005. Selective recovery and preconcentration of mercury with a benzoylthiourea-solid supported liquid membrane system. Anal. Chim. Acta 547, 255–261. http://dx.doi.org/10.1016/j.aca.2005.05.044.

Gao, Y., Canck, E.De., Leermakers, M., Baeyens, W., Van Der Voort, P., 2011. Synthesized mercaptopropyl nanoporous resins in DGT probes for determining dissolved mercury concentrations. Talanta 87, 262–267. http://dx.doi.org/10.1016/j.talanta.2011.10.012.

Gutiérrez-Mosquera, H., Marrugo-Negrete, J., Díez, S., Morales-Mira, G., Montoya-Jaramillo, L.J., Jonathan, M.P., 2021. Mercury distribution in different environmental matrices in aquatic systems of abandoned gold mines, Western Colombia: Focus on human health. J. Hazard. Mater. 404, http://dx.doi.org/10.1016/j.jhazmat.2020.124080.

Hong, Y.S., Rifkin, E., Bouwer, E.J., 2011. Combination of diffusive gradient in a thin film probe and IC-ICP-MS for the simultaneous determination of CH3Hg+ and Hg2+ in oxic water. Environ. Sci. Technol. 45 (15), 6429–6436.

Kurt, G., 2019. Synthesis of new poly-benzoylthiourea and thermal and surface properties. J. Polym. Res. 26, 1–10. http://dx.doi.org/10.1007/s10965-019-1845-y.

Kurt, G., 2021. Mechanical, thermal and surface properties of a new kind of polybenzoylthiourea. Düzce üniv. Bilim Ve Teknol. Derg. 9, 1927–1935. http://dx.doi.org/10.29130/dubited.878203.

Marrugo-Madrid, S., Salas-Moreno, M., Gutiérrez-Mosquera, H., Salazar-Camacho, C., Marrugo-Negrete, J., Díez, S., 2022. Assessment of dissolved mercury by diffusive gradients in thin films devices in abandoned ponds impacted by small scale gold mining. Environ. Res. 208, http://dx.doi.org/10.1016/j.envres.2021.112633.

Marrugo-Negrete, J., Pinedo-Hernández, J., Díez, S., 2017. Assessment of heavy metal pollution, spatial distribution and origin in agricultural soils along the Sinú River Basin. Colombia. Environ. Res. 154, 380–388.

Palacios-Torres, Y., Caballero-Gallardo, K., Olivero-Verbel, J., 2018. Mercury pollution by gold mining in a global biodiversity hotspot, the choco biogeographic region, Colombia. Chemosphere 193, 421–430. http://dx.doi.org/10.1016/j.chemosphere.2017.10.160.

Pelcová, P., Dočekalová, H., Kleckerová, A., 2014. Development of the diffusive gradient in thin films technique for the measurement of labile mercury species in waters. Anal. Chim. Acta 819, 42–48. http://dx.doi.org/10.1016/J.Aca.2014.02.013.

Salazar-Camacho, C., Salas-Moreno, M., Marrugo-Madrid, S., Marrugo-Negrete, J., Díez, S., 2017. Dietary human exposure to mercury in two artisanal small-scale gold mining communities of northwestern Colombia. Environ. Int. 107, http://dx.doi.org/10.1016/j.envint.2017.06.011.

Salazar-Camacho, C., Salas-Moreno, M., Paternina-Uribe, R., Marrugo-Negrete, J., Díez, S., 2021. Mercury species in fish from a tropical river highly impacted by gold mining at the Colombian Pacific region. Chemosphere 264, http://dx.doi.org/10.1016/j.chemosphere.2020.128478.

Shade, C.W., Hudson, R.J.M., 2005. Determination of MeHg in environmental sample matrices using Hg - Thiourea complex ion chromatography with on-line cold vapor generation and atomic fluorescence spectrometric detection. Environ. Sci. Technol. 39, 4974–4982. http://dx.doi.org/10.1021/es0483645.

Turull, M., Elias, G., Fontàs, C., Díez, S., 2017. Exploring new DGT samplers containing a polymer inclusion membrane for mercury monitoring. Environ. Sci. Pollut. Res. 24, 10919–10928. http://dx.doi.org/10.1007/s11356-016-6813-z.

Turull, M., Fontàs, C., Díez, S., 2019. Conventional and novel techniques for the determination of hg uptake by lettuce in amended agricultural peri-urban soils. Sci. Total Environ., volume=668, pages=40–46, doi=10.1016/J.Scitotenv.2019.02.244,.

Turull, M., Komarova, T., Noller, B., Fontàs, C., Díez, S., 2018. Evaluation of mercury in a freshwater environment impacted by an organomercury fungicide using diffusive gradient in thin films. Sci. Total Environ. 621, 1475–1484. http://dx.doi.org/10.1016/j.scitotenv.2017.10.081.

UNEP, 2017. Minamata convention on mercury. pp. 1–67.

Zhang, H., Davison, W., 1995. Performance-characteristics of diffusion gradients in thin-films for the in-situ measurement of trace-metals in aqueous-solution. Anal. Chem. 67, 3391–3400. http://dx.doi.org/10.1021/ac00115a005.

Publicación 5: *Supplementary information*

Benzoylthiourea based polymers as new binding agents for diffusive gradients in thin films technique in labile mercury determination in freshwaters

Marrugo-Madrid, S., Fontàs, C., Kurt, G., Salazar-Camacho, C., Salas-Moreno, M., Gutiérrez-Mosquera, H., Marrugo-Negrete, J. Díez, S.

Figure S1. Photos of binding gels made from three polymeric materials derived from benzoylthiourea (PBTU, BTP1 and BTP2) mixed with a polyacrylamide gel solution at a ratio of 2.3% w/v

Table S1. Mean values ± standard deviation (SD) of physic-chemical parameter: Temperature (^{o}C), pH, dissolved oxygen (DO), conductivity, total dissolved solids (TDS), turbidity, and total mercury concentration in water (THg).

Station	N	W	T (^{o}C)	pH	DO (mg L^{-1})	Conductivity (mS cm^{-1})	TDS (mg L^{-1})	Turbidity (NTU)	THg in water (µg L^{-1})
S1	5°53.1'57.9"	76°45'22.6"	25.3 ± 0.2	8.2 ± 0.0	7.78 ± 0.26	9.5 ± 0.7	1.7 ± 0.1	253 ± 18	0.342 ± 0.043
S2	5°37'49.1"	76°44'10.5	25.5 ± 0.1	7.1 ± 0.3	6.88 ± 0.04	11.5 ± 0.7	2.0 ± 0.1	258 ± 81	0.335 ± 0.040
S3	5°39'58.8"	76°42'32.3"	25.6 ± 0.1	6.6 ± 0.5	5.93 ± 0.78	12.0 ± 1.4	1.7 ± 0.1	255 ± 95	0.299 ± 0.022
S4	5°40'46.4"	76°40'37.8"	25.7 ± 0.1	7.2 ± 0.3	5.60 ± 0.21	12.5 ± 2.1	1.6 ± 0.1	264 ± 136	0.352 ± 0.044
S5	5°40'50.3"	76°39'49.3	24.3 ± 0.5	7.2 ± 0.4	6.26 ± 0.23	29.0 ± 12.7	2.0 ± 0.3	394 ± 45	0.262 ± 0.020
S6	5°42'28.3"	76°40.19.5"	25.2 ± 0.6	7.5 ± 0.3	5.45 ± 0.76	13.5 ± 3.5	2.1 ± 0.6	322 ± 2	0.320 ± 0.036

4.4. Discusión

La técnica DGT es una herramienta efectiva de la química analítica utilizada para la medición de la concentración Hg lábil (fracción biodisponible) en diversas matrices ambientales. La búsqueda, evaluación e implementación de nuevos materiales en la técnica DGT juegan un papel fundamental en el desarrollo y mejora continua de esta técnica, ya que la selectividad y la sensibilidad dependen en gran medida de la elección de los materiales adecuados.

A su vez, la búsqueda de nuevos materiales implica investigar y explorar diversos compuestos, tales como resinas, geles, membranas, entre otros. En el caso de los materiales elegidos para integrar la capa de unión, estos deben tener una alta afinidad y capacidad de retención para el Hg, al tiempo de que su homogeneización y preparación sean relativamente sencillas. Estos dos aspectos fueron fundamentales para el enfoque que se le dió a los artículos presentados en este capítulo.

De igual manera, es importante desarrollar los experimentos necesarios para determinar la eficiencia de los materiales en la captación y acumulación del Hg, y una vez se haya elegido un material potencialmente válido, se procede a la manufacturación de dispositivos DGT. Para ello se utiliza el material seleccionado, y se realizan ensayos de serie temporal para determinar el coeficiente de difusión (D) de los dispositivos, evaluando la optimización de

las condiciones experimentales (temperatura, fuerza iónica, pH, interferencias químicas) para garantizar mediciones precisas y reproducibles.

En esta tesis doctoral se realizaron diversos análisis de materiales de biomasa residual (plumas de pollo, biocarbón, corcho, cáscara de canola y cáscara de arroz) y polímeros derivados de benzoiltiourea (PBTU, BTP1 y BTP2) (ver las estructuras químicas en la Tabla 1 de la publicación Marrugo-Madrid et al. 2022) para evaluar sus propiedades físicas y químicas relevantes en relación a su aplicabilidad en la técnica DGT.

Como se menciona en el primer artículo de este capítulo, los materiales derivados de biomasa que mostraron resultados prometedores en términos de su capacidad de absorción de Hg fueron las plumas, seguidas del biocarbón y el corcho. No obstante, se encontraron muchas dificultades en el tratamiento de las plumas durante los ensayos de homogeneización, debido a su incapacidad de reducir su tamaño y obtener una suspensión homogénea en las soluciones de agarosa o poliacrilamida.

En contraste, el biocarbón base (BC) pudo ser fácilmente macerado y tamizado, adquiriendo una apariencia en forma de un polvo fino similar a la de los polímeros BTP1, BTP2 y PBTU. La pirólisis con S de nuestro BC se realizó con el objetivo de mejorar su afinidad por el Hg, obteniendo un nuevo biocarbón sulfurado (SBC). En las pruebas de preparación de hidrogeles, observamos que la manipulación de los biocarbones BC y SBC era sencilla, por lo que consideramos pirolizar las plumas obteniendo un nuevo biocarbón

(FBC). La homogenización (macerado y tamizado) de los tres biocarbones estudiados (BC, SBC y FBC) se realizó de manera óptima.

Con el fin de verificar la retención de azufre en la estructura de nuestro biocarbón, se utilizó la espectrometría de fluorescencia de rayos X de dispersión de energía (EDXRF). Se compararon muestras de biocarbón original (BC), biocarbón sulfurado (SBC) y una mezcla no pirolizada de BC y S en una proporción de 1:1. El espectro resultante se incluye en la Publicación 4 y muestra un claro aumento de la cantidad de S en el biocarbón modificado respecto al original. Previamente se habían considerado otras técnicas analíticas no destructivas disponibles en el centro, como la espectroscopía infrarroja por transformada de Fourier (FT-IR). Sin embargo, en los espectros obtenidos resultó difícil determinar la señal correspondiente a la presencia de S en las muestras de biocarbones.

En los ensayos de preparación de hidrogeles, se encontró que el polímero PBTU, al carecer de propiedades hidrofóbicas, no pudo generar geles con una consistencia adecuada en ninguno de los ensayos realizados. Mientras, el carácter altamente hidrofóbico tanto de los biocarbones BC, SBC y FBC como los polímeros BTP1 y BTP2, permitieron la formación de geles con una consistencia adecuada para ser cortados y montados como dispositivos DGT, siempre que la cantidad de material en la solución agarosa o poliacrilamida no superara el 3% m/v (masa/volumen). En contraste con el protocolo de preparación de geles de resina 3MFS, que implica una relación de 12% m/v, ninguno de los biocarbones investigados ni los polímeros de benzoiltiourea

demostraron capacidad para gelificar a dicha proporción, lo cual indica una sobresaturación de los geles a tales relaciones. La figura 19 muestra la preparación de geles de unión usando los materiales estudiados.

Figura 20. (A) Biocarbón obtenido a partir de plumas (FBC) para posterior preparación de geles de unión. (B) Preparación de dispositivos DGT-SBC. (C) Preparación de geles de unión con BTP1.

La reducción de las relaciones m/v (1,5% m/v para BC, FBC y SBC/gel de agarosa y 2,3% m/v para BTP1 y BTP2/gel de poliacrilamida) en comparación

con las utilizadas en la preparación de dispositivos DGT con 3MFS (12% m/v en gel de poliacrilamida), no afectaron la eficiencia en la capacidad de captar Hg.

A diferencia de 3MFS y BTP1, que fueron sintetizados para tener una alta afinidad con el Hg, los biocarbones BC, SBC y FBC no son específicos para captar Hg, sino que también pueden mostrar afinidad por otros metales presentes en el medio. Es por esto que para los biocarbones BC, SBC y FBC se llevaron a cabo ensayos de serie temporal en ausencia y presencia de otros metales que pudieran competir con el Hg por los sitios de sorción. Los ensayos de serie temporal permitieron realizar la calibración de los dispositivos y evaluar su eficiencia. Los D a 25 ºC fueron: $5,2\times10^{-6}$ cm^2 s^{-1} para los dispositivos DGT-SBC y $4,0\times10^{-6}$ cm^2 s^{-1} para los dispositivos DGT-BTP1. El orden de magnitud de los D fue similar a los reportados en la literatura, mientras que se observó una fuerte correlación lineal en los resultados obtenidos con dispositivos DGT-SBC (R^2: 0,94) y DGT-BTP1 (R^2: 0.96).

Esta reducción de la cantidad de material usado en la preparación de geles de unión implica una mejora significativa en la relación eficiencia/viabilidad económica, considerando que para la implementación en campo se requiere la manufacturación a gran escala de estos dispositivos, estimando un mínimo de tres dispositivos por cada sitio de muestreo, además de los dispositivos adicionales necesarios para el control de blancos.

Por tanto, uno de los resultados más destacados de este capítulo es la demonstración de dos nuevos materiales con un gran potencial para su

aplicación en la técnica DGT: biocarbón sulfurado (SBC) y el polímero Poli(4-((2-aminonaftaleno-6-carbonotioil) carbamoil) isotiocianato de benzoilo) (BTP1) sintetizado por Kurt (2019).

El biocarbon es un material derivado de la biomasa bastante asequible y de bajo costo, y la modificación de éstos con compuestos azufrados y otros afines al Hg pueden mejorar su capacidad de captación del metal. Los resultados de este capítulo abren la posibilidad de incorporar en la técnica DGT otros tipos de biocarbones modificados con demostrada afinidad por el Hg, tal como grupos tioles (SH), cistenía (Cys), selenio (Se) o Quitosano (también conocido como Chitosán) (Li et. al., 2017; Park et. al., 2019; Li et. al., 2021; Shi et. al., 2022). Sin embargo, es importante tener en cuenta que el proceso de pirólisis con sulfuro debe llevarse a cabo bajo condiciones cuidadosamente controladas para asegurar que el S no se volatilice por completo y el procedimiento se realice en vano.

Considerando la importancia que tienen las diferentes variables fisicoquímicas como pH y fuerza iónica del medio acuático, es importante la evaluación del rendimiento de los dispositivos DGT a diferentes condiciones de estas variables. En el caso del material BTP1, se encontró que la eficiencia de los dispositivos DGT-BTP1 en la captación de Hg lábil en medio acuoso no se vio significativamente afectada por las variaciones de fuerza iónica y el pH. Además, se observó que la eficiencia de los dispositivos DGT-BTP1 en su aplicación en campo fue comparable a los DGT-3MFS, dispositivos que han demostrado una alta fiabilidad en multitud de estudios previos.

En relación a la inclusión de los biocarbones investigados en la técnica DGT, se ha logrado incorporar biocarbones derivados de la biomasa residual y modificados con S en esta técnica para la determinación de Hg lábil. Esta incorporación representa una oportunidad para la valorización de residuos agrícolas en función de su capacidad para el análisis y monitoreo del Hg biodisponible en sistemas acuáticos. En consecuencia, esta tesis doctoral establece una base sólida para futuras investigaciones, algunas de las cuales podrían dar continuidad a este estudio mediante la evaluación de la eficiencia de los dispositivos DGT-SCB en diferentes niveles de pH y fuerza iónica, y su posterior aplicación en campo.

CAPÍTULO 5: Conclusiones

5.1. Conclusiones medioambientales

Las conclusiones de esta tesis doctoral concernientes a la dinámica de la contaminación por Hg asociado al impacto de la MAPE se presentan a continuación:

- Se determinaron las concentraciones de Hg en aguas, pescados, frutas y tubérculos procedentes de zonas afectadas por la MAPE en la cuenca del río Atrato, en el departamento de Chocó. Las concentraciones de Hg y As mostraron variaciones dependiendo del tipo de alimento, con valores por debajo de los límites permitidos establecidos internacionalmente para alimentos contaminantes y reportados en otras regiones del mundo.

- Se observó que los riesgos acumulativos de Hg y As a través del consumo de frutas, tubérculos y pescado superaron el nivel aceptable (HI > 1), lo que indica un riesgo potencial no cancerígeno para la salud de los consumidores.

- En el caso de todos los alimentos evaluados (frutas, tubérculos y pescado), el riesgo carcinogénico debido al As superó el límite aceptable, lo que indica un riesgo potencial de cáncer asociado a la exposición al As a través del consumo de alimentos.

- Se desaconseja el consumo de plátanos, debido a su alta concentración de As (aproximadamente 174 µg kg^{-1}) y especialmente debido al hábito alimenticio de consumir grandes cantidades (alrededor de 500 g/día).

- El aumento en la ingesta de Hg y As en la dieta puede contribuir al desarrollo de diversos trastornos sistémicos, por tanto, es necesario controlar estos contaminantes mediante la implementación de buenas prácticas agrícolas y una clara política que respalde y oriente las acciones de seguridad alimentaria y nutrición, y alineadas con el cumplimiento de los ODS.

- En cuanto a la determinación de las fracciones biodisponibles de Hg, Pb, Cu, Zn, Cd, Ni, Mn y Cr en la cuenca del río Atrato, se encontró que las concentraciones de Hg lábil en el río Atrato fueron más altas en los sitios cercanos a las operaciones mineras en comparación con los sitios de muestreo alejados de las actividades de la MAPE. Además, se encontraron altas concentraciones de Ni, Cu y Zn lábiles.

- En promedio, las concentraciones de Hg total lábil en las AMPs fueron un 50% más altas que en el río Atrato. No obstante, no se encontraron diferencias significativas entre las concentraciones de Hg lábil en las AMPs, lo que sugiere que la biodisponibilidad no está asociada con su tiempo de abandono.

- La obtención de datos precisos, fiables y actualizados sobre el consumo de alimentos y la biodisponibilidad de Hg y otros elementos potencialmente tóxicos, desempeña un papel fundamental en la evaluación de riesgos, ya que permite calcular la exposición de los consumidores a posibles peligros derivados del impacto de la MAPE en la región.

5.2. Conclusiones analíticas

Las conclusiones de esta tesis doctoral referentes a la inclusión de nuevos materiales poliméricos y derivados de la biomasa residual agrícola en la técnica DGT para la determinación de Hg lábil, se presentan a continuación:

- El biocarbón, las plumas y el corcho fueron los materiales derivados de biomasa que exhibieron una capacidad óptima de remoción de Hg en agua con porcentajes máximos de 99%, 94% y 90%, respectivamente. Para mejorar la afinidad del biocarbón original por el Hg, se sometió a pirólisis con S, resultando en la preparación de biocarbón sulfurado (SBC). Por otro lado, las plumas se pirolizaron en condiciones controladas para preservar los grupos tioles de su estructura, lo que dio lugar a la preparación de biocarbón de plumas (FBC). Estas modificaciones fueron confirmadas por EDXRF obteniendo buenos resultados.

- Los dispositivos DGT manufacturados con BC y SBC en agarosa fueron exitosos para la determinación de Hg lábil en condiciones experimentales controladas, mostrando una buena correlación de linealidad entre la absorción de Hg y el tiempo de despliegue.

- Los coeficientes de difusión en agarosa para Hg lábil a 25 ºC fueron $2,8\times10^{-6}$ y $5,2\times10^{-6}$ cm^2 s^{-1} para los dispositivos DGT-BC y DGT-SBC, respectivamente, coincidiendo con los órdenes de magnitud reportado en la literatura.

- A pesar de las altas concentraciones de otros elementos traza (Mn, Cu, Zn, Ni, Pb, Cd y As) en la solución de despliegue, que posiblemente hayan

competido con el Hg por los sitios de sorción en la superficie de BC y SBC, se obtuvo un rendimiento muy satisfactorio de los dispositivos DGT manufacturados con estos materiales.

● Los dispositivos DGT manufacturados con polímeros sintetizados a base de benzoiltiourea como capas de unión y gel de poliacrilamida como capa de difusión demostró ser efectivo para la determinación de especies de Hg lábiles, mostrando una fuerte correlación lineal en los ensayos de serie temporal con dispositivos DGT-BTP1.

● El coeficiente de difusión de dispositivos DGT-BTP1 para el Hg lábil a 25 ºC fue de $4,0 \times 10^{-6}$ cm^2 s^{-1}, mientras que para los dispositivos DGT-3MFS fue de $9,1 \times 10^{-6}$ cm^2 s^{-1}.

● Los dispositivos DGT-BTP1 fueron efectivos para determinar Hg lábil en soluciones acuosas con un amplio intervalo de pH (entre 4,5 y 7,5) y fuerza iónica (0,005 M y 0,01 M).

● Los dispositivos DGT-BTP1 se utilizaron con éxito para mediciones *in situ* de Hg en el río Quito (cuenca del río Atrato) demostrando que son una alternativa prometedora para el monitoreo de Hg en agua dulce.

Referencias

Albanese, S., Ebrahimi, P., Aruta, A., Cicchella, D., De Vivo, B., & Lima, A. (2023). Potentially toxic elements in the soils of Campi Flegrei (south Italy) and the immediate surroundings: Spatial distribution, origin and probabilistic human health risk. Chemosphere, 313, 137297.

ANM (2022). Ficha Colombia. Agencia Nacional Minera. https://mineriaencolombia.anm.gov.co/sites/default/files/2022-02/Ficha%20Colombia%2001%202022.pdf (Retrieved: 05/07/2023).

ATSDR (2005). Toxicological profile for nickel. Agency for Toxic Substances and Disease Registry. Atlanta, US.

ATSDR (2007). Toxicological profile for arsenic. Agency for Toxic Substances and Disease Registry. Atlanta, US.

ATSDR, (2023). What Are the Standards and Regulation for Arsenic Exposure? From: https://www.atsdr.cdc.gov/csem/arsenic/standards.html (Retrieved: 20/05/2023).

Benoit, J. M., Gilmour, C. C., & Mason, R. P. (2003). The influence of sulfide on solid-phase mercury bioavailability for methylation by pure cultures of Desulfobulbus propionicus (1pr3). Environmental Science & Technology, 37(6), 1276-1282.

Berkowitz, B., Dror, I. & Yaron, B. (2008). Contaminant geochemistry, Springer-Verlag. Berlin. 412p.

Bernhoft, R. A. (2012). Mercury Toxicity and Treatment: A Review of the Literature. Journal of Environmental and Public Health, 2012, 1–10.

Bjørklund, G., Dadar, M., Mutter, J., & Aaseth, J. (2017). The toxicology of mercury: Current research and emerging trends. In Environmental Research (Vol. 159, pp. 545–554). Academic Press Inc.

Blesa, M. A., & Castro, G. D. (2015). Historia natural y cultural del mercurio (1st ed.). Asociación Argentina para el progreso de las ciencias. http://www.aargentinapciencias.org/ (Retrieved: 05/07/2023).

Blum, J. D., Drazen, J. C., Johnson, M. W., Popp, B. N., Motta, L. C., & Jamieson, A. J. (2020). Mercury isotopes identify near-surface marine

mercury in deep-sea trench biota. Proceedings of the National Academy of Sciences, 117(47), 29292-29298.

Broussard, L. A., Hammett-Stabler, C. A., Winecker, R. E., & Ropero-Miller, J. D. (2002). The Toxicology of Mercury. Laboratory Medicine, 33(8), 614–625.

Cediel-Ulloa, A., Yu, X., Hinojosa, M., Johansson, Y., Forsby, A., Broberg, K., & Rüegg, J. (2022). Methylmercury-induced DNA methylation—From epidemiological observations to experimental evidence. Frontiers in Genetics, 13.

Clarkson, T. W. (1987). Metal toxicity in the central nervous system. Environmental Health Perspectives, 75, 59–64.

Clarkson, T. W. (2002). The three modern faces of mercury. Environmental Health Perspectives, 110, 11–23.

Clarkson, T., Cranmer, J., Sivulka, D., & Smith, R. (1984). Mercury health effects update: Health issue assessment.

Compeau, G. C., & Bartha, R. (1985). Sulfate-reducing bacteria: principal methylators of mercury in anoxic estuarine sediment. Applied and Environmental Microbiology, 50(2), 498-502.

Córdoba Sola, P. (2018) ¿De dónde procede el mercurio que se encuentra en el medioambiente?. En: Martínez Tarazona, M. R., & López Antón, M. A. (Ed), El mercurio: sus fuentes de emisión, usos e impactos. Consejo Superior de Investigaciones Científicas (CSIC), España

Córdoba-Tovar, L., Marrugo-Negrete, J., Barón, P. A. R., Calao-Ramos, C. R., & Díez, S. (2023). Toxic metal (loids) levels in the aquatic environment and nuclear alterations in fish in a tropical river impacted by gold mining. Environmental research, 224, 115517.

Cruz-Esquivel, Á., Díez, S., & Marrugo-Negrete, J. L. (2023). Genotoxicity effects in freshwater fish species associated with gold mining activities in tropical aquatic ecosystems. Ecotoxicology and Environmental Safety, 253.

DANE (2014) 3er Censo nacional agropecuario. Departamento Administrativo Nacional de Estadística de Colombia. https://www.dane.gov.co/files/CensoAgropecuario/entrega-definitiva/Boletin-4-Pobreza-y-educacion/4-Boletin.pdf (Retrieved: 05/07/2023).

de Paula Gutiérrez, B. F., & Agudelo, C. A. R. (2020). Fish as bioindicators: coal and mercury pollution in Colombia's ecosystems. Environmental Science and Pollution Research, 27(22), 27541-27562.

Díez, S. (2009). Human health effects of methylmercury exposure. In D. M. Whitacre (Ed.), Reviews of Environmental Contamination and Toxicology (Vol. 198, pp. 111–134). Springer.

Díez, S. (2018) El ciclo biogeoquímico del mercurio. En: Martínez Tarazona, M. R., & López Antón, M. A. (Ed), El mercurio: sus fuentes de emisión, usos e impactos. Consejo Superior de Investigaciones Científicas (CSIC), España

Do, S. Y., Lee, C. G., Kim, J. Y., Moon, Y. H., Kim, M. S., Bae, I. H., & Song, H. S. (2017). Cases of acute mercury poisoning by mercury vapor exposure during the demolition of a fluorescent lamp factory. Annals of Occupational and Environmental Medicine, 29(1).

EConcept. (2020). Participación del Banco de la República en la comercialización de oro en Colombia. EConcept Análisis Económico Independiente.

Engstrom, D. R. (2007). Fish respond when the mercury rises. Proceedings of the National Academy of Sciences, 104(42), 16394-16395.

Fahlman, B. D. (2018). Materials Chemistry. In Materials Chemistry. Springer Netherlands.

Gabis, L. V., Attia, O. L., Goldman, M., Barak, N., Tefera, P., Shefer, S., Shaham, M., & Lerman-Sagie, T. (2022). The myth of vaccination and autism spectrum. European Journal of Paediatric Neurology, 36, 151–158.

Gaffney, J., & Marley, N. (2014). In-depth review of atmospheric mercury: sources, transformations, and potential sinks. Energy and Emission Control Technologies, 1.

Gao, Z., Ying, X., Yan, J., Wang, J., Cai, S., & Yan, C. (2017). Acute mercury vapor poisoning in a 3-month-old infant: A case report. Clinica Chimica Acta, 465, 119–122.

Gębka, K., Bełdowski, J., & Bełdowska, M. (2016). The impact of military activities on the concentration of mercury in soils of military training grounds and marine sediments. Environmental Science and Pollution Research, 23, 23103-23113.

Gilmour, C. C., Podar, M., Bullock, A. L., Graham, A. M., Brown, S. D., Somenahally, A. C., ... & Elias, D. A. (2013). Mercury methylation by novel microorganisms from new environments. Environmental Science & Technology, 47(20), 11810-11820.

Gochfeld, M. (2003). Cases of mercury exposure, bioavailability, and absorption. Ecotoxicology and Environmental Safety, 56(1), 174–179.

Google Earth (2023) Satelital image Río Quito, Colombia. Escala: 1:20 m. N:5°27'43", W:76°44'03" Maxar Technologies Landsat / Copernicus. https://earth.google.com/web/@5.46485047,-76.73475986,36.28191287a,1151.92168182d,35y,-7.9232174h,55.1536691t,0r (Retrieved: 23/05/2023).

Greenwood, M. R. (1985). Methylmercury poisoning in Iraq. An epidemiological study of the 1971—1972 outbreak. Journal of Applied Toxicology, 5(3), 148–159.

Gutiérrez-Mosquera, H., Sujitha, S. B., Jonathan, M. P., Sarkar, S. K., Medina-Mosquera, F., Ayala-Mosquera, H., ... & Arreola-Mendoza, L. (2018). Mercury levels in human population from a mining district in Western Colombia. Journal of Environmental Sciences, 68, 83-90.

Gworek, B., Dmuchowski, W., Baczewska, A. H., Brągoszewska, P., Bemowska-Kałabun, O., & Wrzosek-Jakubowska, J. (2017). Air contamination by mercury, emissions and transformations—a review. Water, Air, & Soil Pollution, 228, 1-31.

Hamelin, S., Amyot, M., Barkay, T., Wang, Y., & Planas, D. (2011). Methanogens: principal methylators of mercury in lake periphyton. Environmental science & technology, 45(18), 7693-7700.

Harada, M. (1995). Minamata Disease: Methylmercury Poisoning in Japan Caused by Environmental Pollution. Critical Reviews in Toxicology, 25(1), 1–24.

IEA (2021) The role of critical minerals in clean energy transitions. International Energy Agency. From: https://www.iea.org/reports/the-role-of-critical-minerals-in-clean-energy-transitions (Retrieved: 20/05/2023).

INSG (2023a) What is Nickel? International Nickel Study Group. From: https://insg.org/index.php/about-nickel/what-is-nickel/ (Retrieved: 20/05/2023).

INSST. (2021). Límites de exposición profesional para agentes químicos en España 2021. http://cpage.mpr.gob.es (Retrieved: 05/07/2023).

JECFA. (2011). Safety evaluation of certain contaminants in food.

Kurt, G. (2019). Synthesis of new poly-benzoylthiourea and thermal and surface properties. Journal of Polymer Research, 26(9), 232.

Landner, L., & Reuther, R. (2004). Metals in society and in the environment. A critical review of current knowledge on fluxes, speciation, bioavailability and risk for adverse effects of copper, chromium, nickel and zinc. In Environmental Pollution (Vol. 8). Environmental Pollution, Springer.

Lara-Rodríguez, J. S. (2018). All that glitters is not gold or platinum: Institutions and the use of mercury in mining in Chocó, Colombia. The Extractive Industries and Society, 5(3), 308-318.

Lee, J. H., Moniruzzaman, M., Yun, H., Lee, S., Park, Y., & Bai, S. C. (2016). Dietary vitamin C reduced mercury contents in the tissues of juvenile olive flounder (Paralichthys olivaceus) exposed with and without mercury. Environmental Toxicology and Pharmacology, 45, 8–14.

Lentz, D. L., Hamilton, T. L., Dunning, N. P., Scarborough, V. L., Luxton, T. P., Vonderheide, A., Tepe, E. J., Perfetta, C. J., Brunemann, J., Grazioso, L., Valdez, F., Tankersley, K. B., & Weiss, A. A. (2020). Molecular genetic and geochemical assays reveal severe contamination of drinking water reservoirs at the ancient Maya city of Tikal. Scientific Reports, 10(1).

Li, B., Gong, J., Fang, J., Zheng, Z., & Fan, W. (2021). Cysteine chemical modification for surface regulation of biochar and its application for polymetallic adsorption from aqueous solutions. Environmental Science and Pollution Research, 28, 1061-1071.

Li, F., Ma, C., & Zhang, P. (2020). Mercury deposition, climate change and anthropogenic activities: A review. Frontiers in Earth Science, 8, 316.

Li, H., Dong, X., da Silva, E. B., de Oliveira, L. M., Chen, Y., & Ma, L. Q. (2017). Mechanisms of metal sorption by biochars: biochar characteristics and modifications. Chemosphere, 178, 466-478.

López-Costas, O., Kylander, M., Mattielli, N., Álvarez-Fernández, N., Pérez-Rodríguez, M., Mighall, T., ... & Cortizas, A. M. (2020). Human bones tell the story of atmospheric mercury and lead exposure at the edge of Roman World. Science of the Total Environment, 710, 136319.

Marrugo-Negrete, J., Pinedo-Hernández, J., Marrugo-Madrid, S., & Díez, S. (2020b). Assessment of trace element pollution and ecological risks in a river basin impacted by mining in Colombia. Environmental Science and Pollution Research, 28, 201-210.

Marrugo-Negrete, J., Rodriguez-Espinosa, P. F., Godwyn-Paulson, P., Paternina-Uribe, R. J., Amud, M. Y. I., Rosso-Pinto, M., ... & Jonathan, M. P. (2023). Detecting mass sediment transport and movement tainted by decades of mining activities in river Quito, Western Colombia. Journal of Cleaner Production, 394, 136293.

Marrugo-Negrete, J., Vargas-Licona, S., Ruiz-Guzmán, J. A., Marrugo-Madrid, S., Bravo, A. G., & Díez, S. (2020a). Human health risk of methylmercury from fish consumption at the largest floodplain in Colombia. Environmental Research, 182.

Martín-Doimeadios, R. C. R., Mateo, R., & Jiménez-Moreno, M. (2017). Is gastrointestinal microbiota relevant for endogenous mercury methylation in terrestrial animals? Environmental Research, 152, 454–461.

Mcgeer, J., Henningsen, G., Lanno, R., Fisher, N., Sappington, K., & Drexler, J. (2004). Issue paper on the bioavailability and bioaccumulation of metals.

Medina-Rivas, M. A., Norris, E. T., Rishishwar, L., Conley, A. B., Medrano-Trochez, C., Valderrama-Aguirre, A., ... & Jordan, I. K. (2016). Choco, Colombia: a hotspot of human biodiversity. Revista biodiversidad neotropical, 6(1), 45.

Medina-Rivas, M. A., Norris, E. T., Rishishwar, L., Conley, A. B., Medrano-Trochez, C., Valderrama-Aguirre, A., ... & Jordan, I. K. (2016). Choco, Colombia: a hotspot of human biodiversity. Revista biodiversidad neotropical, 6(1), 45.

Meyer, J. S. (2002). The utility of the terms "bioavailability" and "bioavailable fraction" for metals. Marine Environmental Research, 417–423. www.elsevier.com/locate/marenvrev

Minambiente (2023) Mercurio. Ministerio de Ambiente y Desarrollo Sostenible. Recuperado:20/06/2023, de: https://www.minambiente.gov.co/asuntos-ambientales-sectorial-y-urbana/mercurio/ (Retrieved: 05/07/2023).

Mindat (2023). The mineralogy of Mercury. Hudson Institute of Mineralogy. From https://www.osha.gov/laws-regs/federalregister/2014-10-10 (Retrieved 24/04/2023).

Minenergía (2012) Censo Minero Departamental 2010-2011. Ministerio de Minas y Energía de Colombia.

Ministerio Federal de Finanzas República de Austria (2023). World Mining Data 2023. From: https://www.world-mining-data.info/ (Retrieved 24/05/2023).

MME/UPME/UC (2014). Estudio de la cadena de mercurio en Colombia con énfasis en la actividad minera de oro. Tomos 1-3. Ministerio de Minas y Energía, Unidad de Planeación Minero Energética, Universidad de Córdoba. Bogotá, Colombia.

MME/UPME/UC (2015) Incidencia real de la minería del carbón, del oro y del uso del mercurio en la calidad ambiental con énfasis especial en el recurso hídrico - diseño de herramientas para la planeación sectorial. Ministerio de Minas y Energía; Unidad de Planeación Minero Energética; Universidad de Córdoba. 663 p.

Moniruzzaman, M., Lee, S., Park, Y., Min, T., & Bai, S. C. (2021). Evaluation of dietary selenium, vitamin C and E as the multi-antioxidants on the methylmercury intoxicated mice based on mercury bioaccumulation, antioxidant enzyme activity, lipid peroxidation and mitochondrial oxidative stress. Chemosphere, 273.

Nickel Institute (2023b) Enlace a la página web de donde se toma la información https://nickelinstitute.org/en/about-nickel-and-its-applications/history-of-nickel/ (Retrieved: 05/07/2023).

Nickel Institute, (2023a) Enlace a la página web de donde se toma la información https://nickelinstitute.org/en/about-nickel-and-its-applications/properties-of-nickel/ (Retrieved: 05/07/2023).

Noble, M. J., Decker, S. L., & Zane Horowitz, B. (2016). Inhalational mercury toxicity from artisanal gold extraction reported to the Oregon poison center, 2002–2015. Clinical Toxicology, 54(9), 847–851.

Norilsk Nickel. (2023). Consumption volume of nickel worldwide from 2010 to 2022 (in 1,000 metric tons) [Graph]. In Statista. From https://www.statista.com/statistics/273635/consumption-of-nickel-since-2007/ (Retrieved 20/05/2023).

Oliveira, C. S., Nogara, P. A., Ardisson-Araújo, D. M. P., Aschner, M., Rocha, J. B. T., & Dórea, J. G. (2018). Neurodevelopmental Effects of Mercury. In Advances in Neurotoxicology (Vol. 2, pp. 27–86). Elsevier Inc.

OSHA. (2014). Chemical Management and Permissible Exposure Limits (PELs) | Occupational Safety and Health Administration. From https://www.osha.gov/laws-regs/federalregister/2014-10-10 (Retrieved 24/04/2023).

OSHA. (2023). Hazard Information Bulletins Dimethylmercury | Occupational Safety and Health Administration. From https://www.osha.gov/publications/hib19980309 (Retrieved 21/04/2023).

Palacios-Torres, Y., Caballero-Gallardo, K., & Olivero-Verbel J. (2018) Mercury pollution by gold mining in a global biodiversity hotspot, the Choco biogeographic region, Colombia. Chemosphere. 193: 421-430.

Pan, J., Li, X., Wei, Y., Ni, L., Xu, B., Deng, Y., Yang, T., & Liu, W. (2022). Advances on the Influence of Methylmercury Exposure during Neurodevelopment. In Chemical Research in Toxicology (Vol. 35, Issue 1, pp. 43–58). American Chemical Society.

Park, J. H., Wang, J. J., Zhou, B., Mikhael, J. E., & DeLaune, R. D. (2019). Removing mercury from aqueous solution using sulfurized biochar and associated mechanisms. Environmental pollution, 244, 627-635.

Peijnenburg, W. J. G. M., & Jager, T. (2003). Monitoring approaches to assess bioaccessibility and bioavailability of metals: Matrix issues. Ecotoxicology and Environmental Safety, 56(1), 63–77.

Pérez-Escobar, O. A., Lucas, E., Jaramillo, C., Monro, A., Morris, S. K., Bogarín, D., ... & Antonelli, A. (2019). The origin and diversification of the hyperdiverse flora in the Chocó biogeographic region. Frontiers in Plant Science, 10, 1328.

Pérez-Escobar, O. A., Lucas, E., Jaramillo, C., Monro, A., Morris, S. K., Bogarín, D., ... & Antonelli, A. (2019). The origin and diversification of the hyperdiverse flora in the Chocó biogeographic region. Frontiers in Plant Science, 10, 1328.

Ravichandran, M. (2004). Interactions between mercury and dissolved organic matter—a review. Chemosphere, 55(3), 319-331.

Risher, J. F., Nickle, R. A., & Amler, S. N. (2003). Elemental mercury poisoning in occupational and residential settings. In Int. J. Hyg. Environ.

Health (Vol. 206). http://www.urbanfischer.de/journals/intjhyg (Retrieved: 05/07/2023).

RSC (2023). Arsenic. Royal Society of Chemistry. From: https://www.rsc.org/periodic-table/element/33/arsenic (Retrieved: 20/05/2023).

Salazar-Camacho, C., Salas-Moreno, M., Marrugo-Madrid, S., Marrugo-Negrete, J., & Díez, S. (2017) Dietary human exposure to mercury in two artisanal small-scale gold mining communities of northwestern Colombia. Environment international, 107: 47-54.

Salazar-Camacho, C., Salas-Moreno, M., Marrugo-Madrid, S., Paternina-Uribe, R., Marrugo-Negrete, J., & Díez, S. (2022). A human health risk assessment of methylmercury, arsenic and metals in a tropical river basin impacted by gold mining in the Colombian Pacific region. Environmental research, 212, 113120.

Schuster, P. F., Krabbenhoft, D. P., Naftz, D. L., Cecil, L. D., Olson, M. L., Dewild, J. F., ... & Abbott, M. L. (2002). Atmospheric mercury deposition during the last 270 years: a glacial ice core record of natural and anthropogenic sources. Environmental science & technology, 36(11), 2303-2310.

Science for Environment Policy. (2017). Tackling mercury pollution in the EU and worldwide (N.o 15; In-depth Report 15 produced for the European Commission, Número 15). University of the West of England (UWE), Bristol.

Scudder Eikenberry, B. C., Riva-Murray, K., Knightes, C. D., Journey, C. A., Chasar, L. C., Brigham, M. E., & Bradley, P. M. (2015). Optimizing fish sampling for fish-mercury bioaccumulation factors. Chemosphere, 135, 467–473.

Seccatore, J., Veiga, M., Origliasso, C., Marin, T., & De Tomi, G. (2014). An estimation of the artisanal small-scale production of gold in the world. Science of the Total Environment, 496, 662-667.

Shi, Y., Ma, W., & Wang, D. (2022). Study on Mercury Adsorption and Desorption on Different Modified Biochars. Bulletin of Environmental Contamination and Toxicology, 1-6.

SIMCO (2021) Cifras Sectoriales—Oro. Sistema de Información Minero Colombiano. (2021). https://www1.upme.gov.co/simco/Cifras-Sectoriales/Paginas/oro.aspx (Retrieved: 05/07/2023).

SME (2022). Mining: Produciton and control of Arsenic. Society for Mining, Metallurgy, and Exploration. From: https://www.smenet.org/What-We-Do/Technical-Briefings/Mining-Production-and-Control-of-Arsenic (Retrieved: 20/05/2023).

Tang, W. L., Liu, Y. R., Guan, W. Y., Zhong, H., Qu, X. M., & Zhang, T. (2020). Understanding mercury methylation in the changing environment: Recent advances in assessing microbial methylators and mercury bioavailability. Science of the Total Environment, 714, 136827.

Tsui, M. T. K., Blum, J. D., & Kwon, S. Y. (2020). Review of stable mercury isotopes in ecology and biogeochemistry. The Science of the Total Environment, 716.

Ullrich, S. M., Tanton, T. W., & Abdrashitova, S. A. (2001). Mercury in the aquatic environment: a review of factors affecting methylation. Critical Reviews in Environmental Science and Technology, 31(3), 241-293.

UN (2023) Objetivos de desarrollo sostenible (ODS). Naciones Unidas. https://www.un.org/sustainabledevelopment/es/objetivos-de-desarrollo-sostenible/ (Retrieved: 05/07/2023).

UNEP (2011). Recycling Rates of Metals: A Status Report. United Nations Environment Programme. https://wedocs.unep.org/20.500.11822/8702 (Retrieved: 05/07/2023).

UNEP. (2013). Global Mercury Assessment 2013: Sources, emissions, releases, and environmental transport. United Nations Environment Programme.

UNEP. (2017a). Global mercury supply, trade and demand. United Nations Environment Programme. Chemicals and Health Branch. https://www.unep.org/resources/report/global-mercury-supply-trade-and-demand (Retrieved: 05/07/2023).

UNEP. (2017b). Minamata Convention on Mercury. United Nations Environment Programme https://www.mercuryconvention.org/en/resources/minamata-convention-mercury-text-and-annexes (Retrieved: 05/07/2023).

UNEP. (2019). Global Mercury Assessment 2018. https://www.unep.org/resources/publication/global-mercury-assessment-2018 (Retrieved: 05/07/2023).

UNEP/WHO. (2008). Guidance for identifying populations at risk from mercury exposure. United Nations Environment Programme / World Health Organization. http://www.who.int/foodsafety/en/ (Retrieved: 05/07/2023).

USEPA. (1997). Mercury Study Report to Congress Volume VI: An Ecological Assessment for Anthropogenic Mercury Emissions in the United States. United States Environmental Protection Agency.

USEPA. (2001). Human health criteria - methylmercury. United States Environmental Protection Agency. From https://www.epa.gov/wqc/human-health-criteria-methylmercury (Retrieved 11/04/2023).

USGS (2023a). Mercury production worldwide in 2022, by country (in metric tons) [Graph]. US Geological Survey. In Statista. From: https://www.statista.com/statistics/1005602/global-mercury-production-by-country/ (Retrieved 24/04/2023).

USGS (2023b). Mineral commodity summaries – Arsenic. United States Geological Survey. https://pubs.usgs.gov/periodicals/mcs2022/mcs2022-arsenic.pdf (Retrieved: 05/07/2023).

USGS (2023c). Nickel Statistics and Information. United States Geological Survey. From: https://www.usgs.gov/centers/national-minerals-information-center/nickel-statistics-and-information (Retrieved: 20/05/2023).

USGS (2023d). Mineral commodity summaries. Nickel. United States Geological Survey.

Veiga, M. M. & Baker, R. F. (2004). Protocols for environmental and health assessment of mercury released by artisanal and small-scale gold miners. United Nations Publications.

WHO (2000). Air quality guidelines for Europe, 2nd ed. World Health Organization. Regional Office for Europe.

WHO (2017). Guidelines for drinking-water quality: fourth edition incorporating first addendum, 4th ed + 1st add. World Health Organization.

WHO (2018). Arsenic Primer – Guidance on the investigation& mitigation of arsenic contamination. World Health Organization.

WHO. (2003). Elemental mercury and inorganic mercury compounds : human health aspects. World Health Organization. https://apps.who.int/iris/handle/10665/42607 (Retrieved: 05/07/2023).

World Gold Council (2018). Gold Investor, July 2018. Gold and the electronics sector. From: https://www.gold.org/goldhub/research/gold-investor/gold-investor-july-2018/13231 (Retrieved: 13/05/2023).

Yang, J., Sun, Y., Wang, Z., Gong, J., Gao, J., Tang, S., ... & Duan, Z. (2022). Heavy metal pollution in agricultural soils of a typical volcanic area: Risk assessment and source appointment. Chemosphere, 304, 135340.

Zhang, H., Liu, G., Li, J., Qiao, D., Zhang, S., Li, T., ... & Liu, M. (2023). Modeling the impact of nickel recycling from batteries on nickel demand during vehicle electrification in China from 2010 to 2050. Science of The Total Environment, 859, 159964.